A Role for Hypoxia and Hypoxia Inducible Factor during Chondrogenesis of Bone Marrow Mesenchymal Stem Cells

Taheem, Dheraj

Awarding institution:
King's College London

A Role for Hypoxia and Hypoxia Inducible Factor during Chondrogenesis of Bone Marrow Mesenchymal Stem Cells

Dheraj Kumar Taheem

Thesis submitted for the degree of Doctor of Philosophy

2017

King's College London

Centre for Craniofacial and Regenerative Biology

Acknowledgments

Completing the research for this PhD and writing the thesis has required monumental effort from myself but was made significantly easier by certain people. I would not be in this position without Eileen Gentleman. From the off, she created an atmosphere which was conducive for scientific discussion and which enabled me to develop as a critically-analysing scientist capable of questioning the literature and data generated by myself and others. Her style of management also enabled me to independently construct and answer my own research questions, which will be invaluable in my future career as a scientist. Another key individual was Gavin Jell, whose contribution to the ideas of the project and critique of my research, I hope has enabled me to product a high-quality piece of work. I would also like to acknowledge the PhD students under his supervision who facilitated my hypoxic experiments prior to the arrival of our own hypoxic incubator. Dusko Ilic and Liani Devito have also been invaluable to my research due to them also providing the use of their hypoxic incubator.

I would also like to thank Agamemnon Grigoriadis and his PhD students- Ewa Kania and Sorrel Bunting, who together provided essential advice required for me to design, conduct, analyse and interpret well-controlled experiments for the study of cartilage differentiation. For the same reasons, I would also like to thank Silvia Ferreira and Meghna Motwani who both taught me some of the fundamental aspects of biological research. Together with the rest of the Gentleman lab, they ensured that the day-to-day atmosphere in the lab was a relaxed and constructive one. Another important individual during the last four years was Marcus Dawson. Through sharing of experiment ideas, data analysis and interpretation, equally as well as being there to just chat to, Marcus has been integral in my progression as a scientist. Another individual- Daniel Foyt has also been key in the research shown here with him generating some of the contributing data and also being there discuss scientific and non-scientific matters with.

In addition to those described, help has come in different forms from almost everyone in the Centre for Craniofacial and Regenerative Biology (CCRB). Specifically John Russel, Mark Hintze and those in the corner of the post-graduate office were always there to provide invaluable advice, to chat about inane subjects and to berate me for my political views. Especially over a pint. Other members of CCRB who have helped throughout the last four years are Angela Gates, Chris Healy and Susmitha Rao. These have all provided essential encouragement as well as administrative, logistical and technical help throughout my time in the department.

I would also like to thank my mum, dad, brother, sister and rest of the family for providing the resources and encouragement to get to this stage of the PhD. Without their help and the incessant nagging from my parents to ‘get the work done’ and ‘drink less beer’, the journey to this point would have been much rockier. In addition, various friends including Samuel Thorburn, Christopher Macmorland, Oliver Finlay-Smith and Andrew Marnoch and the aforementioned intake of beer with these individuals and others, have also made the journey more bearable. One of the most important individuals during my PhD and someone that has made my time in London a memorable one, is Maia Duffield. Using a sickeningly overused phrase, she has simply always ‘just been there’. Whether to allow me to vent my frustration during the PhD, to help distract my mind from the inexorable obstacle that was my research or for simply understanding when my PhD commitments stopped us spending time together. She has truly, perhaps unknown to herself, been amazing.

Abstract

Articular cartilage lesions cause pain, morbidity and may progress to osteoarthritis, which in terms of medical care, has been approximated to cost 1-2.5% of the gross national product of USA, UK, France and other countries. Current repair strategies have considerable limitations and have prompted the development of cartilage tissue engineering (CTE) approaches. One of the challenges of CTE is the expansion and differentiation of adult stem cells *in vitro*, into functional articular chondrocytes whilst avoiding hypertrophy. Hypoxia is an important environmental factor required for cartilage development, for stimulating articular chondrogenesis and ECM formation. There remains, however, a number of questions regarding the *in vitro* role of hypoxia and HIF stabilization in the development of CTE strategies. These include: a) the appropriate level of hypoxia required for chondrogenesis, b) determining if artificial HIF stimulation has advantages over physiological hypoxia, c) which of the commonly-used HIF-stimulating compounds most potently induces HIF-mediated articular chondrogenesis and d) if there exists a relationship between mechanostransduction and HIF during chondrogenesis. Compared to normoxia, hypoxia (2%O_2 and 5%O_2) induced the expression HIF target genes (including *VEGFA*, *PGK1* and *EGLN)* but only 5% inhibited hypertrophic collagen type X expression. Artificial stimulation of HIF-1a by DMOG induced greater expression of HIF chondrogenic targets (*SOX9* and collagen-modifying enzymes) than other compounds used ($CoCl_2$ and DFX) and physiological hypoxia. DMOG also reduced collagen type X at the mRNA level compared to the other HIF stabilising compounds. In terms of the effect of hypoxia on mechano-signalling during chondrogenesis, exposure to 2%O_2 induced ROCK activity, actin re-organisation and *SOX9* expression during BM-MSC chondrogenesis on soft polyacrylamide gels. No such changes were induced on stiff substrates. This suggests the existence of specific crosstalk between HIF and stiffness-sensing pathways, which may inform CTE strategies in which hypoxia-mediated chondrogenesis of BM-MSCs is conducted within biomaterial scaffolds of a defined stiffness.

Table of Contents

Figure List

Chapter. Figure. Figure Title…….. Page Number

Abbreviations

Extracellular Matrix (ECM)
Glycosaminoglycans (GAGs)
Osteoarthritis (OA)
Messenger Ribonucleic Acid (mRNA)
Hyaluronic Acid (HA)
T-Box 5/4 (TBX5/4)
Fibroblast Growth Factor 10 (FGF)
Apical Ectodermal Ridge (AER)
Sonic Hedghog (Shh)
Bone Morphogenetic Protein (BMP)
Paired-Related Homeobox 1 (PRX1)
Msh Homeobox 1 (MSX1),
Runt-related transcription factor 2 (RUNX2)
SRY Box-5 (SOX5)
SRY Box-6 (SOX6)
Paired Box (PAX)
Neural Cell Adhesion Molecule (NCAM)
Transforming Growth Factor-Beta (TGF–β)
Matrix Metalloproteinase 13 (MMP13)
Indian hedgehog (Ihh)
Parathyroid Hormone Related Peptide (PTHrP)
Parathyroid Hormone receptors (PTH)
T-cell factor/lymphoid enhancer factor (TCF/LEF)
Autologous Chondrocyte Implantation (ACI)
Cartilage Tissue Engineering (CTE)
Bone marrow mesenchymal stem cells (BM-MSCs)
Adult Stem Cells (ASCs)
Adipose-derived MSCs (AMSCs)
Peroxisome Proliferator-Activated Receptor-γ (PPARγ)
Peripheral Blood Mononucleocytes (PBMCs)
Epithelial-to-Mesenchymal-Transition (EMT)
Lateral Plate Mesoderm (LPM)
Mesenchymal-to-Epithelial Transition (MET)
SRY Box-9 (SOX9)
The International Society for Cellular Therapy (ISCT)
Cluster of Differentiation (CD)
Matrix-assisted ACI (MACI)
Poly(Vinyl Alcohol)-Polycaprolactone (PVA/CL)
Polylactic Acid (PLLA)

Polyethelene Glycol (PEG)
Divalent Iron (Fe^{2+})
Green Fluorescent Protein (GFP)
Complementary Deoxyribonucleic Acid (cDNA)
Oxygen (O_2)
Adenosine Tri-Phosphate (ATP)
Vascular Endothelial Growth Factor (VEGF)
Hypoxia Inducible Factor
CREB-Binding Protein/p300 (CBP/p300)
Pyruvate Kinase (PKM)
HIF-Response Element (HRE)
HIF Ancillary Sequence (HAS)
N-terminal Transactivation Domain (N-TAD)
C-terminal Transactivation Domain (C-TAD)
Prolyl Hydroxylase 2 (PHD2)
Von Hippel–Lindau Tumor Suppressor (VHL)
2-Oxoglutarate (2-OG)
Oxygen-Dependent Degradation Domain (ODDD)
Receptor for Activated C Kinase 1 (RACK1)
Heat Shock Protein 90 (HSP90)
Asparagine-803 (Asn-803)
Factor Inhibiting HIF (FIH)
Protein Kinase B (PKB)
Mammalian Target of Rapamycin (mTOR)
Nuclear Factor kappa-Light-Chain-Enhancer of Activated B cells (NF-κB)
Conditional Knockout (CKO)
Osteochondral Tissue Engineering (OCTE)
Human Articular Chondrocytes (HACs)
Poly(Lactic-co-Glycolic Acid) (PLGA)
Collagen Prolyl Hydroxylase (CP4HA1)
Lysyl Oxidase (LOX)
Alkaline Phosphatase
Myosin Light Chain 2 (MLC2)
Kilopascal (KPa)
Rho-Associated Protein Kinase (ROCK)
Polyacrylamide (PA)
Filamentous Actin (F-Actin)
Focal Adhesion Kinase (FAK)
Ras Homolog Gene Family, Member A (RhoA)
Guanosine Tri-Phosphate (GTP)
Guanosine Tri-Phosphatase (GTPase)

Guanosine Di-Phosphate (GDP)
Guanosine Exchange Factors (GEFs)
Myosin Phosphatase (MYP)
Globular Actin (G-actin)
Yes-Associated Protein
PDZ-binding motif (TAZ)
TEA Domain (TEAD)
Small Interfering RNA (siRNA)
Runt-Related Transcription Factor 2 (RUNX2)
Myocardin-Related Transcription Factors (MRTFs)
Serum Response Factor (SRF)
Linker of Nucleoskeleton and Cytoskeleton
Megakaryoblastic Leukemia (Translocation) 1 (MKL1)
Megapascal (MPa)
Tissue Culture Plastic (TCP)
Dimethyloxalylglycine (DMOG)
Imperial College Healthcare Tissue Bank (ICHTB)
National Institute for Health Research (NIHR)
United Kingdom (UK)
National Health Service (NHS)
Fluorescein Isothiocyanate (FITC)
Phycoerythrin (PE)
Growth media (GM)
Carbon Dioxide (CO_2)
Fetal Bovine Serum (FBS)
Phosphate Buffered Saline (PBS)
Ethylenediaminetetraacetic acid (EDTA)
α-Minimal Essential Media (αMEM)
Dimethyl sulfoxide (DMSO)
Relative Centrifugal Field (RCF)
Dulbeccos MEM (DMEM)
Antibiotic Antimycotic (ABAM)
Chondrogenic Differentiation media (CDM).
Cobalt Chloride ($CoCl_2$)
Desferrioxamine (DFX)
Acriflavine (ACF)
Sodium Hydroxide (NaOH)
Dichlorodimethylsilane (DCDMS)
Tetramethylethylenediamine (TEMED)
Ammonium Persulfate (APS)
sulfosuccinimidyl 6-(4'-azido-2'-nitrophenylamino)hexanoate (Sulfo-SANPAH)

4-(2-hydroxyethyl)-1-piperazineethanesulfonic acid (pH 8.5) (HEPES)
Paraformaldehyde (PFA)
Hydrochloric Acid (HCL)
Double-Stranded DNA (dsDNA)
Cadmium Chloride ($CdCl_2$)
Sodium Dodecyl Sulfate (SDS)
Deionised Water (dH_2O)
Bicinchoninic Acid (BCA)
Bovine Serum Albumin (BSA)
Polyacrylamide Gel Electrophoresis (PAGE)
Polyvinylidene difluoride (PVDF)
Non-fat milk (NFM)
Molecular Weight (MW)
Moloney Murine Leukemia Virus Reverse Transcriptase (MLV-RT)
Polymerase Chain Reaction (PCR)
Quantitative Polymerase Chain Reaction (qPCR)
Nation Centre for Biotechnology Information (NCBI)
4',6-diamidino-2-phenylindole (DAPI)
Poly(ε-Caprolactone) (PE)
Phosphoglycerate Kinase (PGK1)
Gremlin1 (GREM1)
Dickkopf WNT Signalling Pathway Inhibitor 1 (DKK1)
Reactive Oxygen Species (ROS)
Insulin growth factor II (IGF2)
Mitogen Inducible Gene 6 (MIG6)
Inhibin Beta A Subunit (INHBA)
Enzyme-Linked Immunosorbent Assays (ELISAs)
Mitogen-Activated Protein Kinase (MAPK)
Mitogen-Activated Protein Kinase Kinase (MEK)
Extracellular Signal-Regulated Kinase (ERK)
Activator protein 1 (AP-1)
Unfolded Protein Response (UPR)
N-Oxalyl-(d)-Phenylalanine (NOFD)
Distal-less Homeobox 5/6 (Dlx5/6)
Traction Force Microscopy (TFM)
N-Oxaloylglycine (NOG)
Ciclopirox Olamine (CPX)

1. Introduction

1.1. Articular Cartilage

1.1.1. Structure & Function

Articular or hyaline cartilage overlies the subchondral bone within articulating joints. It is an Extracellular Matrix (ECM)-rich tissue consisting of distinct regions from the articulating surface down to the underlying calcified bone, which vary in structural organisation, as shown in **figure 1.1**. Despite this heterogeneity, the constituents of each region are a mixture of collagens, glycosaminoglycans (GAGs), water, and a specialised cell type- the articular chondrocyte. These cells constitute only approximately 1-5% by volume of the whole tissue [2], have a low metabolic activity and are responsible for synthesis of cartilage ECM [3].

The primary functions of articular cartilage are to reduce friction between opposing surfaces of the joint, providing resistance to the compressive and tensile forces on the joint during movement, and protecting the underlying subchondral bone from compression-induced damage [2]. The superficial layer, proximal to the synovial fluid, functions as an impermeable barrier for protection of the remainder of the tissue and enables resistance to tensile forces experienced during limb movement [4]. It consists of tightly arranged network of Collagen Type II and IX fibrils, parallel with the articulating surface of the joint, together with chondrocytes of a high aspect ratio [5, 6]. The middle zone contains collagen fibrils of obliquely-arranged orientation, in addition to proteoglycans and a sparse arrangement of rounded chondrocytes. This region grants the articular cartilage its resistance to compressive forces. It functions in tandem with the deep zone, which consists of collagen fibrils arranged

perpendicularly to the articulating surface and the highest concentration of proteoglycans [3].

Hyaline cartilage is present on the articulating surface of all diarthroidal joints, including the knee, hip and ankle. Despite articular cartilage being largely similar in composition and function between the different joints in which it is present, distinct differences have been identified. These are thought to be due to the varying degree of compressional force which each of these joints encounter. Shepherd and Seedhom made observations on the differences in cartilage thickness between different joint types and found that of the knee to be greater than that of the ankle or hip [7]. Moreover, this thickness appeared to correlate with the size, height and body mass index of the donor, with an inverse relationship identified between thickness and the compressive forces experienced by the joint.

Interestingly, the susceptibility to degradation also varied between joints. Upon dissection from human joints, chondrocytes within the knee were found to be more susceptible to catabolic factors than those in the ankle, which displayed an increased rate of a production of GAGs required for repair [8]. This observation was similar to that described by Eger et al who, in explant models, demonstrated the increased resistance to degeneration of articular cartilage within the ankle compared to that of the knee [9]. It may be hypothesized that the increased load bearing on the articular cartilage within the knee, increases its susceptibility to degeneration. The increased thickness of the articular cartilage within this joint may also result in reduced availability of the tissue to nutrients and regenerative factors from the synovial fluid.

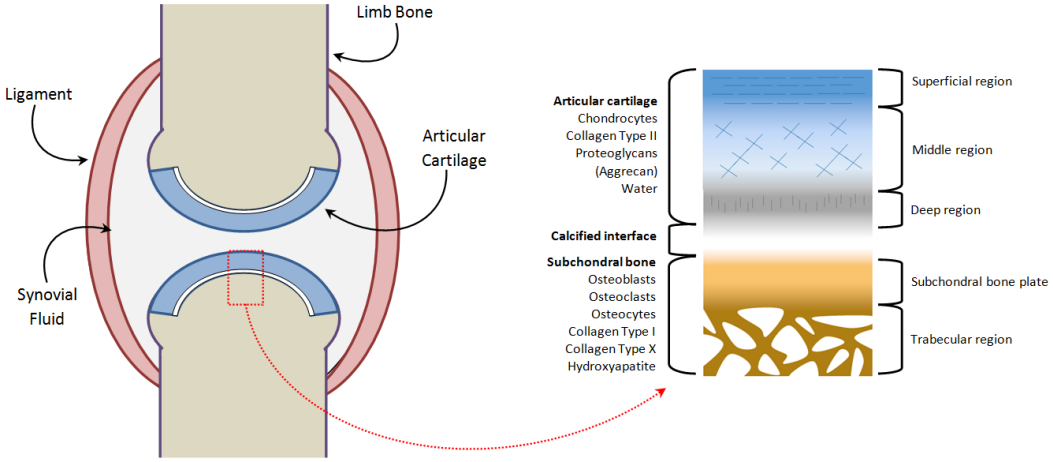

Figure 1.1. Osteochondral Tissue Structure. A: The gross structure of an articulating joint present at the end of limb bones. **B:** Structure and regions of osteochondral tissue.

1.1.2. The components of articular cartilage

1.1.2.1. Articular chondrocytes

The low metabolic rate of the chondrocyte population within articular cartilage is a result of a lack of vasculature and subsequent low nutrient supply [10]. This is in part due to regression of vasculature at the limb bud stage of limb development [11] but also is due to expression of anti-angiogenic protein expression by articular chondrocytes [12]. Proteins such as Chondromodulin-1 inhibit endothelial cell growth, thereby inhibiting vessel formation [13]. If left unhindered, angiogenesis is inhibitory to articular chondrocyte function and is a driver of cartilage degeneration in osteoarthritis (OA) [14, 15]. The development of an essential anti-angiogenic milleu by articular chondrocytes implies that this cell population functions most optimally in a low metabolic state. Corresponding to their low metabolic rate, articular chondrocytes generate a required level of Adenosine Tri-Phosphate (ATP) via glycolytic pathways (Lane, 2015 #1384).

Another advantage of the slow-metabolism and proliferation of chondrocytes is with regards to the stabilisation of articular cartilage ECM. The articular chondrocytes generally do not proliferate and remain in the ECM for a long period of time [10]. It is this aspect which enables them to maintain the ECM of the articular cartilage over the majority of an individual's lifetime. The half-life of collagen type II is estimated to be 117 years [16] with proteoglycans described to reside in the ECM for 3-24 years [17].

Whilst such an ECM turnover rate is benefical for maintance of articular cartilage which is able to maintain the compressive and tensional forces applied during joint

movement [3, 18], it also provides a stable extracellular environment for the articular chondrocytes. For example, interactions with Collagen Type II is thought to inhibit apoptosis of articular chondrocytes via Annexin V [19]. However, despite these advantages of the slow turnover of articular chondrocytes and the ECM in which they reside, repair or acute chondral defects is a major issue as described in later sections of this chapter. Relatively low rates of both chondrocyte proliferation and secretion of new ECM components are inhibitory to endogenous repair of lesions which exceed the superficial layer of articular cartilage [20].

1.1.2.2. The extracellular components of articular cartilage

Water constitutes a large proportion of the wet weight of articular cartilage, approximately 80% in the superficial and 65% of the deep zone composed of water [2]. It functions to maintain a flow of nutrients to the residing chondrocytes and is integral in order for the ECM to maintain the compressive resistance of the tissue to external forces [3]. It is also essential in lubricating the articular surface and inhibiting friction between opposing bones. The other major constituents, Collagen and proteoglycans, each contributing to approximately 10-20% of the total cartilage wet weight.

1.1.2.2.1. Collagen Type II

The major collagen subtype in articular cartilage is Type II Collagen. Its synthesis by articular chondrocytes begins at transcription of the *COL2A1* gene, which encodes the Collagen Type II alpha-helix [21]. The nascent pre-messenger ribonucleic acid

(mRNA) molecule is then processed and spliced to generate the protein-coding mRNA. Two variants of mature *COL2A1* mRNA have been identified and are classified based on the inclusion of exon 2 or not, with their differential expression hypothesized to alter Collagen Type II bio-synthesis [22]. Interestingly, each of these mRNA isoforms have also been shown to mark distinct chondrocyte populations, with mature chondrocytes and chondroprogenitors shown to express differential levels of the exon 2-containing and exon 2–free forms [23]. Inactivation of a single allele of *COL2A1* in developing mice results in a decrease in Collagen Type II protein in the ECM of the cartilage overlying the humerus head [24]. A decrease in the formation of ordered, parallel fibrils was also observed with a softer cartilage being generated as a whole. Complete deletion of *COL2A1* resulted in ECM disorganization of the developing mouse limb which resembled that observed in cases of OA. The importance of *COL2A1* gene transcription for cartilage function was also highlighted by Tiller et al who identified the cause of a large spectrum of chondrodysplasias. The phenotypes observed were due to dominant mutations within the *COL2A1* gene which increases the susceptibility of articular cartilage to degradation [21].

The tertiary protein structure of Collagen Type II in cartilage ECM consists of a triple helix of alpha 1 collagen chains [25]. As described by Bruckner and Van der Rest [25], Collagen Type II is secreted as a pro-collagen molecule, linked to both its C- and N-terminal ends by short sequences known as telopeptides. The C-terminal is important in determining the organisation of each pro-collagen chain and their association with other monomers. Simultaneous with integration into a triple helical arrangement, the N and C-terminal ends of the pro-collagen chain are degraded by specific proteases. A characteristic feature of the collagens is their post-translational

modification during their incorporation into the ECM. Proline hydroxylation of the pro-collagen molecules is required for their assembly in triple helix structures [26] whereas lysine hydroxylation is required for the complete stability of the supramolecular structures formed from multiple triple-helices [27].

Spatial organization of Collagen Type II fibrils as described by Fox et al [3], is dependent on the region of articular cartilage in which they reside. The superficial zone is composed of fibrils which are arranged in a parallel manner relative to the articular surface. Towards the subchondral bone of the joint, the collagen fibrils are arranged in arranged in progressively perpendicular orientation through the middle region to the deep region. To examine the organisation of collagen fibrils via a non-invasive method, Bergholt et al utilized a technique known as Raman Spectroscopy. During Raman Spectroscopy, differential scattering of donor monochromatic light occurs due to differentially-arranged collagen fibrils which enable resolution of the supramolecular structure of this ECM component. Bergholt et al confirmed the observations made by histological methods. They observed the collagen fibrils adopt a parallel, oblique and perpendicular arrangement relative to the articulating surface in the superficial, middle and deep zones respectively [28].

In terms of function, Collagen Type II forms a backbone for Collagen Types IX and XI [29] and together, these fibrillary structures function to maintain the integrity of cartilage in response to shear and tensile stresses. The Collagen Type II proximally-located to the articular chondrocytes are also integral in maintaining the viability of these cells. [30]. Kim and Kirsch identified a role for cartilage collagens in inhibiting the premature hypertrophy of chondrocytes and mineralisation of the surrounding

matrix [19]. This was observed to occur via an interaction of collagen type II with cell-surface marker- Annexin V. The interaction of Collagen Type II and Type XI also stabilizes the GAG network which is required for the maintenance of the mechanical characteristics of the cartilage ECM [18]. Collagen Type II also plays an indirect role in the reduction of friction between opposing articular surfaces. This function of Collagen Type II is mediated by Lubricin [31] which is secreted by articular chondrocytes in the superficial layer and also acts to inhibit chondrocyte apoptosis [32].

1.1.2.2.2. Aggrecan

Articular cartilage contains multiple proteoglycans, and Aggrecan is the most abundant of these. Mutations in the gene encoding its protein core, *ACAN* [33] results in phenotypic outcomes which are grouped together into the Aggrecanopathies. For example a mutation within the ACAN gene has been shown to predispose patients to Osteochondritis Dissecans which in juvenile patients, increases the rate of subchondral bone lesions [34]. In the ECM, the core protein region of Aggrecan consists of 3 globular regions- G1, G2 and G3 [35]. The first of these functions to tether Aggrecan to another major cartilage ECM, Hyaluronic Acid (HA). Between each of globular domains is the inter-globular domain, to which are attached the carbohydrate portion of the proteoglycans – the GAGs, which are classified into chondroitin and keratin sulphates [35]. Aggrecan does not form isolated structures in the ECM of cartilage but rather, multiple Aggrecan molecules via the G1 domains of their protein cores bind to a core HA polymer.

HA is synthesized at the membrane region of cells by HA Synthase [35]. Following production, it is then secreted in the extra-cellular space and forms a coat around the cell where it complexes with Aggrecan molecules. This complex is formed via a link protein which has also plays a role in the protection of HA from HAase-mediated digestion. The chemical structure and ionic charge of the HA-Aggrecan complex enables the cartilage matrix to absorb water and swell in size accordingly [35]. The presence of large amounts of Aggrecan in the chondrocyte extracellular space increases the amount of water retained in the matrix. This results an equilibrium being attained between the swelling of the ECM structure and the tensional force created by the ability of the Collagen Fibrils to resist this swelling. The HA-Aggrecan complex therefore enables cartilage to maintain the viscoelastic nature of cartilage and provide resistance to compressive forces on the joint [35]. This equilibrium between the Aggrecan-induced swelling and Collagen-induced tension, also maintains the resistance of cartilage to fluid flow-induced deformation [36].

1.1.3. Development

During development, articular cartilage is formed during endochondral ossification, a process required for formation of the appendicular skeleton [37]. The initial stage of limb development is the formation of a condensed population of mesenchymal precursors, which go on to form the initial cartilaginous anlage required for bone formation. Following chondrogenesis of the limb bud mesenchyme, vascular infiltration from the perichondrium is the signal for formation of the primary ossification centre of endochondral bones [38]. Hypertrophic differentiation of the

newly formed chondrocytes occurs, resulting in their cell death, remodeling of the cartilage matrix and differentiation of invading osteoblast precursors. Synchronous with this process is the preservation of a population of resting chondrocytes within the growth plate, whose phenotype are maintained and go on to form the articular cartilage.

1.1.3.1. Limb bud specification

At the onset of limb mesenchyme formation, the family of Hox transcription factors expressed in the lateral plate mesoderm [39] stimulate expression of T-Box 5/4 (TBX5/4) [40, 41] which via Fibroblast Growth Factor (FGF) 10, stimulate subsequent expression of FGF8 in the Apical Ectodermal Ridge (AER) [42], a thickened epithelial layer at the distal tip of the prospective limb bud. This process specifies the hind- and forelimbs, with FGF8 initiating and propagating the proximal to distal growth of the pre-cartilage mesenchymal population [43]. Another signalling centre, the zone of polarizing activity [44] functions to specify digit formation along the anterior to posterior axis via Sonic Hedgehog (Shh) signalling [45]. Finally, a 3rd signalling centre- the non-AER limb bud ectoderm, functions to generate the dorsal to ventral polarity of the mesenchymal condensation, via Wnt7a and Bone Morphogenetic Protein (BMP) signalling [46].

The importance of FGF signalling in limb bud formation was shown by studies such as that by Moon et al, who observed skeletal deformation due to a conditional knockdown of *FGF8* in forelimb progenitor cells in addition to downregulation of *SHH* and *BMP2* expression [47]. Overall, prior to chondrogenesis, spatially-controlled

patterns of mesenchymal condensation occurs within the limb bud. These regions are delineated by expression of transcription factors such as Paired-Related Homeobox 1 (PRX1) and Msh Homeobox 1 (MSX1), required for early induction of chondrogenesis [48, 49].

1.1.3.2. Chondrogenic commitment of limb bud progenitors

Following formation of the limb bud, the resident mesenchymal population undergoes chondrogenic differentiation and further division into two sub-populations [50]. One of these populations goes through a proliferative phase, followed by senescence, hypertrophic differentiation and apoptosis, prior to endochondral ossification. The second population enters a resting state and constitute the articular cartilage at the end of long bones.

Between the mesenchymal and proliferative/articular chondrocyte stage, the differentiating cells go through an osteochondral progenitor phase in which the transcription factors SOX9 and Runt-Related Transcription Factor 2 (RUNX2) are both expressed [51], and play key roles in switching the cell fate between that of a chondrocyte or osteoblast. SOX9 has been shown to inhibit the osteoblastic factor, RUNX2 [52] as well as chondrocyte hypertrophy [53], and is indispensable during chondrogenesis, as it functions with SRY Box-5 (SOX5) SRY Box-6 (SOX6) as a transcription factor complex [54], inducing transcription of genes required for cartilage formation such as *COL2A1* [55] and *ACAN* [56]. In addition to this complex, other transcription factors are a requirement during chondrogenesis including Paired Box (PAX) 1 and 9 [57]. Both these transcription factors, as with SOX9, are present

from the limb bud stage throughout articular cartilage patterning [57] and are required for chondroprogenitor specification [58]. Other factors include Nkx3.1/3.2 which are required throughout chondrogenesis, playing roles in chondro-specification [59] and chondrocyte hypertrophy [60].

1.1.3.2.1. Role of cell-cell adhesion

The condensation of mesenchymal populations is deemed a pre-requisite for cartilage development. Accordingly the temporal expression and activity of cell-cell adhesion molecules such as Neural Cell Adhesion Molecule (NCAM) and N-cadherin have been shown to be indispensable during chondrogenesis [61] with their expression reduced following chondrocyte formation [62]. In hMSCs, N-cadherin-mediated cell-cell adhesion has been shown to enhance membrane localization of β-catenin [63], the transcriptional co-activator at the bottom of the canonical Wnt signalling pathway [64]. β-catenin has been shown to be detrimental to mesenchymal progenitor chondrogenesis [65], as well as inducing a bias towards osteoblastic differentiation and bone formation [66]. Cell-cell contact and N-Cadherin binding is therefore integral in minimizing Wnt-induced suppression of chondrogenesis, a function also mirrored by SOX9 [67]. In addition, BMP-induced chondrogenesis was also shown to be inhibited upon blocking of N-Cadherin [68] and was also shown to reduce Transforming Growth Factor-Beta (TGF-β)-mediated chondrogenic differentiation [69]. These studies demonstrate the requirement of cell adhesion in growth factor-mediated cartilage development.

1.1.3.2.2. Role of the TGF-β family of growth factors

A host of growth factor ligand-receptor bindings are required during cartilage development. The TGF-β family of ligands and receptors play an important role in this process, demonstrated by the deletion of BMP receptors or overexpression of BMP inhibitor, Noggin which both result in reduced chondrogenesis [70, 71]. Chondrocyte-specific BMP2 knockdown also reduces proliferation and survival of this cell population in the growth plate [72] as well as inhibiting bone regeneration in a murine fracture model [73]. TGF-β ligands, expressed highly in the mesenchyme and cartilaginous elements, have been shown to enhance initial mesenchyme condensation [74], chondrogenic lineage commitment [75] and arrest chondrocyte hypertrophy [76]. Both BMP and TGFβ ligands exert their effect on cartilage development via the SMAD family of proteins, which transduce the signal generated upon engagement of BMP/TGFβ receptors into transcriptional changes. TGF-βs bind the TGF receptor types 1 and 2 induce activation of SMAD2/3 and binding by SMAD4 before their translocation to the nucleus and transcription of specific target genes. For example nuclear SMAD2/3 enhances SOX9-dependent transcription of chondrogenic genes such as *COL2A1* [77]. Upon binding of a different set of receptors by BMPs, SMAD1/5/8 phosphorylation and activity have been shown to be essential in induction of chondrogenic phenotype from MSCs [78] in addition to cartilage and endochondral bone development [79].

1.1.3.3. Patterning of articular cartilage

Following chondrogenesis and formation of the cartilage growth plate from the mesenchymal limb bud, the chondrocytes then undergo a complex program of events to pattern the formation of mineralised bone and articular cartilage of the limb. From the terminal regions of the prospective long bone, along the longitudinal axis, chondrocytes form distinct groups, each of varying proliferative rates and phenotype. The end of the cartilage template consists of resting chondrocytes. These express genes such as *SOX9*, *SOX5*, SOX6 [80] and *GDF5* [81] in a specific temporal program, creating an ECM rich in Collagen Type II, and XI and Aggrecan [82]. These articular chondrocytes also express *PRG4* [83]. This encodes Lubricin which as described, is important in joint articulation.

Further along the developing bone are a group of highly proliferative chondrocytes, the turnover of which is required for longitudinal bone growth. Further along still, towards the centre of the growth plate are a group of chondrocytes which have left the cell cycle and have begun to de-differentiate into hypertrophic chondrocytes. Following their completion of hypertrophy, these chondrocytes, which exhibit an enlarged morphology, express *RUNX2* and *COL10A1* [84] and secrete a Collagen Type X-rich ECM [85].

The ECM surrounding hypertrophic chondrocytes is also marked by degradation of Collagen Type II and Aggrecan. Matrix Metalloproteinase 13 (MMP13) has been shown to largely govern Collagen Type II degradation prior to the onset of endochondral ossification [86] with Aggrecanases such as Adamts5 [87] digesting Aggrecan in the growth plate. The lack of a proteoglycan and Collagen Type II-rich network as in articular cartilage, results in unique mechanical properties of

hypertrophic cartilage with compared to that at the articulating surface. This is due to a lack of water perfusion of hypertrophic cartilage and a subsequent decrease in resistance to compressive forces. This was demonstrated by Sibole and Herzog who observed the increased deformation of hypertrophic cartilage compared to articular cartilage in response to a compression force on the tissue [88].Following remodeling of the growth plate ECM, apoptosis of the hypertrophic chondrocytes occurs [89] followed by osteoblastic invasion and mineralisation of the vacant space [90].

1.1.3.3.1. Control of articular cartilage patterning by Indian Hedgehog Signalling

Indian Hedgehog (Ihh) signalling is considered the master regulator of chondrocyte de-differentiation during limb development. The Ihh ligand produced by pre-hypertrophic and hypertrophic chondrocytes [91], diffuses along the longitudinal axis of the developing limb, to the pool of proliferative chondrocytes where it binds to Patch1 receptors [92]. This results in inhibition of another transmembrane protein, Smoothened, enabling nuclear translocation of the Gli family of transcription factors. This induces expression and secretion of Parathyroid Hormone Related Peptide (PTHrP) which upon binding to Parathyroid Hormone receptors (PTH) on neighboring pre-hypertrophic and immature chondrocytes, stimulates their proliferation and reduces hypertrophy [93].

Chondrocytes further away from the PTHrP-producing proliferative chondrocytes, undergo hypertrophic differentiation due to a lack of PTHrP-PTH binding. Upon entering the post-mitotic hypertrophic phase these cells in turn, secrete Ihh in a negative feedback loop to maintain the proliferative chondrocyte pool. The anti-

hypertrophic role of the Sox9/5/6 complex has been shown to function through this IHH-PTHRP signalling loop, inducing expression of IHH/PTHRP components required for regulation of chondrocyte phenotype [94]. This system enables controlled rates of chondrocyte proliferation and de-differentiation, required for endochondral bone development [95].

1.1.3.3.2. Control of articular cartilage patterning by Wnt signalling

Another pathway heavily implicated in the progression of chondrocyte hypertrophy is the Wnt signalling pathway. The canonical Wnt pathway acts via the transcriptional co-activator, β-catenin. Upon binding of Frizzled receptor [96] by a canonical Wnt ligand, a protein complex composed of Axin, Glycogen Synthase Kinase, β-catenin and others is dissociated, resulting in nuclear translocation of β-catenin [97]. β-catenin then binds to the T-cell factor/lymphoid enhancer factor (TCF/LEF) family of transcription factors, resulting in transcription of target genes associated with canonical Wnt signalling [98].

As with other pro-hypertrophy signals, the source of Wnt ligands during endochondral ossification is the surrounding perichondrium [99], with the hypertrophic effect of these mediated through RUNX2-dependant mechanisms [100]. Conversely, one of the anti-hypertrophic mechanisms of SOX9 is through inhibition of β-catenin-TCF/LEF [67(Topol, 2009 #217], implicating canonical Wnt signalling as an antagonizing mechanism to Sox9-mediated chondrogenesis. Wnt signalling also drives the key fate switch of mesenchymal limb bud progenitors, inducing a bias for osteoblastic/hypertrophic differentiation rather than

chondrogenesis [66]. Finally, antagonists of canonical Wnt signalling such as those which block Wnt-Frizzled binding have a protective role in OA, preventing de-differentiation of articular chondrocytes [101].

1.2. Cartilage Regenerative Medicine

Acute trauma/stress-related injury to the diathroidal joint may result in damage to the residing articular cartilage [102]. As described by Rai et al, compared to highly vascularized subchondral bone, articular cartilage has a reduced ability to repair itself following the occurrence of lesions which penetrate further than the superficial layer [103]. The articular cartilage is avascular as a result of regression of the blood vessels at the limb bud stage of development and this is coupled with formation of a vascular network at the primary and secondary ossifications centres [104]. The lack of vascular system in the articular cartilage reduces the delivery of nutrients and cells required for cartilage repair. Damage to articular cartilage may result in patient pain, immobility and constitute a large percentage of injury-cases of the diarthoidal knee joint. In a study conducted from 1989-2004, from 25,124 arthroscopies conducted due to various knee joint complications, 67% were deemed to have suffered chondral or osteochondral fractures, with 36% of these lesions measuring over the self-repair threshold in terms of defect size [105].

In addition to symptoms of pain and reduced locomotive ability, chondral lesions may result in damage and remodeling to the surrounding tissue due to abnormal transmission of compressive forces on the joint during movement [106]. This has been documented to result in further cartilage loss [107] and progression to

osteoarthritis if left untreated [108, 109]. The incidence rates of OA are extremely high, with occurrence in 19.2%-27.8% of the US population aged ≥45, and 37% of people aged ≥60. The management of OA also represents a significant economic burden on healthcare systems. As described by Hunter et al – 'the cost of OA in the USA, Canada, UK, France and Australia has been estimated to account for between 1% and 2.5% of the gross national product of these countries' [110].

1.2.1. Current reparative & restorative strategies for cartilage repair

The pain, immobility, and potential progression to OA, emphasises the requirement for immediate repair of acute chondral defects. Current clinical strategies for repair of these defects have been deemed unsuitable for a number of reasons [111]. Autologous/allogeneic transplantation is not a suitable measure for acute lesions due to the risk of disease transmission/immune rejection, the requirement of multiple surgical procedures, donor site morbidity and low tissue availability [112]. Subchondral drilling or microfracture [113] enables access of the lesion to the endogenous source of mesenchymal stem cells within the bone marrow. This technique shows some clinical success, but in younger patients only [114]. In some cases following microfracture, the defect site is occupied with tissue that resembles fibrocartilage [115]. This is mechanically-inferior to articular cartilage, degenerates in the long-term [114] and as a result, may predispose the patient to OA [116].

An improvement on microfracture [117] is Autologous Chondrocyte Implantation (ACI) [118] which works under the principle of implanting isolated and expanded healthy autologous chondrocytes, into the patient defect area [119]. This procedure

requires multiple surgeries however, to harvest autologous cells and for the subsequent implantation, during which the donor site under the periosteal flap may also suffer from hypertrophy [120]. Another key hurdle with ACI is faced during expansion of chondrocytes prior to their implantation. *In vitro* culture of articular chondrocytes and passaging reduces expression of genes which denote the articular chondrocyte phenotype. This is synchronous with their hypertrophic differentiation [121] which reduces their suitability for repair of articular cartilage.

1.2.2. Mesenchymal stem cell-based cartilage tissue engineering.

The problems described in chapter 1.2.1 associated with conventional treatment methods for chondral defects may be alleviated with the use of Cartilage Tissue Engineering (CTE). CTE is the combination of cells, soluble factors and biomaterials for *de novo* cartilage formation, for the purpose of repairing degenerative tissue. One of the key questions which arises when designing a CTE strategy, is that of cell source. For this reason, the use of mesenchymal stem cells for CTE has been under the research spotlight as a genuine alternative to the use of primary chondrocytes. Their ability to be expanded for multiple passages without loss of phenotype [122], their capability for chondrogenic differentiation [123], together with their abundance [124], indicates their advantage to primary chondrocytes for CTE. The potential for BM-MSCs in CTE was demonstrated by their ability to repair chondral defects when implanted into a defect site within a HA hydrogel. When compared with a microfracture technique in which HA without exogenous MSCs were utilized,

patients in the MSC-treatment group exhibited reduced pain and increased joint locomotion [125].

1.2.3. Non bone marrow-derived mesenchymal stem cell types for articular cartilage regeneration

This thesis will focus on the use of BM-MSCs in CTE, however it is important to focus on the potential other cell types for such an application. Whilst the ease of isolation, multipotentcy and self-renewing ability of BM-MSCs [126, 127], denotes them as an appropriate cell choice for cartilage regeneration, other cell types may also be suited for repair of chondral defects. As pertained to, articular chondrocytes, despite their ability to maintain a Collagen Type 2 and GAG-rich ECM [119], are subject to de-differentiation in culture [121, 128]. This inhibits their expansion and the generation of the large cell population required for adequate cartilage regeneration.

A potential source of stem cells which are capable of restoring damaged articular cartilage are those from the periosteum. This tissue forms a vascularized, bone-covering layer and contains a resident population of progenitor cells capable of rapid proliferation, osteogenesis and chondrogenesis [129]. The cartilage regenerative properties of the periosteum have been demonstrated extensively [130]. Following the isolation of periosteal stem cells by Fell, studies have documented the ability of these cells to contribute significantly to the repair of articular cartilage defects when implanted *in vivo* [131] or re-surfacing of the the entire articulating surface [132].

Another potential alterative to BM-MSCs, are mesenchymal stem cells derived from adipose tissue. These cells represent a much more abundant source than that from the bone marrow, with 300-fold more MSCs isolated from 100g of adipose tissue

than the 100ml of bone marrow aspirate [133]. Combined with the ability of adipose-derived MSCs for articular chondrogenesis and cartilage tissue regeneration [134, 135], points to a potentially important reservoir of cells for development of CTE strategies.

1.2.3.1. Bone marrow mesenchymal stem cells

Bone Marrow-derived Mesenchymal Stem Cells (BM-MSCs) residing in the stroma or perivascular region of the bone marrow [136, 137] are Adult Stem Cells (ASCs). ASCs like other stem cell subtypes, are able to self-renew [127] but unlike those types observed at earlier points in development, such as pluripotent embryonic stem cells [138], display a more limited, multipotent potential for differentiation [126]. BM-MSCs were discovered by Friedenstein, who observed colony formation from adherent fibroblast-like cells with the potential for osteogenic differentiation [139]. These were subsequently shown to be capable of differentiation into cartilage, fat, muscle and neural tissue [140].

1.2.3.1.1. Developmental origin

The specification of a mesodermal population occurs as early as the epiblast stage of embryonic development [141] [142]. The mesodermal germ layer is formed during the Epithelial-to-Mesenchymal-Transition (EMT) of the epiblast epithelium as it migrates through the primitive streak, a process known as gastrulation [143]. More specifically, the region towards the posterior side of the primitive streak, forms the

Lateral Plate Mesoderm (LPM) which is located between the extraembryonic and intermediate mesoderm [144]. The mesodermal populations in the LPM undergo a series of EMT and Mesenchymal-to-Epithelial Transitions (MET), one of which divides the LPM into the somatic and Splanchnic LPM epithelial layers [145], with the former generating the mesenchymal-progenitor-containing limb bud [146] and is hypothesized to be the tissue from which resident BM-MSCs are generated. This is suggested due to the similar set of markers expressed in the somatic LPM during limb bud development, and bone marrow mesenchymal stem cells. These markers include alpha-smooth muscle actin [147], Paired Related Homeobox 1 [148] and SRY Box-9 (SOX9) [51].

1.2.3.1.2. Tri-lineage differentiation potential

The predisposition for BM-MSCs to undergo osteogenic, chondrogenic and adipogenic differentiation was shown by Banfi et al. These authors observed an expression of genes conducive for each cell fate decision during their expansion period prior to their induced differentiation [149]. These authors also demonstrated the maintenance of the osteo-chondro differentiation potential throughout the continued passages of BM-MSCs. This culminated in their ability to differentiate following proliferative senescence, which was shown to be reached after 22-25 population doublings following isolation from bone marrow.

Primary BM-MSCs following their isolation, appear to retain a specific epigenetic profile which grants them their tri-lineage differentiation potential. Almeida et al observed the presence of a specific epigenetic profile of BM-MSCs following long-

term culture which was conducive for osteogenic/chondral differentiation. This pre-disposition for cartilage and bone differentiation was greater than that exhibited of Adipose-derived MSCs (AMSCs) [150]. Amongst the osteogenic, chondrogenic and adipogenic lineages, Meyer et al demonstrated an epigenetic prolife of unstimulated BM-MSCs to favour that of osteogenic differentiation [151]. However upon adipogenic induction, these authors demonstrated a clear increase in activating epigenetic marks at the gene loci encoding targets of the master adipogenic transcription factor- Peroxisome Proliferator-Activated Receptor-γ (PPARγ). Herlofsen et al in BM-MSCs, also demonstrated the shift towards a specific pattern of histone marks which delineate activation of a chondrogenic transcriptional profile [152]. The primary nature of BM-MSCs was demonstrated to be key in generating this epigenetic profile conducive for tri-lineage differentiation. Brown et al, demonstrated the increased osteogenic, chondrogenic and adipogenic induction of primary BM-MSCs compared to that of MSC generated from *in vitro* differentiation of embryonic stem cells [153].

1.2.3.1.3. Immunomodulation

The differentiation potential of BM-MSCs therefore presents them as a useful tool for the study of mesenchymal tissue development in addition to a cell source for regenerative strategies for repair of osteochondral tissue. In addition, a unique characteristic of BM-MSCs are their immunomodulatory properties. Puissant et al demonstrated the ability of BM-MSCs to inhibit the activation of lymphocytes, with a reduction in proliferation observed of lymphocytes and Peripheral Blood

Mononucleocytes (PBMCs) [154]. In addition, BM-MSCs have been shown to reduce the activity of both CD4+ and CD8+ T-Cells which were initially activated in response to murine skin engraftment of the MSCs [155].

This immunomodulatory properties of BM-MSCs has implications for regenerative medicine strategies. This was demonstrated for example by Reinders et al who intravenously-delivered autologous BM-MSCs alongside a kidney allograft which was previously subjected to immune-reactivity and rejection by the recipient patient [156]. The delivered BM-MSCs appeared to generate a systemic immunomodulatory milieu which compared to transplantation without BM-MSC treatment, reduced fibrosis and atrophy of the tubular structures in the transplanted kidney. Administration of the BM-MSCs in this study reduced PBMC proliferation and circulating immune-stimulatory cytokine levels such as interferon-γ.

1.2.3.1.4. Isolation and characterisation

In addition to the MSCs, the bone marrow compartment is comprised of multiple cells types including hematopoietic stem cells [157], osteoblasts [158] and lymphocytes [159]. Therefore prior to any study utilising BM-MSCs, including for CTE, it is required to separate these cells from the other contaminating populations. Aside from demonstration of tri-lineage differentiation potential, a primitive selection factor for BM-MSCs is their ability for adherent culture *in vitro*. This separates MSCs from cells of the hematopoietic origin and thus demonstrates a simple method to remove this unwanted cell type [160].

Another major criterion which distinguishes BM-MSCs from other cell types is the expression of specific cell-surface markers. These were originally defined by The International Society for Cellular Therapy (ISCT) [161]. The three markers which are deemed by these guidelines to identify BM-MSCs are Cluster of Differentiation (CD) 105 (CD105)[162], 73 (CD73)[163] and 90 (CD90) [161]. These are involved in transduction of TGF–β signalling during chondrogenesis [162], MSC migration [164] as well as their adhesion to other cells [165] and the surrounding stroma [163]. On their own however or in combination, these markers do not delineate a BM-MSC. Indeed, expression of CD105 and CD73 have been shown to select for both endothelial cells [166] and skin fibroblasts [167]. Fibroblasts have a reduced capacity for colony formation and multi-lineage differentiation compared to MSCs, despite similar morphological characteristics [167]. Therefore, to further separate these stromal stem cells from the hematopoietic compartment of the bone marrow, the absence of expression CD11b or CD14, CD19 or CD79a, CD34, CD45, and Human Leukocyte Antigen-DR, together with the positive expression of CD105, 73 and 90 are required.

Despite the existence of the ISCT guidelines described above, debate exists over the phenotypic markers which distinguish BM-MSCs. For example, CD271 and Mesenchymal Stem Cell Antigen-1 have also been reported to delineate BM-derived cells capable of osteogenesis, chondrogenesis and adipogenesis [168, 169]. Stro-1 was also demonstrated as a marker of BM-MSCs but reports of Erythrocytes also expressing this antigen have prompted the requirement for examining Stro-1 expression in conjunction with other *bona fide* BM-MSC antigens [170]. The ability of MSCs expressing these and other markers for tri-lineage differentiation is suggestive

of a complex set of phenotypic criteria which mark BM-MSCs, beyond that required by ISCT. Cells which are selected based on the ISCT criteria may therefore omit specific subsets of BM-MSCs which are capable of tri-lineage differentiation and represent viable cells for study of mesenchymal development or tissue engineering.

1.2.3.2. Scaffolds for cartilage tissue engineering

A primitive example of CTE is Matrix-Assisted ACI (MACI) in which, akin to ACI, cells are expanded following isolation from the patient. However, unlike ACI, chondrocytes are then seeded onto Collagen Type I/III scaffolds to facilitate proliferation and stabilisation of their phenotype [171]. Despite increasing cartilage regeneration compared to techniques such as microfracture [172], an improvement of clinical success due to MACI was not observed in a direct comparison with ACI [173]. This is also is compounded with MACI also requiring multiple surgical procedures and the time-consuming process of *in vitro* expansion. MACI did however, demonstrate the potential of ECM scaffolds for improving cartilage repair. The use of scaffolds for CTE is demonstrated by the field of mechanotransduction. Research. Mechanotransduction is the mechanism behind cell response to mechanical stimuli in the cell microenvironment. Studies in this field have demonstrated the need for CTE strategies which provide the correct physical cues for tissue repair [174], as described in section 1.4.

1.2.3.2.1. Artificial polymers for cartilage tissue engineering

The choice of scaffold is important due to their ability to dictate cell survival, phenotype and host tissue integration following *in vivo* implantation. Artificial polymers such as Polylactic Acid (PLLA) were utilised in one of the earliest attempts at osteochondral tissue engineering, and was shown to enable survival of implanted rib perichondrial cells into a rabbit defect model, despite promoting formation of fibrous Collagen Type I [175]. Such polymers can be highly customized in terms of attachment of bioactive moieties, are able to be expanded up to production on an industrial scale to meet clinical standards. For example Poly(Vinyl Alcohol)-Polycaprolactone (PVA/CL) nanofiber scaffolds demonstrated great promise when seeded with rabbit-derived mesenchymal stem cells and implanted into a full-thickness defect of a rabbit medial condyle. Repaired tissue showed increased staining for GAGs and Collagen Type II compared to non-treated controls and improved MSC proliferation and differentiation during in vitro, preliminary assays [176].

1.2.3.2.2. Natural scaffolds for cartilage tissue engineering

Natural scaffolds offer a host of advantages compared to artificial polymers. One of these is their increased bioactivity due to the presence of specific sequences within their structure which guides cell growth and tissue formation during development. HA is an example of such a material. It functions as a backbone of articular cartilage ECM, linking Collagen Type II fibrils with proteoglycans and has been shown to be key during limb morphogenesis and formation of the cartilage growth plate. HA synthase is abundantly expressed in the AER of the limb bud [177] and HA is required for cell-

cell adhesion in the pre-cartilage condensation of the limb bud [178]. HA-based scaffolds have demonstrated much promise for CTE with their chondrogenic effect on encapsulated human MSCs have been observed compared to that of inert Polyethelene Glycol (PEG)-based scaffolds [179].

HA was shown to aid the cartilage-forming ability of co-cultured adipose-derived MSCs and human chondrocytes, enhancing GAG synthesis from such cultures whilst inhibiting Collagen Type X production [180]. The translational properties of HA are demonstrated by its use in the clinically-tested product Hyalograft-C which is a combination of autologous chondrocytes and HA-derived matrix. Implantation with Hyalograft-C has been shown to result in a positive outcome for patients with articular cartilage lesions following 3 years post-surgery [181]. Other natural polymers has also shown the potential for their use in CTE. For example, collagen-based hydrogels seeded with human MSCs from the illac crest of donors were shown to enhance chondrogenesis and provide a bias for chondrocyte induction over osteogenesis [182].

1.2.3.3. Supplements for inducing cartilage ECM formation

The continued optimization of BM-MSC chondrogenesis demonstrates the reliance on these cells for CTE strategies. As described below, the role of supplements which stimulate the post-translational processing and secretion of pro-collagen polypeptides have been demonstrated. This is in conjunction with the use of growth factors which induce a transcriptional program within MSCs that is conducive for articular chondrogenesis.

Ascorbic acid is important in the collagen synthesis and maintenance of collagen triple helices. One the initial studies which examined this mechanism behind this phenomenon was that by Murad et al in 1981. These authors built upon previous observation of the increased growth of avian long bones cultured in a Ascorbate-rich medium [183]. Murad et al observed the increase in Collagen biosynthesis in human skin fibroblasts due to Ascorbic acid treatment, with an induction also in the activity of both Lysyl and Prolyl hydroxylases [184]. Corresponding to this, a study by Myllyla et al demonstrated the role of Ascorbic Acid in reducing the oxidized Fe^{3+} ion which is created as a by-product during proline hydroxylation. Following conversion back to the reduced, divalent form of iron (Fe^{2+}), re-activation of the prolyl hydroxylase occurs. This therefore implicates Ascorbate in maintaining hydroxylation of Collagen, thereby maintaining its formation of triple helices and structural integrity of the entire ECM [185]. This role as a potential supplement was shown by studies such as by Temu et al who observed an increase in Collagen Type II protein produced by chondrogenically-induced ATDC5 cells in the presence of Ascorbic Acid [186]. Interestingly, these authors also demonstrated the ability of ascorbate to increase levels of *COL2A1* mRNA and GAG production, indicating the general pro-chondrogenic effect of Ascorbic Acid.

A role for other supplements was also shown in terms of BM-MSC chondrogenesis and cartilage ECM formation. For example, hydroxylated proline residues in Collagen triple helix formation is suggestive of a role for L-Proline in chondrogenic media, to provide the necessary building blocks for Collagen polypeptide biosynthesis [187]. Another major supplement routinely used as an inducer of cartilage formation from BM-MSCs is the steroid, Dexamethasone. Grigoriadis et al demonstrated the dose-

dependent effect on formation of GAG-rich nodules from mouse BM-MSCs [140]. This *in vitro* chondrogenic effect of Dexamethasone was also demonstrated to specifically occur in the presence of TGF-β_1-treated bovine BM-MSCs. In this study, an upregulation of chondrogenic genes was observed, however no such change occurred when Dexamethasone was utilised in conjunction with BMP2 [188].

1.2.3.4. The TGF-β family of growth factors in cartilage tissue engineering

The family TGF-β growth factors are of particular focus due to the role of TGF-$\beta_{1/3}$ and BMP ligands in both cartilage development [189] and regeneration [190]. For example, a TGF-β_1 and BMP-6-supplmented medium was shown to induce a transcriptional program within hBM-MSC pellet cultures that resembles that which occurs during developmental chondrogenesis. This includes specific peaks in the levels of mRNA encoding SOX5, SOX6 and SOX9 and progressive increases in *COL2A1* and *ACAN* expression throughout the chondrogenic differentiating period [191].

Regarding application for CTE, Bian observed an increase in *COL2A1* and *ACAN* expression and increase in GAG production of hBM-MSCs within a HA scaffold loaded with alginate-encapsulated TGF-β_3. This was observed at 4 weeks following subcutaneous implantation of the HA hydrogels, compared to that in which the alginate beads contained no TGF-β_3 [192]. Diao et al. also demonstrated the ability of scaffolds seeded with TGF-β_1-positive plasmids for gene delivery of this growth factor to BM-MSCs [193]. The authors observed an increase in chondrogenesis and cartilage ECM formation upon scaffold-implantation into a rabbit-defect model This was compared to that resulting from implantation of a Green Fluorescent Protein (GFP)-

plasmid-containing scaffold as the control conditions. The cartilage ECM also was observed to remain stable following a 10-week post-operative time period. Pagnotto et al also observed an increase in cartilage regeneration due to ectopic TGF-β_1 expression in human MSCs implanted as pellets within a rat knee defect site. Again, this was compared to hMSCs transduced with GFP Complementary Deoxyribonucleic Acid (cDNA) [194].

The potential of a combinatorial therapy with TGF-β_3 and BMP2 was demonstrated by Tomas et al, who delivered plasmids encoding these two growth factors to BM-MSCs within alginate hydrogels. Following a 28-day *in vitro* differentiating period, a combination of TGF-β_3 and BMP2 compared to treatment of either factor alone, induced formation of ECM which was indicative of articular cartilage [195]. These authors also observed a reduction hypertrophic cartilage and ossified matrix due to the combination therapy.

1.2.4. The risks of chondrocyte hypertrophy in current cartilage tissue engineering strategies

Despite the pro-chondrogenic effect propagated by the TGF-β family of growth factors, their potential to induce chondrocyte hypertrophy in a tissue engineering context has also been demonstrated. For example, TGF-β_3-induced chondrogenesis of BM-MSCs in Poly(ε-Caprolactone) (PE) scaffolds resulted in formation of mineralised tissue consisting of increased calcium content and Alkaline Phosphatase activity [196]. This enzyme is required for mineralisation of tissue following hypertrophy of the growth plate and ossification of the cartilage anlage [197]. This

was also demonstrated by Ichinose et al, who observed the development of a fibroblastic phenotype from BM-MSCs within Alginate capsules, following their chondrogenic induction [198]. This was also accompanied by the presence of Collagen Type X within the ECM.

One mechanism behind these observed cases of hypertrophy may be due to the supraphysiological levels of TGF-β growth factors present in standard chondro-induction protocols. Overexpression of TGF-β_1 in the murine knee results in progression of OA and joint fibrosis, implicating its potential danger in CTE [199]. Gene therapy with DNA encoding BMP-2 or ectopic treatment of the BMP-2 ligand, despite increasing GAGs and Collagen Type II during hBM-MSC chondrogenesis, also produced extensive staining for Collagen Type X and ALP activity [200] [201]. This suggests the hypertrophy of these cultures which is unsuitable due to the contrasting mechanical properties of articular and hypertrophic [202].

The inappropriate hypertrophy and ossification due to such growth factors could perhaps be predicted due to the specific temporal and spatial pattern of their expression and activity during native cartilage development in which hypertrophy is tightly regulated. The TGF-β_1 receptor, ALK5 and BMP receptors ALK3 and ALK6 have been shown to be differentially expressed during embryogenesis with their mRNA levels at a peak during pre-cartilage mesenchymal condensation [203]. This corresponds to experiments in which a severe phenotype was observed due to knockout of the TGF-$\beta_{1/3}$ receptor in pre-cartilage mesenchymal condensations [204]. This contrasts with the milder phenotype observed due to knockdown of these receptors at the onset of chondrogenesis [205]. Evidence also exists for the increased

expression of TGF-β_1 and TGF-β_3 in proliferative and hypertrophic chondrocytes compared to resting, articular chondrocytes [206, 207]. This is suggestive of a temporal role of these growth factors during the transition of immature growth plate chondrocytes into either chondrocytes which contribute to endochondral ossification or articular cartilage, the latter of which being the preferred final product for CTE strategies.

The potential for TGF-β to potently induce a chondrogenic differentiation program but also cause hypertrophy of implanted cartilage grafts, suggests a requirement for additional factors which suppress the negative effect of TGF-β supplements. As described below, one developmental cue which is integral in articular cartilage morphogenesis, is that of hypoxia and its downstream signalling pathways.

1.3. Hypoxia in cell biology – a result of vertebrate evolution

Oxygen (O_2) is integral in biological systems due to its role as an electron vehicle in the final stages of oxidative phosphorylation which is required for ATP)synthesis. Hypoxia, which is defined as the diminished availability of oxygen relative to atmospheric conditions, arose as a result of higher-order metazoan evolution. Oxygen was introduced into our atmosphere approximately 2.5 billion years ago. Accordingly, lesser-evolved species of the metazoan kingdom are able to absorb atmospheric oxygen to such an extent as to supplement all cells in the organism. This includes the *Caenorhabditis elegans* in which oxygen is able to freely diffuse into all cells [208] and in *Drosophila melanogaster* in which the simple gas-perfusion mechanisms enable full-body oxygenation [209]. However, during the evolution of

complex, multi-organ vertebrates in which larger diffusion distances for gases exist, abundant oxygen availability is restricted to certain tissues. Accordingly, the evolution of complex transport systems brought about the introduction of oxygen to organs which would normally be devoid of such a molecule [210].

Despite the mechanisms which serve to increase supply of oxygen to tissues which are not easily perfused by O_2, sub-par levels relative to that of atmospheric conditions are still experienced by multiple organs [211]. This is due to a lack of vasculature in these tissues. This avascularity arises due to specific developmental programs which dictate patterning and regression of the vasculature following early embryogenesis [11]. For example, Iwagaki et al observed a regression of cochlear blood vessels at the onset of development [212]. Accordingly, such tissues have adapted to develop and maintain themselves in hypoxic conditions.

1.3.1. The functions of hypoxia

Hypoxia stimulates signal transduction pathways which result in upregulation of protein such as Erythropoietin and Vascular Endothelial Growth Factor (VEGF) [213, 214]. These are integral for erythropoiesis and angiogenesis respectively and together, increased neovascularization and blood flow to ischemic tissues. Genes upregulated also include those involved in glycolysis, enabling sufficient ATP production in anaerobic conditions [215], as well as those which increase efficiency of electron transfer during oxidative phosphorylation [216].

In addition to enabling metabolic adaptation, hypoxia has a role in tissue development, stimulating proliferation and cell fate changes to enable the correct architecture and function of the tissue. For example, at 8-10 weeks of human gestation, extravillous trophoblasts are thought to exist in a hypoxic environment due to the occlusion of maternal blood [217]. This is thought to promote their differentiation as they are invade the endometrium [218]. The proliferation of villous trophoblasts is also thought to be induced by hypoxia, enabling formation of a population of Syncytiotrophoblasts which is essential for nutrient circulation between the mother and placenta. In heart development, the switch from single to double circulation is in part mediated by hypoxia. The apoptosis of a specific population of cardiomyocytes in the embryonic outflow track is mediated by hypoxic signalling, and this is a pre-requisite for the remodeling-induced switch in circulation [219].

The role of hypoxic signalling in enabling an adaptive response to low-oxygen conditions is also essential in tumour progression. As cancer cells proliferate uncontrollably, they create a mass or tumour that is devoid of vasculature. This creates a subsequent hypoxic microenvironment [220] which in turn upregulates high rates of ATP production via glycolysis, a phenomenon known as the Warburg Effect [221]. There is also an upregulation of angiogenic factors such as VEGFA. This results in formation of a vascular bed within the malignant growth which enables the continued malignancy of the tumor [222].

1.3.2. Hypoxia Inducible Factor – the transducer of hypoxia-mediated transcription

The Hypoxia Inducible Factor [223] complex transduces physiological hypoxia into gene transcriptional changes. This was first discovered by Semenza et al, who observed the increase in expression of erythropoietin by a protein, the levels of which were increased in hypoxic conditions [213]. HIF is a transcriptional complex, principally composed of an alpha subunit, either HIF-1α/HIF-2α and the HIF-1β subunit [224]. Other co-binding partners required for its transcription, include CREB-Binding Protein/p300 (CBP/p300) [225] and the metabolic enzyme Pyruvate Kinase (PKM) 2 [226]. Both HIF-1/2α and HIF-1β contain DNA-binding domains, which recognise a specific sequence of bases in the promoter regions of target genes [227]. This consensus sequence is known as the HIF-Response Elements (HRE) and is also represented in reverse by the HIF Ancillary Sequence (HAS)[213, 228]. When the HREs/HASs are bound by HIF-1/2-HIF-1β dimer, transcription of the corresponding genomic coding to which the promoter belongs, is induced. This induction of transcription occurs via the N- and C-terminal transactivation domains (N-TAD and C-TAD) of HIF-1α [229].

The spatial distribution of HIF-1α and HIF-2α vary, with HIF-1α expressed ubiquitously and HIF-2α expressed in specific tissues such as endothelial cells and lungs during development [230]. There exists a large number of transcriptional targets of the HIF complex, with each HIF-1/2α-containing HIF complexes inducing transcription of a differing subset of genes. HIF-1α induces transcription of genes involved in angiogenesis [213, 214], metabolism [215], cell survival [231], migration [232] and proliferation [233]. HIF-2α, whilst also upregulating pro-angiogenic *VEGFA*

as HIF-1, does not induce glycolytic enzyme synthesis [234]. A third alpha subunit-HIF-3α does not contain a C-TAD, and as such induces transcription to a weaker extent relative to that mediated by HIF-1/2α [235] [236]. Another implicated role of HIF-3α is that of a negative-regulator of HIF-1α, via competition with HIF-1β and inhibition of a functional HIF complex.

1.3.3. Regulation of Hypoxia Inducible Factor-1/2α

1.3.3.1. Protein stability

The rate of HIF-mediated transcription is dependent on the stability of HIF-1/2α and not that of HIF-1β. This is due to the susceptibility of HIF-1/2α to hydroxylation, ubiquitination and degradation by the Prolyl Hydroxylase 2 (PHD2)-Von Hippel–Lindau Tumor Suppressor (VHL) pathway, whilst HIF-1β is constitutively present [237] (**Figure 1.2**). PHD2, a proline-hydroxylating enzyme, requires oxygen, ascorbic acid, Fe^{2+} and 2-Oxoglutarate (2-OG) as substrates for its function [238]. At normoxia in which local oxygen molecules are in abundance, PHD2 is activated and it hydroxylates specific residues (Proline402/564) on the oxygen-dependent degradation domain (ODDD) of HIF-1α [239]. The newly formed hydroxylated residues of HIF1α then serve as recognition motifs by VHL which is part of an E3 ubiquitin ligase complex [240]. VHL binds and causes the ubiquitination of the hydroxylated proline residues of HIF-1α [241], resulting in the subsequent proteasomal degradation of this alpha subunit [242].

In hypoxic conditions, the lack of oxygen available for PHD2 activity results in the downregulation of its HIF-1α-hydroxylating ability, thereby enabling HIF-1α cytosolic accumulation, nuclear translocation and expression of its target genes in the HIF heterodimeric complex. Interestingly, expression of the gene encoding PHD2- *EGLN*, is induced by excessive HIF-1α stabilization. This results in a negative feedback loop to prevent hyper-activation of HIF-mediated transcription [243]. Other pathways central to regulating HIF-1α degradation are The Receptor for Activated C Kinase 1 (RACK1) and Heat Shock Protein90 (HSP90) as demonstrated by Liu et al. RACK1 has been demonstrated to compete with HSP90 in binding to HIF-1α and in doing so, recruits the identical ubiquitinating complex utilised by VHL, thereby resulting in HIF-1α degradation [244]. Conversely, HSP90 functions by binding HIF-1α and blocking RACK1-HIF-1α binding and degradation [245]. RACK1-dependant degradation of HIF-1α is independent of PHD2 function. Liu et al therefore suggest the role of HSP90 and RACK1 and their relative binding affinities for HIF-1α, are to determine the basal, steady state levels of HIF function in different cell types [244]. Calcium signalling has also been shown play a role in the regulation of HIF-1α stability. Liu et al identified the ability of Calcineurin to abolish RACK1-mediated ubiquitination and proteasomal degradation of HIF-1α [246]. Calcineurin is stimulated by increased intracellular Ca^{2+} and calmodulin activity [246].

1.3.3.2. Co-factor binding

Essential for the conformational changes in the HIF-1α-HIF-1β dimer [247] which are required for the induction of gene expression when bound to the HRE in target gene

promoters, is the recruitment of p300/CBP (**Figure 1.2**). Structural crystallography studies of HIF-1α binding to these co-factors have revealed the necessity of this interaction for activation of the CTAD of HIF-1α [247]. This process is required to act synergistically with activity of the NTAD to stimulate HIF-target gene expression, due to the relatively weak ability of NTAD alone in stimulating transcription.

One of the key residues involved in the binding between HIF-1α and p300/CBP is Asparagine-803 (Asn-803) of HIF-1α. This amino acid is a target of another hydroxylase enzyme, Factor Inhibiting HIF (FIH) which regulates HIF transcriptional activity independent of the protein stability of HIF-1/2α [248]. FIH-meidated hydroxylation of Asn-803 of HIF-1α inhibits the binding of p300/CBP to HIF-1α and therefore disrupts formation of the HIF-transcriptional complex [247]. As with PHD2, FIH utilizes oxygen, ascorbic acid, Fe^{2+} and 2-OG [249]. Correspondingly, FIH is inhibited by a lack of local oxygen, thereby enabling CBP/p300 binding to HIF-1α in hypoxic conditions.

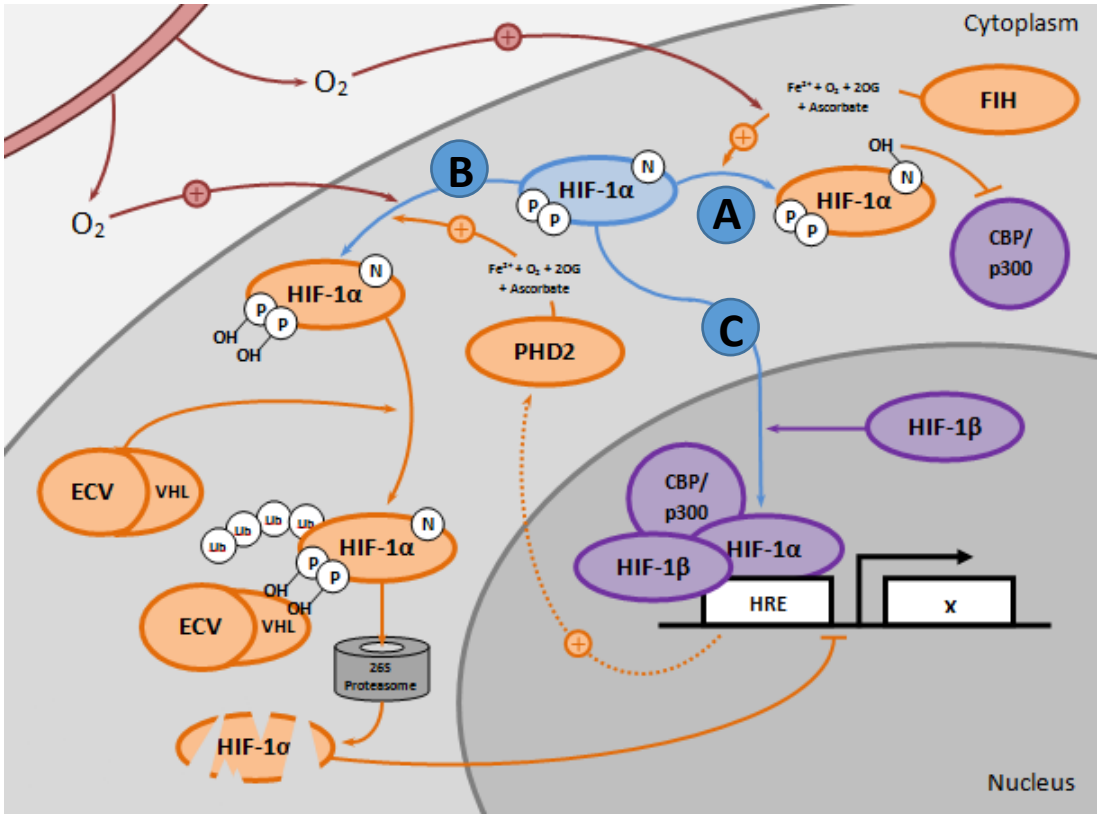

Figure 1.2. Regulation of HIF-mediated transcription by HIF-1α stability and co-factor binding. In response to molecular oxygen from local vasculature for example, FIH and PHD2 each hydroxylate a specific amino acid residue of HIF-1α. **A:** FIH-mediated hydroxylation results in the blocking of the co-factors, CBP/p300 from binding to HIF-1α, thereby reducing HIF transcriptional activity. **B:** PHD2-mediated hydroxylation results in ubiquitination of the ODDD domain of HIF-1α by the VHL component of an E3 ubiquitin ligase, thus promoting the proteasomal degradation of HIF-1α and significantly reducing HIF transcriptional activity. **C:** In hypoxic conditions, PHD2 and FIH remain inactivate, thus enabling HIF-1α to translocate and accumulate in the nucleus, where it activates expression of HIF target genes as part of a transcriptional complex with HIF-1β, CBP/p300 and other co-factors. A negative feedback mechanism exists in which PHD2 expression is also enhanced by HIF activity.

1.3.3.3. Translation

Control of proteasomal degradation and transcriptional co-factor binding, represent the major mechanisms of HIF-1α regulation. However, regulation of HIF-1α protein translation also contributes to the overall rate of HIF-mediated transcription. Growth factor signalling has been heavily implicated in HIF-1α translation both in normoxic and hypoxic conditions. Phosphatidylinositol 3-kinase-protein kinase B (PKB) and mammalian target of rapamycin (mTOR) have together, been shown to stimulate HIF-1α translation and HIF-mediated gene expression [250]. mTOR-mediated translation of HIF-1α is thought to occur through phosphorylation of S6 kinase and 4E-BP1 which results in cap-dependent initiation of translation. Calcium signalling has also been implicated in enhancing HIF-1α translation. Inceased intracellular Ca^{2+} levels result in upregulation of Protein Kinase C, which causes a subsequent induction of mTOR activity and HIF-1α translation [251].

1.3.3.4. Transcription

The contribution of *HIF1A* mRNA to overall HIF-1α levels and HIF-mediated transcription appears to dependant on the cell and tissue type in which it is expressed. For example in Hep3B hepatoma cells, no changes in *HIF1A* mRNA was observed due to hypoxic incubation, despite increases observed in HIF-1α binding of the *VEGFA* promoter [252]. Similar, post-transcriptional regulation of HIF-1α was also observed in lung epithelial cells [253]. These studies are suggestive of the redundancy of *HIF1A* transcription in activity levels of the HIF transcriptional complex, but are

contrasted with that observed by Page et al. These authors demonstrated an increase in mRNA encoding HIF-1α in Vascular Smooth Muscle Cells, not in response to culture at 1%O_2, but by treatment of vasodilative proteins Angiogenin II and Thrombin [254]. *HIF1A* transcription was subsequently shown to occur via Protein Kinase C and PI3K-mediated mechanisms. This demonstrates the HIF-inductive mechanisms required in response to an ischemic microenvironment which increase angiogenic factor expression and tissue blood perfusion [252].

Despite this evidence of hypoxia-independent upregulation of *HIF1A* mRNA, cells incubated at low oxygen levels were shown to induce *HIF1A* expression by Turcotte et al in Renal Cell Carcinoma cells. This was mediated by RhoA-dependent mechanisms [255]. Hypoxia-mediated transcription of *HIF1A* was also demonstrated by BelAida et al who demonstrated an increase in *HIF1A* mRNA due PI3K/PKB-dependent mechanisms in response to hypoxic incubation. A dependence of *HIF1A* transcription was also observed on the activity of the transcription factor; Nuclear Factor kappa-Light-Chain-Enhancer of Activated B cells (NF-κB). Together, these studies demonstrate that transcriptional control of HIF-1α is unlike PHD2/VHL-mediated control of HIF-1α stability which is a conserved mechanism. Instead, the contribution of *HIF1A* mRNA to hypoxia-induced HIF activity is highly context dependent.

In the context of articular cartilage, hypoxia upregulates *HIF1A* mRNA levels during chondrogenesis of cartilage endplate cells [256]. Adult articular chondrocytes have been shown to upregulate *HIF1A* mRNA in response to inflammatory/OA-inducing stimuli without exposure to hypoxic conditions [257]. This again suggests that

hypoxia-induced HIF activity via *HIF1A* transcription is not a conserved mechanism across different tissue types and developmental stages.

1.3.4. The role of hypoxia in osteochondral development

Specific morphogen gradients such as that of Wnt and BMP ligands, exist across developing and adult osteochondral tissue and are essential in the formation and maintenance of distinct regions of cartilage and bone [258]. Another such gradient between vascularised subchondral bone and avascular cartilage, is that of oxygen [259]. This gradient which also exists in the mesenchymal condensations of the limb bud, has been shown to play key roles in the formation and maintenance of the distinct regions of osteochondral tissue.

The oxygen concentrations in adult human articular cartilage are reported to be between 1-6% with that of subchndral bone reaching up to 21% [260]. and as described by Maes et al, the early limb bud and cartilage growth plate are also subject to a hypoxic microenvironment. This is due to the regression of embryonic vasculature [261]. This has been shown in studies by Schipani and Provot who also demonstrated the requirement of HIF-1α-mediated hypoxic signalling for chondrogenesis of the limb bud mesenchymal population, cartilage ECM formation and subsequent survival of the chondrocyte population within the growth plate [259, 262].

The studies by Schipani and Provot are suggestive of an essential role for HIF in mediating a pro-chondrogenic and anti-hypertrophic transcriptome when activated

at low oxygen levels [263]. This effect is reversed in regions of higher O_2 concentration due to downregulation HIF activity, which would result in a bias towards a hypertrophic/osteoblastic cell fate of mesenchymal precursors (**Figure 1.3**).

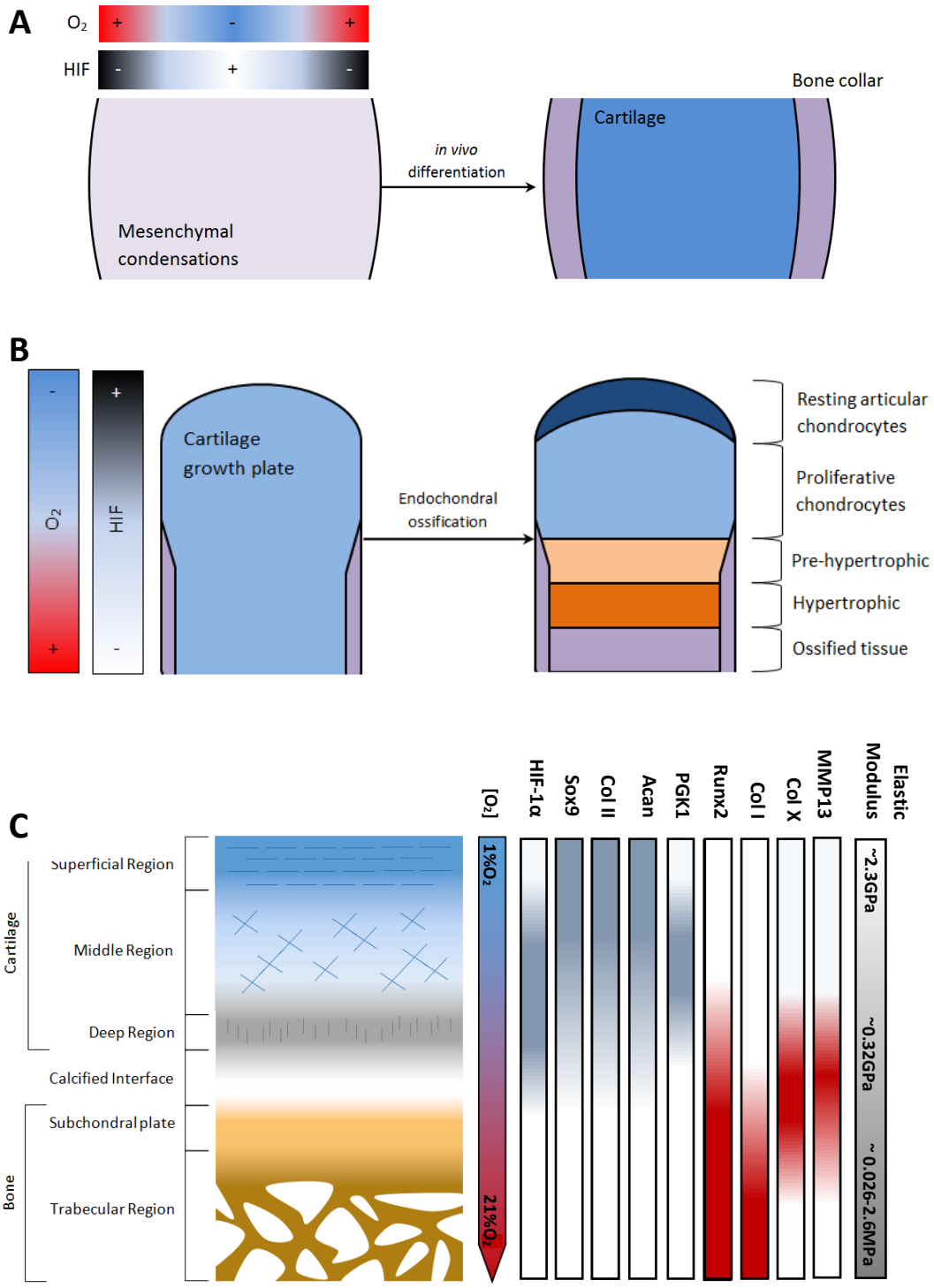

Figure 1.3. The oxygen and HIF gradients present across development and adult osteochondral tissue. Diagrammatic representation of oxygen and result HIF activity gradients present across the mesenchymal limb bud (A) and growth plate (B) stages of limb development. C: Oxygen resulting HIF-1α protein gradients across adult osteochondral tissue with Blue gradients = Proteins upregulated by HIF, Red gradients = proteins downregulated in presence of HIF activity.

1.3.5. The role of hypoxia in osteochondral tissue engineering

Previous efforts of osteochondral tissue engineering (OCTE) via development of two independent bone and cartilage grafts before their attachment by suture or fibrin glue (**Fig. 1.4A**)[264], have been shown to fail due to shearing of the graft by mechanical movement of the joint [265]. Therefore for treatment of such cases, it is advantageous to achieve synchronous regeneration of both the bone and cartilage on the same continuous biomaterial scaffold (**Fig. 1.4B**).

An advantage of osteochondral regeneration within a continuous scaffold is the mimicry of synchronous *in vivo* development of native articular cartilage and subchondral bone. Following formation of the growth plate from the limb bud mesenchymal condensations, the fate of the highly proliferative chondrocytes is that of either hypertrophy or senescence. These two paths which contribute to formation of ossified bone and articular cartilage respectively, occur simultaneously with the fate of growth plate chondrocytes subject to influence by gradients of signals such that of Indian Hedgehog or HIF [91, 266]. This synchronous development of articular cartilage and subchondral is required for the communication of forces between the chondral and bone layers which are applied on the joint during movement.

A case-study in which such a strategy was employed for osteochondral regeneration was conducted by Mohan et al. Within a single biomaterial scaffold, these authors created two opposing gradients of chondrogenic and osteogenic factors respectively which were incorporated within PLGA microspheres [267]. The region of the scaffold that was abundant in the pro-chondrogenic signal (TGF-β_3) with the opposing area rich in osteogenic signals (BMP2 and hydroxyapatite crystals), induced region-specific

formation of cartilage and bone. As identified by Magnetic Resonance Imaging and histological analysis, these scaffolds when implanted into a rabbit osteochondral defect model also resulted in regeneration of distinct cartilage and bone phases *in vivo*.

Aricular cartilage and subchondral bone require differing levels of oxygen for their development and maintenance [259], as decribed in **figure 1.3.** Together with the the pro-chondrogenic and anti-hypertrophic/osteogenic effects of HIF, this suggests the potential HIF for OCTE in which a continuous biomaterial scaffold is utilised. Controlling the spatial organisation of physiological hypoxia however, may be logistically impossible. Therefore it may be advantageous to spatially control chemical agents which stimulate the HIF pathway as an alternative [268].

Agents which act to stabilise the HIF-1α subunit of the HIF transcriptional complex, would therefore enable spatial control of HIF-mediated transcription when themselves deposited in a graded manner on a biomaterial scaffold with seeded cells. It could be envisaged that within a region of graded scaffold that is rich in a HIF-stimulating compound, chondrogenesis would represent the preferred lineage commitment of the scaffold-seeded hBM-MSCs (**Fig. 1.4C**). This would be accompanied by a suppression of with osteoblast differentiation and hypertrophy. This would contrast to regions of the scaffold which are depleted for the HIF-stimulating compound and in which HIF activity is relatively lower. In such a region, there may be a bias for osteoblastic differentiation of the hBM-MSCs when cultured in an osteogenic-chondrogenic co-induction media. This would be due to the lack of osteogenic/hypertrophic-inhibitory signals provided by HIF-mediated transcription

but also due to the bias of BM-MSCs for osteogenesis relative to that for other lineages [151].

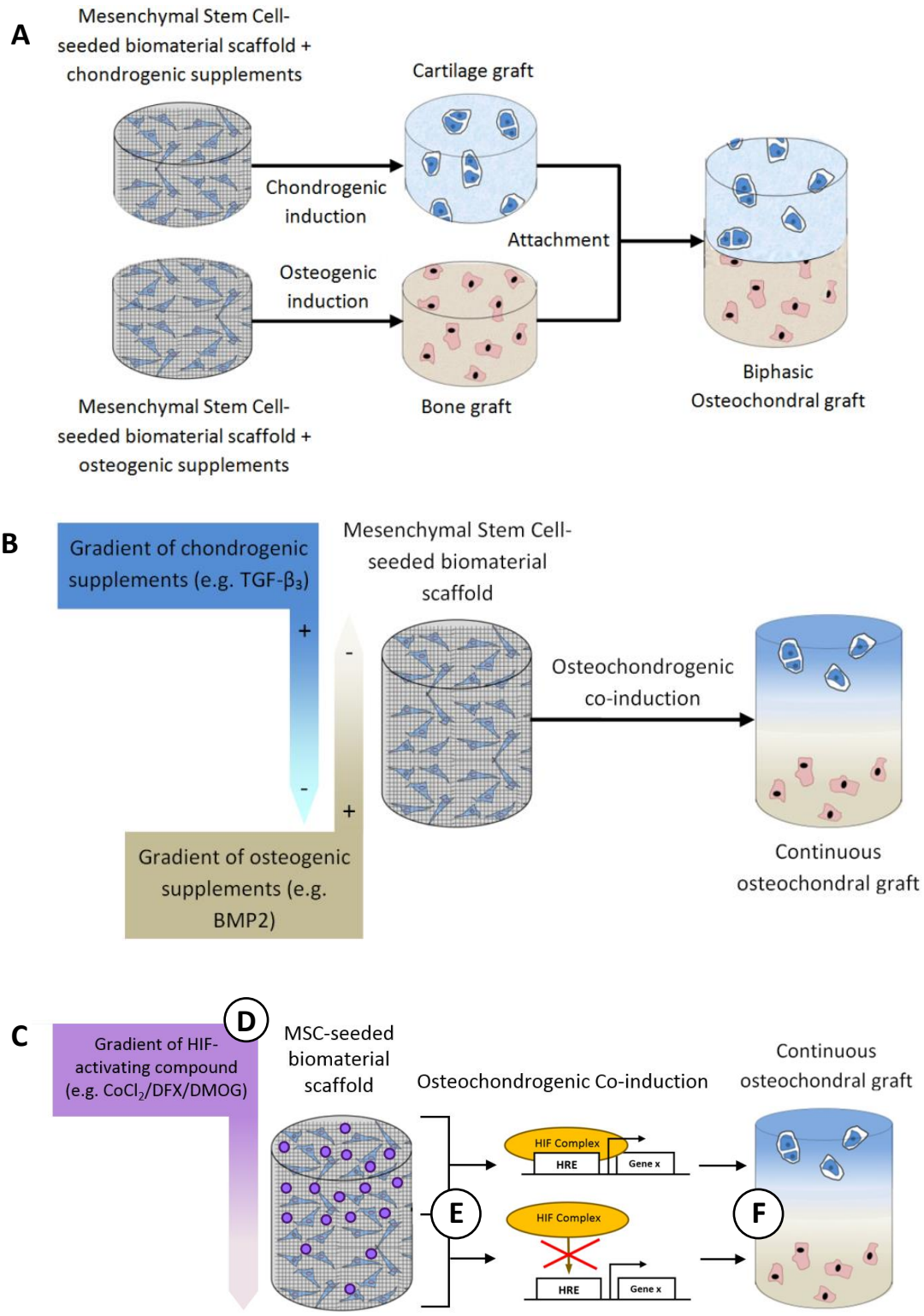
A
Mesenchymal Stem Cell-seeded biomaterial scaffold + chondrogenic supplements
Cartilage graft
Chondrogenic induction
Attachment
Osteogenic induction
Biphasic Osteochondral graft
Mesenchymal Stem Cell-seeded biomaterial scaffold + osteogenic supplements
Bone graft
B
Gradient of chondrogenic supplements (e.g. TGF-β3)
Mesenchymal Stem Cell-seeded biomaterial scaffold
Osteochondrogenic co-induction
Continuous osteochondral graft
Gradient of osteogenic supplements (e.g. BMP2)
C
D
Gradient of HIF-activating compound (e.g. CoCl2/DFX/DMOG)
MSC-seeded biomaterial scaffold
Osteochondrogenic Co-induction
Continuous osteochondral graft
HIF Complex
HRE
Gene x
E
F

(*61) Figure 1.4. Biphasic, Continuous and HIF-graded Scaffolds. A: Biphasic osteochondral graft, generated via attachment of pre-differentiated cartilage and bone tissue engineered grafts **B:** Continuous scaffolds, enabling synchronous development of cartilage and bone regions from one biomaterial and one cell population with a gradual transition from one phase to another, synthesised via incorporation of a graded microenvironment on the scaffold. **C:** HIF-graded scaffold. **D:** MSC-seeded biomaterial scaffold containing a gradient of a HIF-stabilising agent. **E:** During osteochondrogenic co-induction of the scaffold-seeded MSCs, the differential levels of the HIF-activating agent across the scaffold may promote the pro-chondrogenic, anti-hypertrophic and anti-osteoblastic function of HIF in the region of high concentration, whereas this would not occur in the region of low concentration. **F:** The potential continuous osteochondral graft generated using the HIF-regulating scaffold, containing spatially restricted regions of articular cartilage and subchondral bone.

1.3.6. The role of hypoxia and HIF-1α in articular cartilage development and maintenance.

1.3.6.1. Mesenchymal progenitor differentiation

In 2007, Provot et al highlighted the role of HIF-1α in promoting the activity of SOX9, the master chondrogenic transcription factor, in mesenchymal precursors of the limb bud condensations which give rise to the growth plate [262] (**Figure 1.5**). This group showed that upon conditional knockout (CKO) of HIF-1α, expression of the SOX9 target; *COL2A1*, was reduced. HIF-1α CKO also resulted in a disorganised morphology of the resulting cartilage ECM. Concurrent with this study, Amarilio et al demonstrated the role of HIF-1α in stimulating SOX9 expression in pre-chondrogenic precursors during mouse limb development. These authors observed the reduced expression of *SOX9* and its downstream targets *COL2A1* and *ACAN* upon HIF-1α CKO (**Figure 1.5**). They also observed a decrease in mRNA encoding *SOX6* [263].

From an *in vitro* perspective, HIF has been shown to upregulate *SOX9* mRNA and the downstream chondrogenic targets of SOX9 in a BM-MSC line. Following induction of chondrogenesis, reduced SOX9-linked luciferase activity was observed upon deletion of HREs from the SOX9 promoter. This was relative to cells in which the HREs were left intact [269]. Moreover, in rat MSCs, Kanichai et al demonstrated the upregulation of HIF-1α due to hypoxia. This effect was mediated by PKB and p38 mitogen-activated protein kinase resulting in expression of chondrogenic factors [270]. Further cementing the role of HIF in chondrogenesis, adenovirally-delivered HIF-1α was shown to potentiate BMP2-induced chondrogenic induction of MSCs [271]. The role

of HIF-1α in chondrogenesis of BM-MSCs within alginate beads was also observed. This was demonstrated by a lack of *SOX9*, *SOX5*, *SOX6*, *ACAN* and *COL2A1* mRNA upregulation in differentiating conditions in response to treatment of cells with a double-negative HIF-1α vector, compared to the transcriptional profile observed in wild type cells [272].

The interplay between HIF-1α and chondrogenesis is also indicated by observation of HIF-1α upregulation during growth factor-mediated cartilage regeneration at normoxia. In this study, Gelse et al utilised a porcine chondral defect model implanted with autologous porcine BM-MSCs. Following implantation, they observed an increase in HIF-1α in host chondrocytes within the deep zone of the repaired cartilage. This was compared to that within host chondrocytes following implantation of the MSCs without BMP2/insulin growth factor stimulation. These authors also demonstrated the role of *in vitro* periosteal cells to upregulate HIF-1α protein in response to BMP2 and Insulin Growth Factor 1 treatment [275]. Correspondingly, McMahon et al also observed a similar effect of the TGF-β family of transcription factors. In human hepatoma cells, an upregulation of HIF-1α protein and HIF-mediated transcription was observed in response to TGF-β_1 treatment [273].

1.3.6.2. Secretion of cartilage extra-cellular matrix

The specific composition and architecture of the ECM surrounding articular chondrocytes, gives hyaline cartilage its ability to resist compressive forces and tension on the joint. It also enable lubrications between opposing articulating surfaces [3]. Hypoxia has been shown to enhance GAG's and Collagen Type II

synthesis by cultured Human Articular Chondrocytes (HACs), relative to that seen at normoxic conditions [270]. Additionally, reduced oxygen concentration have been shown induce a more ordered morphology of collagen fibrils which is representative of that observed in native articular cartilage. This was observed in chondrocyte pellets cultured at 5%O_2 compared to that at normoxia [274]. Hypoxia has also been shown to have a beneficial effect with regards to ECM production by chondrocytes embedded in biomaterial scaffolds. Coyle et al observed an increase of a GAG and Collagen Type II-rich ECM due to culture of bovine articular chondrocytes at 2%O2, following embedding of the chondrocytes in alginate capsules [275]. A similar pattern of ECM formation was also induced by hypoxic incubation of hypertrophic chondrocytes within a Poly(Lactic-co-Glycolic Acid) (PLGA) scaffold [276].

HIF-1α has been implicated in this hypoxic-induction of cartilage ECM production. Conditional knockdown of HIF-1α in developing murine limbs result in abnormal ECM morphology. Growth plate chondrocytes isolated from HIF-1α-CKO mice also exhibit reduced cartilage proteoglycan and collagen type II production compared to mice in which in which *HIF1A* was left intact [262, 277]. Chemical induction of HIF-1α was shown to also significantly raise Collagen Type II protein levels secreted by HAC's [278] as well as that of Aggrecan, and this effect was abolished in HACs in which HIF-1α was knocked down [279].

In addition to the effect in chondrocytes, HIF has also been shown to increase cartilage ECM in the cultures of various MSC types when induced towards a chondrogenic lineage [270, 272] (**Figure 1.5**). One of the main mechanisms by which HIF increases cartilage ECM production is via enhancement of SOX9 activity and

subsequent *COL2A1* and *ACAN* mRNA [262, 272]. HIF has also been proposed to play a role in the post-translational modification of pro-collagen type II chains which as previously described, is required for stabilisation and function of Collagen Type II within the cartilage ECM. This occurs via upregulation of mRNA encoding Collagen Prolyl Hydroxylase (CP4HA1) which is required for the addition of 4-hydroxyproline residues to single collagen fibrils to enable formation of collagen triple helices [280]. Additionally, HIF induces expression of Lysyl Oxidase (LOX) which is an enzyme whose activity is required for the crosslinking of collagen triple helices. Makris et al observed an increase in expression of *LOX* in response to 2%O_2 culture of bovine articular cartilage explants [285]. They went on to demonstrate the effect of hypoxia in increasing formation of pyridinoline cross-links between collagen fibres, together with an increase in the mechanical stiffness of the explant. These increases were reduced by treatment of the explants with the LOX inhibitor- beta-aminopropionitrile. Together, the findings by Makris et al suggest a role for hypoxia in maintaining a stable articular cartilage ECM via collagen post-translational modification. This crosslinking is required to maintain the overall ECM tensile and compressive strength in response to forces experienced by the joint during locomotion [281].

1.3.6.3. Inhibition of chondrocyte hypertrophy

Signalling gradients such as that of Ihh exist to retain populations of chondrocytes in their non-hypertrophic form, priming them for a permanent, articular chondrocyte cell fate [258]. The oxygen gradient in osteochondral tissue has also been proposed

to limit chondrocyte hypertrophy, with HIF playing a key role in this process (**Figure 1.5**). HIF subunits have been shown to be expressed in human adult chondrocytes [282] and Lafont et al also showed the role of these in maintaining SOX9 expression in articular chondrocytes. This was subsequently shown to be crucial for expression of the downstream transcriptional targets of SOX9 which are required for stabilization of the articular chondrocyte phenotype [283]. This role of HIF was also shown to occur via SOX9-independent pathways [284]. HIF has been shown to downregulate the expression of hypertrophic fibroblast-like markers such as collagen type X, and cartilage degrading enzymes in hypertrophic chondrocytes [279]. In addition to inhibiting hypertrophic factors, hypoxia has also been shown to upregulate chondro-protective proteins such as MMP inhibitors [285] and other anti-catabolic factors [286]. This is also supported by the observation that HIF-1α CKO in developing murine cartilage reduces mRNA expression of articular chondrocyte-specific markers such as Growth Differentiation Factor 5 [263].

The ability of hypoxia to promote an articular chondrocyte phenotype is mediated via a multitude of signalling pathways. Following chondrogenesis of the growth plate, canonical Wnt signalling has been shown to be conducive for chondrocyte hypertrophy in preparation for endochondral ossification [100]. Hypoxia has been correspondingly shown to increase expression of Wnt antagonists during BM-MSC chondrogenesis. This has the downstream effect of increasing expression of articular chondrocyte markers and downregulating mRNA encoding hypertrophic markers. [287]. The Wnt-inhibitory role of hypoxia also functions through HIF-1α which binds and sequesters β-Catenin. This inhibits the primary function of β-Catenin which is the

induction of TCF-LEF target genes such as which are conducive for hypertrophy, such as *MMP13* [288].

HIF is also important in promoting a bias for chondrogenic over osteoblastic differentiation of mesenchymal precursors, a cell fate decision which generates the growth plate or intramembranous bones respectively. The hypoxia-responsive transcription factor via HIF-1α-stabilising compounds [271] or constituitive HIF-1α activation [289] has been shown *in vitro* to downregulate factors involved in osteogenic differentiation and maturation (**Figure 1.5**). This includes RUNX2, Alkaline Phosphatase [290] and Wnt signalling [291] and as such, generate a bias for chondrogenic differentiation over osteoblast formation, and formation of cartilage-specific ECM as opposed to mineral bone matrix.

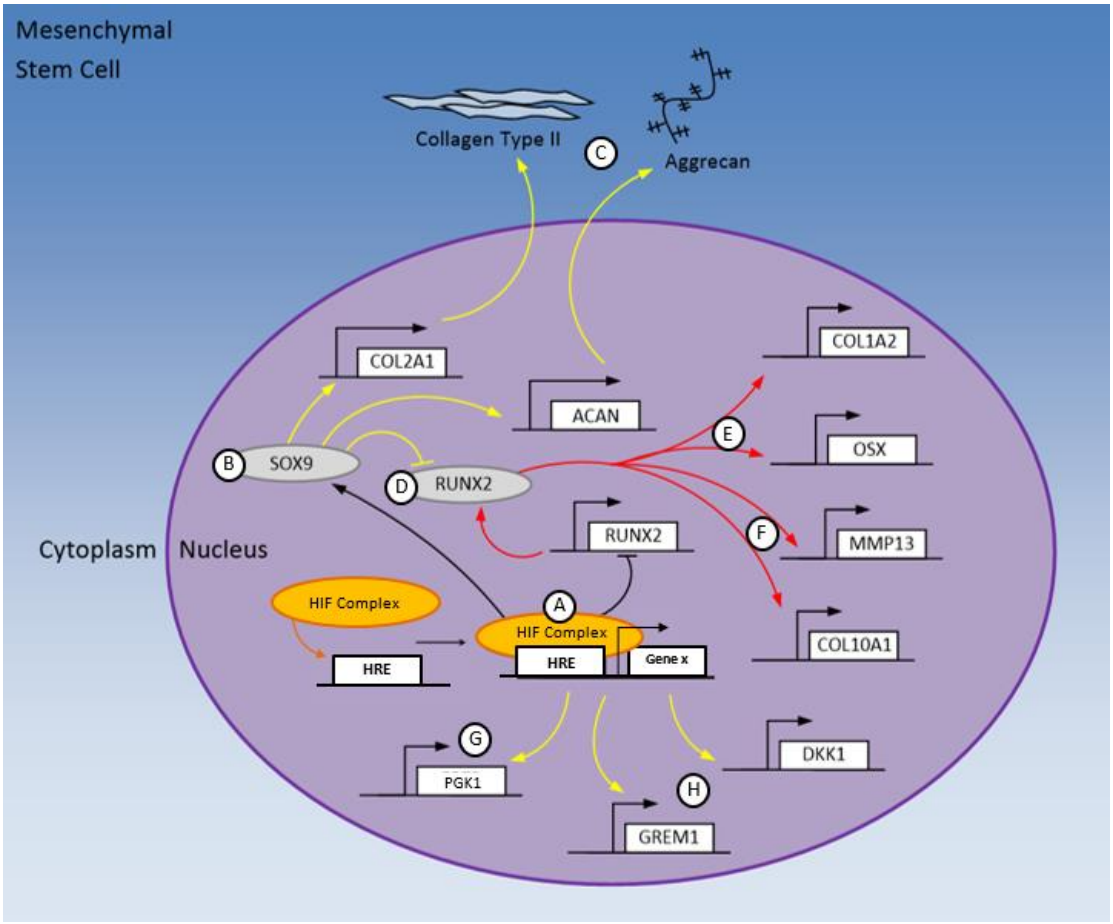

Figure 1.5. Induction of a transcriptional profile by HIF which favours formation of articular cartilage from mesenchymal precursors. A: Following hypoxia-mediated formation of the HIF complex and binding to the HRE of target genes, induction of transcription occurs. **B+C:** Upregulation of *SOX9* transcription (**B**) and subsequent upregulation of SOX9 target gene, *COL2A1* and *ACAN* which results in an increase in secretion of Aggrecan-containing proteglycans and pro-Collagen Type II by the differentiating cell (**C**). **D-F:** SOX9-mediated downregulation of RUNX2 activity and HIF-mediated reduction of *RUNX2* transcription (**D**) together resulting in decrease in transcription of genes encoding osteoblastic (**E**) and hypertrophic factors (**F**). **H:** HIF-mediated transcription of genes which encode anti-hypertorphic factors such as GREM1 and DKK1 which inhibit BMP and canonical Wnt signalling respectively. **G**: HIF-mediated upregulation of genes which encode glycolytic enzymes. Yellow arrows = processes stimulated by HIF, and red arrows = processes inhibited by HIF.

1.4. Mechanotransduction and the influence of hypoxic signalling

Cells are able to respond to changes in the mechanical factors of immediate microenvironment. These mechanical changes, for example the elasticity of the substrate on which they reside, have been shown to influence cell behavior. One aspect of such behavior is chondrogenic differentiation, which has been shown to be heavily influenced by the mechanical properties of the stem cell extracellular space. Furthermore, as described below, evidence exists of the role of hypoxia in regulating mechanotransducive pathways that are involved in BM-MSC chondrogenesis. Insights into the crosstalk between hypoxia and mechanotransducive pathways ay inform CTE techniques where the optimal mechanical microenvironment for chondrogenesis is to be combined with HIF-dependent signalling.

1.4.1. The tensegrity model of the cytoskeleton

As described by Mitchison, the cytoskeleton is composed of actin microfilaments, intermediate filaments and microtubules composed of tubulin monomers [292]. Actin is an ATPase, with ATP bound in lobed structures within the polymer sequence. The steady-state structure of actin is that a homotypic double helix. These helices are unlike the microtubules, display flexibility and yielding in response to tensional forces. This property of actin is required during the formation of high tensed stress fibres which are induced upon contraction of the actin-bound Myosin Light Chain-II (MLC2). As described by Lutz and Lieber, MLC2 contraction is an ATP-dependent process. Following binding of the ‘head’ subunit of MLC2 to the Actin helix, the bound ATP is hydrolysed, which induces the power-stroke movement of the MLC2 head.

This subsequently induces contraction of the actin microfilament, with the sum of tension produced by all actin microfilaments contributing to the tension generated by the cytoskeleton as a whole [293].

Donald Ingber likened the cytoskeletal tension created by MLC contraction to structures whose continuous tension maintains their structural integrity [294]. Such structures include the Buckminsterfullerene, a 60-carbon structure made by Harold Kroto, Robert Curl and Richard Smalley [295]. This structure resembled those discovered by Richard Buckminster Fuller who coined the term 'Tensegrity' upon observation of the ability of such structures to maintain their integrity by increased tension of the inter-carbon bonds [296]. The Buckminsterfullerene did indeed exhibit this same tensegrity, which was investigated due to the observation by Russel Chu that the structure would not be viable without secondary structures in which tensional forces were continuously transferred [297].

Ingber in his comparison between Buckminsterfullerene-like structures and that of the cytoskeleton, suggested that the actin network also experiences changes in tensional forces, with an increase responsible for maintaining cell shape and integrity. This was based on pioneering observations of opposing forces produced by the actin microfilament and the microtubules [298] and of myosin-actin tension orientated towards the centre of the cell [299]. Correspondingly, Harris and Stopak observed a pulling-force by chick cardiac fibroblasts on the surrounding silicon-based surface on which they were seeded, as assessed by the degree of inward 'wrinkling' of the material [300].

1.4.2. Regulation of cytoskeletal tension and cell shape by substrate stiffness

During development, there exists a requirement of ECM which is able to resist deformation in response to cell attachment cell-derived tension. Banerjee et al demonstrated the requirement of a basal lamina during salivary gland development for the maintenance of cell morphology and a specific cytoskeletal arrangement that are conducive for formation of the salivary gland lobular structures [301]. Upon enzymatic digestion of the supporting mesenchyme, these authors observed the loss of cell-ECM attachment, cytoskeletal disorganization and the rounding up of submandibular epithelial cells. Supporting this, Li and Sakaguchi identified the role of cell-ECM attachment during development of the retina [302]. They observed a disruption and 'rounding up' of the retinal lamina upon injection of the embryonic tissue with an antibody which blocked a specific cell surface receptor responsible for mediating cell-ECM interactions. This receptor is a member of the Integrin family which are integral in mediating the transmission of signals from the ECM through the cell. The exact molecular nature of this is described in subsequent sections of this chapter.

In addition to the effect of either the presence or absence of ECM on cell behaviour, the magnitude of tensional force applied by the cell onto its ECM is determined by elasticity of the ECM. The elasticity or stiffness of a substrate on which a cell is seeded is defined as the extent to which it resists deformation in response to tensional forces produced by the cell. As pertained to, the attachment point of a cell to its ECM is primarily mediated by Integrin receptors, which enables formation of focal adhesion complexes at discrete regions along the cell-ECM interface. As described by Ingber,

it is the elasticity of the ECM between these attachment points which determines the tension generated within the cell. A substrate of relative high stiffness will not deform between sites of cell attachment and adhesion formation. This will result in a high tensional forces generated by the cell cytoskeleton to reach an equilibrium with the tension generated within the ECM [303]. Morphologically, this results in cell spreading and observation of visible actin stress fibres [304].

On a relative soft substrate, despite cells exhibiting lower cytoskeletal tension compared to those on a stiff substrate, actin-myosin contraction is present. Therefore when present on an ECM which undergoes deformation more readily in response to a pulling force, a cell generates a rounded morphology. This is due to a cytoskeletal tension-mediated retraction of the actin network towards the nucleus in a concentric manner, which occurs due to the low relative tension and binding affinity of cell-ECM anchors. Mih et al demonstrated the importance of myosin contraction in generating a rounded cell morphology by observation of fibroblast spreading on a soft substrate in response to Blebbistatin treatment. This was compared to cells without inhibitor treatment in which a round morphology was observed [305]. This was also observed in the study by Vishavkarma et al in which the cell area of murine MSC on a substrate of 3-4 Kilopascal (KPa) increased in response to Blebbistatin treatment [306].

1.4.3. Regulation of lineage commitment by cytoskeletal tension and actin arrangement

A study by McBeath et al observed how changes in cytoskeletal tension and cell shape affected MSC fate. When cultured at high density, MSCs were shown to adopt a rounded cell shape. This change in cell shape was shown to mediate the bias towards adipogenic differentiation over that of an osteoblast, despite culture of the MSCs in media containing factors conducive for differentiation down either lineage [307]. Furthermore, when MSC spreading was restricted on 1024μm^2 islands, there was a bias for adipogenesis of seeded cells compared to an osteogenic cell fate which was preferred on larger, 10,000μm^2 islands. In further experiments, a reduction in osteogenesis was observed on the large island in the presence of an inhibitor of myosin contraction. Also, transfection of a constitutively-active Rho-Associated Protein Kinase (ROCK) which functions to induce cytoskeletal tension, decreased adipogenesis of MSCs cultured on the smaller substrate. These observations demonstrate the control of lineage commitment by cell shape is dependent on cytoskeletal tension.

1.4.4. Regulation of cytoskeletal tension-mediated lineage commitment by substrate stiffness

Supplementing that observed by McBeath et al, a seminal study by Engler et al also demonstrated a correlation between substrate stiffness and cytoskeletal tension-mediated lineage commitment. These authors observed, on a Collagen Type I coated soft Polyacrylamide surface, in non-differentiating media, thats MSCs adopted a relatively smaller cell shape with which a neural fate was favoured. Neural specific proteins were expressed in MSCs on the soft substrate with an associated branching

morphology observed, resembling native neurons. This is in contrast with MSCs on a stiff substrate on which a spread morphology and increased propensity for osteoblast differentiation was exhibited. This conclusion were made due to the increased expression of Osteocalcin and formation of a rigid ECM resembling mineralised bone [304]. Critically, as substrate stiffness increased, these authors observed a positive correlation with actin stress fibre formation, contraction of MLC2 and stiffness of the cells. The role of increased cytoskeletal tension in dictating the stiffness-mediated differentiation of the MSCs was then confirmed by use of the inhibitor of myosin contraction- Blebbistatin. Treatment of MSCs on all substrates with Blebbistatin reduced the commitment down the originally-preferred lineages.

Guvendiren and Burdick demonstrated a similar phenomenon to Engler et al, upon the culture of hMSCs on soft, stiff and dynamic stiffening Polyacrylamide (PA) substrates [303]. They observed a round and spread cell morphology on the soft and stiff surfaces respectively, with a 10-fold increase in traction force generated by cells on the 30KPa substrate compared to those at 3KPa. MSCs on the dynamic gel exhibited a cell morphology and traction force indicative of culture on the soft substrate which transformed into that indicative of a stiff surface following *in situ* stiffening of the PA gel. Corresponding to the changes in cell shape and traction forces, which correlate with the tensional forces within the cytoskeleton [308], a predisposition for adipogenic and osteogenic differentiation was induced on the 3 and 30KPa substrates respectively.

Finally, Guvendiren and Burdick conducted the differentiation of cells on the dyanomic stiffening substrate following a 14-day culture period. In response to gel-

stiffening at day 1 of the differentiating period, a clear bias for osteogenesis was observed. However, upon stiffening at day 7 of the culture period, MSCs within the culture appeared to differentiate down both lineages with an approximate 50% difference observed between adipo- and osteogenesis. This implies that early responses to substrate stiffness are integral in determining cell fate, compared to stiffness-mediated stimuli at latent stages of differentiation. Again, cytoskeletal tension mediated the switch in cell fate as observed by the abolishment of osteogenesis and preservation of adipogenesis in response to inhibition of myosin contraction.

1.4.5. Mechanisms by which substrate stiffness regulates cytoskeletal tension

1.4.5.1. Sensing of substrate stiffness by integrin receptors

Cells sense the stiffness of their environment via integrin receptors which link the extracellular environment with the cell cytoskeleton, and different subtypes exhibiting affinity with different ECM proteins [309, 310]. Upon engagement of ECM by the extracellular domains of integrins and binding of their cytoplasmic tails by Talin [311] and Kindlins [312], clustering occurs of multiple integrin receptors [313]. This results in the formation of focal adhesion complexes. These complexes, consisting of proteins such as Vinculin and Paxicillin, via Focal Adhesion Kinase (FAK) initiate a downstream cascade of events resulting in contraction of MLC2 and formation of Filamentous Actin (F-Actin) bundles [314, 315].

Upon engagement of integrin receptors by ligands in the ECM and actin-myosin contraction, the cell generates tension if present on a non-compliant substrate which results in a strengthening of the integrin-ECM interaction. This induces further focal adhesion maturation in a positive feedback loop, enabling continued response to the stiffness of the cell environment which actin stress fibres [316]. If the cell is present on a softer substrate, it will be unable to generate tension against a more easily deformed ECM substrate, therefore generating relatively weak integrin-ECM interactions. This generates a cortical actin organisation within the cell with few accompanying actin stress fibres.

1.4.5.2. Transduction of mechanical stiffness to the nucleus by RhoA and ROCK

One of the key mechanisms by which integrin-ECM binding is transduced into cytoskeletal tension, is via modulation of the Homolog Gene Family, Member A (RhoA)/ROCK pathway [307]. FAK is auto-phosphorylated in the focal adhesion complex [317], promotes the hierarchal addition of proteins to this complex [318] and indirectly activates RhoA [319]. RhoA is a member of the (Guanosine Tri-Phosphatase) GTPase family of proteins which in an active conformation, hydrolyses its bound (Guanosine Tri-Phosphate) GTP to Guanosine Di-Phosphate (GDP) and in doing so becomes inactive. The re-activation of RhoA is induced by the exchange of GDP for GTP which itself is mediated by Guanosine Exchange Factors (GEFs). Zaidel-Bar et al observed the ability of integrin-stimulated FAK in increasing activity of a RhoA-specific GEFs [319].

Activation of ROCK by RhoA [320, 321] stimulates the dual effect of ROCK on MLC2 – 1) direct phosphorylation of MLC2 [322] and 2) Inhibition of myosin phosphatase (MYP) [323] which functions to de-phosphorylate MLC2. This process is also simultaneous with the polymerisation of Globular Actin (G-actin) into F-actin-rich stress fibers [324]. This is induced by ROCK via inhibition of actin-binding protein, cofilin which enables polymerisation of G-Actin monomers [325, 326]. Together, RhoA/ROCK-mediated actin polymerization and contraction of MLC generates cytoskeletal tension.

1.4.6. Mechanisms by which cytoskeletal tension regulates gene expression

1.4.6.1. YAP/TAZ

The precise steps between ROCK-mediated cytoskeletal tension and induction of specific gene expression patterns observed are poorly understood. However, one transcription factor complex, Yes-Associated Protein [327] [327]/Transcriptional Coactivator with PDZ-Binding Motif (TAZ) has been shown to be central to this process [327]. This complex is classically the effector of the Hippo signalling pathway. Upon cell-cell contact and engagement of the Fat4 receptor, specific kinases negatively regulate YAP by phosphorylating and targeting it for proteosomal degradation. Conversely when the Hippo pathway is inhibited, non-phosphorylated YAP translocates to the nucleus where it binds to TEA Domain (TEAD) transcription factors and induces gene expression [328].

The ability of YAP/TAZ to respond to changes in substrate stiffness has also been shown, both via [329] and independently of the Hippo pathway [330]. On substrates of increased stiffness on which cytoskeletal stress fibre formation is induced, YAP/TAZ are localized to the nucleus. This was shown to be mediated by ROCK-induced MLC contraction, by observation that treatment with Blebbistatin or ROCK inhibitor, Y-27632 abolished stiffness-mediated YAP translocation. Nuclear shuttling of YAP also requires inhibition of Cofilin and de-repression of actin polymerization [331].

On a relative stiff ECM, following YAP/TAZ translocation into the nucleus, a cell fate switch occurs which was previously demonstrated by MSCs on this substrate [307]. That is, a bias towards osteogensis at the expense of adipogenesis. Conversely, adipogenesis was higher in MSCs on a softer substrate, within which cytoplasmic YAP/TAZ was observed [330]. Small Interfering RNA (siRNA) knockdown of YAP and TAZ in MSCs on the stiff substrate appeared to abolish osteogenesis, whilst inducing adipogenesis. Correspondingly, TAZ has been shown to bind to and potentiate the function of the key regulator of osteogenesis, RUNX2 whilst inhibiting the key regulator of adipogenesis, PPAR-γ [332].

1.4.6.2. MRTF-SRF

In addition to YAP/TAZ, other transcription factors which are regulated by cytoskeletal tension are the Myocardin-Related Transcription Factors (MRTFs) which are co-activators of Serum Response Factor (SRF)-target genes [333]. MRTF nuclear import is inhibited by actin de-polymerisation within the cell [334]. Recue of MRTF

nuclear import requires RhoA activity, ROCK-mediated phosphorylation of Cofilin and G-actin polymerisation [335]. MRTF-SRF functions to maintain the mechanosensing ability of the cell in a positive feedback loop. Their targets include genes whose products are involved in actin and ECM re-organization in addition to those required for cell-cell adhesion [336]. *TAZ* mRNA and expression of YAP-TEAD targets have also been shown to be stimulated by MRTF-SRF activity [337].

1.4.6.3. The LINC complex and Nuclear Lamins

Observations have been made of the effect of integrin-mediated cytoskeletal tension on inducing corresponding tension with the nucleus [338]. This has been shown to require in part, the Linker of Nucleoskeleton and Cytoskeleton [339] [339] complex. This complex connects the actin-myosin cytoskeleton with the nucleoskeleton [340] and mediates the force transmitted to the nucleus in response to cytoskeletal tension [341]. Nuclear YAP localization and subsequent transcription of TEAD-targets has been shown to depend on the LINC complex in strain-responsive cells [342], indicating a link between nuclear tension and changes in gene expression.

Another class of structural components within the nucleus, the Lamins, may also play key roles in the transduction of mechanical signals from the cytoplasm [343]. Lamins regulate nuclear architecture, chromatin organization [344] and epigenetic control of gene expression [345]. They are localisaed to the nuclear lamina, between the LINC complex and chromatin bundles [346]. LaminA expression in MSCs correlates with tissue stiffness and has also been shown to be greater in cells exposed to stiffness-mediated increases in cytoskeletal tension [347]. LaminA has also been shown to

coordinate actin dynamics of the cytoskeleton. It ensure formation of contracted actin bundles, and nuclear translocation of mechanoresponsive transcription factors, YAP [347] and Megakaryoblastic Leukemia (Translocation) 1 (MKL1) [348] [349].

1.4.7. Mechanotransduction during articular cartilage development and maintenance

There is a multitude of evidence suggesting the role of mechanotransductive pathways during maintenance of the articular chondrocyte phenotype. Correlation between cell shape and stability of the articular chondrocyte phenotype has long been suggested, with spread articular chondrocytes compared to those of a smaller, polygonal shape exhibiting hypertrophic characteristics [350]. Reducing substrate adhesion and cell spreading enhances the cartilage ECM-producing ability of chondrocytes [351] and this is concomitant with that shown by Kim et al. These authors observed a progressively-higher susceptibility of chondrocytes to develop an OA-phenotype when cultured on substrates of increasing stiffness [352]. This OA-phenotype was marked by increased mRNA expression of *MMP13* and *ADAMTS5*, whilst reducing *SOX9*, *COL2A1* and *ACAN* mRNA. These changes in chondrocyte phenotype were shown to be mediated via ROCK-induced cytoskeletal tension due to observations of reduced OA development upon treatment with Y-27632 and Blebbistatin.

1.4.7.1. Effect of substrate stiffness, cytoskeletal tension and actin organisation during chondrogenesis

Cell shape is an influential aspect of mesenchymal progenitors in the limb bud condensation and the subsequent chondrogenic differentiation program. Ray et al demonstrated the round actin arrangement of chick limb bud mesenchymal cells prior to formation of the growth plate. Treatment of this *ex vivo* culture with Cytochalasin D inhibited myosin contraction and the round actin arrangement required for *SOX9* and *COL2A1* mRNA expression [353]. This implies that cortical actin organization is a product of cytoskeletal tension in limb bud cells and is responsible for their observed round morphology and downstream chondrogenesis. Gao et al investigated the effect of cell spreading on the chondrogenesis of hMSCs. Collagen Type II protein and *SOX9* mRNA were increased in hMSCs which were chondrogenically-induced on 1024μm^2 islands compared to that on 10,000μm^2 islands [354]. This study therefore directly implicates cell shape in downstream chondrogenic differentiation programs.

The specific stiffnesses of cartilage and subchondral bone are important in directing osteochondral mesenchymal progenitors down the chondrogenic [355]/osteoblastic lineages [304], in addition to being required for the specific functions of each tissue. The elastic modulus from subchondral bone, through to articular cartilage has been shown to vary in the order of three magnitudes – ranging from approximately 2.3GPa to 2.6MPa for bone and cartilage respectively [356, 357] (**Fig. 1.3**) [1]. Allen et al utilised Collagen Type I-coated polyacrylamide gels to demonstrate stiffness mediated differences in hMSC chondrogenesis which were independent of a change

in cell shape or area [355]. In this study, despite fewer long stress fibres and more cortical actin observed in hMSCs on the 0.5 Megapascal (MPa) substrate compared to those on the 1.1MPa, no significant change in cell morphology was observed. Despite this lack of shape change, hMSCs on the 0.5MPa surface upregulated transcription of *SOX9*, *COL2A1* and *ACAN* compared to that at 1.1MPa.

In the study by Allen et al, chondrogenesis on the 0.5MPa substrate in which a cortical actin arrangement was present in hMSCs, was reduced by ROCK inhibition. This same inhibition appeared to increase cartilage differentiation on the stiff substrate on which hMSCs displayed long actin stress fibres. This, suggests the importance of ROCK-mediated cortical actin organization for chondrogenesis, as opposed to ROCK-mediated long stress fibre formation which is detrimental to chondrogenic induction. Kwon et al observed an increase in *SOX9* and *COL2A1* mRNA and Collagen Type II protein by murine BM-MSCs on a 1KPa substrate, compared to those on a 150KPa substrate [358]. Blebbistatin treatment was observed to reduce the increases in chondrogenic mRNA levels on the 1KPa substrate, implicating MLC2 contraction in generating the specific cortical actin organization required for chondrogenesis. Together these studies point to polar-opposite effect of cytoskeletal tension on chondrogenesis, dependent on the elasticity of the substrate on which cells are seeded. On a soft substrate RhoA/ROCK-mediated actin reorganization may be conducive for chondrogenesis by inducing cortical actin formation of differentiating cells. This is as opposed to cells on a stiff substrate in which ROCK induces stress fibre formation and a spread actin network and in which chondrogenesis is inhibited.

1.4.7.2. Role of RhoA/ROCK during chondrogenesis

The role that RhoA/ROCK plays in generating and maintaining an articular chondrocyte phenotype is context-dependent. In micromass cultures ROCK inhibition abolished the early expression of SOX9 targets and transcriptional co-activators in murine limb bud mesenchymal stem cells (Woods, 2006). This decrease in chondrogenesis is also induced by cytoskeletal destabilisation, whilst stimulation of actin polymerisation increased chondrogenesis [307]. The culture system utilized in this study was a high-density, micromass culture, in which a rounded/oval morphology has been shown to be adopted by individual cells [307]. Therefore the finding by Wood and Beier supports previous reports of the role of RhoA/ROCK-mediated cortical actin organization for chondrogenesis. This is also supported by the observation that ROCK inhibition decreases the expression of chondrogenic genes in ATDC5 cells on softer substrates where fewer long stress fibres and increased cortical actin is displayed [355]. This is contrasted with observations on comparatively stiff substrates where ATDC5 stress fibre formation is increased and on which, chondrogenesis is enhanced by ROCK inhibition. This again indicates that ROCK is required to maintain both cortical organization and long stress fibre formation on soft and stiff substrates respectively. However ROCK is required for chondrogenesis only when differentiating cells take on a round morphology, for example when present on ECM of low stiffness or in high-density cultures.

In addition to mediating the mechanotransducive effect on chondrogenesis, RhoA/ROCK is able to regulate SOX9 activity directly. The stability of SOX9 in ATDC5 cells is dependent on the phosphorylation state of serine-211 within its polypeptide

sequence [359]. In chondrosarcoma cells, Haudenschild et al identified a specific amino acid sequence within the SOX9 polypeptide which denotes it as a target of ROCK-mediated phosphorylation [360]. These authors then observed the ROCK-mediated dose-dependent increase of SOX9 phosphorylation. Nuclear localization of SOX9 is required for transcription of its chondrogenic target genes [361]. Therefore observation of the abolishment of TGF-β_1-induced nuclear SOX9 translocalisation by ROCK inhibition, suggests the requirement of ROCK activity for SOX9 function during chondrogenesis [360]. The activity of RhoA and ROCK have also been demonstrated to positively-influence the TGF-$\beta_{1/3}$-Smad2/3 pathways during chondrogenesis. Xu et al observed on an inhibition of TGF-β_1-induced *SOX9*, *COL2A1* and *ACAN* transcription in synovium-derived MSC, due to inhibition of RhoA or ROCK [362]. This was shown to be due to the requirement of RhoA-stimulated ROCK activity in the phosphorylation of Smad2 and Smad3.

1.4.7.3. Role of YAP/TAZ during chondrogenesis

The consensus for the role of YAP/TAZ during chondrogenesis is that of a down-regulatory one. Deng et al observed a progressive decrease in *YAP1* expression during the differentiation of chondro-progenitor cells into those capable of depositing a GAG-rich ECM [363]. This was synonymous with observations during endochondral bone development in which the cartilage growth plate expresses low levels of un-phosphorylated, and therefore active YAP. This is in contrast to the increased expression in that of surrounding perichondrium, containing osteoblasts required for formation of the primary ossification centre. Adenoviral delivery of *YAP1* to

chondroprogenitor cells results in a significant reduction in GAG and Collagen Type II production and instead, halts their differentiation whilst maintaining their proliferative state [363]. Karystinou et al observed a reduction in YAP1 mRNA and protein in response to TGF-β_1-mediated chondrogenic induction of synovium-derived MSCs [364]. These authors also observed a decrease in chondrogenesis of the MSC cell line, C3H10T1/2 in response to retroviral delivery of the *YAP1* gene. This was marked by reduced *SOX9* and *COL2A1* mRNA expression in addition to diminished Alcian Blue staining of GAGs. Mechanistically, this was proposed to be via downregulation of BMP signalling due to observation of reduced Smad1/5/8 phosphorylation in *YAP1*-delivered MSCs.

Zhong et al observed the decrease in transcription of *RUNX2* and *COL1A1* in response to siRNA knockdown of *YAP1* in rat BM-MSCs [365]. This was accompanied by an increase in *SOX9, COL2A1* and *ACAN* expression. Together this demonstrated the role of YAP in promoting a pro-osteogenic and anti-chondrogenic transcriptional program in mesenchymal progenitors. The requirement of YAP downregulation for maintenance of the chondrocyte phenotype has also been demonstrated by observation that its siRNA-mediated knockdown result in increases in *SOX9, COL2A1* and *ACAN* mRNA [366]. This corresponded with observations in the same study of the downregulation of these chondrogenic transcripts in response to siRNA knockdown of *LATS1*. This gene encodes a kinase which inhibits YAP nuclear translocation [367].

1.4.8. Effect of hypoxia and HIF on mechanotransductive pathways

1.4.8.1. Regulation of cytoskeletal tension and organisation by hypoxia and HIF

The effect of hypoxia and HIF on formation of actin stress fibres and cytoskeletal tension has been extensively investigated. Overall, the evidence points to the ability of hypoxia to upregulate stress fibre formation in a variety of cell types. For example, Vogler et al demonstrated the increased spreading of L929 Fibroblasts upon incubation at 1%O_2 compared to cells cultured in normoxic conditions [368]. This was associated with increased intensity of actin staining in cortical patterns around the nucleus in addition to a greater number of actin focal points. These structures denote regions where the cytoskeleton is linked with the ECM via adhesion complexes thereby signifying increased cytoskeletal tension [369]. Cytoskeletal contraction and re-arrangement also occurs due to hypoxia in many cancer cell types such as neuroblastoma [370], adenocarcinoma cells [371] and breast cancer cells [372]. In the case of the latter, incubation at 1%O_2 for 24 hours increased the number of visible actin stress fibres in the MDA-MB-231 breast cancer cell line compared to culture at 20%O_2. Hypoxia was also observed to increase tension within these breast cancer cells, as assessed by their ability to retract the Collagen Type I gel onto which they were seeded. This was accompanied by increased MLC2 phosphorylation denoting contraction of this myosin sub-type.

The ability of hypoxia-incubated MDA-MB-231 cells to generate focal adhesions compared to that at normoxia was demonstrated. A group observed increased immunodetection of Vinculin-containing adhesion complexes due to hypoxic

incubation of the breast cancer cells. This corresponded with greater levels of FAK phosphorylation which is indicative of downstream integrin signalling in cells of a high tensegrity [373]. HIF has also been shown to regulate cytoskeletal rearrangement in endothelial cell spheroid cultures. In this study, Weidemann et al observed an increase in the concentric F-Actin arrangement around the nucleus in response to treatment with HIF-1α stabilizing agent- Dimethyloxalylglycine (DMOG) [374]. Again in breast cancer cells, siRNA knockdown of HIF-1/2α abolished hypoxia-mediated increases in cell contraction, focal adhesion formation and phosphorylation of FAK, similar to levels observed at normoxic conditions [372].

Cofilin is an actin-binding protein which by performing its function, blocks G-actin polymerization which is required for stress fibre formation. Knockdown of PHD2, the oxygen-sensing hydroxylase responsible for targeting HIF-1α for degradation, was observed to increased stress fibre formation in HeLa cells [375]. This phenomenon is mediated by increased phosphorylation and inactivation of Cofilin and was replicated by treatment of wild type cells with DMOG.

Another mechanism by which HIF increases focal adhesion formation and cytoskeletal contraction, is via transcriptional induction of genes encoding Integrin receptors. For example, Skuli et al observed increases in protein levels of Integrin-β_5 in response to hypoxic incubation in a glioma cell line, and this also was accompanied by increases in Vinculin and FAK phosphorylation [376]. siRNA knockdown of Integrin-β_5 inhibited hypoxia-mediated increases of phosphorylated FAK. This suggests the requirement of increased integrin-mediated ECM adhesion in generating downstream cytoskeletal tension. Hypoxia was also shown to increase

mRNA levels encoding Integrin-α_6 in a breast cancer cell line, and this increase was abolished by HIF-1α knockdown [377]. Identification of a HIF-response element within the gene encoding this integrin subtype is suggestive of the ability of hypoxic-induced transcription to directly upregulate integrin-mediated signalling.

1.4.8.2. The regulation of RhoA/ROCK by hypoxia and HIF

Corresponding to the majority of the literature which describes the positive effect of hypoxia on stress fibre formation, low oxygen tension has been shown to induce the activity levels of the both RhoA and ROCK. In breast cancer cells, Gilkes et al identified HIF-response elements in the promoter regions of both *RHOA* and *ROCK1*, demonstrating an ability of this transcription factor complex to directly upregulate *RhoA* and *ROCK1* expression [372]. Indeed, these authors demonstrated an increase in mRNA encoding RhoA and ROCK1 in response to incubation in 1%O_2 compared to culture at normoxia, in addition to observing increases in the corresponding proteins. These increases were also shown to be abolished by HIF-1/2α knockdown. Therefore hypoxia-induced HIF is implicated as the regulatory mechanism of RhoA/ROCK activity during breast cancer cytoskeletal contraction.

González Rodríguez et al identified the hypoxia-mediated regulation of RhoA/ROCK in rat cardiomyocytes [378]. Interestingly, despite a lack of effect on *RHOA* and *ROCK1* mRNA due to a 4-hour hypoxic incubation, an increased in RhoA and ROCK1 protein were observed in addition to an induction of RhoA activity. Additionally, RhoA activity was not enhanced in myocytes in which a constitutively active HIF-1α

was present. Despite demonstrating a hypoxia-mediated induction of RhoA/ROCK protein, this study is suggestive of a context-dependent regulation of *RHOA* and *ROCK1* transcription by HIF, despite both these genes containing HIF-response elements in their promoter regions. Following on from this, in colon cancer cells, Mizukami et al observed an increase in the active, GTP-bound form of RhoA due to hypoxic incubation, despite no overall increases in RhoA protein [379]. This increase was abolished by inhibition of phosphoinositide 3-kinases demonstrating a novel pathway by which hypoxia regulates RhoA activity. This effect of hypoxia on RhoA induction was also observed to be required for induction of the transcription of *VEGFA*, a long established HIF target [379]. This was demonstrated by hypoxia-mediated increases in *VEGFA* mRNA being abolished by RhoA or ROCK inhibition. This indicates the potential requirement of RhoA and ROCK in mediating hypoxia-induced HIF signalling.

With regards to evidence of increased ROCK activity due to hypoxia, Nakanishi et al demonstrated the increase of ROCK activity due to hypoxia in lung smooth muscle *in vivo* [380]. In response to incubation of a mouse in a mild hypoxia (10%O_2), the authors observed an upregulation of MLC2 phosphorylation within smooth muscle cells of the lung. This was accompanied by an increase in phosphorylation of myosin phosphatase. These changes were abolished by ROCK inhibition with Y-27632 thereby demonstrating the ability of hypoxia to induce activity of ROCK that is conducive for myosin light chain contraction.

1.4.8.3. Effect of hypoxic pathways on YAP/TAZ function

Hypoxia has been shown to influence the availability of YAP as a binding partner for TEAD transcription factors in a number of cancer cell types. In prostate cancer cells [381], hepatocellular carcinoma cells [382] and breast cancer cells [383], the nuclear localisation of YAP is induced by hypoxic culture. This is simultaneous with a decrease in the inactive, phosphorylated YAP. In the study by Ma et al, hypoxia downregulated the hippo pathway and increased levels of activated YAP. This increased in YAP was shown to be mediated via an increase in expression of Zyxin which plays a key role in the focal adhesion complex in response to integrin engagement [384]. The findings by Ma et al are therefore suggestive of a role for hypoxia in regulating the levels of active YAP via changes in formation of the cell adhesion complex and the transduction of ECM stiffness by the cell.

1.5. The research aims of the thesis - utilising hypoxia and HIF signalling in BM-MSC chondrogenesis

Hypoxia plays critical roles during chondrogenesis of mesenchymal progenitors and cartilage ECM formation, both during limb development and *in vitro* chondrocyte specification. This suggests the role that hypoxia may play in achieving a cell phenotype and ECM composition from BM-MSCs which mimics articular chondrocytes and native articular cartilage in which they reside. Generation of native-like articular cartilage is required for the repair of chondral defects. This may enable the desired mechanical properties of the regenerated cartilage which would enable resistance to the compressive and tensional forces on the joint during locomotion. However, a disparity exists with regards to the specific hypoxic state

required to achieve optimal chondrogenesis and cartilage ECM formation, whilst inhibiting chondrocyte hypertrophy – a common issue with current CTE strategies. Therefore the first results chapter of this thesis - **chapter 3**, describes data which compares the effects of 5% with 2%O_2 during hBM-MSC chondrogenesis.

The primary mediator of signalling in response to physiological hypoxia is the HIF transcriptional complex. During BM-MSC chondrogenesis, the functions of HIF and its alpha subunit – HIF-1α are required for expression of articular chondrocyte markers and an ECM which mimics native articular cartilage. Therefore, the use of chemical agents which upregulate HIF-1α may provide a valid alternative to the use of hypoxia during hBM-MSC chondrogenesis.

The use of HIF-1α-stimulating compounds would avoid the potential pitfalls associated with the incubation of BM-MSCs at low-oxygen conditions. These include the upregulation of the unfolded protein response which may reduce the protein translation required for stem cell differentiation. The use of HIF-1α-upregulating compounds would also enable spatial control of hypoxic signaling in BM-MSCs on a biomaterial scaffold. Therefore **chapter 4** describes a study which compares the role of three widely-used HIF-1α-stimulating compounds during BM-MSC chondrogenesis. The aim of this study was to compare which of Cobalt Chloride, Desferroxamine and Dimethyloxaloylglycine are able to stimulate articular chondrogenesis, formation of articular cartilage ECM and inhibition of chondrocyte hypertrophy.

The final results section – **chapter 5**, aims to investigate the crosstalk between hypoxic signaling, with those pathways that are stimulated in response to the

mechanical stiffness of the cell microenvironment. As described in section____, mechanotransducive pathways have been shown to be integral during BM-MSC chondrogenesis, with ROCK-mediated cytoskeletal tension and a round cell morphology required for chondrocyte differentiation. In addition to the role of hypoxia during chondrogenesis, regulation of components of the mechanotransducive pathway by low-oxygen conditions has been demonstrated. Together, these suggest the potential of hypoxia in upregulating mechanotransducive pathways that are conducive for chondrogenesis. The results in **chapter 5** investigates this effect of hypoxia with observations potentially informing CTE strategies in which hypoxic culture of BM-MSCs is combined with biomaterial scaffolds of a defined stiffness.

The overarching hypothesis for the thesis is as follows: hypoxia is able to improve chondrogenesis of BM-MSCs and inhibit hypertrophy. This improvement of chondrogenesis is able to be replicated by the use of a HIF-1α-stabilising compound. Finally, hypoxia induces BM-MSC chondrogenesis through regulation of mechanotransducive pathways via generation of cytoskeletal tension and cell shape that are conducive for articular chondrocyte differentiation. Together, **chapters 3-5** detail results which inform the improvement of BM-MSC chondrogenesis to achieve an articular chondrocyte phenotype which more closely mimics those present in native articular cartilage. Such improvements utilising hypoxia would enable the development of CTE strategies for repair of chondral defects by ensuring production of an articular cartilage ECM and inhibition of chondrocyte hypertrophy. This would enable the regenerated tissue to exhibit the specific mechanical properties required

of articular cartilage whilst inhibiting inappropriate ossification of the graft when implanted *in vivo*.

2. Materials & Methods

2.1. Isolation of hBM-MSC

hBM-MSCs were provided by Dr. Holgar Auner of Department of Medicine, Imperial College London. Due to this material being provided by a collaborator and not isolated by within the lab of Dr. Eileen Gentleman, it was not possible to obtain BM-MSCs from more than a from a single donor . This introduces a caveat to the present study due to the heterogeneity exhibited by BM-MSCs harvested from different donors with regards to their chondrogenic potential. However, there exists a concordance between observations made of BM-MSCs here with that in the literature, such as the HIF-response to hypoxic incubation and chondrogenic-induction by TGF-β_3. This suggests that the novel observations made here are not indicative of an anomalous BM-MSC donor source but instead, may represent BM-MSCs of similar characteristics as utilized in the literature. Thereby, these findings may inform the development of chondrogenic induction protocols for BM-MSCs.

Human samples used in this research project were obtained from the Imperial College Healthcare Tissue Bank (ICHTB, HTA license 12275). ICHTB are supported by the National Institute for Health Research (NIHR) Biomedical Research Centre based at Imperial College Healthcare National Health Service (NHS) Trust and Imperial

College London. ICHTB is approved by the United Kingdom (UK) National Research Ethics Service to release human material for research (12/WA/0196), and the samples for this project were issued from sub-collection R16052. Bone marrow aspirates were collected and plated in CellSTACK® (Corning) culture chambers at a density of 10-25x10^6/636cm^2. Cells were then cultured in αMEM supplemented with 5% human platelet lysate (Stemulate) and cultured under standard conditions. When cell confluence of 90-100% was achieved (10-14 days), cells were detached with recombinant trypsin (Roche) and reseeded at 5000 cells/cm^2.

Cultures were immunophenotyped and found to express CD90, CD105, CD73 and not express hematopoietic markers CD34 and CD45 (data now shown). Antibodies used identify expression of these markers were: CD90-Fluorescein Isothiocyanate (FITC) [166-095-403], CD105-Allophycocyanin [385-094-926], CD73- Phycoerythrin (PE) [385-095-182], CD34-PE [385-081-002], and CD45-FITC (#130-098-043; all from BD Biosciences) using a FACSCalibur™ Analyser (BD Biosciences).

2.2. Expansion and cryopreservation of hBM-MSC, bovine chondrocytes and C28/I2 cell line

Following their isolation, hBM-MSCs were plated onto T-175 tissue culture flasks for their expansion in the following conditions: 20%O_2, 5% Carbon Dioxide (CO_2) at 37°C. Growth media (GM; 10% (v/v) Fetal Bovine Serum (FBS; Life Technologies) in α-Minimal Essential Media (αMEM; Life Technologies)) was added to each flask and replaced twice a week until cultures reached 90% confluency. At this point, cultures

were passaged by an initial wash in Phosphate Buffered Saline (PBS; Life Technologies) and enzymatic dettachment from the flask surface with treatment with 0.05% (v/v) Trypsin-Ethylenediaminetetraacetic acid (EDTA) (Life Technologies) for 3 minutes at 37°C. Following collection of resulting cell suspension and washing of residual cells from the flask with GM, cells were centrifuged at 1200 Relative Centrifugal Field (RCF) for 5 minutes. The resulting pellet from one flask was then re-suspended in GM and divided equally between three recipient flasks which was also each added to with GM. Flasks were incubated for 24 hours before their inspection on a Zeiss brightfield microscope and subsequently incubated for a further 48 hours before the GM was changed and expansion was carried out.

For cryopreservation of hBM-MSCs, trypsin-EDTA was used for cell detachment and suspensions were pelleted as with the passaging protocol but pellets from each flask were instead re-suspended in a 1:1 mixture of GM and Cryopreservation media (20% (v/v) Dimethyl sulfoxide (DMSO; Sigma Aldrich) in FBS). The suspension from one flask was then transferred to a single cryopreservation vial which was frozen at -80°C in an iso-propanol container before transfer to storage in liquid nitrogen.

For thawing of frozen cells, each vial was removed from liquid nitrogen storage and thawed rapidly at 37°C. This was subsequently followed by dilution of the cell suspension in GM in a 1:10 ratio. Suspensions were then centrifuged at 1200 RCF for 5 minutes, before re-suspension of the pellet and division between three T-175 flasks each containing GM. Flasks were incubated for 24 hours before their inspection on a Zeiss brightfield microscope, changing of the GM and expansion as described above. Bovine chondrocytes and C28/I2 cells were expanded, cryopreserved and thawed

with identical protocols to that used for hBM-MSC culture with the exception of the composition of GM. GM consisted of Dulbeccos MEM (DMEM; Sigma Aldrich) + 10% (v/v) FBS + 1% (v/v) Antibiotic Antimycotic (ABAM; Sigma Aldrich) for the bovine chondrocytes and DMEM + 10% (v/v) FBS for the C28/I2 cell line.

2.3. Chondrogenic Induction of hBM-MSC and bovine chondrocytes as monolayers, pellets and on PA gels.

Frozen vials of hBM-MSCs and bovine chondrocytes were thawed and expanded up until passage 5, before their trypsinisation and plating into multi-well tissue culture plates for monolayer chondrogenic induction. Following the cell counting of the BM-MSC suspension, separate dilutions of this suspension were made in GM for seeding into tissue culture plates of each size of well. The cell suspensions were diluted such that when set volumes were pipetted into each well, a universal cell density of 30,000/cm^2 or 5000/cm^2 was achieved for TCP or PA subtrates respectively . See **appendix figure 1** for cell concentrations and pipetting volumes for wells of each size. See **appendix figure 2** the overall workflow detailing the chondrogenesis of hBM-MSCs.

In addition to the universal cell densities used, other control measures were put into place to minimize the effect of sample-to-sample cell number variation due to proliferation/cell death. hBM-MSC cell number in control conditions did not vary significantly (p=<0.05) throughout chondrogenesis **appendix figure 3**. In conditions in which cell number at time of sample harvest did vary from the control condition, normalization of chondrogenic assay outputs to cell number was undertaken. See

each assay entry in this chapter for how quantitiative/semi-quantitative data was normalized to cell number .

In addition to chondrogenic induction of hBM-MSCs, bovine chondrocytes were utililsed as a positive control for cartilage ECM formation. By detection of GAG's produced by bovine chondrocytes, it was possible to optimize Alcian Blue staining for GAGs in addition to allowing selection between TGF-β_1 or TGF-β_3 for future chondrogenic-induction experiments.

For pellet chondrogenesis, hBM-MSC and bovine chondrocytes were divided into aliquots of $2x10^5$ cells in 15ml flacon tubes before their centrifugation at 1200 RCF for 5 minutes. Monolayer cultures and pellets were incubated for 24 hours in GM, prior to induction using standard chondrogenic differentiation media (CDM). CDM consisted of High Glucose Dulbecco's Modified Eagle Medium (Sigma Aldrich) + 2mM L-Glutamine (Thermo Fisher Scientific) + 100nM Dexamethasome (Sigma Aldrich) + 1% (v/v) Insulin, Transferrin, Selenium Solution (Thermo Fisher Scientific) + 1% (v/v) ABAM solution (Sigma Aldrich) + 50µg/ml Ascorbic acid-2-phosphate (Sigma Aldrich) + 40µg/ml L-proline (Sigma Aldrich). This was then supplemented with either 10ng/ml TGF-β_1 or TGF-β_3 (Peprotech).

For upregulation of HIF-1α, CDM was supplemented with the following compounds (Sigma Aldrich): 100µM Cobalt Chloride ($CoCl_2$), 50µM Desferrioxamine (DFX) and 200µM DMOG. For hypoxic incubations, hBM-MSCs in un-supplemented CDM were incubated in a cell culture incubator which was set to 5%O_2 + 5%CO_2 or in an incubator set at 2%O_2 + 5%CO_2. To achieve HIF-1α inhibition, media was further supplemented with 500nM Acriflavine (ACF; Santa Cruz). Preliminary experiments

were conducted to identify which of TGF-β_1 or TGF-β_3 were more optimal for chondrogenesis with bovine chondrocyte cultures used as a positive control for cartilage ECM production.

hBM-MSCs and bovine chondrocytes were also differentiated as pellet cultures to ensure CDM promoted the production of cartilage ECM in 3D culture (**Appendix Fig. 4**). This was due to the premise that results in the present study may enable improvement of strategies for cartilage tissue engineering within 3D biomaterial scaffolds. Pellet cultures at time points specificed were washed in PBS and fixed in 4% (w/v) Paraformaldehyde (PFA) before histological processing (**Appendix Fig. 5**). Following paraffin wax embedding, sectioning of pellets into 10µm slices and mounting onto glass cover slides, samples were then histochemically stained as described in **Appendix Fig. 6**.

2.4. Polyacrylamide gel synthesis and hBM-MSC culture

Synthesis of PA gels was conducted by Daniel Foyt who also aided in carrying out experiments in which BM-MSCs were chondrogenically-induced on these gels. 0.5ml of 100mM Sodium Hydroxide (NaOH) was dispensed evenly onto a 25mm glass coverslip and the water was allowed to evaporate at 80°C leaving a thin crystalline layer of NaOH. 0.2 mL of (3-Aminopropyl)triethoxysilane was dispensed evenly onto the NaOH coated coverslip and allowed to react for 5 min after which the coverslip was thoroughly washed with DI water and placed in 2ml of 0.5%(v/v) glutaraldehyde in PBS for 30min. Coverslips were then removed from the glutaraldehyde solution and allowed to air dry at room temperature. 40% (w/v) acrylamide, 2% (w/v) N,N'-

methylenebis(acrylamide), and PBS were mixed in the proportions shown in **appendix figure 10A**. Gel precursors were degassed under strong vacuum for 15min. Glass microscope slides were coated with 0.1 ml of Dichlorodimethylsilane (DCDMS) and allowed to react for 2min. Microscope slides were washed with DI water and dried. Tetramethylethylenediamine (TEMED) and ammonium persulfate (APS) were added to the gel precursors according to the ratios above and vortexed for 30 sec. 0.05ml of gel solution was dispensed onto the DCDMS coated microscope slides. Coated coverslips were then placed coated side down onto the gel solution and the gel was allowed to cure for 30 min. Substrates were washed over night in 10 ml of PBS with gentle agitation.

Substrates were washed again 3 times in 5ml of PBS for 5 min. 0.5ml of 0.5mg/ml sulfosuccinimidyl 6-(4'-azido-2'-nitrophenylamino)hexanoate (Sulfo-SANPAH) dissolved in 50mM 4-(2-hydroxyethyl)-1-piperazineethanesulfonic acid (pH 8.5) (HEPES) was dispensed onto the substrates and substrates were exposed to UV light for 20min. Substrates were wash 3 times in 5ml of HEPES. Substrates were placed in 2ml of 0.015mg/ml fibronectin solution in HEPES and agitated gently over night at 4°C. Fibronectin coated substrates were washed 3 times in PBS and stored at 4°C for up to 2 weeks.

After washing in PBS overnight, one PA gel was placed in each well of a 6-well plate prior to seeding with hBM-MSCs and chondrogenic induction for which the following procedure was followed. hBM-MSCs were detached from the plastic surface with 0.05% (v/v) Trypsin-EDTA, re-suspended in GM and cells were carefully distributed in a 200µl aliquot to cover the entire surface of each gel at $3x10^4$ cells/cm^2. Following

an initial 4-hour attachment period at 20%O_2, 5%CO_2 and 37°C, each well containing a single PA gel was supplemented with 2ml GM. A further 24-hour incubation period was carried out and GM was then replaced by CDM containing TGF-β_3 with each gel incubated further at either 20%O_2 or 2%O_2 conditions as indicated. The length of the final incubation step is indicated in each figure legend and represents the 'chondrogenic-induction phase' of the experiment. Where also indicated, CDM was further supplemented with 10µM Y-27632 to achieve ROCK inhibition.

2.5. PicoGreen assay for quantification of dsDNA and cell number

At indicated time points, samples were washed in PBS and snap-frozen at -80 °C followed by their digestion in 400µg/ml Papain in a 0.2M Trisodium Phosphate buffer which also included 10mM EDTA and 10mM L-Cysteine. This digestion step was carried out at 65°C for 18 hours with constant agitation after which the cell lysates were frozen at -20°C until quantification of double stranded DNA using a PicoGreen kit (Thermo Fisher Scientific). PicoGreen dye was diluted in a 1:200 ratio with TE buffer which consists of 10mM Tris-Hydrochloric Acid (HCL) and 1mM EDTA at pH 7.5. PicoGreen dye was then further diluted in a 1:1 ratio with one of each of the Papain-digested lysates in a single well of an opaque 96-well plate. Samples of each lysate were prepared in triplicate in this manner. Following a subsequent 10-minute incubation step in the dark at room temperature, fluorescence intensity was quantified with a Flexstation fluorescent plate reader. Using double-stranded DNA (dsDNA) standards provided in the PicoGreen kit, a linear relationship was observed between PicoGreen fluorescence intensity and dsDNA. Lysates of known hBM-MSC

number were also used to determine a linear relationship between hBM-MSC number and PicoGreen fluorescence intensity.

2.6. Neutral Red Assay for quantification of cell viability

At the time points specified, cultures were washed with PBS and replaced with identical media + 10% Neutral red dye (Sigma-Aldrich). Samples were then incubated with hBM-MSCs for 2 hours in identical culture conditions as that prior to Neutral Red treatment. This was followed by sample fixation in 0.1% (w/v) Cadmium Chloride ($CdCl_2$) + 0.5% (w/v) PFA. Dye retained by hBM-MSC was solubilised in 1% (v/v) Acetic Acid + 50% (v/v) Ethanol for 10 mins with gentle agitation. Quantification of solubilised Neutral Red was then performed on an absorbance spectrophotometer at 540nm. Samples of known hBM-MSC number were also used to determine a linear relationship between hBM-MSC number and PicoGreen fluorescence intensity.

2.7. Sodium Dodecyl Sulfate-Polyacrylamide Gel Electrophoresis for separation of proteins in cell lysate based on molecular weight

Following 24-hours of culture, cells were washed once in PBS and lysed in a buffer consisting of 2M urea, 4.8% (v/v) Sodium Dodecyl Sulfate (SDS), 8% (w/v) sucrose (all Sigma Aldrich) in Deionised Water (dH_2O) for 10 minutes on ice. Lysates were then removed from the cell culture vessel with a cell scraper and transferred to 1.5ml Eppendorf tubes where they were passed through a 23-guage needle with a 1ml syringe. Samples were then stored at -20°C until quantification of total protein with the BCA assay kit from Thermo Fisher Scientific. Total protein levels were quantified

to enable equal loading of each conditions for the SDS-PAGE, thereby normalizing for changes in cell number at time of sample harvest .

For the Bicinchoninic Acid (BCA) assay, 25µl of each sample was mixed with 200µl BCA solution (1:50 ratio of 4% (w/v) cupric sulfate:sodium carbonate+sodium bicarbonate+BCA+sodium tartrate in 0.1M sodium hydroxide) in a single well of a 96-well plate followed by incubation for 30 mins at 37°C with gentle agitation throughout. The protein levels were then quantified using an absorbance spectrophotometer at 562nm wavelength. If sample were suspected to be highly concentrated or if lysate volume was low, samples were diluted by 2x or 5x in killer lysis buffer before mixing with BCA solution. 1, 0.8, 0.6, 0.4 and 0.2mg/ml solutions of Bovine Serum Albumin (BSA) were ran alongside samples of unknown protein concentration to generate a standard curve from which unknown concentrations could be determined.

For running on the SDS-Polyacrylamide Gel Electrophoresis (PAGE), all samples quantified using the BCA assay were diluted to the same concentration. Each sample was then further diluted in a 1:4 ratio with Laemmli loading buffer (Biorad) containing 10% (v/v) 2-mercaptoethnol (Sigma Aldrich) and boiled at 95°C for 5 minutes before resting on ice for 10 minutes. 40µl Prepared lysates in loading buffer were loaded into 10% (w/v) pre-cast PA gels (Biorad) and SDS-PAGE was performed at 120v for 45 minutes in which the Kaleidoscope™ ladder (Biorad) was also ran to enable determination of protein molecular weight in samples. The buffer used in the SDS-PAGE consisted of 0.3% (w/v) Trizma Base (Sigma Aldrich) + 1.4% (w/v) Glycine (Sigma Aldrich) + 1% (v/v) SDS (Sigma Aldrich) in dH_2O. Protein from the SDS-PAGE were

transferred using the Trans-Blot Turbo Transfer System (Biorad) onto Polyvinylidene difluoride (PVDF) membranes which were pre-soaked in absolute Ethanol and transfer buffer (40% (v/v) absolute ethanol + 20% (v/v) BioRad Transfer Buffer in dH_2O).

2.8. Western Blot for detection of proteins separated by SDS-PAGE

Following protein transfer, PVDF membranes were soaked in blocking solution (5% Non-fat milk (NFM) solution in TBST buffer (0.1% (v/v) Tween-20 (Sigma Aldrich) + Tris-HCL (Sigma Aldrich) in dH_2O)) for 1 hour at room temperature with gentle agitation. Membranes were then cut and the half in which proteins were of 100Kda or above were incubated in a solution of anti-HIF-1α antibody (h-206; Santa Cruz) diluted 1:200 in 5%NFM solution, overnight at 4°C with gentle agitation. The portion of the membrane in which proteins were below that of 100KDa in Molecular Weight (MW) were incubated with anti-β-Actin antibody (ab8227; Abcam) for 1 hour at room temperature with gentle agitation. β-Actin is a commonly-detected housekeeping protein whose expression does not change in response to hypoxic incubation. This therefore enabled normalization of the band due to HIF-1α to total protein/cell number of each sample .

Following multiple washes in TBST, membranes were treated with a horseradish peroxidase-conjugated secondary antibody (sc-2004; Santa Cruz) for 1 hour at room temperature with gentle agitation. Membranes were washed again in TBST and signal was generated from bound secondary antibody with the Chemiluminescent ECL substrate (Biorad) and was detected on a Chemidoc Touch imaging platform

(Biorad). HIF-1α and protein levels were generated by densitometric analysis with ImageJ and normalised to that of β-Actin.

2.9. Quantitative Polymerase Chain Reaction for quantification of mRNA

At time points specified, samples were washed in PBS, lysed in buffer consisting of 1% (v/v) 2-mercaptoethanol in RLT buffer (Qiagen) and stored at -80°C until RNA extraction procedure. RNA was extracted from lysates using the RNeasy Mini Kit (Qiagen) in which samples were lysed further by passing through Qiashredder spin columns before subsequent washes in RW1 and RPE buffers in RNeasy spin columns. RNA was eluted from the spin columns in RNase-free H_2O and quantified on a NanoDrop spectrophotometer.

100ng of RNA per sample was then reverse transcribed by first incubating with Random Primers (Promega) at 70°C for 5 minutes. cDNA complimentary to the input RNA was synthesized by incubation of the RNA-Random Primer solution for 1 hour at 42°C with a solution consisting of 4% (v/v) Moloney Murine Leukemia Virus Reverse Transcriptase (MLV-RT; Promega) + 20% (v/v) MLV-RT buffer (Promega) + 5.4% (v/v) Polymerase Chain Reaction (PCR) Nucleotide Mix (Promega) all in molecular biology H_2O (Sigma Aldrich). Resulting cDNA of 25µl final volume was stored at -20°C until amplification and quantification of specific transcripts with quantitative polymerase chain reactions (qPCR). The loading of 100ng of RNA in the RT of each sample ensures that the expression value obtained from the qPCR assay is normalized to cell number/total RNA content .

qPCR was carried out in a CFX384 (Biorad). Each qPCR reaction mixture consisted of 4ng cDNA template + 50% (v/v) Brilliant III Ultra-Fast SYBR® Green QPCR Master Mix

(Agilent) was used in conjunction with 250/500nM primers (IDT Technologies) specific to genes of interest. See qPCR reaction conditions and primer sequences in **Appendix Fig. 7A** and **Appendix Fig. 7B** respectively.

Raw cycle of Ct values were converted to transcript copy number by the relative standard curve method of analysis, and expression levels were normalised to transcript levels of *RPL13A* . Following normalisation to the housekeeping gene, expression levels were then normalised to that of the untreated control to determine fold change in expression induced by each treatment.

Optimal primers were identified through the use of cDNA from cell types theorised to express high levels of each transcript to which the primer is specific for. Each primer set tested following prediction of binding target with Nation Centre for Biotechnology Information (NCBI) Primer Blast was used to amplify serially diluted cDNA from these positive controls in order to generate standard curves. These standard curves were used to identify the existence of a linear expression between input cDNA concentration and Ct value in addition to enabling quantification of the reaction efficiency. Selection criteria for each gene of interest: single predicted product in NCBI Primer Blast results, a single peak in melt curve compared to no-template control in which dH_2O replaces the cDNA template and an R^2 value of >0.9, theoretical reaction efficiency of 90-110%.

2.10. Immunodetection of proteins in cultures on tissue culture plastic

Cultures were washed in PBS, fixed in 4% (w/v) PFA for 15 minutes before further PBS washes and storage at 4°C until immunofluorescent staining protocol. Following a blocking and permeabilisation period of 1 hour at room temperature in 10% (v/v)

goat serum (Sigma Aldrich) + in 0.1% (v/v) Triton X-100 (Sigma Aldrich) in H_2O (PBT), fixed monolayers were treated with primary antibody (see **Appendix Fig. 8** for specific antibodies and concentrations) made up in blocking solution overnight at 4°C. After binding of the primary antibody to the specific antigen, monolayers were washed in 0.1% (v/v) PBT. Rabbit-derived primary antibodies were visualised by incubating monolayers with ab150077 (Abcam) for one hour at room temperature (dilutions in blocking solution are specified in **Appendix Fig. 8** for detection of each primary antibody). Mouse-derived primary antibodies were detected by treatment with biotin (ab6788, Abcam) for one hour at room temperature and Streptavidin (S11223, Thermo Fisher Scientific) for one hour at room temperature with both diluted by 1:350 in blocking solution. Cultures were counterstained with 0.1µg/ml 4',6-diamidino-2-phenylindole (DAPI; Sigma Aldrich) for 1 hour min to visualise cell nuclei and fluorescent signal was imaged on an Axiovert200M microscope (Zeiss).

2.11. Immunofluorescence staining of proteins in cultures on PA gels

Cultures were washed in PBS, fixed in 4% (w/v) PFA for 15 minutes before multiple 15-minute PBS washes with gentle agitation. Samples were stored at 4°C until immunofluorescent staining protocol. Following a blocking and permeabilisation period of 1 hour at room temperature in 5% (w/v) BSA + in 0.1M Triton X-100 in H_2O (PBT), fixed PA gels were treated with primary antibody (see **Appendix Fig. 8** for specific antibodies and concentrations) made up in 5% (w/v) BSA + PBT overnight at 4°C. After binding of the primary antibody to the specific antigen, monolayers were washed in 3% (w/v) BSA (Sigma Aldrich) + PBT with gentle agitation. Rabbit-derived primary antibodies were visualised by incubating monolayers

with ab150077 (Abcam) for one hour at room temperature (dilutions in 5% (w/v) BSA + PBT are specified in **Appendix Fig. 8** for detection of each primary antibody). The secondary antibody solution also included 0.1µg/ml DAPI to visualise cell nuclei and fluorescent signal was imaged on an Axiovert200M microscope (Zeiss). Following imaging of signal generated due to detection of specific antigen, PA gels were re-stained with Phalloidin (Sigma Aldrich) at 1:200 dilution in PBS for visualisation of the actin cytoskeleton.

2.12. Alcian Blue Staining for detection of glycosaminoglycans

At time point specified, cultures were washed in PBS, fixed in 4% (w/v) PFA, washed subsequently in PBS and stored at 4^{O}C until Alcian Blue staining protocol. Staining procedure was as follows. Samples were first washed in 0.1N HCL and stained overnight at room temperature with 1% (w/v) Alcian Blue solution, pH 1.0 (Sigma Aldrich) prepared in 0.1N HCL. Following another 0.1N HCL wash, stained cultures were then rinsed repeatedly in PBS until the waste PBS no longer contained any residual Alcian Blue dye. Samples were then counterstained with Haematoxylin (Vector Laboratories) to visualise cell nuclei and washed in PBS until the waste PBS no longer contained any residual Haematoxylin dye. Staining was imaged with an Axiovert200M microscope (Zeiss).

2.13. Glycosaminoglycan quantification

At day 21 of chondrogenesis, cultures were washed in PBS and frozen at -80 °C before their digestion in Papain buffer as described in protocol for cell lysis for the PicoGreen assay. Glycosaminoglycans were quantified from papain-digested lysates using the

GAG assay kit by Blyscan™ in which GAGs were dyed with 1,9-dimethyl-methylene blue and subsequently dissociated with Propan-1-ol solution before quantification on an absorbance spectrophotometre at 640nm. Values per culture were normalised to levels of dsDNA, which were quantified using the PicoGreen assay .

2.14. Immunofluorescence quantification

Immunofluorescence images were captured using identical gain, exposure and offset for all conditions in each experiment. These were determined with positive controls that expressed the antigen of interest, and negative controls in which the primary antibody was omitted. The same threshold fluorescence intensity for images of all conditions within an experiment was set and signal below this threshold was negated as non-specific immunofluorescence. The signal produced above the threshold was regarded as *bona fide* protein detection and was used to create a binary representation of the protein localisation pattern of each image. The percentage of immunofluorescence staining present within a specified area was then determined for each image within each condition. This percentage was then normalized to the number of DAPI-positive cells to account for changes in cell number due to proliferation/cell death .

2.15. Quantification of cell colonies, area, circularity and HIF-1α/YAP nuclear localisation

For quantification of cell colonies, area, circularity and HIF-1α/YAP nuclear localisation, images were analysed in ImageJ. For quantification of colonies,

Phalloidin staining of actin cytoskeleton was used. The same threshold of fluorescence intensity was set for images of all conditions within a single experiment and below this threshold, the signal produced was negated as non-specific immunofluorescence. The signal produced above the threshold was regarded as *bona fide* protein detection and was converted to a binary representation of the protein localisation pattern of each image. Using the corresponding DAPI channel as a reference, colonies were counted based on classification of direct cell-cell contact occurring with those not engaged in cell-cell contact classified as single cells (**Appendix Fig. 10B**).

Number of single cells and colonies were quantified in this manner and total cells quantified in DAPI channel. Area of counted single cells and colonies in addition to single cell circularity were also quantified using the 'measure' function in ImageJ following thresholding and creation of binary images as described above.

For quantification of HIF-1α/YAP nuclear localisation, DAPI channel and Alexa488 channel indicating HIF-1α/YAP signal were used. As before, thresholding and binary representations were created from each image. Each DAPI-stained nuclei was selected in each image and these selections were superimposed onto the corresponding Alexa488 channel. ImageJ's 'measure' function was utilised to quantify the percentage of signal present within each DAPI-demarcated area in the Alexa488 channel.

2.16. Statistical Analysis

All statistical analyses were performed in Prism7 (GraphPad) with the Mann-Whitney test used to compare two conditions and Kruskal-Wallis with Dunn's Correction for

multiple condition comparisons. Non-parametric tests were used as we were unable to demonstrate normality in all datasets. Data comprise biological replicates (n stated in figure legends), where each replicate represents a single cell culture experiment. *marks all differences which were statistically significant (p<0.05).

3. The role of low oxygen concentration during chondrogenic induction of human bone marrow-derived mesenchymal stem cells.

3.1. Introduction

CTE is required due to the insufficiency of palliative, reparative and restorative strategies for treatment of acute chondral and osteochondral defects. hBM-MSCs may represent the most suitable source for CTE due to their ease of isolation, ability to be expanded without loss of multipotency and the patient specificity of autologous cells. However, a potential limitation to the use of this cell type in articular CTE is the propensity for their differentiation into cells with hypertrophic characteristics. This is suggested due to observation of *COL10A1* and *COL1A1* mRNA expression in BM-MSCs prior to chondrogenesis [386, 387]. This indicates a priming of these cells for secretion of collagens required for hypertrophic and fibrotic cartilage respectively. BM-MSC pellet culture and chondrogenesis has also been shown to progressively upregulate the expression of both *COL10A1* and *IL1B* mRNA compared to that prior to induction [388]. *IL1B* encodes Interleukin-1β which is a pro-inflammatory cytokine shown to induce articular cartilage hypertrophy [389] and development of an osteoarthritic phenotype [390]. As pertained to, TGF-β-mediated CTE may also result in chondrocyte hypertrophy [198] which may result in mineralisation of the regenerated tissue within the chondral defect site [196].

From formation of the limb bud, through to cartilage growth plate formation and during homeostasis of adult articular cartilage, there exists a hypoxic state in which the mesenchymal progenitors and articular chondrocytes reside. Hypoxia and HIF

play essential roles in the proliferation, differentiation and maintenance of the articular chondrocyte phenotype. Unlike that of specific growth factors which are expressed in specific temporal patterns, hypoxia is constitutively present and plays active role throughout articular cartilage development [259, 262]. This suggests a potential role for hypoxia and HIF in CTE. Hypoxia has been shown to block chondrocyte hypertrophy and ossification. This demonstrates its potential for reducing the drawbacks associated with TGF-β treatment, whilst still allowing chondro-induction and cartilage formation.

The potential for hypoxic signalling in CTE is demonstrated, for example, in a study in which BM-MSCs and chondrocyte co-cultures were differentiated within PE micro-fibre scaffolds. Hypoxic incubation of differentiating cultures within these constructs induced expression of chondrogenic mRNA and GAG production, in addition to reducing activity of ALP [391]. Duval et al also demonstrated a role for hypoxia in improving the chondrogenic differentiation of hBM-MSCs cultured in alginate beads. These authors observed the induction of chondrogenic mRNA and reduction of transcripts which encode factors conducive for chondrocyte hypertrophy. An increased formation of a Collagen Type II and GAG-rich ECM was also observed of hypoxia-induced, alginate-encapsulated MSCs following subcutaneous implantation into mice [272]. The ability of hypoxia to alleviate chondrocyte hypertrophy in PLGA scaffolds was also demonstrated. Tan et al observed a decrease in expression of *RUNX2* and *COL10A1* and an increase in the ratio of *COL2A1*/*COL1A1* mRNA due to 2%O_2, compared to incubation at 20%O_2 [392]. Hypoxia in this study also increased detection of Collagen and GAGs in the ECM within the PLGA scaffolds compared to normoxic controls.

The role of hypoxia in chondrogenic differentiation and maintaining the phenotype of articular chondrocytes relative to CTE approaches conducted at normoxia, highlights the potential role for hypoxia in the repair of acute chondral defects. A key question however, is that which asks of the severity of hypoxia required to promote articular chondrogenesis. The studies by Meretoja and Duval described above utilised 5% oxygen as their hypoxic condition, with others performing chondrogenic induction of BM-MSCs at 3% oxygen for example [393]. Without a direct comparison during chondrogenic induction, it is impossible to determine the optimal oxygen concentration required to improve this process. For example, the oxygen concentrations in the studies by Meretoja and Duval cannot be directly compared with that by Bornes et al, due to the use of differing biomaterial scaffolds, which may influence the chondrogenic differentiation program of seeded cells.

Foldager et al demonstrated a trend towards increased mRNA expression of *SOX9, ACAN and COL2A1* with the oxygen concentration decreased from 21, to 5, to 1% during both scaffold and monolayer culture of primary articular chondrocytes [394]. Increased GAG release was also observed from human osteoarthritic chondrocytes due to 2% oxygen compared to those cultured at 5%O_2 [395]. These and other studies identifying lower oxygen concentrations as more potent HIF stabilisers [396] points to the importance of identifying the optimal hypoxic oxygen concentration for MSC-based CTE efforts. However, to date there exists no such direct comparison of 5% and lower values during hBM-MSC chondrogenesis. Therefore, the aims, hypothesis and objectives for the current chapter are as follows:

- **Aim**: Identify which of 5% or 2% oxygen induces greater chondrogenic induction of hBM-MSCs in a 2D system on tissue culture plastic (TCP).

- **Hypothesis**: 2% oxygen stimulates greater stabilisation of HIF transcriptional complex than 5%O_2, resulting in a greater level of chondrogenic induction.

- **Objectives**:
    - To identify which of 2% or 5%O_2 more potently stimulates HIF stabilisation and downstream transcriptional activity during *in vitro* hBM-MSC chondrogenic induction on TCP.
    - To identify which of 2% or 5%O_2 more potently stimulates articular chondrogenesis and cartilage ECM formation during *in vitro* hBM-MSC chondrogenic induction on TCP.
    - To identify which of 2% or 5%O_2 more potently inhibits hypertrophy during chondrogenesis during *in vitro* hBM-MSC chondrogenic induction on TCP.

3.2. Results

3.2.1. Comparison of TGF-β_1 and TGF-β_3 during chondrogenic induction of hBM-MSCs as monolayer and pellet cultures

A difference between 2% and 5% oxygen regarding the degree of hBM-MSC chondrogenesis induced may inform CTE strategies in which hypoxia is to be utilised. We initially optimised chondrogenic induction of primary hBM-MSCs in a 2D monolayer culture system . This is due to the heterogeneity exhibited by BM-MSCs from different donors in terms of regulation of the molecular pathways required for their expansion and chondrocyte differentiation. BM-MSCs from female donors for example, exhibit higher clone-forming ability than their male counterparts, resulting in a higher proliferation rate [397]. BM-MSCs from differing donors also underwent varying degrees of chondrogenic induction, with changes in SOX9, Aggrecan and Collagen Type II protein demonstrated [398].

TGF-β ligands via SMAD3 are the most established drivers of *in* vitro chondrogenesis from hBM-MSCs [77]. The indispensable role of TGF-β ligands in chondrogenic differentiation of limb bud progenitors and cartilage ECM production during limb development rationalizes their use within an *in vitro* model of stem cell chondrogenesis [189]. Current methods for *in vitro* chondrogenesis utilise either TGF-β_1 or TGF-β_3 with no overwhelming preference for either demonstrated in the literature. Therefore a comparison of these two growth factors during chondrogenesis at was employed, with Alcian Blue staining for GAG's utilised at day 21 of culture. As shown previously, Alcian Blue staining is a rudimentary indicator of

chondrogenesis with GAGs representing a large constituent of cartilage ECM [399], with a timepoint such as day 21 chosen to maximize the presence of GAGs .

The concentration of 10ng/ml used for TGF-β_1 and TGF-β_3 represents that used by the vast majority of studies in which BM-MSCs are chondrogenically induced . In addition, to ensure that differentiating BM-MSCs were exposed to a bioactive concentration of either TGF-β ligand throughout the differentiating period, cultures were replaced with fresh chondrogenic media at 3-4 day intervals . Treatment of TGF-β1/TGF-β_3 was also combined with culture of hBM-MSCs at a high cell density. This is due to the importance of mesenchymal condensation of the limb bud at the onset of embryonic chondro-induction [400]. TGF-β_1/TGF-β_3 were also used in conjunction with Dexamethasome, L-Proline and Ascorbic Acid-2-Phosphate due to the role of these supplements in promoting cartilage ECM production *in vitro* [140, 184, 401] .

Following 21 days of BM-MSC chondrogenic induction, no difference was observed in Alcian Blue staining of GAGs between cultures exposed to TGF-β_1 or TGF-β_3-containing chondrogenic induction media (**Figs. 3.1A-3.1C**). This time point was chosen due to previous demonstration that abundant GAG production represents later stages of chondrogenic induction [402]. Adult bovine chondrocytes have also previously been used as an *in vitro* cartilage model due to the ability of these cells to abundantly produce cartilage ECM proteins in response to stimulatory conditions [403]. Therefore the effect of TGF-β_1 and TGF-β_3 again at 10ng/ml was compared with regards to GAG production from Bovine chondrocytes following 7 and 14 days of culture. At both time points, GAG production by bovine chondrocytes was greater due to TGF-β_3 (**Figs. 3.1E+3.1G**) compared to that induced by TGF-β_1 (**Figs. 3.1D+3.1F**)

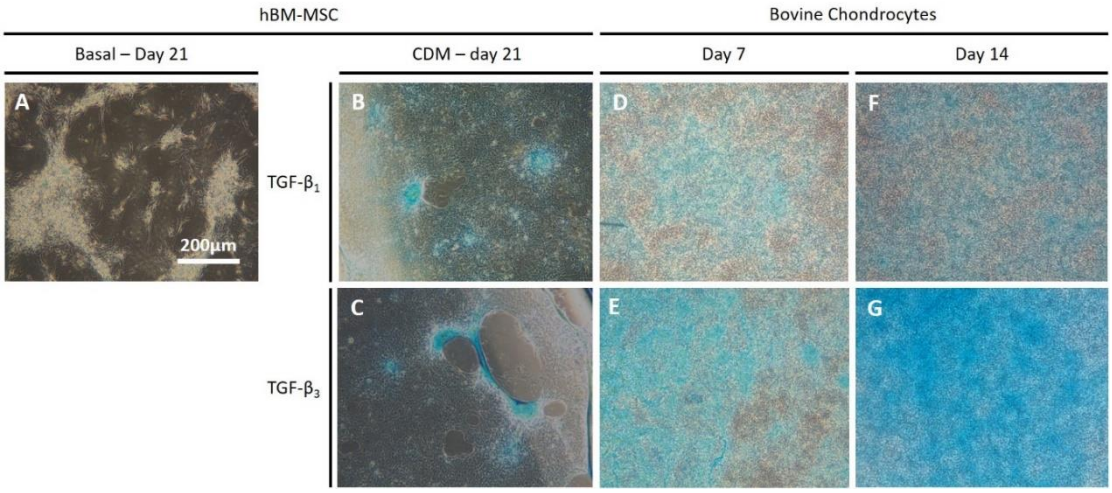

Figure 3.1. Comparison of TGF-β_1 and TGF-β_3 for inducing presence of GAGs in ECM. Alcian Blue staining of GAG's in the ECM surrounding hBM-MSCs and Bovine Chondrocytes in presence of TGF-β_1/TGF-β_3-containing chondrogenic media. A: hBM-MSCs at day 21 of culture in expansion conditions. B+C: hBM-MSCs at day 21 of chondrogenic induction in presence of TGF-β_1 (B) and TGF-β_3 (C). D+E: Bovine chondrocyte cultures at day 7 of culture in chondrogenic media consisting of TGF-β_1 (D) and TGF-β_3 (E). F+G: Bovine chondrocyte cultures at day 14 of culture in chondrogenic media consisting of TGF-β_1 (F) and TGF-β_3 (G).

3.2.2. Effect on Collagen Type II mRNA and protein synthesis by human Bone Marrow-derived Mesenchymal Stem Cells following TGF-β_3-mediated chondrogenic differentiation

Following observation that TGF-β_3 enhanced GAG production from chondrogenically-induced hBM-MSCs compared to that due to TGF-β_1, an effect on Collagen Type II mRNA and protein was assessed due to TGF-β_3. This is due to the importance of Collagen Type II both during chondrogenesis and in cartilage ECM function [29]. mRNA encoding the alpha helix of Collagen Type II was examined due to the importance of *COL2A1* transcription during cartilage development [404] . Immunostaining of Collagen Type II in chondrogenically-differentiated cultures was also conducted due to the large number of post-transcriptional regulatory elements of Collagen Type II. Visualisation of Collagen Type II protein therefore indicates formation of mature articular cartilage ECM [394] and as with GAG production , was examined at day 21 due to this stage representing that at which adult cartilage is formed *in vitro* ((Solchaga, 2011 #1364)) . Expression of Collagen Type mRNA has previously been shown to be upregulated prior to Collagen Type II production and incorporation into the ECM at day 21. This therefore prompted investigation of *COL2A1* expression at 14 of *in vitro* cartilage induction [269] .

Figure 2 displays the optimisation of protocols conducted for *COL2A1* mRNA quantification and Collagen Type II immunostaining. The suitability of primers which enabled specific amplification of the *COL2A1* gene was assessed by generation of a standard curve in which the concentration of serially-diluted cDNA from the chondrocyte cell line; C28/I2 were plotted against cycle number (**Fig. 3.2A**). This was

also repeated for identification of an optimal housekeeping gene to which all expression values in this study were normalised. Primers specific to the housekeeping gene; *RPL13A* were used (**Fig. 3.2B**). The *COL2A1* and *RPL13A* standard curves demonstrate a linear relationship between cDNA concentration and cycle number in addition to amplifying target cDNA with a theoretical efficiency between 90-110%. **Fig. 3.2D** demonstrates the binding of Collagen Type II by the primary antibody used in the immunostaining protocol here, following 21 days of chondrogenic induction. This is in contrast to that at day 0 of chondrogenesis (**Fig. 3.2C**) . The lack of signal in figure **3.2E** demonstrates that the signal observed in **Fig. 3.2D** is due to the primary antibody and is not background signal or that due to the secondary antibody to which the fluorophore is conjugated.

mRNA was extracted from differentiating cultures at day 14 and TGF-β_3 was observed to increase levels of the *COL2A1* transcript by 3-fold compared to that induced without TGF-β_3. This was confirmed statistically by comparison of the averaged expression values due to each condition using a Mann-Whitney test (**Fig. 3.3A**). Even in the absence of TGF-β_3, differentiating cultures at day 21 produced condensed clusters of Collagen Type II (**Fig. 3.3B**) and GAGs (**Fig. 3.3D**) as assessed by Collagen Type II immunostaining and the Alcian Blue histochemical stain respectively . This suggests an ability of high-density cultures + non-growth factor supplements in enabling a degree of cartilage ECM formation. This may perhaps have been predicted due to the ability of Dexamethasome, L-Proline and Ascorbate-2-Phosphate to induce ECM production. Despite this however inclusion of TGF-β_3 appeared to increase the levels of Collagen Type II and GAGs (**Figs. 3.3C+3.3E**), demonstrating the use of this growth factor and overall culture system (cell density of 30,000/cm^2 on

TCP) in our model of chondrogenesis. These precise culture conditions were therefore utilised throughout this chapter and chapter 5 of this document.

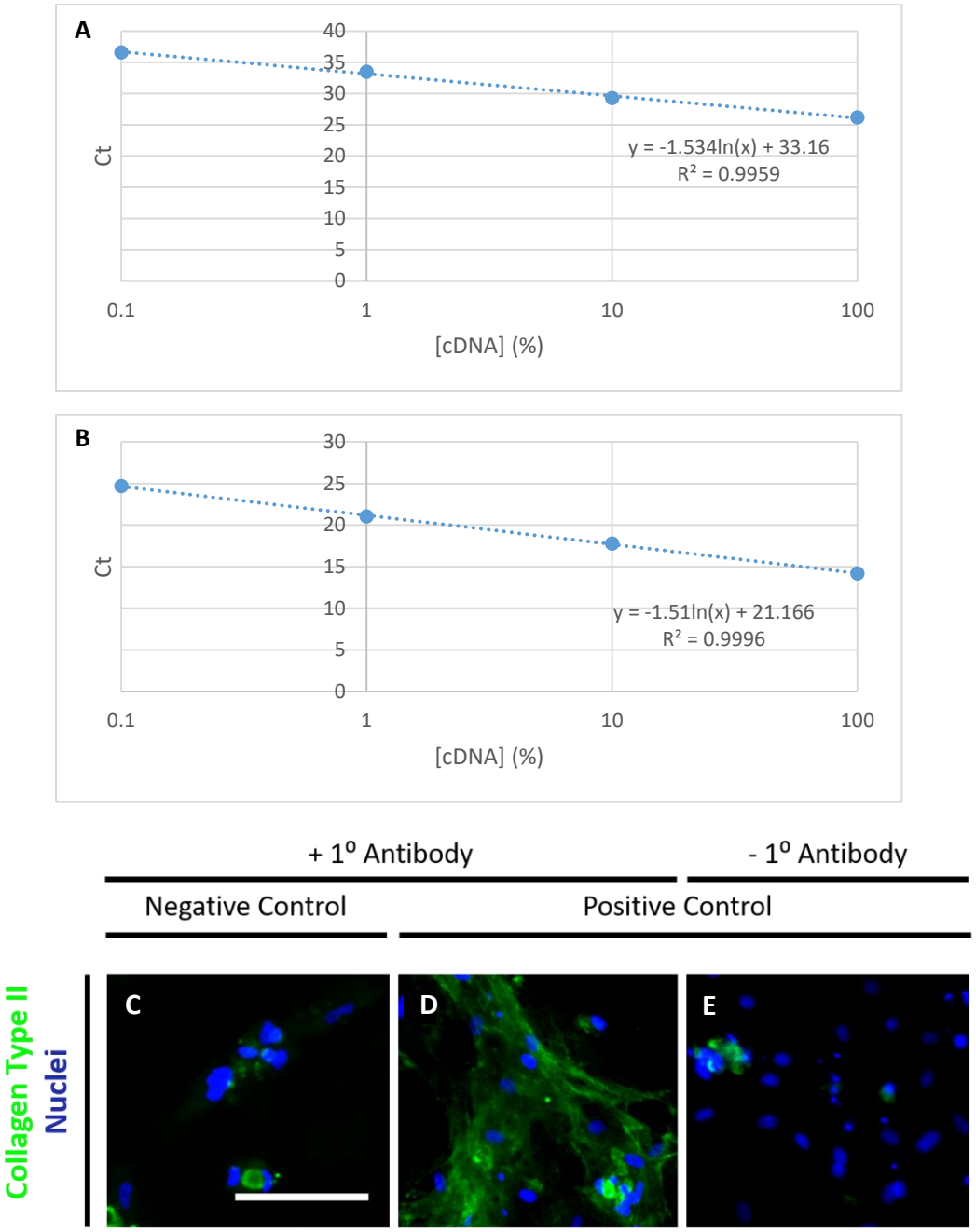

Figure 3.2. Identification of *COL2A1*-specific primers and optimization of Collagen Type II immunostaining. (A+B) Standard curve which demonstrates a linear relationship between input cDNA concentration and cycle (Ct) number when amplified using *COL2A1* (A) and *RPL13A* (B)-specific primers. (C-E) Immunostaining of Collagen Type II in BM-MSC cultures incubated at 20%O_2 at days 0 (C) and 21 (D+E) of chondrogenesis. Images C+D demonstrate immunofluorescent signal following an immunostaining protocol in which the primary antibody was included. Image E was taken following an immunostaining protocol in which the primary antibody was omitted. Scale bar = 200µm.

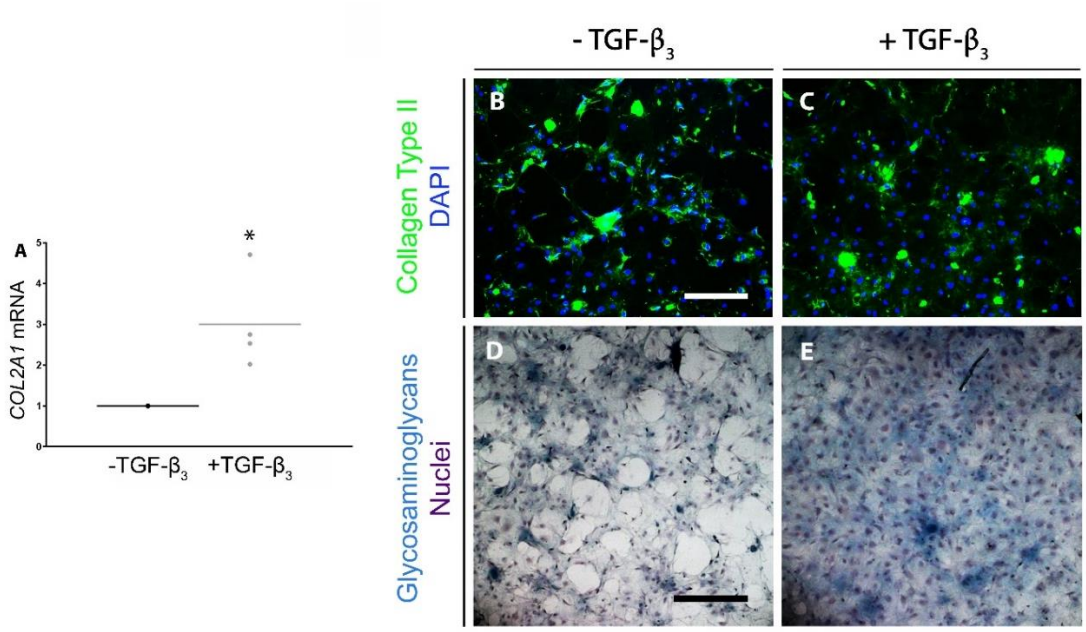

Figure 3.3. TGF-β$_3$-containing chondrogenic differentiation medium enhances chondrogenesis of hBM-MSCs. (A) mRNA expression of COL2A1 at day 14 of differentiation under normoxic conditions after normalization to expression of the housekeeping gene; *RPL13A*. Values plotted are fold change relative to -TGF-β3 condition from 4 independent experiments, with the solid line representing the mean. *denotes p<0.05 compared to -TGF-β$_3$ when compared with a Mann Whitney test. (B+C) Collagen Type II immunostaining with DAPI counterstain at day 21 of differentiation. Scale bar = 400µm. Representative images of 3 independent experiments are shown. (D+E) Alcian Blue staining for glycosaminoglycans with haematoxylin counterstain at day 21 of differentiation under normoxic conditions. Scale bar = 400µm. Representative images of 3 independent experiments are shown.

3.2.3. Hypoxia Inducible Factor stabilisation by 5% and 2%O_2

Following identification of TGF-β_3-containing induction media as a driver of *in vitro* BM-MSC chondrogenesis, the next aim was to examine the ability of either hypoxic state; 2/5%O_2 in stimulating the HIF pathway – the archetypal response of cells to physiological hypoxia. Each hypoxic state was induced by the culture of BM-MSCs within incubators into which specific levels of Nitrogen gas are introduced to displace the oxygen and alter its bioavailability to cultured cells . BM-MSCs were induced with TGF-β_3-containing chondrogenic media as before in a 2D, TCP system but incubated at either hypoxic state for the full differentiating period. The phenotype of the chondrogenically-induced cultures which were incubated at hypoxia were compared with cultures differentiated at the normoxic (20%O_2) condition.

Cultures were exposed to hypoxia throughout the entire differentiating protocol due to the constitutive presence of this factor during *in vivo* cartilage development [259, 262] . Compared to normoxic conditions, constitutive hypoxia *in vitro* did not negatively affect cell number throughout the differentiating process, thus suggesting their suitability for further experiments . This is illustrated by immuno-labelling and counting the number of nuclei in day 21 BM-MSC cultures which were chondrogenically induced at 20%, 5% and 2%O_2 (**Fig. 3.4A**).

One of the key biological markers of physiological hypoxia is increased total HIF-1α – the oxygen-responsive subunit of HIF as well as its enhanced nuclear localization. HIF-1α protein levels are controlled by the hydroxylase; PHD2 whose inhibition reduces HIF-1α degradation and correspondingly, increases its stabilization [405] . Therefore, increased HIF-1α due to either 2 or 5%O_2 compared to normoxic conditions would

demonstrate the ability of these hypoxic states to block availability of oxygen to the active sites of PHD2 and in doing so, stimulate the HIF pathway. This may therefore indicate the ability of 2 and 5% O_2 to induce BM-MSC chondrogenesis compared to normoxic conditions, due to HIF activity being shown to enhance cartilage formation *in vitro* [272]. When assessed by whole-cell Western Blot, which is a common method utilised to determine total HIF-1α levels and therefore its stability [406] , both 5% and 2%O_2 increased HIF-1α stabilisation at day 1 of chondrogenesis compared to normoxic controls (**Fig. 3.4B**). This was validated by densitometric analysis of each biological repeat in which the levels to due to either hypoxic state were shown to be significantly higher than that at normoxia, as assessed by the Mann Whitney test (**Fig. 3.4C**). The day 1 time point was selected due to the relatively rapid and acute upregulation of HIF-1α protein by hypoxia under chondrogenic conditions [407] .

As with total HIF-1α protein levels, HIF-1α nuclear localization is an indicator of PHD2 inhibition and suppression of HIF-1α degradation . This is due to evidence which demonstrates the passive translocation of HIF-1α into the nucleus and inhibition of this phenomenon occurring only due to PHD2-mediated HIF-1α degradation [44] . Conversely, increased levels of this protein results in enhanced nuclear translocation of HIF-1α and binding to target DNA sequences with the HIF complex [408] . The ability of 5% and 2%O_2 to induce HIF-1α nuclear localisation was assessed by immunostaining for this protein. This was followed by semi-quantification of HIF-1α within the subcellular compartments of BM-MSCs in the resulting immunofluorescent images. As with analysis of total HIF-1α protein, this was conducted at day 1 of chondrogenesis. Under each condition, the total area of immunofluorescent signal due to the HIF-1α-specific antibody used, whose intensity

was above a standardized threshold, was measured in the nucleus of each cell. This value was then converted into a percentage of the total nucleus area of each cell which was demarcated by DAPI immunostaining .

Both reduced oxygen concentrations appeared to induce more nuclear HIF-1α (**Figs. 3.4E+3.4F**) compared to the normoxic control (**Fig. 3.4D**). Quantification of HIF-1α translocation in these images validated this observation in which nuclear localization due to either hypoxic state were shown to be significantly higher than that at normoxia, as assessed by the Mann Whitney test (**Fig. 3.4G**). At each hypoxic level compared to that at normoxia, there was an increased number of BM-MSCs in which over 50% of the nucleus was occupied by HIF-1α.

Interestingly, HIF-1α protein was detected in normoxic cultures by Western Blot (**Fig 3.4B**) but localisation appeared to be solely restricted to the perinuclear region of differentiating BM-MSCs (**Fig. 3.4D**). This perinuclear localisation of HIF-1α was also observed in each hypoxic condition which accompanied the increased nuclear presence of this protein (**Fig. 3.4E+3.4F**). **Figure 3.4H** illustrates that the signal generated in BM-MSC cultures at 2%O_2 compared to 20%O_2 is due to the HIF-1α antibody used and background fluorescence or due to the secondary antibody. It is important to note that nuclear fractionation of chondrogenically-induced BM-MSCs was attempted for the purpose HIF-1α semi-quantification by Western Blot in the nuclear compartment only. However, low levels of total protein per sample prevented us from doing so .

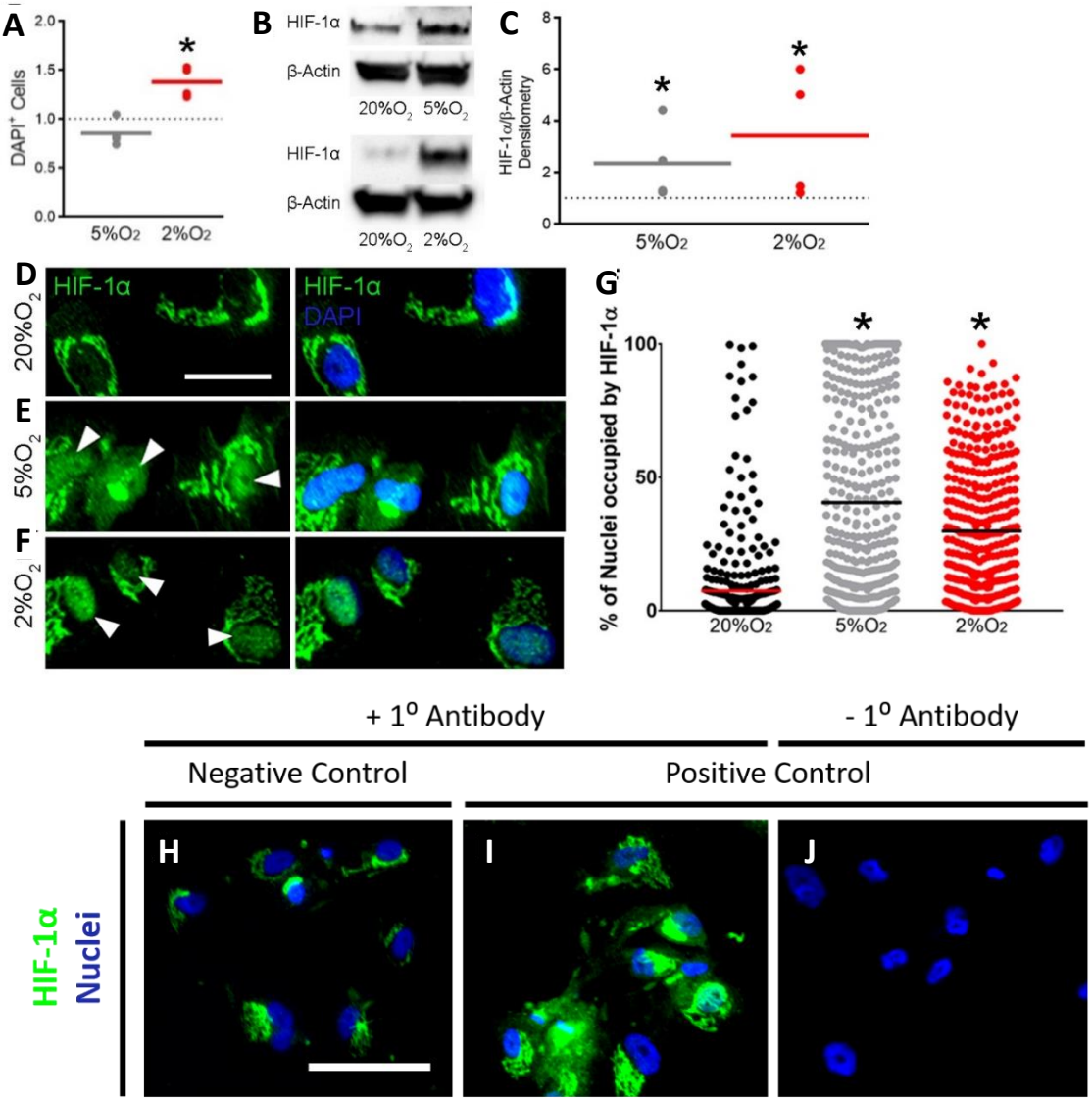
A
DAPI+ Cells
5%O2
2%O2
B
HIF-1α
β-Actin
20%O2
5%O2
HIF-1α
β-Actin
20%O2
2%O2
C
HIF-1α/β-Actin Densitometry
5%O2
2%O2
D
20%O2
HIF-1α
HIF-1α
DAPI
E
5%O2
F
2%O2
G
% of Nuclei occupied by HIF-1α
20%O2
5%O2
2%O2
+ 1° Antibody
- 1° Antibody
Negative Control
Positive Control
H
I
J
HIF-1α
Nuclei

Figure 3.4. Both 5% and 2% oxygen levels increase total HIF-1α levels and nuclear localisation. (A) Detection of HIF-1α, and housekeeping protein β-Actin at day 1 of chondrogenesis by Western Blot. Representative image of 4 experimental repeats shown. (B) Protein blots of HIF-1α were quantified by densitometric analysis and normalised to levels of β-Actin. Values plotted represent magnitude difference to 20%O_2 condition represented by the horizontal dotted line, with the solid coloured lines representing the mean for each condition and *denoting p<0.05 compared to 20%O_2 when assessed by the Mann Whitney test. (C-E) HIF-1α immunofluorescence staining at day 1 of chondrogenesis. Scale Bar = 50μm. Representative images of 3 independent repeats shown. Images were cropped and magnified to clearly visualise localisation of HIF-1α. Brightness and contrast was adjusted for all channels to an equal degree between all conditions. (F) Quantification of nuclear HIF-1α immunofluorescence at day 1 of chondrogenesis. Each value plotted represents the percentage of a single DAPI-stained nucleus that is occupied by HIF-1α. Values from 3 independent repeats shown with the red/black horizontal lines representing the mean and *denoting p<0.05 compared to 20%O_2 when assessed by the Mann Whitney test. (B-D) Immunostaining of HIF-1α in BM-MSC cultures incubated at 20%O_2 at days 1 of chondrogenesis at 20% (H) and 2%O_2 (I+J). Images H+I demonstrate immunofluorescent signal following an immunostaining protocol in which the primary antibody was included. Image J was taken following an immunostaining protocol in which the primary antibody was omitted. Scale bar = 100μm.

3.2.4. Induction of Hypoxia Inducible Factor target gene expression by 5% and 2%O_2

Following HIF-1α stabilisation and increased nuclear localization, an indicator of HIF-1α upregulation is expression of genes whose promoters contain a HRE to which the HIF complex binds and induces transcription. In addition to being regulated by PHD2-mediated HIF-1α degradation, the hydroxylase; FIH when active, hydroxylates HIF-1α and inhibits binding by its co-factors that are required for transcription of target genes. Therefore, expression of HIF target genes in BM-MSCs during TGF-β_3-mediated chondrogenesis at 2/5%O_2, may indicate inhibition of both PHD2 and FIH and induction of HIF activity by these hypoxic states .

To assess HIF-mediated transcription of target genes, qPCR was utilised to quantify exact number of mRNA transcripts. BM-MSC cultures differentiated in the TGF-β_3-mediated chondrogenic conditions optimized here, at 20%/5%/2%O_2, were lysed and RNA was collected at specific time points. A day 1 time-point was selected to complement the studies into HIF-1α protein level and localization shown above and to assess early, acute effects of each oxygen concentration . PGK1, EGLN and VEGFA mRNA was also quantified at day 14 at which point, mature chondrogenic differentiation of progenitor cells is undergoing [269]. This would indicate HIF stabilisation and expression of HIF targets during chondrogenesis . Analysis of HIF target expression at day 14 would enable correlations to be made between the expression of established HIF targets, with those indicating chondrogensis .

The mRNA levels of three established HIF targets were assessed. *VEGFA* encodes a growth factor which is upregulated in response to ischemic conditions, as a primary mediator of vasculogenesis [409]. The product of *PGK1* – Phosphoglycerate Kinase 1

(PGK1) is part of the array of glycolytic enzymes upregulated in response to hypoxia which enables the switch from aerobic to anaerobic respiration [410]. *EGLN* encodes the hydroxylase, PHD2 which is upregulated by HIF to provide a negative feedback loop and preventing hyper-activation of HIF-mediated transcription [411] . *RPL13A* has been shown to be the most appropriate housekeeping gene for gene expression analysis of cultures exposed to physiological hypoxia. Its expression does not change significantly in response to hypoxic stimulation unlike that of *GAPDH* or *ACTB* [412] . *RPL13A* was therefore used throughout this and the next two chapters for normalization of gene expression data.

The suitability of primers specific to *VEGFA*, *PGK1* and *EGLN* were assessed by generation of a standard curve in which the concentration of serially-diluted cDNA from the chondrocyte cell line; C28/I2 were plotted against cycle number (**Figs. 3.5A-3.5C**). Each standard curve demonstrated a linear relationship between cDNA concentration and cycle number in addition to amplifying target cDNA with a theoretical efficiency between 90-110%.

Following identification of optimal primers, *VEGFA*, *PGK1* and *EGLN* transcripts were amplified and quantified in differentiating cultures. Both 5% and 2%O_2 significantly (p=<0.05) increased expression of *VEGFA* (**Fig. 3.5D**), *PGK1* (**Fig. 3.5E**) and *EGLN* (**Fig. 3.5F**), at day 1 of chondro-induction compared to that at 20%O_2. However at day 14 of culture, only 2%O_2 maintained this increase of all three genes compared to normoxic conditions (**Figs. 3.5G-5I**). Furthermore, 2%O_2 induced expression of *VEGFA* (**Fig. 3.5G**) and *EGLN* (**Fig. 3.5I**) to significantly higher levels than induced by 5%O_2. *PGK1* expression was increased by 5%O_2 at day 14 compared to 20%O_2 (**Fig. 3.5H**).

Overall both 2 and 5%O_2 appear to induce HIF-1α stabilisation and expression of HIF target genes, but only 2%O_2 maintained this at later stages of chondrogenesis.

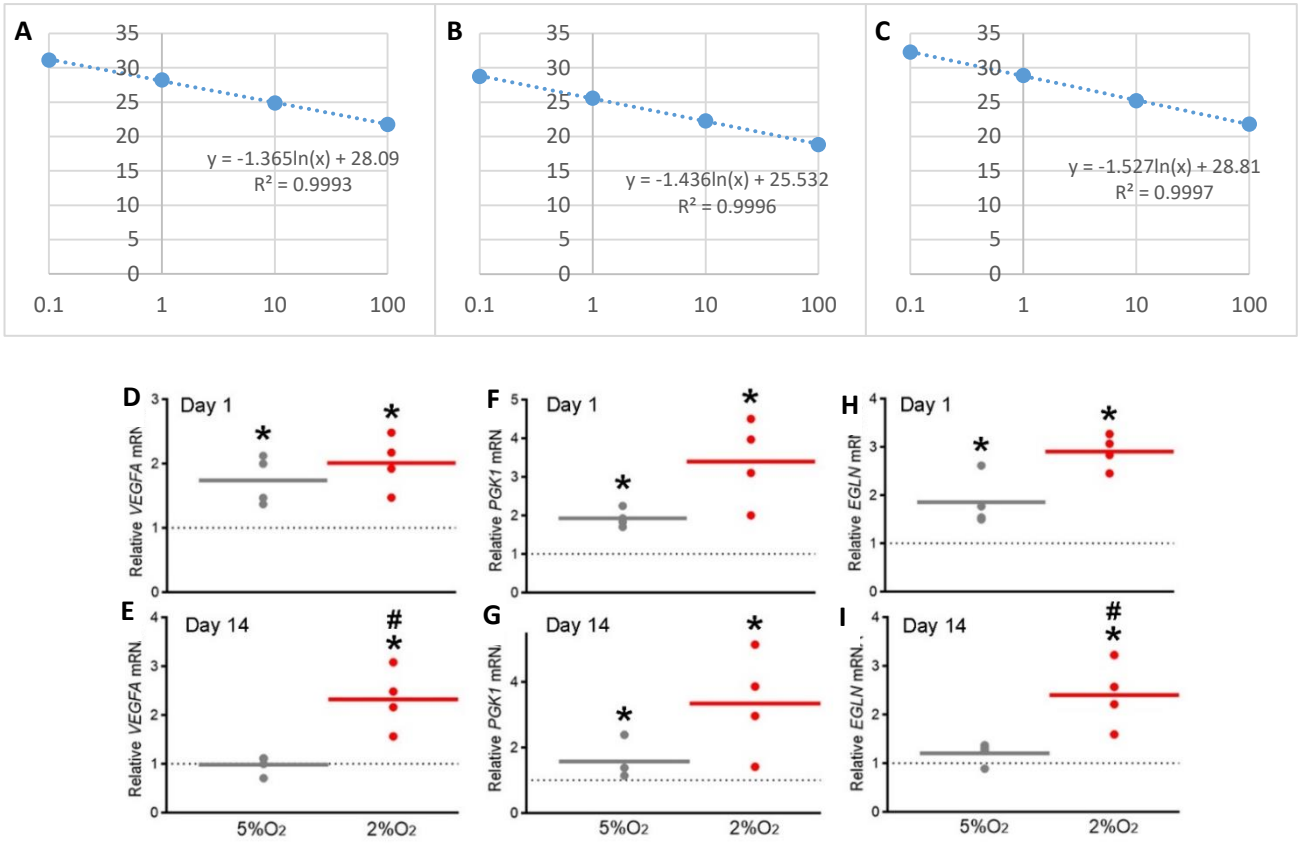

Figure 3.5. 2%O_2 induces constitutive expression of HIF target mRNA and 5%O_2 induced expression of these genes at day 1 only. (A-C) Standard curves which demonstrate a linear relationship between input cDNA concentration and cycle (Ct) number when amplified using *VEGFA*- (A), *PGK1*- (B) and *EGLN*-specific (C) primers (y axis = Ct, x axis = [cDNA] (%). (D-I) mRNA expression of *VEGFA* (D+E), *PGK1* (F+G) and *EGLN* (H+I) throughout chondrogenesis. Values plotted are from 4 independent experiments and are fold change compared to the 20%O_2 condition which is represented by the horizontal dotted line. The solid coloured lines represent the mean for each condition with *denoting $p<0.05$ compared to 20%O_2 and #denoting $p<0.05$ between 2% and 5%O_2. Significant changes were determined by Mann Whitney statistical tests.

3.2.5. Effect of 5% and 2%O_2 on chondrogenesis of hBM-MSCs

As both 2% and 5%O_2 increased levels of HIF-1α protein, HIF-1α nuclear translocation and expression of HIF target genes, the ability of these oxygen concentrations to increase chondrogenesis, utilising the same chondrogenic protocol was then assessed. Again, day 1 and 14 time-points were chosen to represent both early and more latent chronic effects of hypoxia during chondrocyte differentiation of BM-MSCs . These time-points were also chosen to enable correlation between expression of established HIF target genes (*VEGFA, PGK1, EGLN*) with those involved in chondrogenesis.

SOX9 is the master chondrogenic transcription factor that is essential during limb bud chondro-specification, *in vitro* chondrogenesis, production of an articular cartilage-like ECM and inhibition of chondrocyte hypertrophy [94]. As described in section 3.2.2, the product of *COL2A1;* Collagen Type II, plays key roles in the biology of chondrocytes in addition to maintaining the mechanical properties of articular cartilage. It is also a well-established transcriptional target of SOX9 and together with this transcription factor is part of a gene expression signature used to denote chondrogenesis [53] . Also part of this signature of cartilage differentiation is the gene *ACAN*, encoding Aggrecan which constitutes the largest proportion of the proteoglycans in cartilage ECM [413] . As with Collagen Type II, these proteoglycans are required to maintain the resistance of cartilage to compressive forces on the joint and residing articular cartilage [29].

The suitability of primers specific to *SOX9* and *ACAN* were assessed by generation of standard curves in which the concentration of serially-diluted cDNA from the

chondrocyte cell line; C28/I2 were plotted against cycle number (**Figs. 3.6A+3.6B**). Each standard curve demonstrated a linear relationship between cDNA concentration and cycle number in addition to amplifying target cDNA with a theoretical efficiency between 90-110%. At day 1 of chondrogenesis, only 5%O_2 significantly (p=<0.05) increase mRNA of *SOX9* but not at day 14 (**Fig. 3.6C+3.6D**). Increased expression of *COL2A1* was only observed at day 14 of chondrogenesis due to 5%O_2 compared to normoxic controls (**Fig. 3.6F**) with no changes observed due at day 1 (**Fig. 3.6E**). Despite not enhancing either *SOX9* or *COL2A1* expression, 2%O_2 increased the mRNA of the gene encoding Aggrecan at both day 1 and day14 with no change observed in the levels of this transcript due to 5%O_2 (**Figs. 3.6G+3.6H**).

As 5%O_2 enhanced *SOX9* and *COL2A1* mRNA, both of which were not affected by 2%O_2, we expected to see an increase in Collagen Type II protein incorporated into the ECM due to 5%O_2 only. However, despite observing a subtle increase (p=<0.05) in Collagen Type II due to 5%O_2 compared to the normoxic control (**Figs. 3.7A+3.7B**), a much more drastic increase due to 2%O_2 was observed (**Fig. 3.7C**). This immuno-detection of Collagen Type II was quantified and the increase due to 2%O_2 was statistically significant compared to both the normoxic cultures and those incubated at 5%O_2 (**Fig. 3.7D**). When this quantification was normalised to the number of DAPI-stained cells in each condition, the difference between 2% and 5%O_2 was no longer statistically significant, with both hypoxic states inducing an increase compared to the normoxic control (**Fig. 3.7E**). 2%O_2 also increased the number of DAPI-positive cells relative to that at normoxia, with no changes observed due to 5%O_2 (**Fig. 3.7F**).

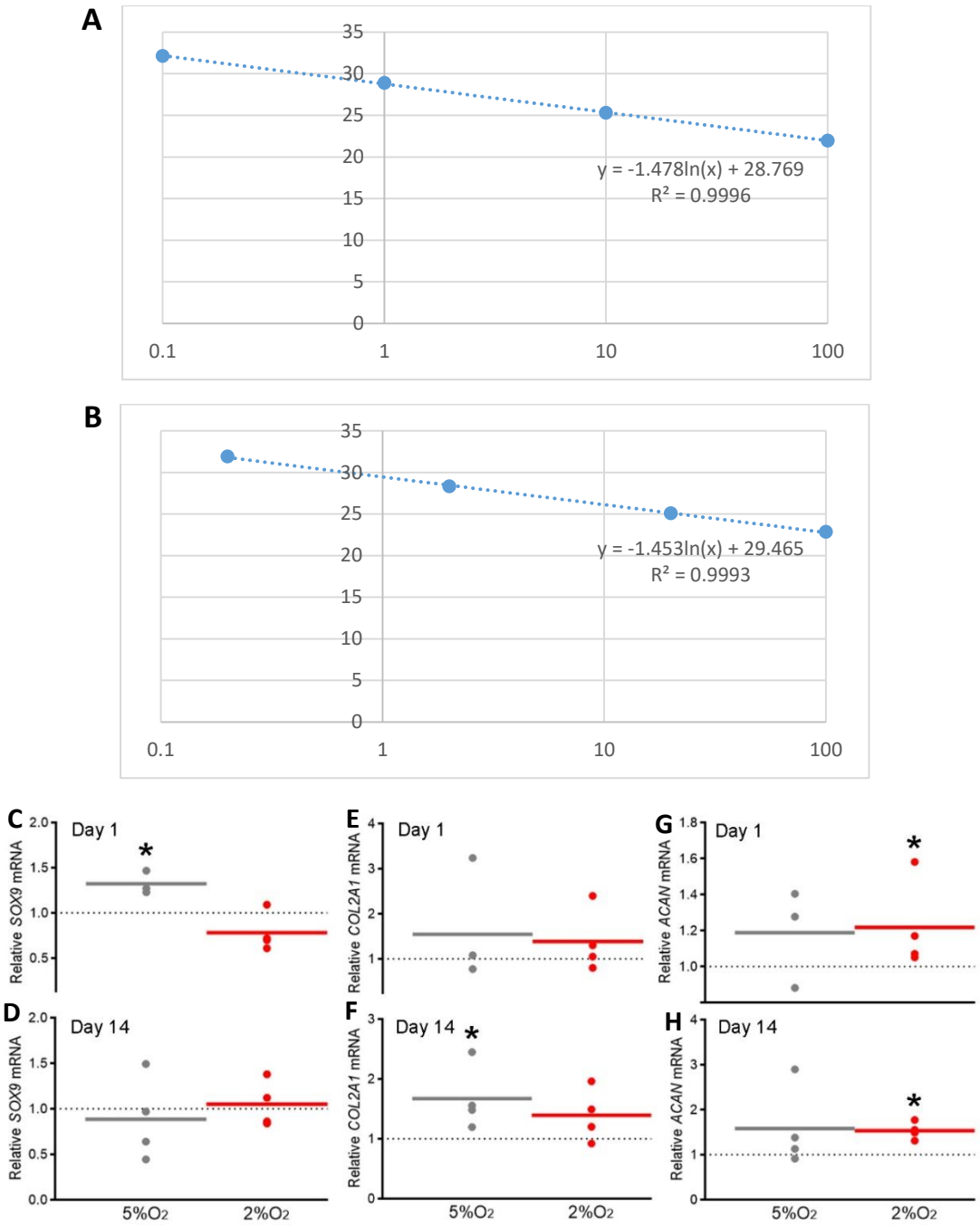

Figure 3.6. 5% but not 2%O_2 induces expression of *SOX9* and *COL2A1* with 2% but not 5%O_2 increasing *ACAN* mRNA. (A+B) Standard curves which demonstrate a linear relationship between input cDNA concentration and cycle (Ct) number when amplified using *SOX9*- (A) and *COL2A1*-specific (B) primers (y axis = Ct, x axis = [cDNA] (%). mRNA expression of *SOX9* (C+D), *COL2A1* (E+F) and *ACAN* (G+H) at days 1 and 14 of chondrogenesis due to 5% and 2%O_2. Values plotted are from 4 independent experiments and are fold change compared to the 20%O_2 condition which is represented by the horizontal dotted line. The solid coloured lines represent the mean for each condition with *denoting p<0.05 compared to 20%O_2.

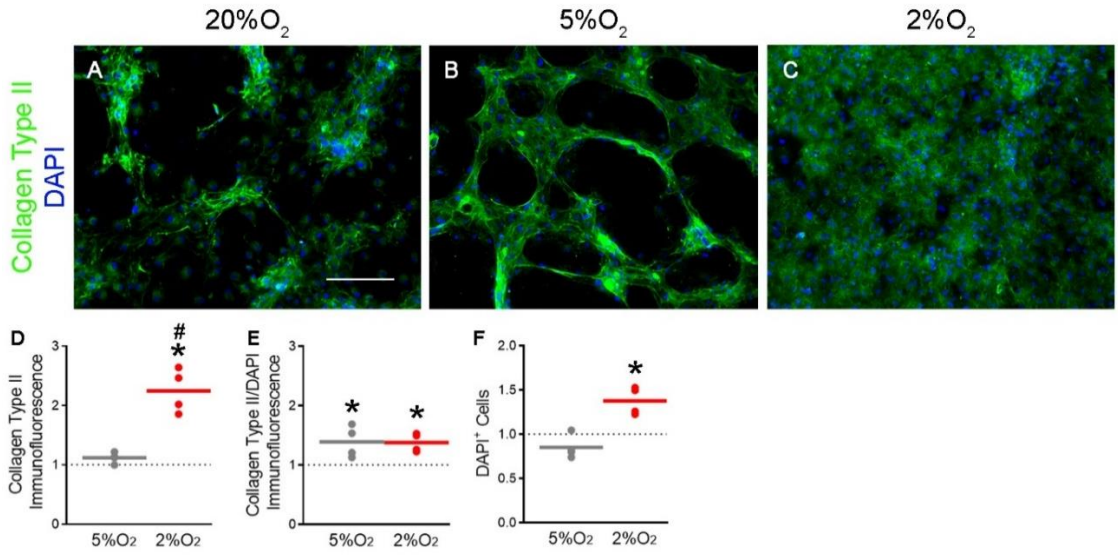

Figure 3.7. 2%O_2 increases total Collagen Type II deposition in the extracellular matrix with both hypoxic states inducing increases in this ECM protein per cell. (A-C) Collagen Type II immunofluorescence staining at day 21 of chondrogenesis due to incubation at 20% (A), 5% (B) and 2%O_2 (C). Scale Bar = 400µm. Representative images of 4 independent repeats shown. (D) Quantification of Collagen Type II immunofluorescence at day 21 of chondrogenesis and (E) normalised to DAPI immunofluorescence which equates to cell number. (F) Number of DAPI-positive cells at day 21 of chondrogenesis. Values plotted are from 4 independent experiments and are fold change compared to the 20%O_2 condition which is represented by the horizontal dotted line. The solid coloured lines represent the mean for each condition. *denote p<0.05 compared to 20%O_2 and $^{\#}$between 5% and 2%O_2.

3.2.6. Effect of 5% and 2%O_2 on hypertrophy of chondrogenically-induced hBM-MSCs

Having determined that 5% and 2% O_2 induced changes in the level chondrogenic mRNA and proteins during BM-MSC differentiation, the effect of these hypoxic states on chondrocyte hypertrophy were assessed. This is due to the significant problem of hypertrophy observed in current CTE strategies which may promote unwanted mineralisation upon implantation of the cartilage graft into the defect site [414]. Previous evidence demonstrates the ability of hypoxia in inhibiting hypertrophic signaling during chondrogenesis and stabilising the articular chondrocyte phenotype [272]. A key transcription factor involved in hypertrophy is RUNX2 [415] . This is responsible for expression of *COL10A1*, encoding the archetypal hypertrophic marker- Collagen Type X, and *MMP13* whose gene product is responsible for degrading Collagen Type II during endochondral ossification and OA pathogenesis [86].

Again to correlate with the expression of chondrogenic markers and established HIF targets, days 1 and 14 were selected as time points for harvesting RNA from differentiating cultures . **Figure 3.8A** details the standard curve generated by the *RUNX2*-specific primers used to amplify this gene. In chondrogenically-induced BM-MSCs, RUNX2 expression was inhibited (p=<0.05) by 2%O_2 at day 1 of chondrogenesis (**Fig. 3.9A**) with no change observed at day 14 (**Fig. 3.9B**) and no regulation due to 5%O_2 observed at either time point.

One of the drawbacks however, of quantifying the transcript level of a single gene is the lack of biological mechanism that this describes. All cellular processes require the

function of multiple gene products, whether it is the post-translational modification of Collagen or transcriptional induction of a specific gene locus. Therefore, due to the multipotency of hBM-MSCs and the relative ease of an epigenetic shift towards an osteoblastic/hypertrophic phenotype [151], the ratio of *SOX9* expression to that of *RUNX2* was analysed. The phenotype of limb bud progenitors have been described to be controlled by the opposing actions of SOX9 and RUNX2, with overexpression of either shown to negate the effect of the other [416]. In the study here when RNA was analysed for expression of these two master transcription factors, despite the decrease in *RUNX2* due to 2%O_2, no change was observed in the ratio of *SOX9*/*RUNX2* at either time point at either hypoxic state (**Figs. 3.9C+3.9D**).

COL10A1 is an established target gene of RUNX2, and together expression of these genes denotes progression of chondrocyte hypertrophy [417] . In the present study, the standard curve for the *COL10A1*-specific primers utilized here, demonstrate reactions within the accepted efficiency window in addition to a linear relationship between cDNA concentration and cycle number (**Fig. 3.8B**). During BM-MSC chondrogenesis, both hypoxic conditions inhibited *COL10A1* expression (p=<0.05) at day 1 (**Fig. 3.9E**). However at day 14, a decrease was observed due to only 5%O_2 with an increase in *COL10A1* mRNA induced by 2%O_2 at this time point (**Fig. 3.9F**). Similar to the ratio of *SOX9* mRNA to that of *RUNX2*, the ratio of *COL2A1/COL10A1* may indicate a transcriptional program that is conducive for production of articular or hypertrophic cartilage ECM. Both 2% and 5%O_2 enhanced the ratio of *COL2A1* to *COL10A1* at day 1 (**Fig. 3.9G**), with 5%O_2 significantly increasing this ratio at day 14, compared to both the normoxic control and 2%O_2 (**Fig. 3.9H**). Together, these results indicate that whilst 5%O_2 is unable to reduce *RUNX2* expression as observed due to

2%O_2, it clearly inhibits expression of the established hypertrophic marker *COL10A1* at the mRNA level.

In terms of investigating the mechanistic details behind chondrocyte hypertrophy such as *COL10A1* expression and its inhibition by hypoxic signaling, a number of key pathways are implicated. Signaling in response to BMP ligands, via binding of BMP receptors and phosphorylation of intracellular proteins; SMAD1/5/8 has been shown to be involved in progression of chondrocyte hypertrophy [418]. Similarly, the canonical Wnt signaling pathway which is propagated by conical Wnt ligand-Frizzled receptor binding and β-catenin-mediated transcription also induces chondrocyte hypertrophy [100]. In addition, there exist regulatory mechanisms which limit the signaling output of the BMP and Wnt pathways and the subsequent hypertrophy which these pathways mediate. One such class of regulatory mechanism is via the inhibition of the receptors to which BMP and canonical Wnt ligands bind. For example, Gremlin1 (GREM1) and Dickkopf WNT Signalling Pathway Inhibitor 1 (DKK1) are expressed during limb development and control of chondrocyte hypertrophy [419, 420] via their inhibition of canonical BMP and Wnt signalling respectively [101].

The control of hypertrophy by Gremlin1 and DKK1-mediated inhibition of the BMP and Wnt pathways presents one of the mechanisms by which hypoxic signaling regulates this unwanted transformation of articular chondrocytes . *GREM1* and *DKK1* expression have previously been shown to be increased in response to hypoxia during BM-MSC chondrogenesis [287]. **Figure 3.8C+3.8D** illustrate the ability of *GREM1* and *DKK1*-specific primers to amplify target cDNA with a theoretical

efficiency of 90-110%, ensuring a linear relationship between cDNA input and cycle number.

During BM-MSC chondrogenesis only 2%O_2 appeared to inhibit expression (p=<0.05) of *GREM1* at day 1 of chondrogenesis (**Fig. 3.9I**) with no changes observed at day 14 (**Fig. 3.9J**) or with regards to *DKK1* mRNA at any time point (**Figs. 3.9K+3.9L**). These results suggest that the reduction of *COL10A1* expression by culture at 5%O_2 is not due to increases in *GREM1* and *DKK1,* perhaps negating a role for Wnt and BMP signaling inhibition in that observed due to this hypoxic state.

Collagen Type X immunostaining was utilised to investigate the protein levels of this hypertrophic marker at day 21 of chondrogenesis – a time point at which hypertrophy is observed to occur, following chondrocyte differentiation [421] . 5%O_2 appeared to inhibit the production of Collagen Type X compared to that observed in the normoxic control (**Figs. 3.10A+3.10B**), with no noticeable change observed due to 2%O_2 (**Fig. 3.10C**). Together, 5%O_2 appears to confer advantages in terms of BM-MSC chondrogenesis compared to that conducted at 20% and 2%O_2 due to its unique ability to inhibit expression of hypertrophy, both at the mRNA and protein level. This therefore warrants its use in chapter 5 of the present thesis in which the role of HIF in CTE is further explored.

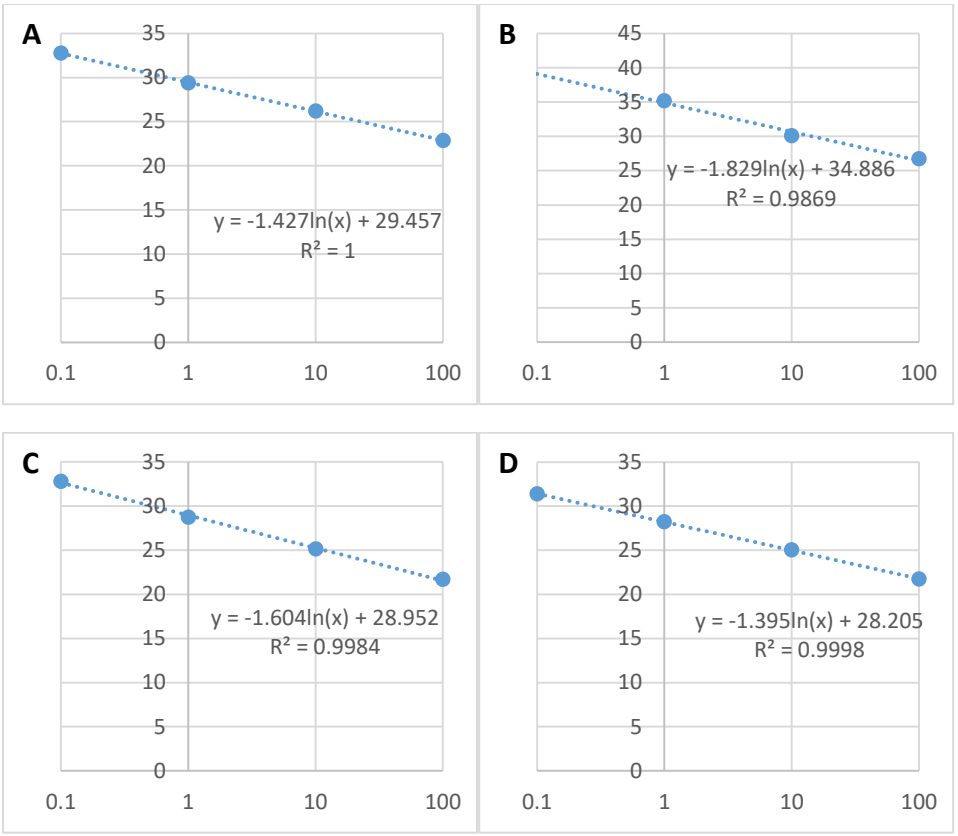

Figure 3.8. Standard curves which demonstrate a linear relationship between input cDNA concentration and cycle (Ct) number when amplified using *RUNX2*- (A), *COL10A1*- (B), *DKK1*- (C) and *GREM1*-specific (D) primers (y axis = Ct, x axis = [cDNA] (%).

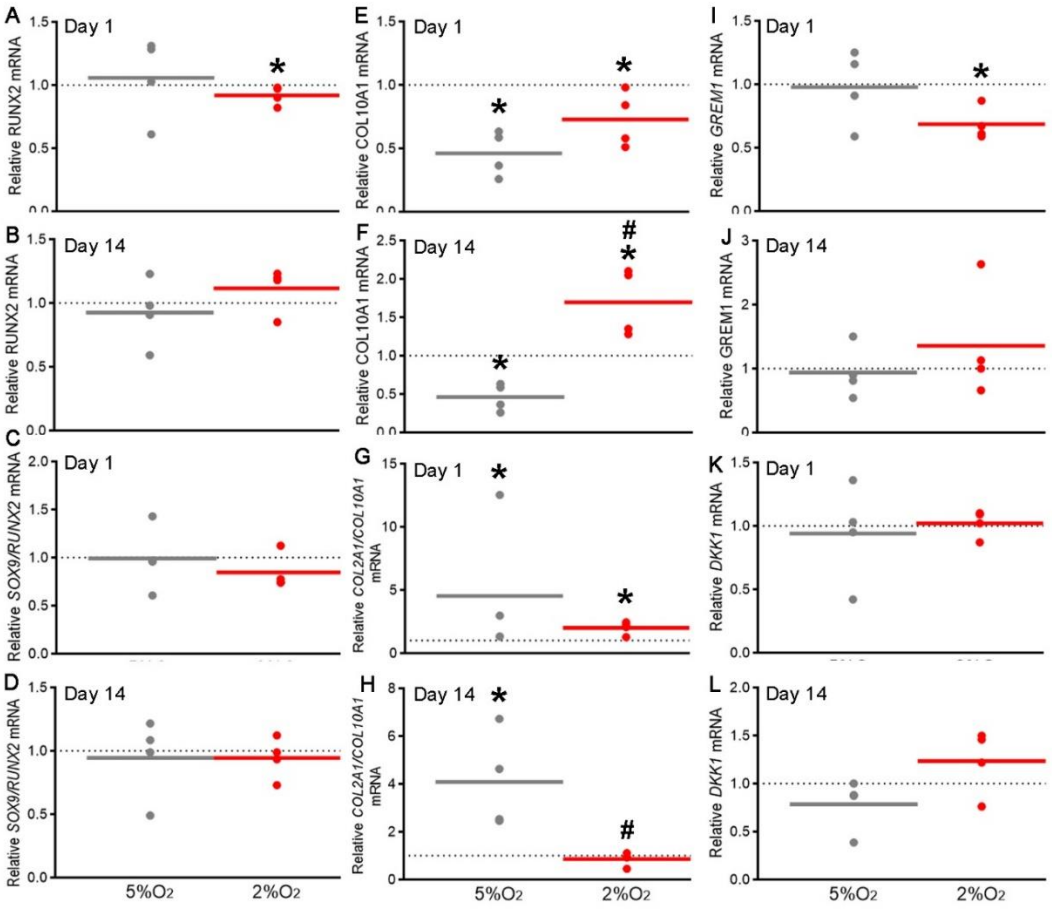

Figure 3.9. 5%O_2 but not 2%O_2 inhibits hypertrophic mRNA expression throughout chondrogenesis. mRNA expression of *RUNX2* (A+B), *COL10A1* (E+F), *GREM1* (I+J) and *DKK1* (K+L) at days 1 and 14 of chondrogenesis due to 5% and 2%O_2. Ratios of mRNA of *SOX9*:*RUNX2* (C+D) and *COL2A1*:*COL10A1* (G+H) at days 1 and 14 of chondrogenesis due to 5% and 2%O_2. Values plotted are from 4 independent experiments, and are fold change compared to the 20%O_2 condition, represented by the horizontal dotted line.The solid coloured lines represent the mean for each condition with *denoting p<0.05 compared to 20%O_2 and $^{\#}$denoting p<0.05 between 2% and 5%O_2.

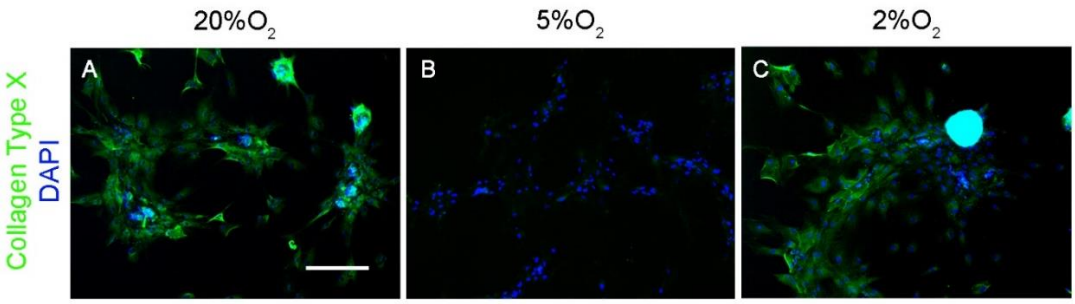

Figure 3.10. 5%O_2 but not 2%O_2 reduces Collagen Type X protein during chondrogenesis of hBM-MSCs. (A-C) Collagen Type X immunofluorescent staining at day 21 of chondrogenesis due to incubation at 20% (A), 5% (B) and 2%O_2 (C). Scale Bar = 400µm. Representative images of 3 independent repeats shown.

3.3. Discussion

Many developing and adult tissues exist within a hypoxic microenvironment [422] [423]. Correspondingly, many genes which contain a HRE [424] are expressed in these tissues in response to transcriptional-induction by the HIF complex [211, 425]. One population of cells which depend on HIF signaling in response to hypoxic stimulation, are BM-MSCs. These cells exist within a hypoxic niche within the bone marrow [426] and as a result, respond to *in vitro* hypoxic conditions with changes in a variety of cellular behaviors. Such changes induced by hypoxia include migration, proliferation and differentiation [427]. In terms of differentiation, the lineages of differentiation of BM-MSCs have been shown to be differentially altered in response to hypoxia, with adipogenesis and chondrogenesis being elevated by hypoxia and osteogenesis inhibited [272, 428].

Despite the conserved PHD2 and FIH-mediated mechanisms which exist to respectively control HIF-1α stabilisation and co-factor binding, the level of oxygen required to induce maximal HIF-mediated transcription varies from one tissue to another. Stroka et al demonstrated this via exposing a mouse model to systemic hypoxia and analysing HIF-1α stabilisation in different organs. They found that cells within the liver and kidney achieved maximal HIF-1α levels following 1 hour of hypoxic exposure, whereas a maximum was reached in 5 hours within cells of the brain. This demonstrates a differential sensitivity to oxygen, of the mechanisms regulating HIF-1α between the brain, lung and kidney, [211].

This variation in the sensitivity of the HIF-regulatory mechanisms to oxygen is mediated by the milieu of signals within the specific cellular niche of each organ.

These impact the regulatory elements controlling HIF-1α availability. Stroka et al for example, observed reduced basal levels of HIF-1β at normoxia in the brain whereas in the lung and brain it is present at constitutively higher levels [211]. Alternatively, variation in expression of the HIF-1α-regulatory elements such as PHD2 results in cell-specific regulation of HIF-1α and its participation in the HIF complex [406].

In developing cartilage or *in vitro* chondrogenesis of stem cells, factors other than the PHD2/VHL/FIH pathway may regulate the participation of HIF-1α in the HIF complex. These may alter the induction of HIF in response to reduced local oxygen concentration compared to that observed in other systems. The TGF-β family of proteins may be such factors. Porcine periosteal cells when transfected with a *BMP2*-overexpressing adenovirus, raised HIF-1α protein in the deep layer of articular cartilage following implantation back into a pig chondral defect [429]. Induction of HIF-1α by BMP2 was mediated by the Mitogen Activated Protein Kinase (MAPK) Kinase (MEK)/Extracellular Signal-Regulated Kinase (ERK) pathway, with TGF-β_1 also shown to induce HIF-1α protein via SMAD2/3-mediated mechanisms in hepatoma and fibrosarcoma cell lines [273]. The elevated expression of TGF-β and its downstream signalling during limb development, together with its established use during *in vitro* chondro-induction protocols, may therefore suggest its role in regulating HIF-1α induction by hypoxia.

Another factor utilised during *in vitro* chondrogenesis is Ascorbate. In addition to promoting collagen post-translational modification through induction of the Collagen-specific prolyl hydroxylase, Ascorbate has been shown to regulate HIF-1α levels [430]. Kuiper et al identified the potent effect of ascorbate in overcoming both

5%O_2 and chemical stabilisation of HIF-1α to reduce levels of this HIF subunit. This implicates its potential role during hypoxia-mediated chondrogenesis. The chemical stabilisers used in this were PHD2 inhibitors, and therefore this suggests that Ascorbate plays a role in HIF-1α regulation independently of its ability to promote PHD2 activity through recycling of the Fe^{2+} ion. This was also suggested by Miles et al who observed an increase in HIF-1α protein and HIF-mediated transcription in response to Ascorbate treatment of human melanoma cells [431]. These authors negated a role of PHD2 in their observations upon siRNA knockdown of PHD2 which had no effect on Ascorbate-mediated increased in HIF-1α.

Factors such as TGF-β ligands or Ascorbate that during chondrogenesis, may affect hypoxic-induction of HIF-α, necessitate an investigation into the effect of varying oxygen concentration on chondrocyte differentiation. This would enable determination of the levels of oxygen required to mimic the *in vivo* function of hypoxia in promoting articular chondrogenesis. The existence of an oxygen gradient across the mesenchymal limb bud [262] and growth pate cartilage [259] and the observation that HIF-1α stabilisation can vary significantly through such an oxygen gradient [396] supports the requirement for such a study. A study by Bracken et al suggested that the relationship between oxygen concentration and HIF-1α levels in certain cell types is not linear, and significant stabilisation of HIF-1α occurs only following a threshold hypoxic level [396].

Overall, the present study demonstrates key differences between mild (5%O_2) and more severe (2%O_2) hypoxic conditions on hBM-MSC chondrogenesis. Despite inducing expression of established HIF targets during chondrogenesis at all time

points examined, 2%O_2 appeared to induce a transcriptional program independent of that involved in chondrogenesis. Without stimulating expression of *SOX9* or *COL2A1* and inhibiting hypertrophy, this oxygen concentration raised only *ACAN* expression and increased Collagen Type II protein. At the same time points however, 5%O_2 induced formation of an anti-hypertrophic, chondrogenic expression profile. This is suggestive of an important role for mild hypoxic signalling in CTE due to the risk of hypertrophy and mineralisation in current strategies for repair of acute chondral defects .

As suspected and shown previously [396], both 5% and 2%O_2 increased total HIF-1α protein and nuclear localisation in hBM-MSCs following 24-hour incubation. These increased protein levels demonstrate the inhibition of PHD2 by hypoxic conditions, which have been shown to result in increased nuclear localisation of HIF-1α where it is able to function as part of the HIF transcriptional complex. An interesting result however, is the observation of HIF-1α protein present in the normoxic conditions, where PHD2 would theoretically be most active. One explanation may be based on observations of PHD2 inhibition by TGF-β1 treatment via SMAD2/3 [273]. Therefore the TGF-β_3 in the induction media used in the present study may reduce HIF-1α hydroxylation. This would result in a net increase in HIF-1α in the presence of 20% oxygen. Additionally, BM-MSCs compared to MSCs from other sources and non-MSC cell types, appear to show reduced senstivity to PHD2 activity with regards to HIF-1α levels [432]. This is suggested by Palomaki et al to be due to the increased transcript levels encoding HIF-1 α in BM-MSCs which would result in increased HIF-1α levels in the face of PHD2 activity .

Whatever the mechanism is behind the observed HIF-1α at normoxia, it appears to almost exclusively localise to a peri-nuclear region of the cell under normoxic conditions unlike at 2%/5%O_2 where it localizes to within the nucleus. Moreover, the discrete, clustered pattern of peri-nuclear HIF-1α suggests encapsulation within an intracellular organelle as opposed to being freely diffusible within the cell. Storage of HIF-1α within perinuclear golgi has been shown *in* vitro, within colon cancer cells [433] and bovine chondrocytes [434], where it has been hypothesised to act as a reservoir to allow cells to respond to a rapid metabolic changes. Coimbra et al observed a reduction in nuclear HIF-1α in human articular chondrocytes in monolayer compared to suspension culture at normoxia [282]. These authors also observed under normoxic conditions, reduced nuclear HIF-1α in osteoarthritic chondrocytes compared to those from healthy cartilage. This suggests a deregulation of HIF-1α upon removal form the *in vivo* niche. There may also exist, a role of the golgi as a scaffold for HIF-1α which may facilitate modification to its amino acid sequence such as that by PHD2. This is supported by the evidence that OS9, as a HIF-1α-downregulatory factor, plays key roles in trafficking proteins from the endoplasmic reticulum to the golgi [435].

VEGFA, *PGK1* and *EGLN* represent HIF target genes. With the exception of *PGK1*, the increases in the expression of these due to 5%O_2 at day 1 of chondrogenesis, did not occur at day 14. This is unlike that due to 2%O_2 which induced transcription of all three genes at both time points. A limitation of this study may be the relatively few genes chosen to represent HIF targets as a proportion of the total genomic sequences which contain one or more HREs. Hypoxia has been shown to induce different subsets

of genes between relative short and long-term culture [436]. Therefore by analysing a small subset of genes here, those regulated by 5%O_2 other than *VEGFA*, *PGK1* and EGLN, would be omitted. However, the continued upregulation of *VEGFA*, *PGK1* and *EGLN* by 2%O_2 at day 14 is suggestive of a tolerance of the hBM-MSCs to 5%O_2 at this time point, following an initial period of hypoxic stimulation.

As validated by its use as a HIF target gene, *EGLN* when upregulated by hypoxic conditions, propagates a feedback loop via its product- PHD2, which increases HIF-1α degradation [243]. It is therefore plausible to suggest the inability of 5%O_2 to initially raise nuclear HIF-1α to levels beyond which it be abolished by this PHD2-mediated negative feedback loop. As previously demonstrated [396], this may be at odds with that due to 2%O_2 which overcomes the PHD2-mediated tolerance to stimulate constitutive expression of HIF target genes. If indeed, PHD2-mediated negative feedback and suppression of *VEGFA*, *PGK1* and *EGLN* transcription did occur, this may highlight another limitation of the present study. The lack of longer term time points than 14 days may omit observations of latent recovery of HIF target mRNA after this time point which is a pattern described generally of negative feedback loops [437].

An alternative explanation to the reduced effect of 5%O_2 at day 14 may be due to the specific nature of HIF regulation in BM-MSCs. These cells have been shown to express increased mRNA levels of *HIF1A* which increases subsequent protein levels of HIF-1α, even in normoxic conditions [432]. This may therefore suggest that the chondrogenically-induced BM-MSCs require severe hypoxic conditions (i.e. 2%O_2 compared to 5%O_2) to induce HIF activity to levels beyond that observed in basal

conditions. A similar mechanism may be induced by TGF-β_3 treatment in this study which has been shown to raise the basal levels of HIF-1α at normoxia [273]. Inclusion of TGF- β_3 in the chondrogenic media may therefore result in the inability of a mild hypoxic state such as 5%O_2 to raise basal levels of HIF-mediated transcription in a sustained manner, beyond a TGF-β_3-augmented level. This theory is also supported by a study in which the HRE sequence was deleted within the *SOX9* promoter in chondro-induced ST2 cells. Robins et al in this investigation, observed the inhibited expression of *SOX9* at 20%O_2 due to this deletion [269]. This therefore suggests that high levels of HIF-mediated transcription exist at basal/normoxic conditions. With regards to the current study, this again suggests that a more potent hypoxic state is required to elevate HIF activity to levels beyond the basal levels.

Corresponding to the increase in HIF target mRNA at day 1 of chondrogenesis due to 5%O_2, this oxygen concentration also induced expression of the master regulator of chondrogenesis, *SOX9* following 24 hours of induction. This matches previous studies such as that by Robins et al who observed an increase in *SOX9* mRNA 24 hours following chondro-induction of ST2 cells [269]. These authors demonstrated the role of HIF in that observed by identification of four HREs within the promoter region of the *SOX9* gene which when deleted, reduced hypoxia-mediated transcription. Duval et al also investigated the mechanisms behind hypoxia-mediated chondrogenesis and observed an abolishment of HIF binding at the *SOX9* promoter in response to treatment with the inducer of proteasome activity, $CdCl_2$ [272]. This study demonstrated that hypoxia-mediated increases in chondrogenic mRNA such as *SOX9* are due to inhibition of PHD2/VHL-mediated degradation of HIF-1α which suggests a similar mechanism in the present study. Again corresponding to the lack of increase

in *VEFGA* and *EGLN* due to 5%O_2 at day 14, *SOX9* expression was also not raised as this time point. This may suggest that *SOX9* and those genes classically upregulated by hypoxia are regulated by similar mechanisms.

COL2A1 was raised by only 5%O_2 at day 14 of chondrogenesis. Induction of this gene at a similar time point was also previously demonstrated [269]. The product of *COL2A1;* Collagen Type II, plays an essential role cartilage ECM by forming a water-perfused network with HA-Aggrecan to generate a structure capable of withstanding compressive forces on the joint. The importance of Collagen Type II in cartilage ECM is demonstrated by phenotypic observations following a deletion in the *COL2A1* gene. A specific mutation within the alpha helix gene results in degradation of Collagen Type II molecules and replacement with Type I and III collagens [438]. This predisposed the articular cartilage in developing limbs to OA. This was denoted as osteoarthritic due to the increased protein expression of Collagen Type X which is shown to be a common consequence of other mutations within the *COL2A1* gene [439] [440].

The promoter region within the *COL2A1* contains multiple SOX9 binding sites [441] and this is concomitant with studies demonstrating the dependence of *COL2A1* expression on SOX9 activity during cartilage development [442]. The recovery of an articular chondrocyte phenotype from a hypertrophic state is also propagated by SOX9-dependant *COL2A1* transcription [443]. In studies examining the relationship between SOX9 and *COL2A1* during chondro-induction of hBM-MSCS, overexpression of *SOX9* increases *COL2A1* mRNA [272]. The early *SOX9* transcription observed in the present study due to 5%O_2 and the latent increase in *COL2A1* mRNA has been

described previously as an *in vitro*-specific phenomenon. *SOX9* expression is increased at an early time point during *in vitro* chondrogenesis of chick limb bud micromass cultures [402] whereas *COL2A1* expression *in vitro* is generally thought to occur at latent stages of differentiation [444]. This contrasts with that which occurs during *in vivo* development in which both *SOX9* and *COL2A1* expression are observed at early points in the pre-cartilage cranial mesenchyme and at later time points [445]. This pattern of early *SOX9* expression and latent *COL2A1* expression by hypoxia *in vitro* was also demonstrated by Robins et al. These authors observed an increase in *COL2A1* mRNA at day 16 due to incubation of mesenchymal progenitors at 1%O_2.

BM-MSCs incubated at 5%O_2 were unable to maintain the day 1 increase in *SOX9* expression relative to normoxic conditions through to day 14. This perhaps indicates the sufficiency of early increases in *SOX9* for transcription of its target genes, as also described by Gadjanski et al [446]. In the present study however, SOX9 cannot be implicated in *COL2A1* transcription induced by 5%O_2 by solely correlative evidence of increasing *SOX9* and *COL2A1* mRNA levels. This represents a limitation of this study with SOX9 deletion being required to implicate this protein in hypoxia-induced *COL2A1* mRNA expression. Additionally, analysis of the mRNA expression encoding SOX9 binding partners, SOX5 and SOX6 in addition to protein analysis of these three transcription factors would enable a more robust conclusion to be made with regards to the effect of 5%O_2 on the chondrogenic differentiation program.

Unexpectedly, despite constitutive upregulation of *VEGFA, PGK1 and EGLN* and unlike that observed due to 5%O_2, 2%O_2 did not increase *SOX9* expression at either time point investigated. As pertained to above, a caveat to this observation may be

that any increases in *SOX9* mRNA due to 2%O_2 would not be observed in this study if occurred between days 1 and 14 due to only these two timepoints utilised. This therefore prevents the dismissal of 2%O_2 in raising *SOX9* expression during chondrogenesis.

Due to *SOX9* transcription occurring due to 5%O_2 here, it may be suggested that 2%O_2 stimulated expression of genes which do not require SOX9 to accompany the increases in *VEGFA, PGK1 and EGLN*. For example, Mitogen Inducible Gene 6 (MIG6) and Inhibin Beta A Subunit (INHBA) mRNA were induced by incubation of human articular chondrocytes cultured at 1%O_2. These increases which were inhibited by HIF-1α deletion but were unaffected by SOX9 deletion [447]. MIG6 is involved in preventing hypertrophy of articular cartilage and ossification [448]. INHBA dimerises to form Activin A which inhibits secretion of MMP3 [449] and induces expression of tissue inhibitor of metalloproteinase-1. This is an anti-catabolic factor of cartilage [450].

Unlike *MIG6* and *INHBA,* expression of *COL2A1* relies on *SOX9* activity. Due to the observation in the current study that expression of *SOX9* and *COL2A1* were not increased by 2%O_2 but increases were observed of established HIF target mRNA, this oxygen concentration may induce a SOX9-independent subset of genes in contrast to 5%O_2. The stimulation of expression of different and specific subsets of genes by different hypoxic states has been suggested in the literature and is dependent on the ability of each hypoxic state to inhibit FIH as well as PHD2. FIH inhibition induces expression of HIF target genes distinct from that observed due to inhibition of PHD2 [451]. The differentiation sensitivity of PHD2 and FIH to oxygen deprivation indicates

the ability of varying hypoxic states to inhibit PHD2 and FIH to different magnitudes [452]. This correlates with that shown by Tian et al, who observed a greater resistance of FIH (compared to PHD2) to hypoxia-mediated inhibition [453]. Therefore, in the present study, it could be hypothesized that 5% compared to 2%O_2 may stimulate HIF target gene expression primarily through PHD2 inhibition. In the presence of a more severe hypoxia at 2%O_2, the BM-MSCs may exhibit expression of an alternate subset of genes through dual inhibition of PHD2 and FIH. However, with the observations made in this study, this theory is purely speculative. This therefore requires further analysis of the contribution of FIH and PHD2 before conclusions on the role of these enzymes can be made.

ACAN is the most abundant non-collagenous protein in cartilage ECM, providing the essential structural integrity for joint function in the face of compressional load and fluid flow experienced during locomotion. Mutations in the *ACAN* gene can result in skeletal abnormalities and development of severe OA [413] which demonstrates the essential nature of this structural protein in cartilage ECM. Co-localisation of Aggrecan and SOX9 delineates skeletal progenitors which go onto the form the growth plate [454]. Expression of ACAN has been shown to be dependent on SOX9 expression and activity. For example, *SOX9*-specific siRNA reduces *ACAN* expression in articular chondrocytes [455]. Liu et al identified an enrichment of SOX9 and SOX6 at the *ACAN* promoter in a growth plate chondrocyte cell line [456]. In addition, ACAN mRNA and Alcian Blue staining of GAGs were reduced upon deletion of *SOX9* in developing cartilage [457] with overexpression of *SOX9* in chondro-induced hBM-MSCs inducing *ACAN* transcription [272]. Hypoxic conditions have been repeatedly shown to induce expression of ACAN and increase GAG abundance in cartilage ECM.

This was shown to be mediated via HIF-1α during hBM-MSC and limb bud chondrogenesis [263, 272]. In the present study, 5%O_2 did not affect expression of ACAN despite its induction of *SOX9* and *COL2A1* transcription. This may suggest a lack of complete chondrogenic differentiation induced by 5%O_2. This conclusion may be made due to *ACAN* expression denoting late stages of chondrocyte formation from mesenchymal precursors [402]. This lack of *ACAN* expression induction by 5%O_2 may correspond with the lack of sustained expression of HIF targets- *VEGFA* and *EGLN*, in addition to *SOX9* at day 14. Alternatively, an increase in *ACAN* expression may have been observed if mRNA was collected from differentiating cultures at day 21, due to this stage of *in vitro* chondrogenesis denoting the end-point for differentiating cultures [458].

In BM-MSCs in which *COL2A1* expression remains constant, an increase in cell number would result in a cumulative increase of Collagen Type II incorporated into the ECM [459]. The increased cell number observed here due to 2%O_2 may therefore represent the mechanism behind the high levels of total Collagen Type II protein observed compared to that induced by normoxia and 5%O_2. Such a conclusion may be made due to the observed reduction in Collagen Type II fluorescence to similar levels to that of 5%O_2 when the quantity of signal was normalised to the number of DAPI-stained cells. Interestingly, the amount of Collagen Type II in the ECM at 5%O_2 was enhanced to a significant level compared to 20%O_2 only when normalised to cell number and not without normalisation. This increase per cell correlates with the induction of *COL2A1* transcription due to 5%O_2. A notable caveat to these observations is that quantification of Collagen Type II immunofluorescence is only a semi-quantitative measurement of its protein. In order to discern the accurate effect

of differential hypoxic cultures on Collagen Type II protein, Enzyme-Linked Immunosorbent Assays (ELISAs) must be conducted. This would enable quantification of Collagen Type II protein and dismiss the contributing effect of background fluorescence to the semi-quantitative observations here.

Despite inducing transcription of *SOX9*, 5%O_2 did not reduce *RUNX2* mRNA as previously demonstrated [460] and 2%O_2 induced a very marginal decrease in its expression. The relative activity levels of SOX9 and RUNX2 determines the respective chondrogenic or osteogenic lineage commitment in osteochondral progenitors which arise from the mesenchymal limb bud [52]. In cells destined to become resting chondrocytes, SOX9 overcomes the activity of RUNX2 to provide a bias towards articular rather than hypertrophic chondrogenesis. This has been theorised to occur due to the hypoxic nature of the developing limb bud, resulting in HIF-mediated upregulation of SOX9 [259]. Following this activation, SOX9 then inhibits the function of RUNX2 [461] which as a master transcription factor, stimulates chondrocyte hypertrophy and endochondral ossification if left unhindered [462].

In the present study, the lack of significant increase in the ratio of *SOX9* to *RUNX2* due to either hypoxic state suggests that the transcriptional programs induced by these conditions are not conducive for chondrogenesis at the expense of ostegenesis. However this observation may also be explained by the specific time points chosen for RNA isolation here and the possibility of significant changes in *SOX9*:*RUNX2* expression occurring at other points throughout BM-MSC chondrogenesis. An example of such as time point may be the terminal stages of chondrogenesis where hypertrophic differentiation is thought to occur [463].

Irrelevant of the time points chosen to examine the relative expression of *SOX9* and *RUNX2*, both oxygen concentrations induced changes in the expression of *COL10A1*, a marker of hypertrophy as well as changes in the expression ratio of *COL2A1*:*COL10A1.* The ratio of these compounds is suggestive of the type of ECM that is produced by differentiating BM-MSCs or chondrocytes, with increases in this ratio indicating articular cartilage ECM and a decrease suggesting hypertrophic cartilage [464]. Expression of *COL10A1* and other hypertrophic factors such as *MMP13* [415] as well as induction of Wnt-mediated hypertrophy [100] are downstream effects of *RUNX2*-mediated transcription.

In the present study, both hypoxic states inhibited *COL10A1* expression at day 1 and the ratio of expression of *COL2A1*:*COL10A1* at this time point. This early suppression suggests the bias of the condensed mesenchymal population to articular chondrogenesis and not hypertrophy. This function of hypoxia is suggestive of its role in patterning articular cartilage and growth plate cartilage destined to become ossified bone [100]. However as with any cellular process, progression of hypertrophy is not denoted by expression of a single gene. Therefore, analysis of other hypertrophic markers such as MMP13 and ADAMTS5 at the mRNA and protein level would be required in order to strengthen the conclusion of hypertrophy inhibition by hypoxia.

Despite that observed at day 1 due to either hypoxic states, inhibition of *COL10A1* mRNA and increase in the ratio of *COL2A1*:*COL10A1* mRNA was induced by only 5%O_2 at day 14. Conversely 2%O_2 increased *COL10A1* expression at this time point. A reduction of Collagen Type X protein was observed in the ECM in cultures exposed to

5%O_2 with a lack of change induced by 2%O_2. This suggests a requirement of constitutive inhibition of *COL10A1* transcription may be required for corresponding changes in protein levels to be exhibited. It is imperative to reduce protein levels of this hypertrophic marker to inhibit the downstream hypertrophic signalling which it induces which results in apoptosis of this cells and spontaneous ossification [465]. These observations therefore suggest that 5%O_2 compared to 2%O_2 is suitable for CTE due to its ability to induce a transcriptional profile and corresponding ECM that is suggestive of articular and not hypertrophic cartilage.

In terms of the mechanism behind this decrease in *COL10A1* expression due to 5%O_2 at day 14, it could be suggested that HIF activity was not required as indicated by a lack of observed increase in HIF targets- VEGFA, PGK1 and EGLN at this time point. The increase in *COL2A1* due *to* 5%O_2 at this time point also suggests that HIF activity is not required for latent expression of this gene due to hypoxia. Representing a limitation of the present study, this lack of correlation between *COL10A1/COL2A1* and HIF targets may be due to the relatively low number of time points or HIF targets chosen. By not utilising time points between days 1 and 14, and with *VEGFA*, *PGK1* and *EGLN* not representing the full complement of HIF target genes, observation of HIF-mediated transcription required for *COL10A1*/*COL2A1* regulation may have been omitted. However in terms of hypertrophy, HIF-independent inhibition of this process in hypoxic conditions was demonstrated by Lee et al [466]. These authors observed the role of PI3K/Akt-dependent mechanisms in hypoxia-mediated suppression of hypertrophy.

The increase in *SOX9* expression due to 5%O_2 may be involved in the latent suppression of *COL10A1* mRNA, due to the role that SOX9 plays in inhibition of RUNX2-mediated hypertrophy. However, as described earlier, ablation of SOX9 would be required in order to implicate this transcription factor in the suppression of hypertrophy observed due to 5%O_2. This rationale would also apply in order to dismiss the role of HIF in regulation of *COL10A1*/*COL2A1* expression due to 5%O_2.

The increase in *COL10A1* mRNA at day 1 due to 2%O_2 may be due to an absence of hypertrophic-suppressive mechanisms. For example in this study, mRNA encoding the inhibitor of BMP signalling- Gremlin1, is reduced at day 1 by 2%O_2. Gremlin1 acts to inhibit hypertrophic signalling induced by specific BMP ligands upon binding to their receptors in articular chondrocytes [101]. The decrease in *GREM1* due to 2%O_2 observed here suggests a role for BMP signalling in raising *COL10A1* mRNA in BM-MSCs cultured at this hypoxic state. However, as with the role of HIF and SOX9 in the observations due to hypoxia here, data regarding this role of Gremlin1 is correlative only. This therefore requires manipulation of the BMP antagonist at the genetic or protein level in order to discern its role in hypoxia-mediated chondrogenesis.

4. Comparison of HIF-stimulating compounds in the chondrogenenic differentiation of BM-MSCs.

4.1. Introduction

The previous chapter demonstrated the ability of both 5% and 2% oxygen to induce transcriptional and proteomic changes during hBM-MSC chondrogenesis, thereby suggesting a role for either in CTE for repair of acute chondral defects. Despite this however, the use of physiological hypoxia may be associated with inherent risks and logistical problems with regards to generating a translational product for use in the clinic. In addition to functioning through HIF, hypoxia has been shown to stimulate HIF-independent mechanisms to induce a global decrease in protein translation. This phenomenon occurs via inhibition of mTOR signalling [467]. mTOR controls global translation machinery by inducing ribosomal protein S6 kinase, eukaryotic initiation factor 4E binding protein 1 and eukaryotic elongation factor 2 kinase [468]. Hypoxia has been shown to inhibit mTOR signalling via a number of mechanisms as described by Wouters & Koritzinsky [469] with the overall effect being a reduction in cap-dependent initiation of protein translation.

Also independently of HIF, hypoxia has also been shown to induce activity of the Unfolded Protein Response (UPR), a cell response to endoplasmic reticulum stress and inefficient protein folding which results in targeting of unfolded proteins for proteasomal degradation [470]. HIF independent regulation of protein translation and UPR may have severe consequences in terms of CTE. Placing brakes on translation machinery may have a negative effect on chondrogenic induction of hBM-

MSCs. This is due to the requirement of protein synthesis for propagating transcriptional programs and processing of cartilage ECM [471]. This also correlates with findings that protein synthesis is the key regulatory mechanism of cellular processes during differentiation [472] as opposed to protein degradation [473].

Another potential drawback of hypoxia is the susceptibility of its downstream pathways to negative feedback loops, suppressing the pro-chondrogenic activity required throughout chondrogenic induction [289]. This was indeed observed in the previous chapter due to 5%O_2, in which the increase in HIF target gene expression observed at day 1 of chondrogenesis was abolished at day 14. Such a situation may arise due to hypoxia-induced UPR, shown to enable tolerance of tumour cells to hypoxic conditions for progression of the malignancy [474].

Logistically, hypoxia may present complications during translation to the clinic for CTE. As described by Liu et al, a current paradigm for repairing chondral defects is the requirement of injectable scaffolds loaded with a specific cell source and bioactive factors for regeneration [475]. Biomaterial scaffolds have evolved to retain these factors and release them over a sustained period of time ensuring a reservoir of pro-regenerative signals to the donor cells for *in vivo* defect repair [476]. The use of hypoxia would prove difficult for this strategy due to the requirement to reduce the bioavailability of oxygen *in situ* as opposed to its release.

The use of hypoxia may also be limited for tissue engineering applications where both the articular cartilage and underlying subchondral bone are damaged, as observed in full osteochondral breaks [111]. As described in section 1.3.5, a continuous scaffold may be the most appropriate strategy for OCTE with compounds which stabilize HIF-

1α perhaos enabling spatial control of cartilage and bone regeneration. In addition to the potential role for OCTE, the use of HIF-1α-stimulating compounds would also ameliorate the other pitfalls of utilising hypoxia. Injectable scaffolds with a sustained release of a HIF-stablising compound may aid *in vivo* CTE efforts, promoting articular chondrogenesis and inhibiting hypertrophy. In addition, stimulating HIF during hBM-MSC chondrogenesis, as opposed to the full complement of hypoxic effects, such as HIF-independent mTOR inhibition or UPR stimulation would avoid the decrease in overall translation and tolerance of hypoxic pathways required for chondrocyte differentiation.

$CoCl_2$, DFX and DMOG are the most widely used of the HIF-stabilising compounds and each target PHD2 and/or FIH via different mechanisms of action. As observed in regions of diminished oxygen concentration, PHD2 inhibition has the net effect of inhibiting HIF-1α prolyl hydroxylation and its degradation with FIH inhibition reducing asparagine hydroxylation of HIF-1α which would result in blocking of its transcriptional co-factors [268]. DMOG strongly binds to the 2-OG binding pocket of both FIH and PHD2, acting as a competitive inhibitor [44]. DFX sequesters and reduces intracellular Fe^{2+} thereby reducing activity of both FIH and PHD2 due to their dependence on this ion [477]. This is unlike the effect induced by $CoCl_2$ which binds directly to the PHD2 active site and demonstrates specificity for this hydroxylase [453].

Evidence exists of the use of $CoCl_2$, DFX or DMOG for cartilage regeneration. Duval et al demonstrated the role for $CoCl_2$ in such a context. They observed an increase in SOX9 binding to the promoters of target genes in $CoCl_2$-treated BM-MSCs

encapsulated within alginate beads, in addition to a corresponding increase in chondrogenic mRNA expression due to $CoCl_2$ [272]. In an investigation by Huang et al, DFX in conjunction with TGF-β_1 increased expression of *SOX9*, *COL2A1* and *ACAN* in chondrogenically-induced ATDC5 cells compared to TGF-β_1 supplementation alone [478]. This was also shown to increase the detection of GAGs in the ECM, again compared to the use the growth factor alone. Finally DMOG's potential role in CTE was also implicated by Thoms et al who observed an increase in SOX9 protein in human articular chondrocytes treated with DMOG [278]. This corresponds to a study by Gelse et al, in which *SOX9* mRNA was induced in murine chondrocyte cultures due to DMOG treatment, together with an inhibition of *COL1A1* expression, required for matrix ossification [479].

In addition to aiding the CTE field, use of compounds such as $CoCl_2$, DFX or DMOG enable insights to be made into the regulation of HIF by the HIF hydroxylases during chondrogenesis. Generally speaking, hypoxia induces complete PHD2 inhibition whilst FIH activity has been shown to remain in cells cultured at low oxygen levels [453]. This was demonstrated by Tian et al in the renal cell carcinoma line, RCC4. These authors observed an inhibition of HIF-1α hydroxylation due to incubation at 1%O_2 compared to those at normoxia. At this oxygen concentration, Asparagine hydroxylation remained and was reduced only by the much more severe hypoxia of 0.01%O_2. This study demonstrated the reliance of hypoxic conditions in inhibiting PHD2-mediated HIF-1α degradation which, in the presence of residual FIH activity, is still able to induce HIF activity [480].

Inhibition of FIH and asparagine hydroxylation however, is not redundant and has been shown to act synergistically with PHD2 suppression, stimulating maximal activation of HIF and expression of its target genes. An example of such a study was that by Huang et al who observed in mouse myoblast cells, a synergistic effect of PHD2 and FIH knockdown. Due to this combinatorial knockdown, these authors observed an increase in fluorescence of a HIF-response element-tagged reporter compared to knockdown of either hydroxylase alone, in addition an increase in mRNA encoding angiogenic factors in response to PHD2 and FIH ablation [481]. In addition, evidence exists for the role of FIH inhibition in propagating a specific transcriptional program that is separate from that induced by PHD2 ablation. FIH inhibition is able to induce expression of a subset of hypoxia-inducible genes, not observed during PHD2 ablation [451].

There is a lack of clear evidence of the precise mechanisms between HIF regulation during chondrogenesis and the contribution of PHD2 and FIH during this process. By comparing the effect of distinctly-functioning hydroxylase inhibitors on HIF-1α stabilisation, HIF-mediated transcription and chondrogenic induction, it may be possible to determine key mechanistic details behind HIF signalling during cartilage development. Therefore due to this lack of clarity of HIF regulation during hypoxic cartilage development, and an absence of studies which compare the roles of $CoCl_2$, DFX and DMOG for cartilage regeneration, the following aim, hypothesis and objectives were proposed.

- **Aim:** To determine which of $CoCl_2$, DFX or DMOG most strongly induces HIF-mediated transcription, hBM-MSC chondrogenesis and inhibition of hypertrophy.
- **Hypothesis**: DMOG due to its high specificity compared to $CoCl_2$ or DFX which may target other iron-utilising enzymes will induce the largest effect during hBM-MSC chondrogenesis in terms of induction of chondrogenic mRNA expression and cartilage ECM production.
- **Objectives**:
    - To identify non-toxic doses of $CoCl_2$, DFX or DMOG for use in a 21-day protocol
    - During hBM-MSC chondro-induction, to identify which of $CoCl_2$, DFX or DMOG more potently stimulates HIF stabilisation and downstream transcriptional activity
    - To identify which of $CoCl_2$, DFX or DMOG more potently stimulates articular chondrogenesis and cartilage ECM formation.
    - To identify which of $CoCl_2$, DFX or DMOG more potently inhibits hypertrophy during chondrogenesis.
    - To confirm that $CoCl_2$, DFX or DMOG function though HIF-1α during their effect on hBM-MSC chondrogenesis.

4.2. Results

4.2.1. Identification of non-toxic doses of $CoCl_2$, DFX and DMOG for 21-day hBM-MSC chondrogenesis

Observation of the hypoxia's effect on chondrogenesis in chapter 3 suggests the role of compounds which stimulate HIF- the primary transducer of physiogical hypoxia, during chondrocyte lineage commitment and cartilage ECM formation. $CoCl_2$, DFX and DMOG, which al stimulate HIF-1α were therefore included in separate TGF-β_3-containing chondrogenic induction media to determine their ability to induce HIF activity and subsequent chondrogenesis of hBM-MSCs. Demonstration of the ability of these compounds to stimulate formation of articular cartilage, whilst inhibiting hypertrophy may indicate new strategies for CTE. In addition, the differential mechanisms of action of $CoCl_2$, DFX and DMOG may illuminate the regulatory mechanisms by which HIF activity is controlled during chondrogenesis.

As previously pertained to, hypoxia and HIF activity are present throughout the entire phase of articular cartilage development from the limb bud mesenchyme up to the resting chondrocyte population. This indicates the requirement of constitutive HIF activity during hBM-MSC chondrogenesis for CTE. Therefore to avoid any deleterious effects of each of the HIF-stabilising compounds on the hBM-MSCs during chondro-induction, $CoCl_2$, DFX and DMOG were included in TGF-β_3-containing chondrogenic induction media at varying concentrations. BM-MSCs in each of these media compositions were then cultured in the identical culture system utilised in chapter 3. These concentrations chosen which are shown in **figure 4.1A** , were based on those

most widely used in the literature (DMOG: 1mM (Nguyen, 2013 #343), $CoCl_2$: 200µM [272], DFX: 200 µM [234]) . These values however, were utilised in cultures of relatively short incubation times in the studies references – approximately 24 hours-7days, compared to the culture period utilised in the current study of 14-21 days. Therefore, the toxicity of a range of reduced values than those shown as shown previously [453], were tested to ensure high cell viability throughout chondrogenic induction of BM-MSCs .

The majority of assays used to assess cell viability rely on quantification of cell metabolism such as the Alamar Blue or MTT assays, or quantify metabolic enzyme activity such as the Lactate Dehydrogenase assay. These cell parametres are affected by hypoxia independently of cell viability, therefore invalidating their use in the resent study. The neutral red assay which quantifies the neutral red dye taken up by viable cells within their lysosomes, was therefore used to assess cell viability. This was compared with the PicoGreen assay which enable cell number to be determined by quantification of double-stranded DNA. **Figures 4.1B** and **4.1C** demonstrate a linear relationship between cell number and Neutral Red/PicoGreen quantification respectively. To ensure the functionality of the Neutral Red assay as a measurement of viability, vehicle-only and high, toxic doses of $CoCl_2$, DFX and DMOG were utilised as respective negative and positive controls.

Throughout this study, the effect of each of the three HIF-stabilising compounds, in addition to being assessed against an untreated control at normoxia, were also compared to the effect of 5%O_2. This oxygen concentration was preferred to 2%, due

to the ability of only 5% in reducing hypertrophic marker expression which is a key problem faced in CTE strategies .

1mM of $CoCl_2$ resulted in zero viability at days 7, 14 and 21 compared to the no-treatment control (p<0.05) as determined by the Kruskal-Wallace multiple-comparison test (**Fig. 4.1D**) . Throughout the 21-day period, 50, 100 and 200µM $CoCl_2$ did not alter viability until day 21 at which point the 200µM appeared to reduce vaibility compared to the untreated control (p>0.05) . The toxic, 1mM dose of DFX resulted in complete ablation of viability after 14 days (p<0.05) (**Fig 4.1E**) . The 100 and 200µM doses of DFX appeared to reduce viability of the differentiating BM-MSCs compared to the no-treatment control at days 14 and 21 (p>0.05) . Conversely the 20 and 50µM doses of DFX did not reduce viability compared to the untreated control as observed due to 100 and 200µM (p>0.05) . 5mM of DMOG also completely reduced viability at days 7, 14 and 21 (p<0.05) (**Fig. 4.1F**) . At days 7 and 14, no obvious change in viability was induced by any of the other DMOG doses compared to the untreated control. At day 21 however 500 and 1000µM concentrations of DMOG appeared to reduce viability (p>0.05) , with no apparent effect observed due to 100 or 200µM.

Overall, 100µM of $CoCl_2$ (**Fig 4.1D**), 50µM of DFX (**Fig 4.1E**) and 200µM of DMOG (**Fig 4.1F**) were the highest concentrations of each compound to not induce ≥25% decrease in viability compared to the untreated control. To ensure the viability assay translated into actual cell number, the PicoGreen assay was used to quantify dsDNA throughout differentiation. None of the doses chosen of each compound altered the cell number throughout chondrogenesis compared to the untreated control when

analysed using the Kruskal-Wallace multiple-comparison statistical test (**Fig 4.1G**) (p>0.05) . Together these results indicate that 100, 50 and 200μM are the highest concentrations of $CoCl_2$, DFX and DMOG respectively to be taken forward for experiments in which thier effect on BM-MSC chondrogenesis is to be assessed. These results also coccur with studies such as that by Tian et al, in which these doses of each compound are shown to increase HIF-1α protein levels by similar magnitudes [453].

A	$CoCl_2$	DFX	DMOG
Negative Control (µM)	0	0	0
Concentration #1 (µM)	20	20	100
Concentration #2 (µM)	50	50	200
Concentration #3 (µM)	100	100	500
Concentration most widely used in literature (µM)	200	200	1000
Toxic Dose (µM)	1000	1000	5000

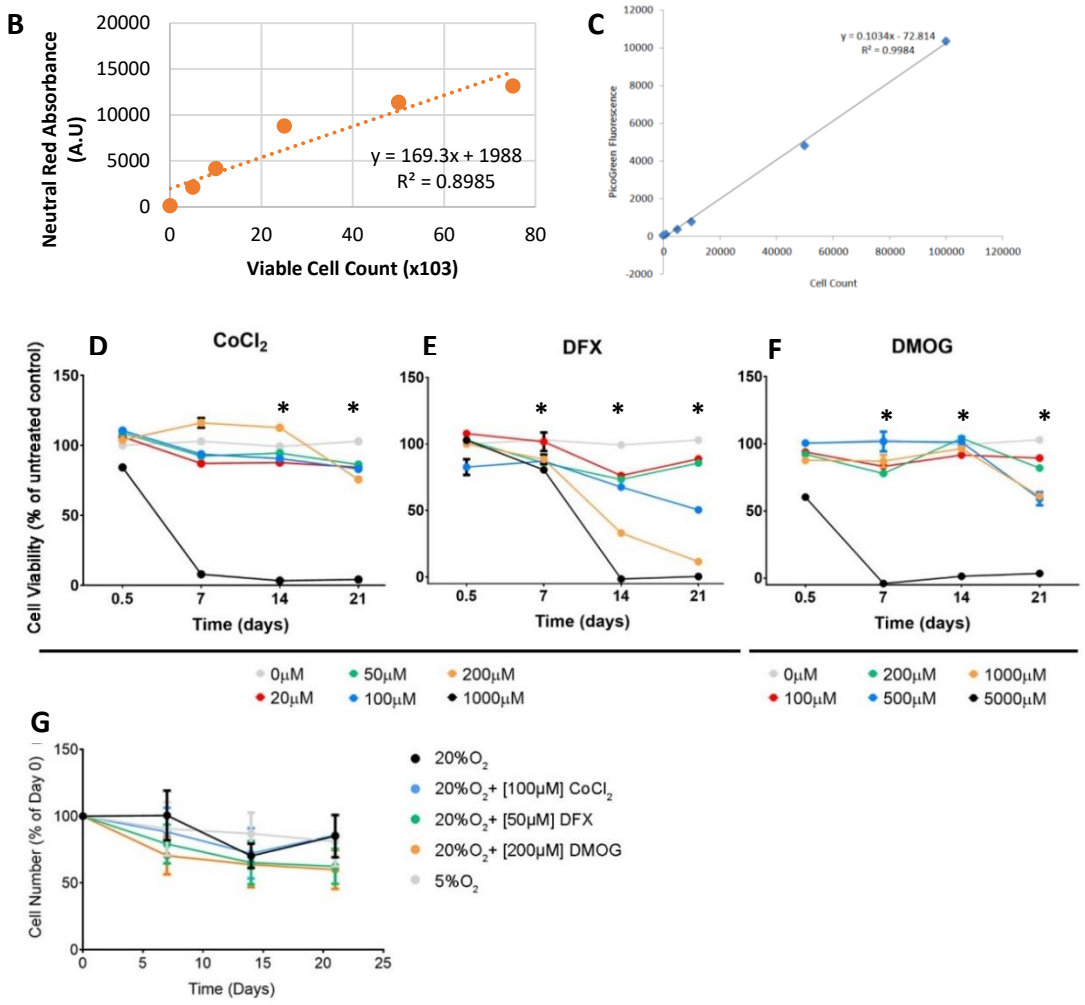

Figure 4.1. CoCl2 at 100µM, DFX at 50µM and DMOG at 200µM do not reduce cell viability to below 75% during 21-day chondrogenic differentiation and do not reduce cell number during this incubation period. (A) Table detailing concentrations of $CoCl_2$, DFX and DMOG tested. (B+C) Standard curves detailing linear relationship between Neutral Red (B)/PicoGreen (C) readings and cell number. (D-F) Cell viability throughout 21-day chondrogenic differentiation with varying concentrations of CoCl2 (D), DFX (E) and DMOG (F) included in the induction media as measured by the neutral red toxicity assay. Values plotted are a percentage of the untreated control which is represented by the grey line. *represents significant difference (p<0.05) between the positive (1000/5000µM for $CoCl_2$+DFX/DMOG respectively) and no treatment (0µM) control. when analysed with a Kruskal-Wallace test with Dunn's correction. (G) Cell number during the chondrogenic differentiation of hBM-MSC in the presence of CoCl2, DFX, DMOG or 5%O_2. Values plotted represent the mean from 3 independent experiments and are a percentage of the cell number at day 0. Error bars show the standard error of the mean.

4.2.2. Induction of HIF-1α stabilisation by $CoCl_2$, DFX and DMOG

$CoCl_2$, DFX and DMOG are all described as hypoxia-mimicking agents due to their ability to increase HIF-1α protein levels, induce its nuclear translocation and stimulate expression of HIF-target genes. Therefore as with experiments in which the stimulation of hypoxic pathways were investigated in choater 3, HIF-1α stabilisation by Western Blot, immunolocalisation and mRNA quantification of HIF-target transcripts were undertaken in BM-MSCs in response to treatment with either $CoCl_2$, DFX and DMOG. As in response to hypoxia, a change in these parametres would demonstrate inhibition of PHD and/or FIH – two hydroxylases in the HIF pathway [453]. As qualitatively assessed by Western Blot and densitometric analysis, no compounds increased total HIF-1α levels significantly compared to the untreated control, however all treatments did induce a trend towards its increase (**Fig. 4.2A+4.2B**).

As with assessment of HIF-1α stabilisation by hypoxia, increase in nuclear HIF-1α localisation occurs as a result of PHD2 inhibition [482]. All three compounds induced HIF-1α nuclear localisation compared to the untreated control upon immunostaining of HIF-1α in the presence of each compound for 24 hours. A higher proportion of the nucleus of each cell was occupied by HIF-1α in the presence of CoCl2, DFX or DMOG compared to that due to the untreated control (**Fig 4.2C**). This quantification represents the images in **Figures 4.2D-4.2K** with HIF-1α-occupation of the nuclei increased due to each compound compared to the untreated control. Interestingly in each condition, a clear peri-nuclear localisation of HIF-1α was observed. This peri-

nuclear staining was observed in discrete patterns suggesting localisation within a subcellular organelle.

Overall, all three HIF-1α-stimulating compounds used here induced HIF-1α nuclear localization. This suggests their potential for increasing formation of an active HIF transcription complex and subsequent transcription of HIF target genes. A selection of such HIF-target genes are those whose products mediate articular chondrogenesis and are inhibitory to chondrocyte hypertrophy. This has been demonstrated by inhibition of HIF-1α during hypoxia-mediated chondrogenesis inhibiting chondrogenic transcript and ECM formation in BM-MSCs, whilst stimulating hypertrophy [272]. This demonstrates the suitability of $CoCl_2$, DFX and DMOG for experiments in which their effect on BM-MSC chondrogenesis is to be investigated. Such a study would enable suitability of such compounds for CTE strategies for repair of acute chondral defects.

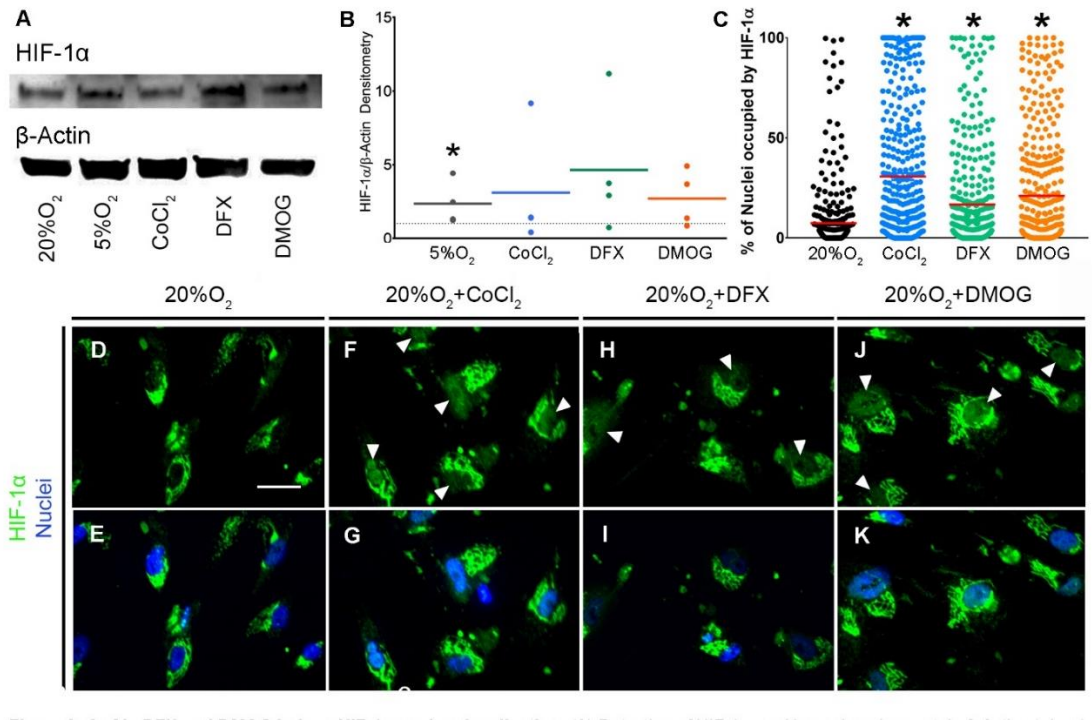

Figure 4.2. CoCl2, DFX and DMOG induce HIF-1α nuclear localisation. (A) Detection of HIF-1α, and housekeeping protein β-Actin at day 1 of chondrogenesis by Western Blot. (B) Protein blots of HIF-1α were quantified by densitometric analysis and normalised to levels of β-Actin. Values plotted represent magnitude difference to the untreated control which is represented by the horizontal dotted line. The solid coloured lines represent the mean for each condition with *denoting $p<0.05$ compared to the untreated control. (C) Quantification of nuclear HIF-1α immunofluorescence at day 1 of chondrogenesis. Each value plotted represents the percentage of a single DAPI-marked nucleus that is occupied by HIF-1α. Values from 3 independent repeats shown with the coloured horizontal lines representing the mean and *denoting $p<0.05$ compared to the untreated control. (D-K) HIF-1α immunofluorescence staining at day 1 of chondrogenesis. Scale Bar = 50μm. Representative images of 3 independent repeats shown. Images were cropped and magnified to clearly visualise localisation of HIF-1α.

4.2.3. DMOG induced constuitive expression of HIF target genes compared to that induced by $CoCl_2$ or DFX

To determine if the increased HIF-1α nuclear localisation induced by $CoCl_2$, DFX and DMOG translated into enhanced functional activity of the HIF transcriptional complex, we used qPCR to quantify mRNA of established HIF targets throughout the entire chondrogenic induction period. The genes analysed are identical to those used in chapter 3 in which the effect of hypoxia was investigated. DMOG treatment at days 1, 7 and 21 increased expression of *VEGFA* by approximately 5, 10 and 15x that of the untreated control respectively (**Fig. 4.3A**). At all 4 time points, DMOG also upregulated expression of *PGK1* (4x, 7x, 6x, 6x respectively for days 1, 7, 14 and 21; **Fig 4.3B**) and *EGLN* (7x, 10x, 27x, 9x respectively for days 1, 7, 14 and 21 **Fig 4.3C**). DFX induced expression of *PGK1* at day 14 (**Fig 4.3B**) and *EGLN* at day 21 (**Fig 4.3C**) compared to the untreated control with $CoCl_2$ not inducing expression of any the three HIF-targets chosen.

Taken together, despite all three compounds inducing HIF-1α nuclear localization only DMOG appeared to constituitively induce expression of genes documented to contain HREs are which are responsive to HIF induction. This therefore suggests that 2-OG analogues compared to those which sequester Fe^{2+} ($CoCl_2$/DFX) may induce stonger transcriptional activity at the promoter regions of HIF-target genes. This indicates that 2-OG inhibitors may represent the more appropriate class of inhibitor for CTE in which HIF-1α is required required to be elevated increased articular chondrogenesis.

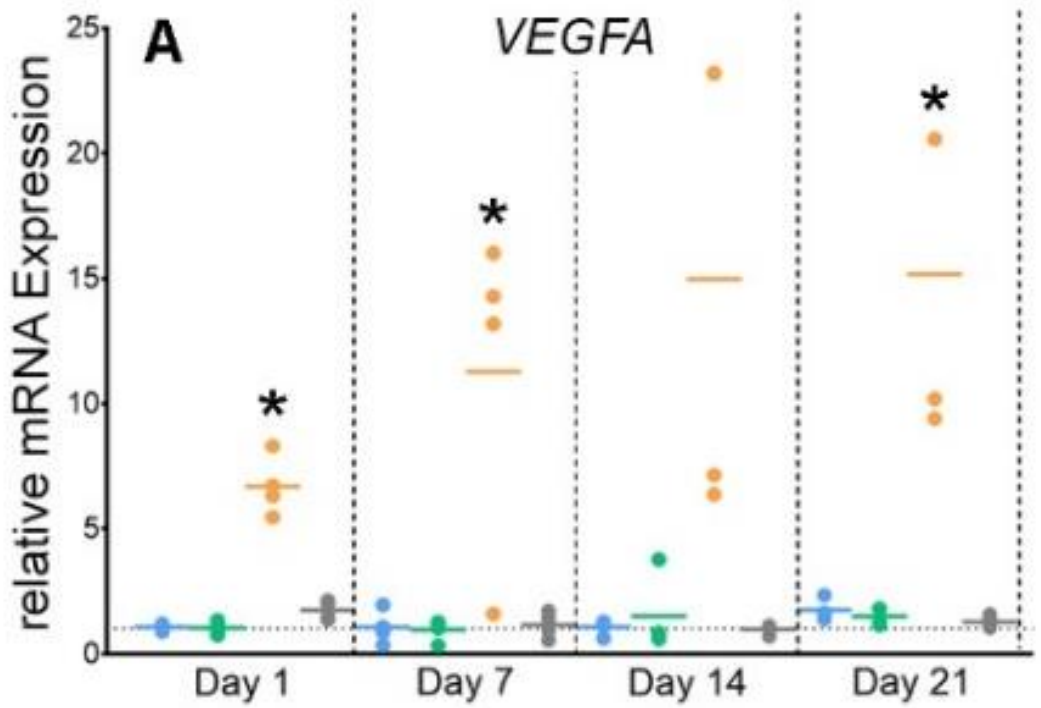
A
VEGFA
relative mRNA Expression
25
20
15
10
5
0
*
*
*
Day 1
Day 7
Day 14
Day 21

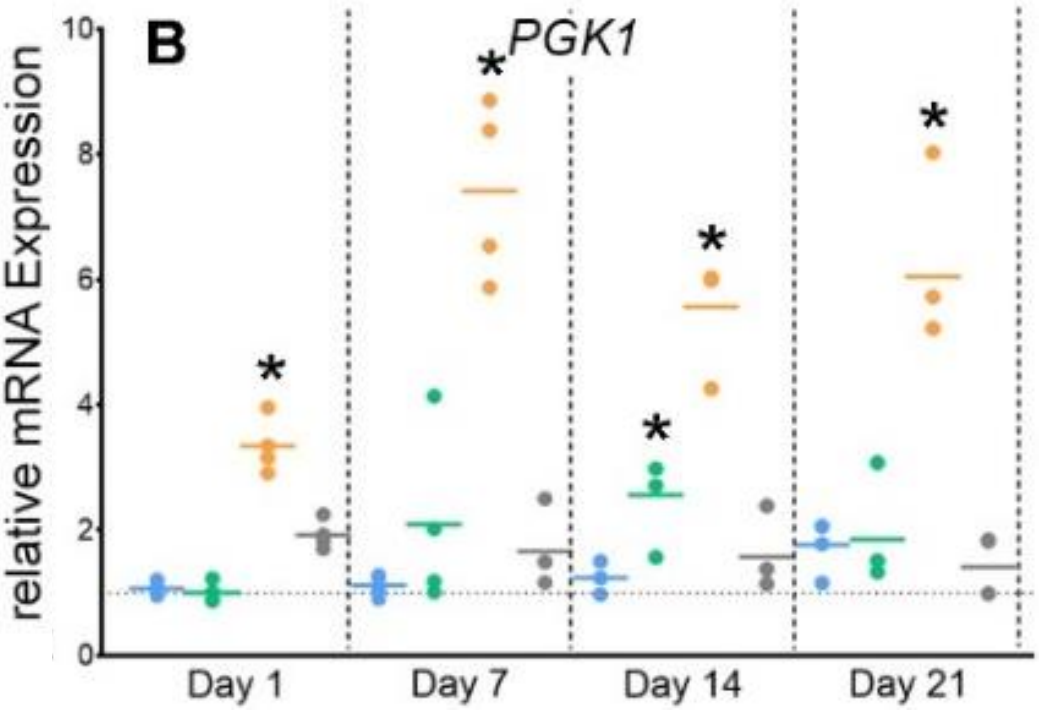
B
PGK1
relative mRNA Expression
10
8
6
4
2
0
*
*
*
*
Day 1
Day 7
Day 14
Day 21

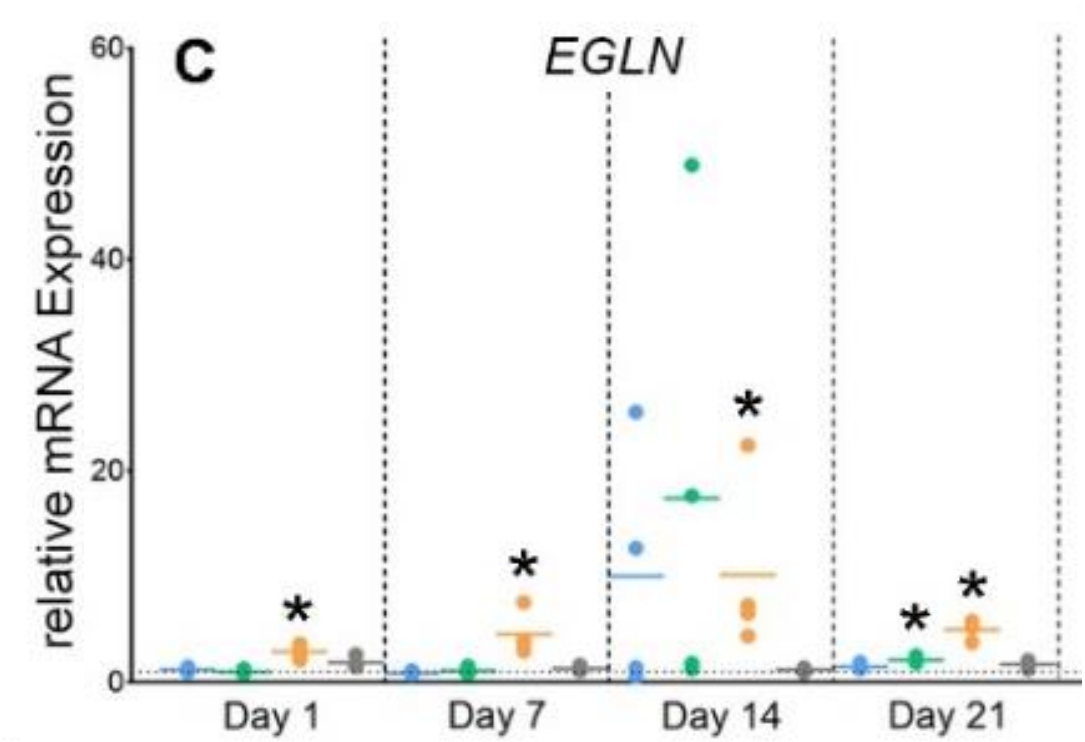

Figure 4.3. DMOG stimulates transcription of HIF targets constuitively throughout the 21-day chondrogenic induction period. mRNA expression of *VEGFA* (A), *PGK1* (B) and *EGLN* (C) throughout chondrogenesis. Values plotted are from 4 independent experiments and are fold change compared to the untreated control which is represented by the horizontal dotted line. The solid coloured lines represent the mean for each condition with *denoting $p<0.05$ compared to the untreated control.

4.2.4. Effect of $CoCl_2$, DFX and DMOG on transcription conducive for hBM-MSC chondrogenesis

Expression of *SOX9* and its downstream targets- *COL2A1* and *ACAN* are essential for chondrogenesis and cartilage ECM formation. Together, these are required for the repair of chondral defects in CTE strategies, and replacement with tissue which mimicks native articular cartilage, both biochemically and mechanically. Stimulation of HIF-1α during chondrogenesis is important for hypoxia-mediated chondrocyte differentiation and expression of *SOX9*, *COL2A1* and *ACAN* [262, 269]. Therefore, to investigate the ability of $CoCl_2$, DFX and DMOG to stimulate expression of these genes during chondrogenesis qPCR was utilised to quantify their corresponding mRNA levels. The major role of SOX9 during chondrogenesis, from early chondrogenic lineage commitment to inhibition of hypertrophy promoted investigation at days 1, 7, 14 and 21 of chondrogenesis. As in chapter 3, latent, day 14 expression of *ACAN* and *COL2A1* which precedes cartilage ECM formation, denotes a typical chondrogenic differentiation program.

Compared to the untreated control, DMOG induced significant expression of *SOX9* at days 7 and 21 by approximately 4x at each of these time points (**Fig. 4.4A**). DFX appeared to show a trend towards increasing *SOX9* transcripts at days 14 and 21, but these were not statistically significant. Unlike that shown in **chapter 3, figure 3.3** where we observed increases in *SOX9* due to 5%O_2 at day 1, those differences were no longer statistically significant when analysed using the multi-variant Kruskal-Wallace test in which the effects of DMOG were included. Despite these increases observed due to only DMOG, all conditions appeared to significantly increase

expression of its target, *COL2A1* (approximately 3.5x, 4x, 3x, 1.5x by $CoCl_2$, DFX, DMOG and 5%O_2 respectively; **Fig. 4.4B**). However, no conditions significantly raised expression of *ACAN* despite each treatment showing trend towards increases in this transcript (approximately 7.5x, 11x, 5x by $CoCl_2$, DFX and DMOG respectively; **Fig. 4.4C**).

In addition to investigating the expression of 'classic' chondrogenic markers, it is also important to quantify expression of gene whose products play other key role during cartilage ECM formation. *P4HA1* which encodes the CP4HA1 and *LOX* which encodes LOX and plays key roles in the formation of the collagen helical structure important in native cartilage ECM function and polymerisation of multiple collagen helices. A key facet therefore of any CTE strategy is maintaining these post-translational modifications of the collagen helices, which are important for function of the collagen network in cartilage ECM [483]. The product of *P4HA1* catalyses the hydroxylation of specific proline residues [484]. LOX coverts lysine and hydroxylysine residues to their aldehyde form which facilitates covalent crosslinks between individual collagen fibrils [483]. Both of these enzymes have been shown to be upregulated by HIF and hypoxia [280, 485] and indeed both DFX and DMOG induced *LOX* expression significantly by approximately 2x and 3x respectively compared to untreated controls (**Fig. 4.4D**). *P4HA1* was significantly upregulated by approximately 6x in response to DMOG treatment (**Fig. 4.4E**). **Figures 4.4F+4.4G** demonstrate the suitability of *LOX* and *P4HA1*-specific primers with regards to the efficiency of the qPCR reaction which they mediate and a linear relationship between cycle number and input cDNA.

Overall, DMOG displayed the greatest advantages with regards to induction of chondrogenic mRNA during BM-MSC chondrocyte differentiation. It enhanced expression of the master chondrogenicn transcription factor; *SOX9* throughout chondrogenesis with no change seen due to $CoCl_2$ or DFX. DMOG also induced expression of *LOX* and *P4HA1* – genes whose products are integral in Collagen deposition in cartilage ECM. Together, these suggests that DMOG may have the greatest potential with regards to its inclusion in a CTE strategy.

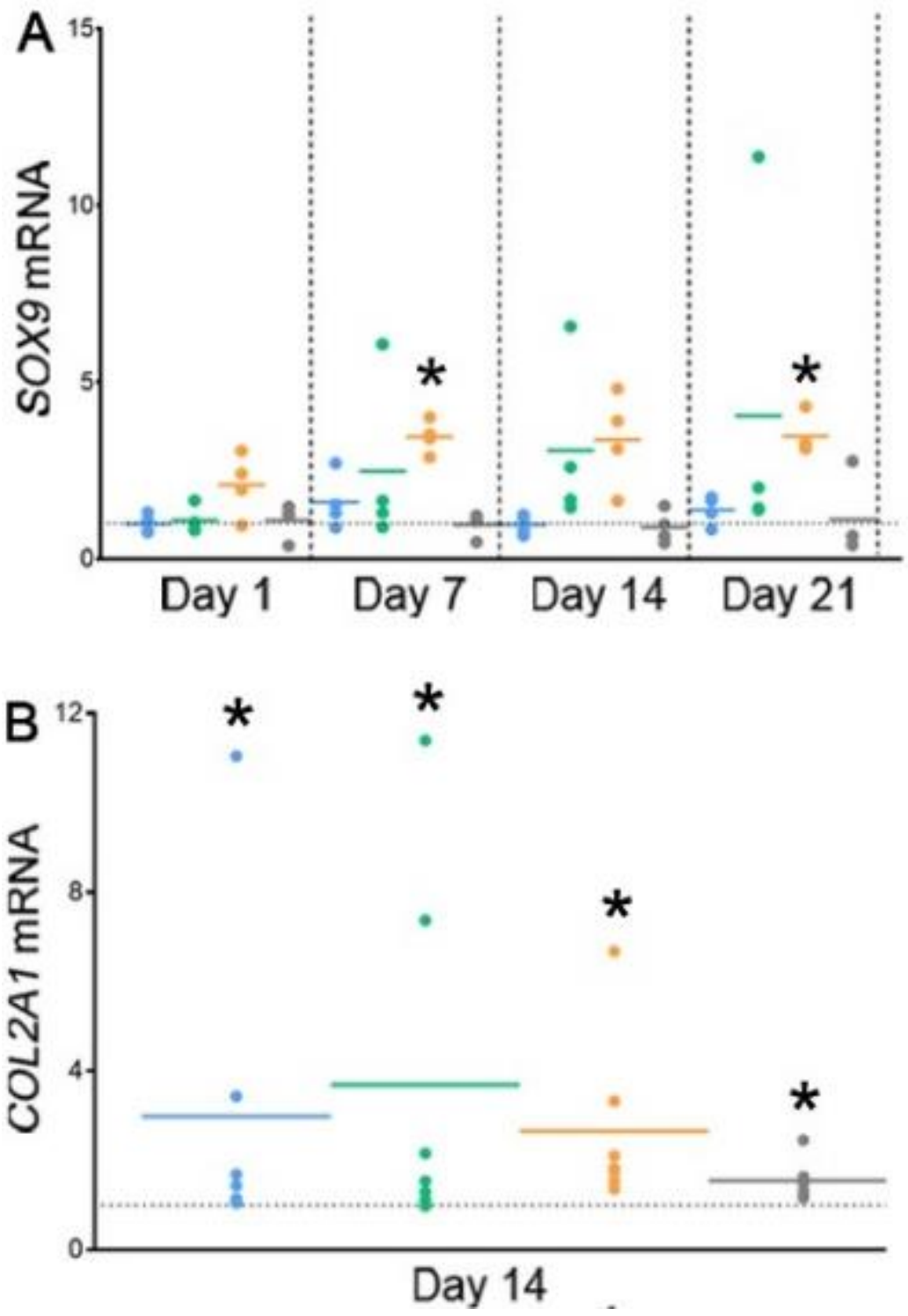
A
SOX9 mRNA
15
10
5
0
*
*
Day 1
Day 7
Day 14
Day 21
B
COL2A1 mRNA
12
8
4
0
*
*
*
*
Day 14

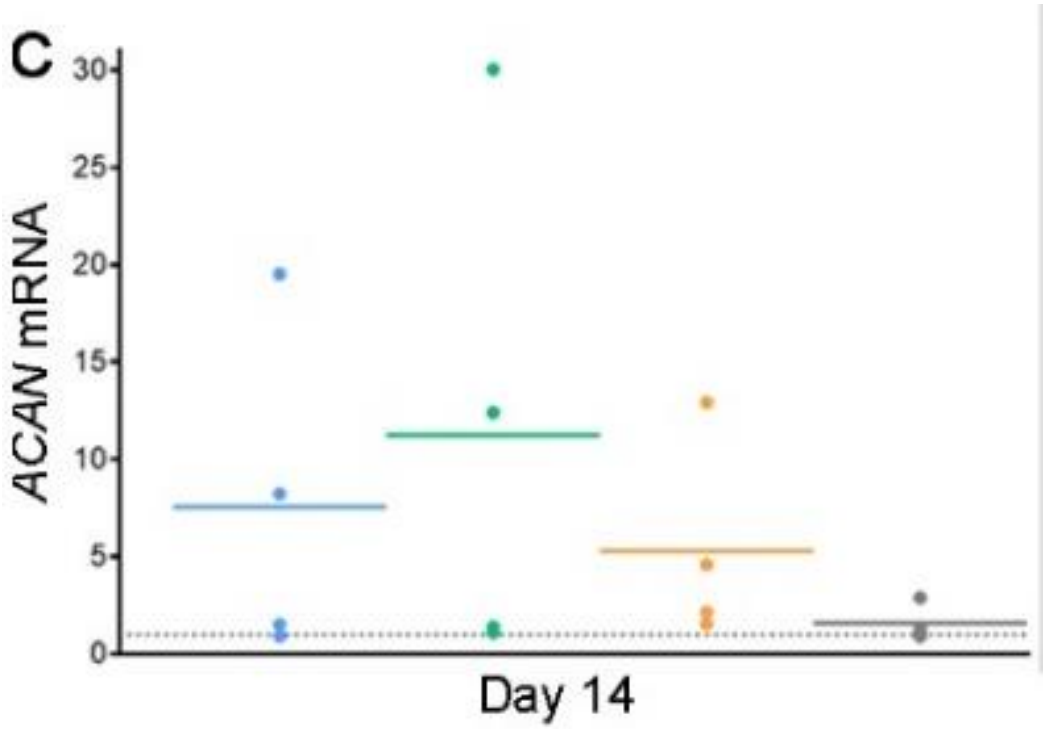
C
ACAN mRNA
30
25
20
15
10
5
0
Day 14

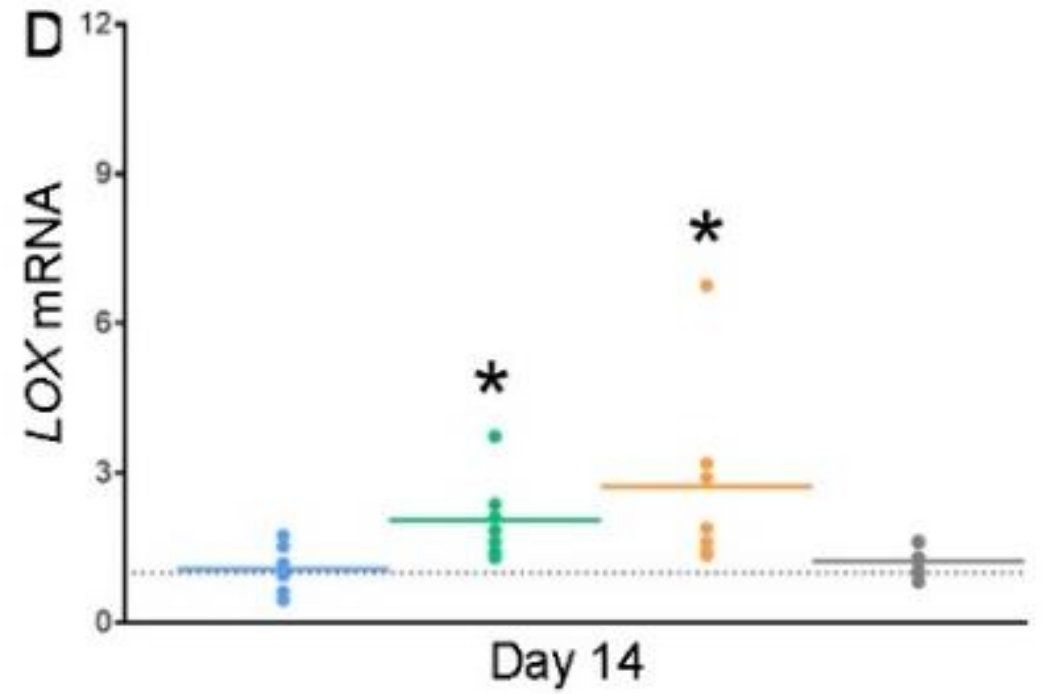
D
LOX mRNA
12
9
6
3
0
*
*
Day 14

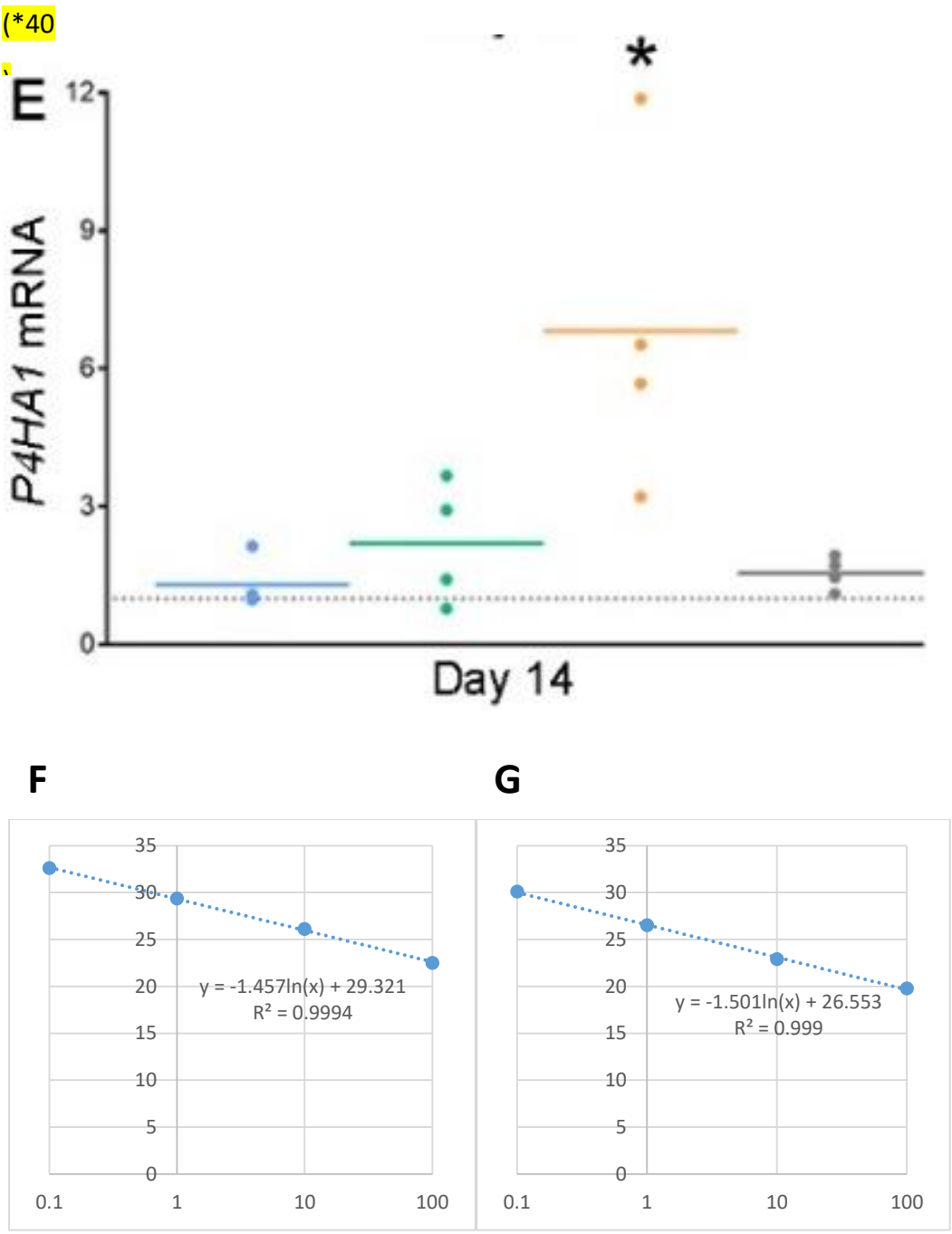

Figure 4.4. DMOG induces a transcriptional profile in differentiating BM-MSCs which is conducive for chondrogenesis and cartilage formation. mRNA expression of *SOX9* (A), *COL2A1* (B), *ACAN* (C), *LOX* (D) and *P4HA1* (E) throughout chondrogenesis. Values plotted are from 4 independent experiments, and are fold change compared to the untreated control which is represented by the horizontal dotted line. The solid coloured lines represent the mean for each condition with *denoting $p<0.05$ compared to 20%O_2. (F+G) Standard curve which demonstrates a linear relationship between input cDNA concentration and cycle (Ct) number when amplified using *LOX* (F) and *P4HA1* (G)-specific primers.

4.2.5. DMOG inhibits the presence of Collagen Type II and GAGs in the ECM during chondrogenesis of hBM-MSCs

To assess if the changes in chondrogenic gene expression due to $CoCl_2$, DFX and DMOG translates into an increased presence of deposited cartilage ECM components, we examined the presence of Collagen Type II and GAGs in the produced by differentiated hBM-MSCs. This was accomplished by immunostaining and Alcian Blue histochemical staining for Collagen Type II and GAGs respectively at day 21 of chondrogenesis. Such an investigation would indicate the suitability of $CoCl_2$, DFX and DMOG for inclusion in a CTE strategy due to the requirement of a Collagen Type II and GAG-rich ECM for articular cartilage function [33, 438].

Neither $CoCl_2$ (**Fig. 4.5B**) nor DFX (**Fig. 4.5C**) induced changes in Collagen Type II compared to the untreated control (**Fig. 4.5A**). This was also mirrored by a lack of change in staining for GAGs due to $CoCl_2$ (**Fig. 4.5F**) or DFX (**Fig. 4.5G**) compared to the untreated control (**Fig. 4.5E**). DMOG however appeared to inhibit both incorporation of Collagen Type II (**Fig. 4.5D**) and GAG's (**Fig. 4.5H**) into the ECM. Quantification of Collagen Type II immunofluorescence confirmed this inhibition due to DMOG when the signal due to the presence of Collagen Type II was normalised to the number of DAPI-stained nuclei in each image (**Fig. 4.5I**). This significance was determined by a Kruskal Wallace multiple comparison test ($p<0.05$). The decrease in GAGs due to DMOG were not significant ($p<0.05$) when total GAGs were quantified and normalised to cell number as determined by the PicoGreen assay (**Fig. 4.5J**).

Overall, despite DMOG demonstrating advantages at the mRNA levels with regards to BM-MSC chondrogenesis, it appeared to reduce the production of Collagen Type

II by these cultures. This represents a major issue with regards to use of DMOG in CTE. This is due to the requirement of cartilage ECM for maintaining viability of the resident chondrocytes, enabling resistance to compressive forces applied on the containing joint and providing lubrication between articulating surfaces.

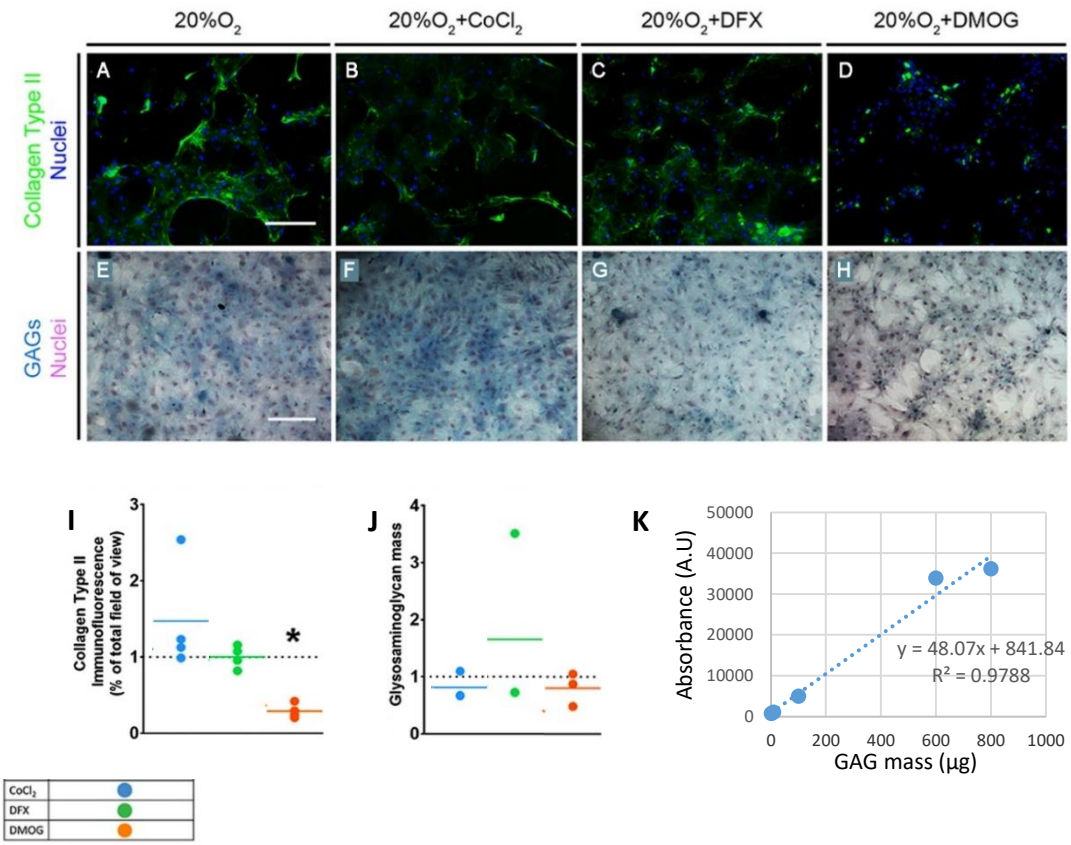

Figure 4.5. DMOG inhibits Collagen Type II deposition in the extracellular matrix by reducing its production per cell. (A-D) Collagen Type II immunofluorescence staining at day 21 of chondrogenesis. Scale Bar = 400µm. Representative images of 4 independent repeats shown. Alcian Blue staining for glycosaminoglycans with nuclear haematoxylin counterstain at day 21 of differentiation. Scale bar = 400µm. Representative images of 3 independent experiments are shown. (I-J) Quantification of Collagen Type II immunofluorescence (I) and Glycosaminoglycans (J) at day 21 of chondrogenesis both without and with values normalised to DAPI immunofluorescence/total double stranded DNA. Values plotted are from 4 independent experiments, and are fold change compared to the untreated control, represented by the horizontal dotted line. The solid coloured lines represent the mean for each condition and *denotes $p<0.05$ compared to the untreated control. (K) Standard curve illustrating linear relationship between GAG mass and absorbance reading.

4.2.6. DMOG induced an anti-hypertrophic transcriptional profile and inhibits Collagen Type X protein levels

To identify any changes in hypertrophy of the chondrogenically-induced hBM-MSCs as observed due to 5%O_2 in chapter 3, we investigated changes in transcription of *RUNX2* and *COL10A1* but also quantified *MMP13* mRNA in response to $CoCl_2$, DFX and DMOG treatment. Increased expression of *MMP13* is observed during chondrocyte hypertrophy [486], plays a significant role in OA pathogenesis via digestion of Collagen Type II [487], and is downregulated by hypoxia and HIF [288]. Together, an effect on hypertrophic mRNA expression would demonstrate the suitability of either compound for CTE strategies. Chondrocyte hypertrophy during BM-MSC differentiation is a significant pitfall of current attempts articular cartilage regenerative medicine due to the subsequent mineralisation which subsequently occurs [414].

No conditions induced increases in *RUNX2* mRNA at any time point during chondrogenesis (**Fig. 4.6A**). DMOG treatment caused a significant increase in the ratio of *SOX9:RUNX2* mRNA at days 7, 14 and 21 (approximately 4x, 3x, 3x respectively) compared to the untreated control (**Fig. 4.6D**). DMOG also significantly inhibited expression of *COL10A1* mRNA (**Fig. 4.6B**) and this significantly increased the ratio of *COL2A1*:*COL10A1* by approximately 6x due to DMOG compared to the untreated control (**Fig. 4.6E**). No changes were apparent in *MMP13* expression due to any condition (**Fig. 4.6C**). In terms of Collagen Type X protein, both DFX (**Fig. 4.7C**) and DMOG (**Fig. 4.7D**) reduced immunostaining for this hypertrophic marker

compared to the untreated control (**Fig. 4.7A**), with $CoCl_2$ inducing a more subtle decrease (**Fig. 4.7B**).

Overall, DMOG at the transcript level, demonstrated clear advantages with regards to promotion of an articular chondrocyte phenotype and inhibition of hypertrophy. Compared to that induced by $CoCl_2$ or DFX, an increase of *SOX9* compared to levels of *RUNX2* and inhibition of Collagen Type X (at the mRNA and protein level) by DMOG, suggests its use in programming BM-MSCs down an articular chondrocyte lineage only in CTE.

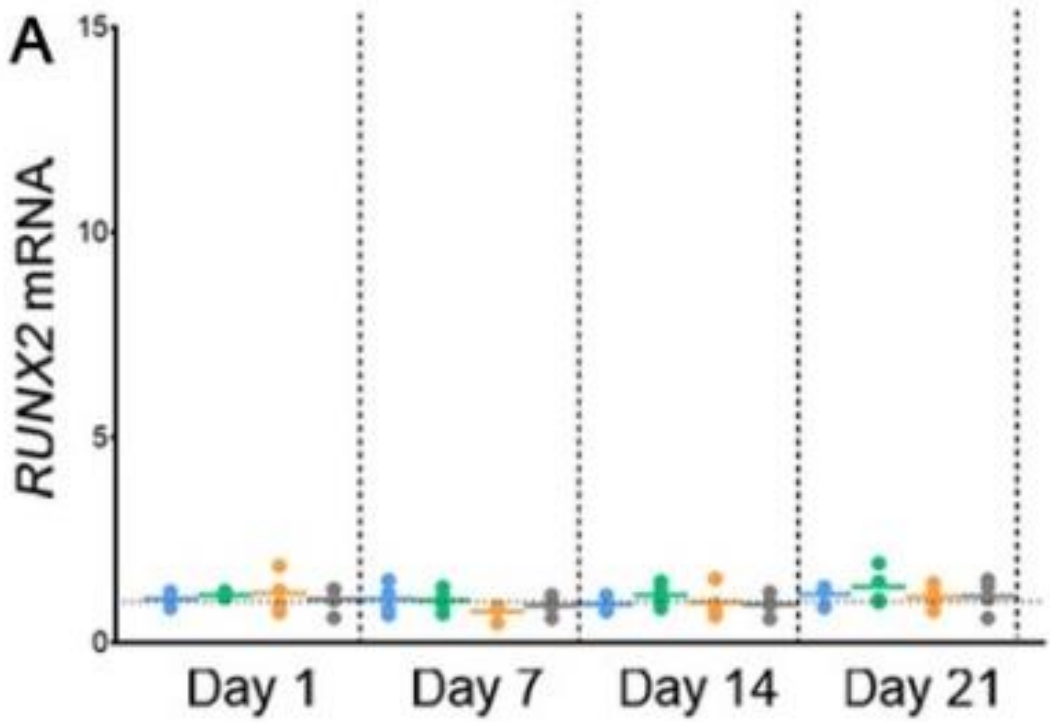
A
RUNX2 mRNA
15
10
5
0
Day 1
Day 7
Day 14
Day 21

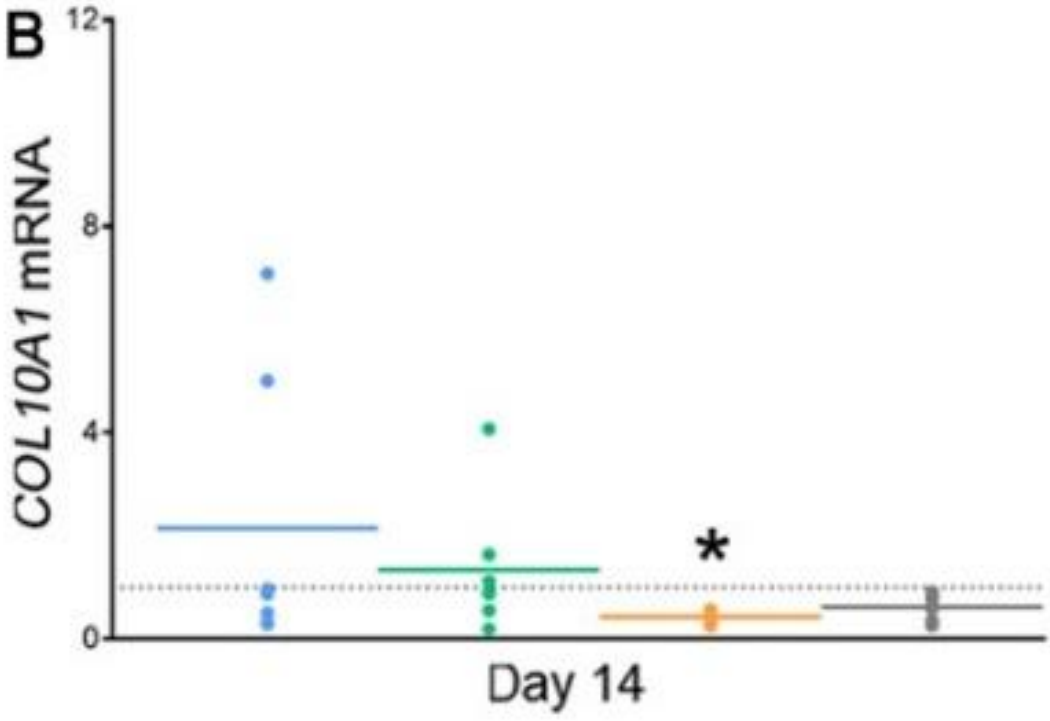
B
COL10A1 mRNA
12
8
4
0
*
Day 14

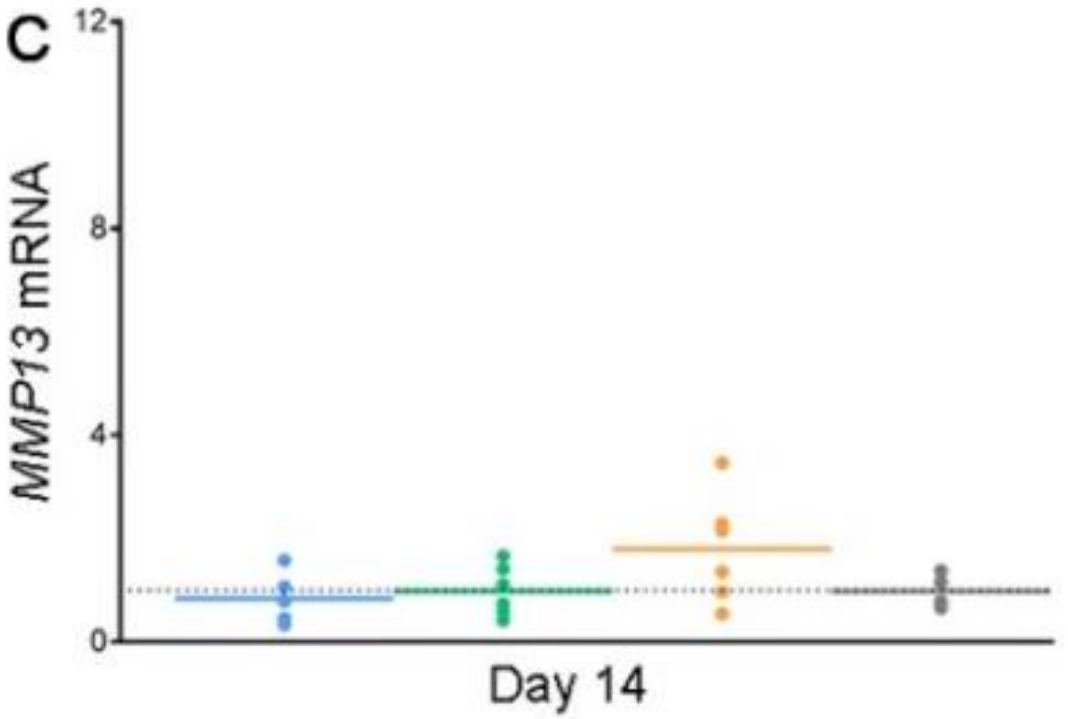
C
MMP13 mRNA
12
8
4
0
Day 14

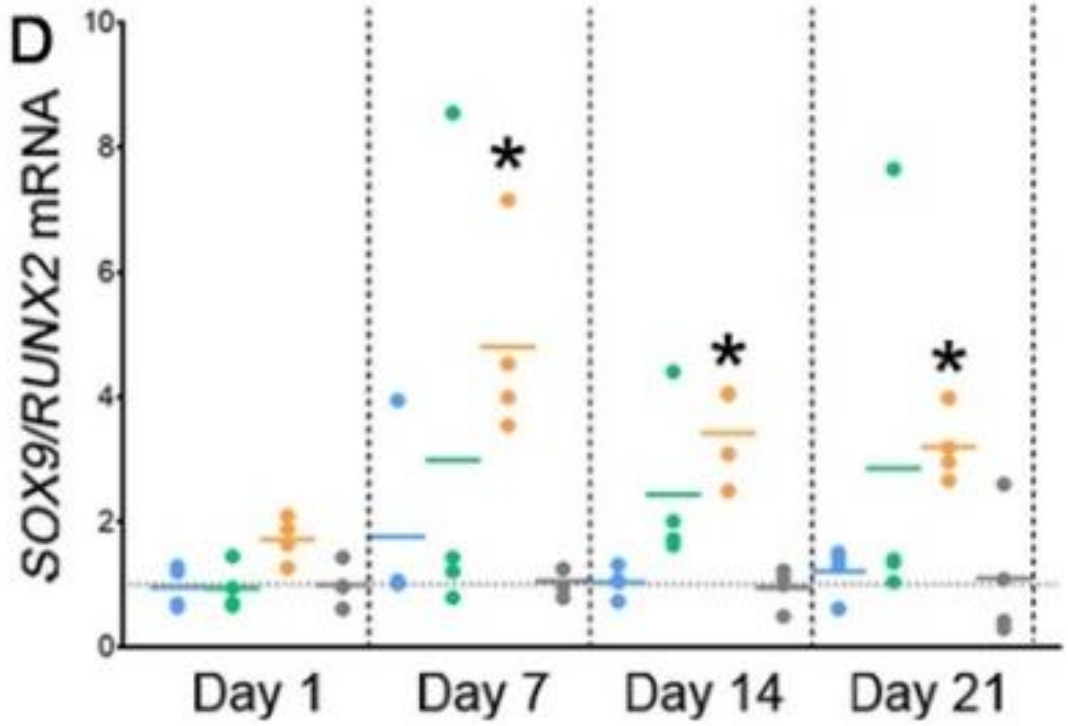
D
SOX9/RUNX2 mRNA
10
8
6
4
2
0
*
*
*
Day 1
Day 7
Day 14
Day 21

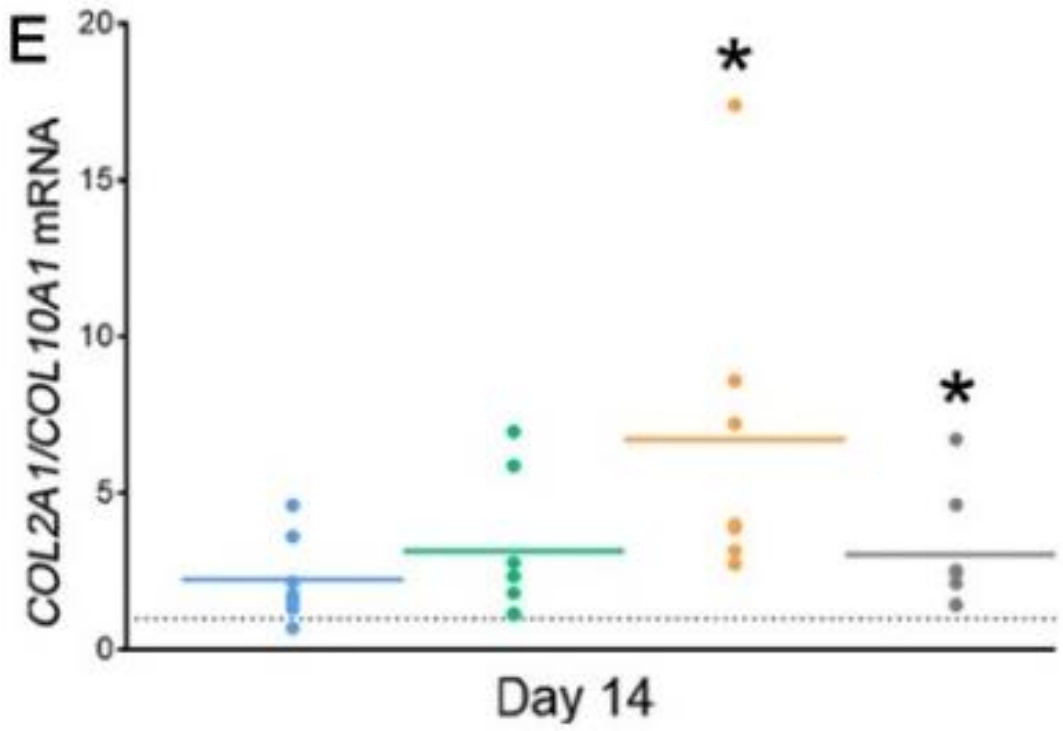

Figure 4.6. DMOG induces a transcriptional profile in differentiating BM-MSCs which is inhibitory to chondrocyte hypertrophy. mRNA expression throughout chondrogenesis of *RUNX2* (A), *COL10A1* (B), *MMP13* (C) and *SOX9* & *COL2A1* normalised to *RUNX2* & *COL10A1* respectively (D+E). Values plotted are from 4 independent experiments and are fold change compared to the untreated control which is represented by the horizontal dotted line. The solid coloured lines represent the mean for each condition with *denoting $p<0.05$ compared to the untreated control.

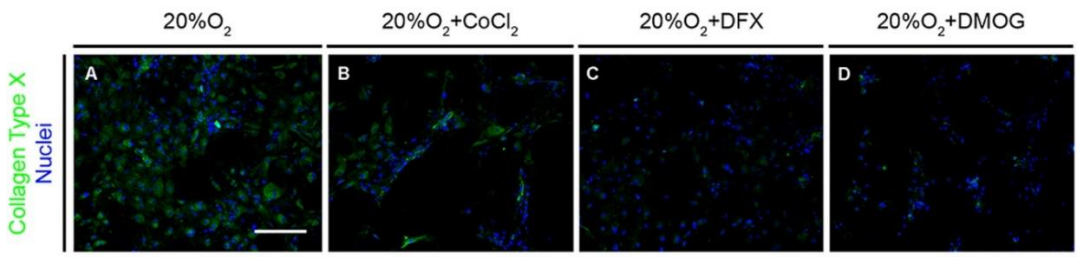

Figure 4.7. DFX and DMOG reduce Collagen Type X protein in chondrogenically-differentiating hBM-MSCs. (A-D) Collagen Type X immunofluorescent staining at day 21 of chondrogenesis. Scale Bar = 400µm. Representative images of 3 independent repeats shown.

4.2.7. Effect of $CoCl_2$, DFX and DMOG on expression of Bone Morphogenetic Protein, Indian Hedgehog and Wnt pathway components during hBM-MSC chondrogenesis

The differential effects $CoCl_2$, DFX and DMOG on the chondrogenic gene expression profile during induction of hBM-MSCs prompted investigation into the expression of components of other pathways important during cartilage development. Canonical Wnt signalling plays a key role during limb development. β-Catenin activity is required for early limb bud initiation via FGF signalling [488] and plays key roles in determining cell fate of the early mesenchymal limb bud population between the osteoblastic or chondrogenic cell fates [66] It is also involved in propagating chondrocyte hypertrophy and endochondral ossification [100]. Secondly, BMP signaling has also been shown to mediate hypertrophic signaling during cartilage development and *in vitro* [489, 490].

The importance of Wnt and BMP signaling in cartilage hypertrophy prompted investigation of the effect of the HIF-1α-stabilising compounds on genes whose products regulate the activity of Wnt and BMP signalling. Such data may provide insights into how these compounds are able to inhibit hypertrophy during BM-MSC chondrogenesis which is an essential facet of any CTE strategy. As described in chapter 3, hypoxia has been shown to upregulate Wnt and BMP antagonists- DKK1 and Gremlin1 during chondrogenesis of BM-MSCs. As HIF-1α is known to play key roles during hypoxia-mediated chondrogenesis, we therefore examined expression of *DKK1* and *GREM1* here in response to treatment of $CoCl_2$, DFX and DMOG. In addition, the expression of canonical β-Catenin target genes was examined.

Expression of these targets- *AXIN2* and *LEF1* may give a diect indication of the activity of the Wnt pathway during chondrogenesis of BM-MSCs. This may therefore enable correlations to be made with hypertrophic marker expression and how these together are regulated by HIF-1α-stabilising compounds.

Compared to the untreated control, expression of *DKK1* appeared to follow a trend towards downregulation at day 1 and upregulation at day 21 due to DMOG (**Fig. 4.8A**). DFX induced a trend of upregulation in *DKK1* at days 7, 14 and 21 of differentiation (**Fig. 4.8A**). No effect on *DKK1* expression appeared to be induced by $CoCl_2$. Compared to the untreated control, all compounds appeared to also show trends towards increases of Wnt targets *AXIN2* (**Figs. 4.8C**) and *LEF1* (**Figs. 4.8D**) at day 14, with an increase in *LEF1* also observed at day 1 due to DMOG. Interestingly, this effect at day 14 was also preceded by a suppression of *AXIN2* at day 7 due to all compounds compared to the no-treatment control (**Figs. 4.8C**). In terms of expression of the BMP antagonist- *GREM1*, $CoCl_2$ and DMOG appeared to more strongly induce *GREM1* expression at days 7 14 and 21 compared to that observed due to DFX and the untreated control (**Figs. 4.8B**).

Overall, all 3 compounds appeared to induce *DKK1* or *GREM1* expression, however this did not appear to correlate with expression of Wn targets, *AXIN2* and *LEF1*. In addition, the inhibition of hypertrophy specifically by DMOG shown previously did not appear to correlate with an inhibition of Wnt or BMP signaling. This perhaps indicates that DMOG's anti-hypertrophic effect is not mediated through inhibition of Wnt/BMP-induction of *RUNX2*/*COL10A1* etc.

Indian Hedgehog signalling is another pathway whose output is important in regulating the phenotype of different populations of chondrocytes during endochondral ossification. It maintains articular chondrocytes distally located from the primary ossification centre, whilst inducing hypertrophy in those more proximal to the centre of the developing bone. The gene product of *IHH,* which upon binding to Patch1 receptors on articular chondrocytes, sitmulates expression of *PTHRP* whose product inhibits hypertrophic progression. Therefore, expression of *IHH* and *PTHRP* in response to treatment of chondrogenically-induced BM-MSCs with HIF-1α-stabilising compounds, would also illustrate regulation of hypertrophic signaling by these compounds.

Despite there being no significant changes in expression of the genes encoding the two ligands- *IHH* (**Figs. 4.8E**) and *PTHRP* (**Figs. 4.8F**), there was a trend towards increase in the mRNA of those at day 14 in the presence of all compounds. There was also a similar trend at in expression of *IHH* at day 1 due to DMOG (**Figs. 4.8E**). Overall and as with expression of Wnt/BMP antagonists, there appeared to be no correlation between the DMOG's unique inhibition of hypertrophy and expression of anti-hypertrophic Indian Hedghog signaling genes. Instead all three compounds appeared to upregulate *IHH* and *PTHRP*, indicating the ability of $CoCl_2$, DFX and DMOG to provide an anti-hypertophic signaling milleu during BM-MSC chondrogenesis. **Figure 4.8G-4.8J** demonstrate the ability of AXIN2, LEF1, IHH and PTHRP-specific primers to amplify input cDNA with reaction efficiencies between theoretical values of 90-110%. Linear relationships were also demonstrated between input cDNA and cycle number.

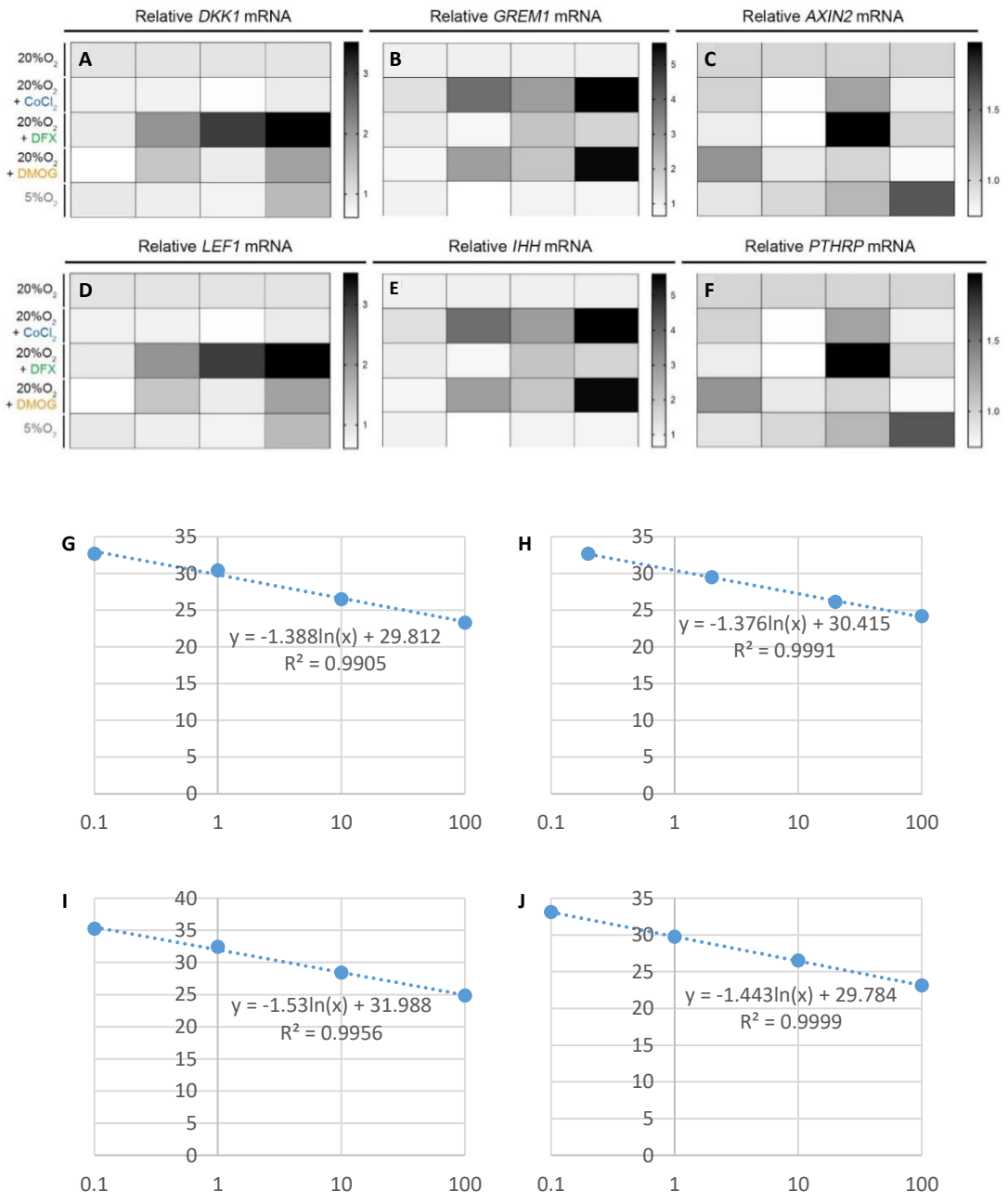

Figure 4.8. During BM-MSC chondrogenesis, CoCl2, DFX and DMOG induce changes in the mRNA of genes whose products are involved in the Bone Morphogenetic Protein, Wnt and Indian Hedgehog signalling pathways. (A-F) mRNA expression of *DKK1* (A), *GREM1* (B), *AXIN2* (C), *LEF1* (D), *IHH* (E) and *PTHRP* (F) throughout chondrogenesis. Values plotted represent the mean value of 4 independent experiments and are fold change compared to the untreated control (20%O_2). Data illustrated as scatter plots in **appendix figure 6**. [491] Standard curves which demonstrate a linear relationship between input cDNA concentration and cycle (Ct) number when amplified using *AXIN2*- (G), *LEF1*- (H), *IHH*- (I) and *PTHRP*- (J) specific primers (y axis = Ct, x axis = [cDNA] (%).

4.2.8. Identification of a HIF-1α inhibitor for use during hBM-MSC chondrogenesis

The regulation of HIF-1α during chondrogenesis of BM-MSCs is poorly understood. The use of $CoCl_2$, DFX and DMOG during this process may enable elucidation of HIF-1α control due to the differential mechanism of action of these compounds and varying extent to which they inhibit PHD2 and FIH. However, before any interpretation can be made from experiments in which $CoCl_2$/DFX/DMOG stimulate chondrogenesis, it is required to confirm that these effects are indeed mediated via HIF-1α. Therefore, to determine if the potent transcriptional effect of DMOG is mediated via stabilisation of HIF-1α, we sought to identify an inhibitor of its HIF-1α that is downstream of the proposed effect of DMOG which inhibits PHD2 and FIH-mediated hydroxylation of HIF-1α.

One such compound is Acriflavine which acts to block the dimerization of HIF-1α with an essential transcriptional co-factor in the HIF complex- HIF-1β [492]. ACF has therefore been demonstrated to reduce the availability of HIF-1α in the HIF transcriptional complex, without affecting its protein levels [493]. To determine if ACF retained this biological effect when used in conjunction with TGF-β_3-containing chondrogenic media and DMOG, we quantified the effect of 5μM ACF on the levels of mRNA encoding established HIF targets after a 24 hour treatment period. DMOG induced expression of *VEGFA, EGLN, PGK1* and *GLUT2* by approximately 9x, 2.5x, 3x and 4x respectively compared to the untreated control, and these increases were abolished in the presence of ACF (**Fig. 4.9A**). To ensure ACF treatment did not significantly alter cell number throughout chondrogenic differentiation we measured the number of DAPI-stained nuclei after 14 days of culture. No difference in cell

number was observed due to ACF in the presence of DMOG compared to DMOG treatment alone (**Fig 4.9B**).

Together, these results demonstrate that ACF can be used to inhibit DMOG-mediated expression of HIF targets without negatively affecting cell number for 14 days, at which point chondrogenic transcripts are upregulated by hypoxia and HIF stimulation.

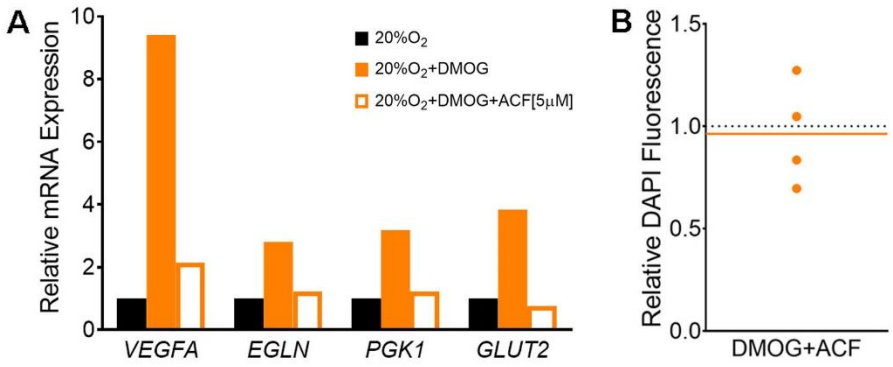

Figure 4.9. Acriflavine abolished DMOG-mediated upregulation of HIF target transcription and does not alter cell number after 21 days in DMOG-supplemented conditions. (A) mRNA expression of *VEGFA*, *EGLN*, *PGK1* and *GLUT2* following a 24-hour incubation period (n=1). Values plotted are fold change compared to the untreated control without DMOG. (B) Quantification of DAPI-stained nuclei following 14-day incubation in chondrogenic conditions in the presence of DMOG+/-Acriflavine. Values plotted are from 4 independent repeats and are fold change compared to DMOG treatment without Acriflavine which represented by the horizontal is dotted line. The mean value is represented by the horizontal orange line.

4.2.9. DMOG-mediated changes in transcription during hBM-MSC chondrogenesis are mediated by HIF-1α

Acriflvaine was shown to be a suitable HIF-1α inhibitor to investigate the mechanism of DMOG-mediated gene expression changes and thereby give insight into HIF-1α regulation during chondrogenesis. The effect of ACF at day 14 of BM-MSC differentiation was subsequently examined due to many of the DMOG-induced expression changes occurring at this time point, relative to the untreated control. Such changes include genes involved in correct folding and polymersiation of Collagen Type 2 triple helices as well as those involved in chondrocyte hypertrophy.

The significant increases in *SOX9* mRNA due to DMOG compared to the untreated control (approx 6x), were abolished in the presence of ACF (**Fig. 4.10A**) and this pattern was observed when the expression of HIF targets- *VEGFA* and *EGLN* were quantified. DMOG as before induced significant increases in both *VEGFA* (**Fig. 4.10B**) and *EGLN* (**Fig. 4.10C**) at day 14 of chondrogenesis compared to the untreated control (increases of 20x and 6x respectively) and these significant differences were not present following ACF treatment. The significant increase in *COL2A1* mRNA by DMOG compared to the untreated control (approximately 2x) was also abolished by ACF (**Fig. 4.10D**) and the significant downregulation of *COL10A1* mRNA due to DMOG compared to the untreated control (approx. 0.5x) was also abolished in the presence of ACF (**Fig. 4.10E**). A corresponding significant reduction in the ratio of *COL2A1:COL10A1* due to DMOG was observed in the presence of ACF. This is in comparison to the ACF-free conditions in which the *COL2A1:COL10A1* ratio was increased by DMOG compared to the untreated control (**Fig. 4.10F**).

ACF also had an effect with regards to the gene expression induced by 5%O_2. In the ACF-free conditions, 5%O_2 induced no changes in expression of *SOX9* and *COL2A1* mRNA. In the presence of ACF, hypoxic incubation significantly reduced *SOX9* (**Fig. 4.10A**) and *COL2A1* (**Fig. 4.10D**) mRNA, as well as the ratio of *COL2A1:COL10A1* (**Fig. 4.10F**).

The global effect of DMOG on HIF target and chondrogenic transcripts are shown in **Figures 4.10G-4.10N**. DMOG induced a trend towards the upregulation of *SOX9* (**Fig. 4.10G**), *COL2A1* (**Fig. 4.10H**), *VEGFA* (**Fig. 4.10I**), *EGLN* (**Fig. 4.10J**), *DKK1* (**Fig. 4.10K**) and *LOX* (**Fig. 4.10L**) *mRNA* and inhibits *COL10A1* (**Fig. 4.10N**) transcription compared to all other conditions. The effect of ACF in reducing the observed expression changes due to each of the three HIF-stimulating compounds is most apparent in the presence of DMOG. The reduction in DMOG-mediated gene expression changes by ACF appear to be larger than the differences observed in the presence of either $CoCl_2$ or DFX. In addition, for *COL10A1* expression, the decreases induced by $CoCl_2$ and DFX were not reversed as emphatically by ACF as observed in the presence of DMOG (**Fig. 4.10N**).

Overall, DMOG's effects on stimulating the expression of pro-chondrogenic mRNA at day 14 of chondrogenesis were inhibited by ACF treatment. This demonstrates the importance of HIF-1α in the HIF transcriptional complex in response to DMOG treatment and its integral role in expression of HRE-containing genetic loci. In addition ACF had a greater impact on DMOG-mediated gene expression compared to the effect of ACF when used in conjunction with $CoCl_2$/DFX. This indicates that HIF-1α mediates DMOG's effect to greater extents than $CoCl_2$/DFX's effects and suggests that during chondrogenesis, the HIF-1α hydroxylases; PHD2 and FIH are dependant

more on 2-OG than Fe^{2+}. This also has importance implications for CTE strategies and indicates the role that 2-OG inhibitors may play in enhancing BM-MSC articular chondrogenesis via HIF-1α. The use of such inhibitors may be essential due to demonstration that HIF-1 deletion in adult articular cartilage results in chondrocyte death and development of an OA-like phenotype [288]. 2-OG inhibitors may therefore enable formation of a cell population that faithfully mimics those found in native articular cartilage.

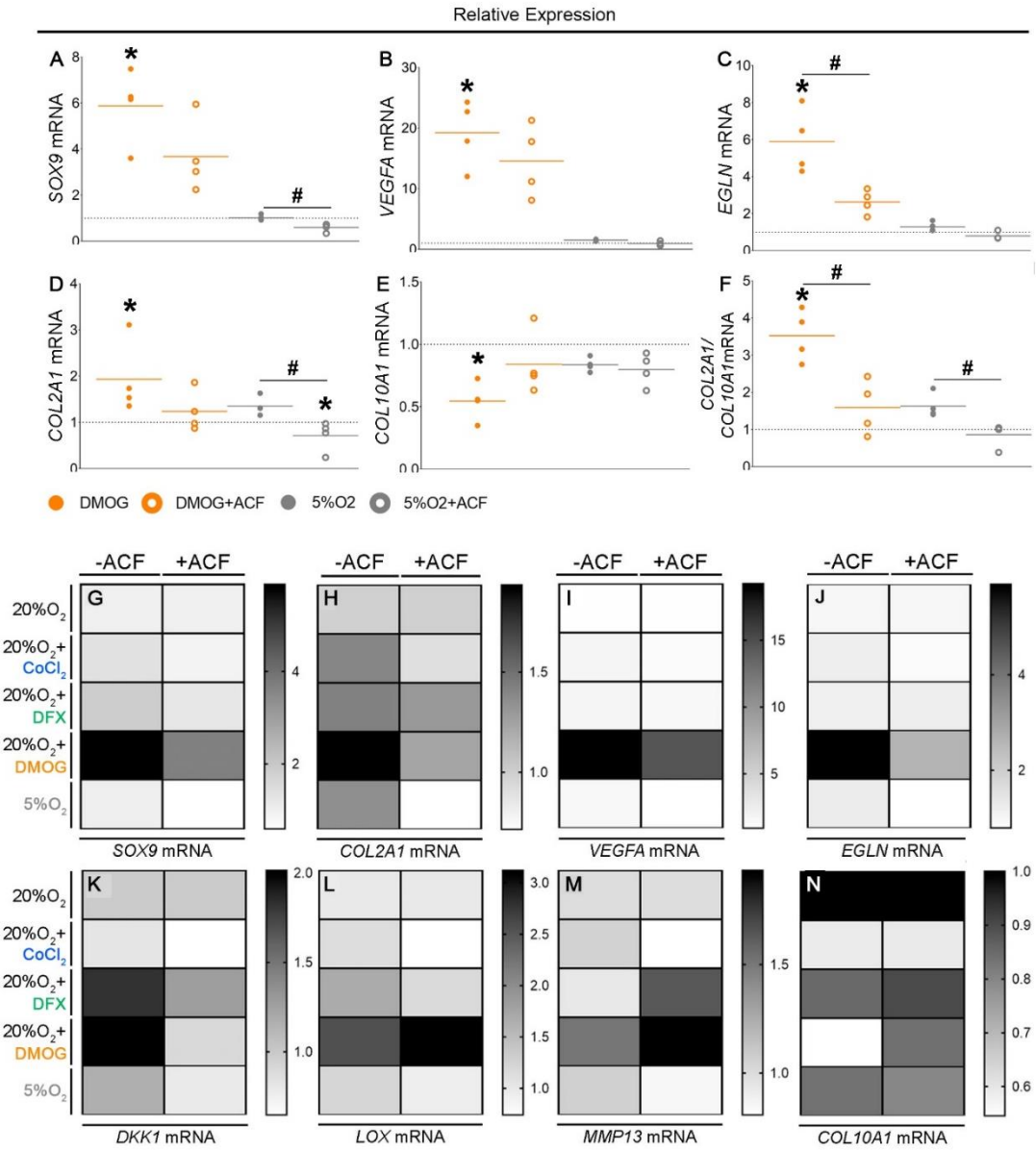

Figure 4.10. Acriflavine, an inhibitor of HIF-1α+HIF-1β binding, reduces DMOG-mediated transcriptional changes during chondrogenesis. mRNA expression throughout chondrogenesis of *SOX9* (A), *VEGFA* (B), *EGLN* (C), *COL2A1* (D), *COL10A1* (E) and the ratio of *COL2A1/COL10A1* (F). Values plotted are from 4 independent experiments and are fold change compared to the untreated control without DMOG which is represented by the horizontal dotted line. The solid coloured lines represent the mean for each condition. *denotes $p<0.05$ when compared to 20%O_2+/-ACF and #denotes $p<0.05$ between +/-ACF conditions within DMOG and 5%O_2 groups. The heat maps shown in G-N illustrate the effect of Acriflavine in the presence of each HIF-stabilising compound. Each value represents the mean fold change over the untreated control.

4.2.10. HIF-1α inhibition alleviates the decrease in Collagen Type II observed due to DMOG

With observation that the gene expression changes induced by DMOG are mediated by HIF-1α, we sought to identify if the ability of DMOG to inhibit incorporation of Collagen Type II into the ECM was also mediated by HIF-1α. As previously, DMOG reduced Collagen Type II in the ECM (**Fig. 4.11B**) compared to the untreated control (**Fig. 4.11A**), and this decrease was alleviated slightly in the presence of ACF (**Fig. 4.11C**). This is represented in the quantification of this immunofluorescent staining in which the significant decrease due to DMOG, is rendered no longer significant by the addition of ACF (**Fig. 4.11D**). This result indicates that the DMOG's determental effect on Collagen Type 2 production by BM-MSCs is in part mediated by HIF-1α.

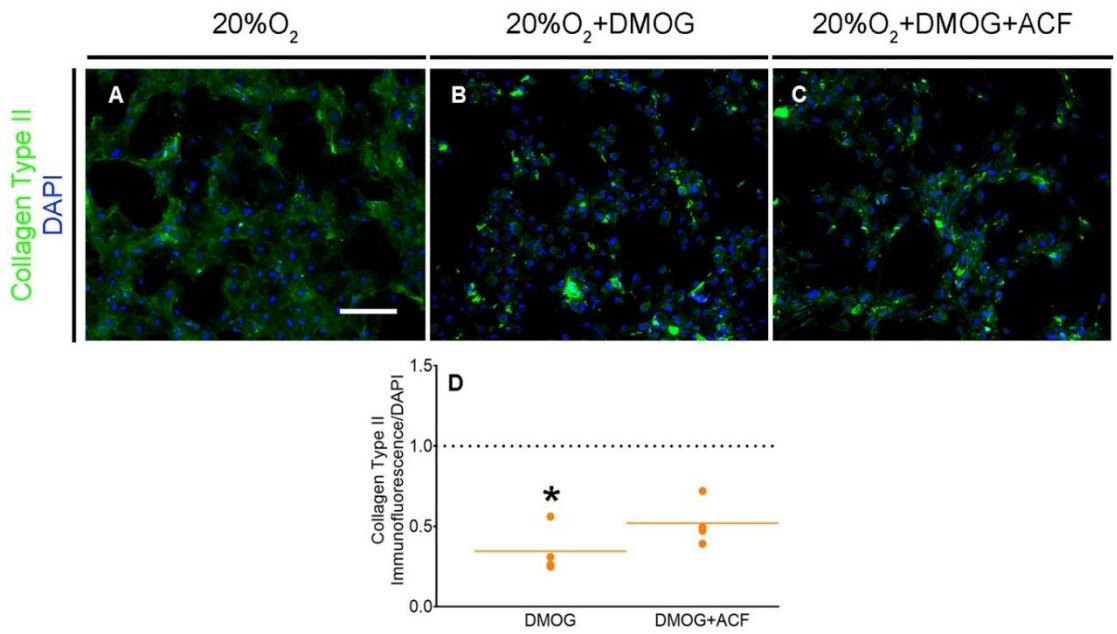

Figure 4.11. Inhibition of HIF-1α partially rescues the DMOG-mediated decreases in the presence of Collagen Type II in the ECM. (A-C) Collagen Type II immunofluorescent staining at day 14 of chondrogenesis due to DMOG in the absence and presence of Acriflavine. Scale bar = 400µm. Representative images of 3 independent repeats shown. (D) Quantification of Collagen Type II immunofluorescence at day 14 of chondrogenesis due to DMOG in the absence and presence of Acriflavine. Values plotted are from 4 independent experiments, and are fold change compared to the untreated control without DMOG which is represented by the horizontal dotted line. The solid orange lines represent the mean for each condition and *denotes $p<0.05$ compared to the untreated control without DMOG.

4.2.11. Late treatment of DMOG induces pro-chondrogenic transcriptional changes whilst maintaining cartilage ECM

To attempt to alleviate the effect of DMOG in inhibiting production of Collagen Type II which is an important structural component of articular cartilage, the period of DMOG treatment during hBM-MSC chondrogenesis was adjusted. Treatment of DMOG for the final 7 days of chondrogenic induction could potentially reduce the cumulative inhibitory effect on Collagen Type II incorporation into the ECM. Chondrogenic transcript quantification by qPCR and collagen type 2 immunostaining were performed at day 21 of chondrogenesis following either continuous DMOG treatment or supplementation for the final 7 days of culture.

Treatment of DMOG for days 14-21 of the chondrogenic protocol only did not reduce Collagen Type II in the ECM (**Fig. 4.12C**) compared to the untreated control (**Fig. 4.12A**) as was observed due to continuous treatment for the full 21 days of chondrogenesis (**Fig. 4.12B**). This was confirmed by quantification of the immunostaining which were normalised to the number DAPI-stained cells (**Fig. 4.12D**). Despite achieving similar Collagen Type II protein compared to the untreated control, DMOG treatment for days 14-21 enhanced mRNA expression of *SOX9* (**Fig. 4.12E**), *P4HA1* (**Fig. 4.12G**) and HIF targets- *VEGFA* (**Fig. 4.12H**) and *EGLN* (**Fig. 4.12I**), as observed due to continuous treatment for 21 days. Unlike these transcripts, the *SOX9* target- *COL2A1* was not induced by late treatment as with continuous dosage (**Fig. 4.12F**).

Overall, late DMOG treatment appeared to alleviate the determinal effect of continuous treatment on Collagen Type II production by BM-MSCs, whilst still

maintaining the strong induction of transcription of chondrocgenic mRNA. This therefore indicates tha late DMOG treatment may be a valid CTE strategy for improving chondrogenic differentiation of BM-MSCs whilst maintaining the cartilage ECM required for articular cartilage function in the joint.

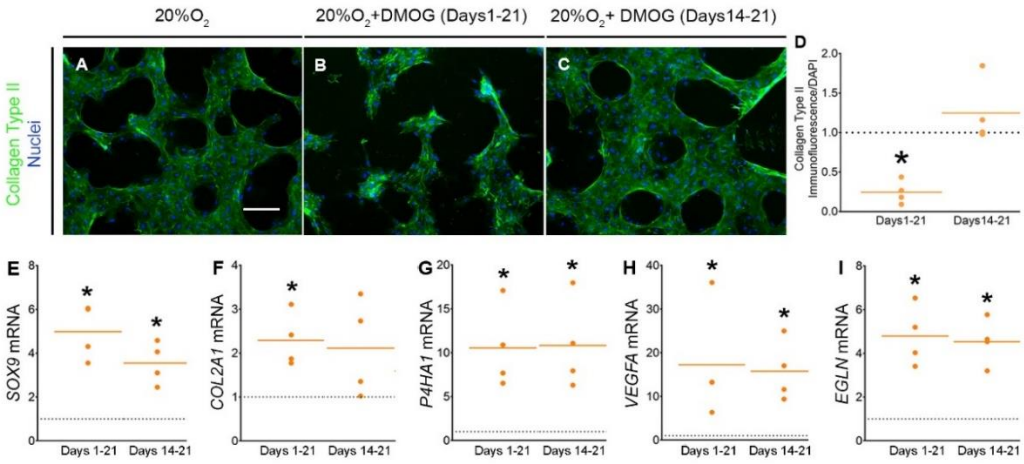

Figure 4.12. Late treatment of DMOG does not reduce Collagen Type II in the ECM as with continuous exposure, but still induces chondrogenic gene expression in differentiating BM-MSCs. (A-C) Collagen Type II immunofluorescence staining at day 21 of chondrogenesis. Scale Bar = 400µm. Representative images of 4 independent repeats shown. (D) Quantification of Collagen Type II immunofluorescence at day 21 of chondrogenesis which was normalised to DAPI immunofluorescence. Values plotted are from 4 independent experiments and are fold change compared to the untreated control without DMOG which is represented by the horizontal dotted line. The solid coloured lines represent the mean for each condition and *denotes $p<0.05$ compared to the untreated control without DMOG. (E-I) mRNA expression throughout chondrogenesis of *SOX9* (E), *COL2A1* (F), *P4HA1* (G) *VEGFA* (H) and *EGLN* (I). Values plotted are from 4 independent experiments and are fold change compared to the untreated control without DMOG which is represented by the horizontal dotted line. The solid orange lines represent the mean for each condition with *denoting $p<0.05$ compared to the untreated control without DMOG.

4.3. Discussion

The pro-chondrogenic effects of hypoxia are thought to be mediated primarily through HIF-1α which is part of an active transcription factor complex at target genes. It has been shown to mediate not only initial chondrogenic differentiation of mesenchymal precursors [262] but also have a role in stabilising the articular chondrocyte phenotype [288] and ensuring cartilage ECM production [277]. Therefore it is not overly presumptive to predict that compounds which stimulate HIF-1α, may improve *de-novo* articular cartilage formation. Previous studies have examined the effect of $CoCl_2$ [272], DFX [494] and DMOG [278]; compounds with HIF-α-stabilising ability, for enhancing cartilage ECM formation from articular chondrocytes, reducing hypertrophy or even rescuing from an osteoarthritic phenotype. However, no evidence exists for the comparison of the effect of DMOG, a 2-OG analogue with that of Fe^{2+} analogue and chelator, CoCl2 and DFX [467] during chondrogenesis of hBM-MSCs.

The results detailed in this chapter clearly indicate an advantage of DMOG in stimulating expression of chondrogenic mRNA including those whose products are quired for chondrocyte differentiation and complete folding and polymerization of Collagen Type II triple helices. In addition, compared to that observed due to $CoCl_2$ or DFX, DMOG inhibited expression of hypertrophic markers at the mRNA and protein leevsl. Together, these suggest the suitability of DMOG for incorporation into a CTE strategy in which BM-MSCs or a similarly multipotent cell population are directed down an articular chondrocyte lineage within a 3D biomaterial scaffold. The ECM synthesized by BM-MSCs that are differentiated in the presence of DMOG may

produce cartilage that resembles that which arises during native articular cartilage development – essential for repair of acute chondral defects. However, a potential pitfall is demomstrated by the decrease in Collagen Type II protein induced by DMOG treatment. This was alleviated by treatment of DMOG for the final 7/21 days of chondrogenesis only whilst maintaining the transcriptional changes induced by this 2-OG inhibitor.

Prior to assessing the role of these HIF-stabilising compounds for chondrogenic induction, it was imperative to identify concentrations which were not toxic to the hBM-MSCs and did not significantly reduce cell number during the 21-day differentiating period. The highest concentrations of each compound which were used as a positive control for cell death, did not cause a complete abolishment in cell viability at 0.5 days for $CoCl_2$ and DMOG and not at day 0.5 or 7 for DFX. This suggests either a lack of drug absorption by the cells prior to 0.5 days which would have otherwise resulted in a cumulative toxic dose.Alternatively, and particularly in the case of DFX, hBM-MSCs may retain have been able to excrete/metabolise the compounds at early time points before their toxicity took effect. The constitutive treatment and build-up of each compound following 0.5-7 days may then have overcome any ability of the cell for excretion or metabolism.

Another possibility for the lack of toxicity at these early time points is that observed may be due to the initial ability of hBM-MSC treated with these compounds to inhibit apoptotic processes via HIF-mediated mechanisms. Although HIF-1α stabilisation was not examined at 0.5 days, each compound increased nuclear HIF-1α at 24 hours, indicating a possibility of HIF-induced tolerance to drug toxicity. This has been shown

previously in breast cancer cells, where resistance to a chemotherapeutic agent being abolished upon HIF-1α deletion [495], and also in a hepatocyte cell line in which fatty acid-induced apoptosis was inhibited by HIF-1α overexpression [496]. Following the initial tolerance, DFX appeared to cause a larger drop in viability due to the 100 and 200μM doses. This was unlike that observed due to $CoCl_2$ at these doses. This may suggest the propensity of DFX, which is a specific iron-chelating agent, to sequester Fe^{2+} ions from enzymes responsible for maintaining cell viability, such as cytochrome complexes of the mitochondria [497].

Following identification of appropriate doses to use of each compounds, the ability of $CoCl_2$, DFX and DMOG to induce HIF-1α nuclear localisation was confirmed. In addition, as with hypoxic incubations, treatment with each of the compounds did not alter the peri-nuclear localisation of HIF-1α observed in the control conditions. Subcellular localisation of the HIF hydroxylases is important in their regulation of HIF-1α. It has been reported that PHD2 protein primarily resides and hydroxylates of HIF-1α within the nucleus in certain cell types [498] which perhaps rationalises the presence of HIF-1α external to the nucleus. This is also supported by the observation of increased hydroxylase activity of nuclear PHD2 compared to the cytoplasmic fraction [498]. In normoxic untreated conditions, this may result in a net increase in hydroxylation, ubiquitination and degradation of nuclear HIF-1α and comparatively, a preservation of HIF-1α in the cytoplasm.

Despite each compound inducing nuclear HIF-1α localisation compared to the untreated control, only DMOG appeared to constitutively induce mRNA expression of HIF targets throughout chondrogenesis, with DFX inducing fewer changes and

$CoCl_2$ causing no transcriptional effect. Increases in *VEGFA* and *EGLN* mRNA by DMOG were shown through the use of Acriflavine, to be mediated by HIF-1α interacting with HIF-1β in the HIF transcriptional complex. As with observations in the previous chapter, a limitation in this study may be the relatively low number of HIF-target genes selected to denote activation of HIF-mediated transcription. PHD2 and FIH inhibition stimulates differential HIF-mediated gene expression programs, with these hydroxylases inhibited by $CoCl_2$, DFX and DMOG to different extents [453]. This therefore suggests that expression of alternative HIF target genes than those shown here may be induced by $CoCl_2$ and DFX which may have validate their potency as inducers of HIF activity.

The differences in HIF-mediated transcription induced by Acriflavine in the presence of DMOG were larger than the effect of Acriflavine in the presence of DFX. This suggests the transcriptional changes induced by DMOG compared to that stimulated by DFX were dependent to a greater extent on the participation on HIF-1α. Interestingly DMOG's potent transcriptional effects relative to both the untreated control and DFX were not a result of increased HIF-1α protein induced by the 2-OG analogue. This is demonstrated by the lack of observed differences in the total levels and nuclear localisation of HIF-1α between that induced by DFX and DMOG. One limitation of this study is the lack of analysis of HIF-1α protein throughout chondrogenesis induced by these compounds after day 1. This would have enabled correlation or a lack thereof between HIF-1α protein, transcription of HIF targets and chondrocyte differentiation. Furthermore, as opposed to HIF-1α semi-quantification, it may be required to quantify absolute levels of HIF-1α both in the whole cell and

nuclear compartments using ELISAs or DNA-binding ELISAs. This may enable the discerning of any subtle changes in HIF-1α stabilization between $CoCl_2$, DFX and DMOG treated cultures.

These differences in expression of HIF targets due to these HIF-stimulating compounds may therefore highlight distinct mechanisms by which the different hydroxylase inhibitors function, and by which HIF-1α is regulated in hBM-MSCs. Tian et al examined the ability of each of the presently used compounds to inhibit the activity of PHD2 and the HIF asparagine hydroxylase, FIH. In a renal carcinoma cell line, Tian et al utilised identical concentrations of $CoCl_2$, DFX and DMOG identical to that used in the present study. They observed a complete reduction in FIH activity due to DMOG as evidence by abolishment of HIF-1α asparagine hydroxylation. This was accompanied by a decrease in proline hydroxylation which is indicative of PHD2 inhibition. Due to DFX, the decrease in asparagine hydroxylation did not occur as robustly as with DMOG and a lack of change in this was observed in response to treatment with 100μM $CoCl_2$ compared to the untreated control. However both DFX and $CoCl_2$ induced similar decreases in proline hydroxylation as observed due to DMOG in this study. Overall the observations made by Tian et al suggest the role of FIH and PHD2 inhibition in mediating DMOG's effect on HIF target gene expression compared to that stimulated by DFX and $CoCl_2$ which may primarily function solely via PHD2 inhibition. This corresponds to the lack of effect of $CoCl_2$ in the present study. $CoCl_2$ here may be unable to sufficiently inhibit FIH, which would result in high HIF-1α asparagine hydroxylation and a lack of HIF enrichment at the promoters of *VEGFA*, *PGK1* and *EGLN*. Alternatively, at odds with that induced by DMOG and DFX,

a lack of FIH inhibition by $CoCl_2$ may induce a different subset of HIF targets [451] which were not investigated here and which may validate $CoCl_2$ as a potent HIF-stimulator during chondrogenesis.

Further supporting a role for FIH in the observations made here in response to DMOG treatment, FIH compared to PHD2 has an increased K_m value for 2-OG [499]. This translates into a requirement of FIH for greater levels of 2-OG than required by PHD2 for these two enzymes reach the same activity level. DMOG treatment also increased HIF-mediated transcription compared to that observed in the presence of a PHD2-selective inhibitor [44]. Together these studies suggest that FIH is more sensitive than PHD2 to DMOG and this enhances HIF-mediated transcription relative to PHD2-only inhibition. Furthermore, Palomaki et al suggested the greater dependence on inhibition of FIH rather than PHD2 for HIF-mediated transcription specifically in BM-MSCs. This is due to the observation in this study of increased HIF-1α mRNA levels observed in this cell type [432]. This increased transcription and corresponding protein levels of HIF-1α was hypothesised to compensate for any decrease in HIF-1α stability due to PHD2-mediated hydroxylation.

The studies described above, may rationalise the potent effect of DMOG in the present study and suggests this compound as potent FIH inhibitor compared to DFX or $CoCl_2$. In mouse myoblasts, FIH knockdown was shown to induce significant higher levels of HIF-mediated transcription compared to PHD2 knockdown which demonstrates the potential for a FIH-selective mechanism that is stimulated by DMOG here [481]. These rationalisations of the contrasting effects of $CoCl_2$ and DMOG on HIF-target gene expression observed and the contribution of FIH and PHD2

inhibition to these observations are of course, only speculative. Aside from the use of Acriflavine which inhibits HIF-1α-HIF-1β heterodimerisation and is therefore downstream of FIH and PHD2 activity, no manipulation of the PHD2/FIH/HIF signalling pathways was conducted during $CoCl_2$/DFX/DMOG-treated chondrogenesis.

If DMOG does indeed induce its transcriptional effects via inhibition of PHD2 and FIH, as opposed to PHD2 inhibition alone as induced by DFX and $CoCl_2$ this would correlate with our observations of DMOG's effect on inducing a chondrogenic gene expression profile. Chan et al compared the effects of PHD2-specific inhibitor, IOX2 and FIH-specific inhibitor, N-Oxalyl-(d)-Phenylalanine (NOFD) with that of DMOG on transcription of HIF targets in MCF-7, Hep3B, and U2OS cell lines [500]. These authors observed an increase in *SOX9* expression due to DMOG but not due to IOX2 or NOFD. This implies that *SOX9* is a genetic locus that is regulated by HIF in a manner dependent on inhibition of both PHD2 and FIH by DMOG as opposed to inhibition of either hydroxylases alone.

In the present study, DMOG-mediated upregulation of HIF-target gene expression appeared to correlate with the generation of a chondrocyte expression profile, including an induction of *SOX9* expression. As with expression of HIF targets described above, the role of dual FIH and PHD inhibition in mediating the effect of DMOG on *SOX9* expression here is only theoretical. Confirmation of such a mechanism would require genetic or inhibitor-based manipulation of PHD2 and FIH during DMOG-mediated chondrogenesis. Also observed was an upregulation of *SOX9* mRNA over that of *RUNX2* which suggests a bias towards chondrogenic

differentiation over that of an osteoblast/hypertrophic chondrocyte. This would confer advantages to any CTE strategy. For example, Ma et al created a doxycyline-inducible *SOX9* transgene within C3H10T1/2 cells which when seeded subcutaneously into a mouse model resulted upregulation of cartilage ECM formation upon Doxycycline treatment [501].

Despite only DMOG inducing significant *SOX9* expression, all three compounds appeared to induce expression of its target gene- *COL2A1* at day 14. Provot et al deleted *HIF1A* in the limb bud mesenchyme. Despite observing an abolishment in *COL2A1* mRNA at the onset of chondrogenesis, *SOX9* mRNA was largely unaffected both at the same developmental time point, and at the earlier stage of mesenchymal condensation [262]. This implicates a SOX9-independent induction of *COL2A1* during HIF-1α-mediated cartilage development or at least an uncoupling of *SOX9* transcription with that of *COL2A1* in response to HIF-1α stimulation. A similar mechanism may be induced by $CoCl_2$ and DFX due to observations of an absence of *SOX9* expression accompanying the increase in *COL2A1* by these compounds. As shown previously [272] HIF-1α may upregulate *SOX5/6* which would increase *COL2A1* expression by facilitating SOX9-mediated transcription of this genetic locus [502]. This would therefore require no increase in *SOX9* expression to achieve increased *COL2A1* expression. Again, the correlative observations of *SOX9* and *COL2A1* transcription here enable only a suggestion of the mechanisms which dictate the levels of their mRNA in respect of each other. For any such mechanism to be validated, genetic manipulation of SOX9 in addition to SOX5 and SOX6 would be a requirement. In addition, without utilising more frequent time points between days

1 and 7 or between days 7 and 14, it is not possible to rule out an increase in *SOX9* transcription prior to the increase in *COL2A1* mRNA at day 14.

Unlike *COL2A1* transcription which is upregulated by all three compounds, *COL10A1* involved in chondrocyte hypertrophy appeared to be selectively downregulated by DMOG only. This also resulted in a corresponding upregulation of the ratio of *COL2A1:COL10A1* mRNA. This pattern appears to manifest in the protein levels of Collagen Type X which were also reduced by DMOG treatment. This and increased *SOX9* expression, therefore suggests DMOG compared to $CoCl_2$ or DFX as the chemical agent which offers advantages regarding hBM-MSC-based CTE. However, a significant limitation of this study is represented by the difference of 2D culture on TCP with 3D culture of hBM-MSCs in a biomaterial scaffold. In a 3D microenvironment created by a scaffold, a multitude of regulatory cues exist compared to 2D culture. This is summarised by Sart et al who gathered evidence of studies in which cartilage induction of MSCs was regulated differentially by 2D and 3D aggregate culture [503]. Therefore before the role of DMOG may be suggested for CTE applications, it is a requirement to assess its effect on BM-MSC chondrogenesis in a 3D, biomaterial scaffold environment. Chondrocyte hypertrophy is a significant problem in CTE so therefore a small molecule which is able to reduce hypertrophic signalling within scaffold-seeded mesenchymal progenitors would be highly advantageous.

Regarding the design of continuous scaffolds for full osteochondral tissue repair, spatial control of hypertrophic expression (in addition to that of *SOX9*) would also enable corresponding organisation of articular cartilage and endochondral bone. As

described by Sun and Beier [504], strategies in which hypertrophy is able to be spatially controlled would be advantageous due to the opposing requirements of hypertrophy during cartilage and bone formation. Such a strategy would also enable formation of the hypertrophic 'tidemark' present between native articular cartilage and subchondral bone. This region plays an important structural role in osteochondral tissue by facilitating communication between the cartilage and bone layers. This is required for complete joint function and to enable communication between tissues with such contrasting structural, mechanical and biochemical properties. Da et al observed an enhanced tensile and shear strength of an interface-containing scaffold compared to that containing none They also observed increased *in vivo* regeneration of osteochondral tissue following implantation into a rabbit defect model [505]. Clinical trials of a collagen type I-hydroxyapatite multiphasic scaffold inclusive of an interface region were implanted into osteochondral defects of the femoral condyle. Patients were reported as having experienced good clinical outcome following 2 years post-operative observations [506].

Interestingly, despite *COL10A1* being downregulated by DMOG, MMP13 was not inhibited by this compound. DMOG also did not downregulate *RUNX2* mRNA compared to the non-treated control throughout chondrogenesis. This perhaps suggests that DMOG-induced HIF activity did not reduce *COL10A1* expression by reducing *RUNX2*-mediated transactivation of the *COL10A1* promoter. Correspondingly, expression of *MMP13* was also not altered by DMOG treatment at the same time as the observed *COL10A1* downregulation. *MMP13* is thought to be regulated are part of a RUNX2-mediated transcriptional program which simultaneously regulates *COL10A1* transcription [507, 508]. An increase in only

COL10A1 mRNA here suggests that DMOG is not inhibiting the entire regulatory network conducive for hypertrophy but instead is targeting *COL10A1* expression specifically. Of course, expression of both *RUNX2* and *MMP13* may be regulated by DMOG at time points other than those observed here. Regardless of time points chosen however, the role of RUNX2-mediated *COL10A1* and *MMP13* regulation in the present study is speculative without genetic manipulation of *RUNX2* during DMOG-treated chondrogenesis.

As opposed to regulating *RUNX2,* upregulation of *SOX9* by DMOG may indicate the potential role of SOX9-mediated repression of *COL10A1* transcription. This has been shown to occur via co-binding of SOX9 target sites by the Gli transcription factors which causes a decrease in *COL10A1* transcription by SOX9 [53]. In the present study, we can also negate a role for HIF-2α in the mechanism of action of DMOG. HIF-2α has repeatedly been shown to induce a hypertrophic and osteoarthritic transcriptional profile within *in vivo* murine models [509]. The lack of upregulation of both *MMP13* and *COL10A1* suggests upregulation of HIF-1α due to DMOG as opposed to HIF-2α. This also corresponds to previous reports which indicate a bias for HIF-1α over HIF-2α stabilisation upon PHD2 and FIH inhibition [396]. Again, if the role of factors such as SOX9 or HIF-2α are to be investigated during DMOG-mediated chondrogenesis, their genetic manipulation would need to be undertaken.

Despite a lack of effect on expression of *SOX9* or hypertrophic markers due to $CoCl_2$ and DFX, these compounds both stimulated changes in mRNA encoding the articular chondrocyte markers, Gremlin1 and DKK1. Throughout chondrogenesis, DFX appeared to increase *DKK1* mRNA with an increase at day 21 observed due to DMOG.

A trend was also observed towards increased expression of BMP antagonist- *GREM1* from day 7 onwards due to $CoCl_2$ or DMOG treatment. This demonstrates again that during hBM-MSC chondrogenesis, the effect of HIF-1α activation on target gene expression is not an 'all or nothing' response and that different mechanisms of HIF-1α upregulation may result in different subsets of HIF-targeted genes being transcribed. Iron chelation by DFX appears to generate an anti-Wnt signalling milieu within the cell whereas competitive inhibition of PHD2 by $CoCl_2$ or DMOG appears to upregulate the BMP antagonist. However, these observations on the differential transcription of *DKK1* and *GREM1* do not robustly validate a conserved mechanism by which HIF controls expression of these genes. This instead would be demonstrated by the use of other iron-chelators and competitive PHD2 inhibitors. This would determine if the effects on *DKK1* and *GREM1* expression is a specific effect of the compounds used here or not.

Studies suggest a requirement for β-catenin-mediated transcription during chondrocyte hypertrophy. There exists therefore a requirement to inhibit canonical Wnt signalling during the latter stages of BM-MSC chondrogenesis to suppress hypertrophy. This therefore may correspond to the expression patterns here of the Wnt antagonist- *DKK1* which was induced by DFX throughout chondrogenesis and by DMOG at day 1. An observation which was not made here and one in which would determine the necessity of Wnt inhibition during chondrogenesis, is that of β-catenin activity. This would allow a greater or lesser significance to be drawn of DFX/DMOG-mediated *DKK1* transcription, dependent on the relative activity levels of the canonical Wnt pathway, as denoted by β-catenin levels.

Despite changes in expression of the Wnt antagonist; DKK1, there was a lack of corresponding decrease in expression of *AXIN2,* a gene which is designated as a conserved canonical Wnt signalling target [510]. There was also a lack of decrease in expression of *LEF1* which is another transcriptional target of β-Catenin whose product is part of the TCF-LEF complex active at Wnt target genes [511]. As described, this lack of correlation in *AXIN2* and *LEF1* mRNA may be due to the relatively few time points utilised as a proportion of the total differentiating period. Regulation of *AXIN2* and *LEF1* may occur by DMOG after day 14 of chondrogenesis, following *DKK1* upregulation at this time point. Despite observing no changes in *AXIN2* and *LEF1* mRNA due to DFX, we did observed a trend towards an increase in *LEF1* mRNA at day 1 due to DMOG. This may be suggestive of a DMOG-mediated mechanism for increasing Wnt signalling at this early time point in chondrogenesis at which point it is required for early chondrocyte specification. DMOG may stimulate the role of LEF1 as the co-factor required for expression of Wnt target genes. To confirm this role of DMOG, it would be required to genetically downregulate components of the Wnt pathway such as β-Catenin. If DMOG does indeed increase Wnt signalling during its during early chondro-induction, robust knckdown of β-Catenin may reduce the potent effects of DMOG on the chondrogenic gene expression observed.

In terms of Indian Hedgehog signalling, we also observed a trend for increase at day 1 due to DMOG, which would also correspond to a role for this compound in inhibiting hypertrophy. This is due to the role of IHH ligand in suppressing progression of hypertrophy in pre-hypertrophic chondrocytes via increased *PTHRP* expression [93]. However, we observed no changes in expression of *PTHRP* at this same time point. This may be due to a requirement of the paracrine action of IHH which is a

required process during spatial regulation of hypertrophy and normal bone development. This is as opposed to an autocrine mechanism of action which may be observed here, in which the entire cell population increases expression of *IHH*. As with regulation of Wnt signalling by DMOG, it may be required to examine time points other than those utilised here to enable suggestion that Indian Hedgehog signalling is stimulated in response to DMOG treatment.

Despite its strong transcriptional induction of chondrogenic genes, DMOG had a negative effect on cartilage-like ECM production. This was shown to be partly mediated via HIF-1α, but a large decrease in Collagen Type II due to DMOG was observed still in the presence of Acriflavine. DMOG has been shown to reduce the activity of CP4HA1 which is required for processing of collagen fibrils [278]. Correspondingly, both FIH and CP4HA1 have similar affinities for 2-OG which is represented by a similar K_m value of these enzymes for this co-factor [512]. This would manifest in an equal sensitivity of FIH and CP4HA1 to DMOG. This suggests the strong induction of HIF target genes due to DMOG via FIH inhibition would be accompanied by a similarly potent inhibition of Collagen processing and incorporation into the ECM. It is also worth noting that the suggested inhibition of CP4HA1 by DMOG would also negate the positive effect of the increases observed in *CP4HA1* and *LOX* mRNA due to DMOG. The lack complete folding and formation of collagen triple helices due to CP4HA1 inhibition, would make further mRNA expression of *CP4HA1* and *LOX*, redundant in terms of an effect on Collagen Type II in the ECM. It is also important to note that current observations here are merely suggestive of this mechanism of DMOG-mediated inhibition of CP4HA1. As proposed

above in which suggestions were made to examine the role of PHD2 and FIH in the effects observed due to DMOG, the role of CP4HA1 may be investigated by its genetic overexpression. Via examination of Collagen Type II protein in response to this overexpression, the role of CP4HA1 in the detrimental ECM changes induced by DMOG would be validated.

Timed exposure of the hBM-MSCs to DMOG may help alleviate the negative effect on Collagen Type II incorporation into the ECM. Treatment with DMOG for the final 7 days of induction did at least in part restore the poor levels of type II collagen secretion that resulted from continuous treatment. This could have been mediated by a lack of continuous inhibition of the CP4HA1. In addition we observed enhanced expression of HIF targets *VEGFA* and *EGLN* and chondrogenic marker *SOX9*, to similar levels as observed with continuous DMOG treatment. This suggests a role of late DMOG treatment in CTE strategies as opposed to continuous treatment. However, late DMOG treatment was not able to stably induce expression of SOX9 target, *COL2A1*. This suggests that HIF activity is required throughout the early and late phases of differentiation in order to induce expression of SOX9 targets, including *COL2A1*. This may be predicted due to the constitutive role of SOX9 throughout chondrogenic induction [94].

5. The role of hypoxia in regulation of mechanosensing during chondrogenesis.

5.1. Introduction

As already pertained to, the low oxygen state which persists throughout cartilage development and adult cartilage, plays essential roles in generating and maintaining the articular chondrogenic phenotype. The relative permanence of hypoxia and its downstream transcription factor- HIF, suggest this stimulus is one of the fundamental factors residing in the limb bud and chondrocyte cell niche. This is demonstrated by the loss of the cartilage growth plate/articular cartilage upon HIF-1α conditional deletion at various stages throughout limb development [259, 262].

As described in this introduction, another set of omnipresent cell signals during cartilage development are those which activate intracellular pathways in response to mechanical changes in the cell microenvironment. Evidence exists for a role of these pathways from the mesenchymal limb bud stage through to the resting articular cartilage, as observed with hypoxia-stimulated pathways. Condensation of the limb bud mesenchyme is required to initiate chondrogenesis in formation of the growth plate [178]. The role of mechanical signals in pre-condensation mesenchymal progenitors was demonstrated by Carrion et al. These authors observed the effect of soft PEG hydrogels on the induction of condensation and chondrogenesis of encapsulated mesenchymal progenitor line, ATDC5 [513]. Hydrogels with a shear modulus of 7.5KPa exhibited more compact arrangement of cells compared to those in gel of 25KPa and induced greater levels of chondrogenesis as assessed by *COL2A1* mRNA, Collagen Type II and Aggrecan protein. The condensed limb bud mesenchyme

was shown to exhibit differential tension as assessed by atomic force microscopy, between its centre and flanking regions [514]. The increase in tension due to FGF8 treatment of the flanking regions was reduced by an inhibitor of Actin polymerisation. This suggests that the specific mechanical properties of the limb bud are maintained by a cytoskeletal-mediated mechanism.

Takahashi et al demonstrated the mechanosensing ability of mouse embryonic limb bud cells for their chondrogenesis. Static compressive loading was observed to increase *SOX9* mRNA and both Aggrecan and Collagen Type II protein secretion from limb bud cells cultures in Collagen Type I scaffolds [515]. A dose-dependent relationship between the magnitude of static compression and *COL2A1* expression was also demonstrated. One of the mechanisms behind this response to mechanical compression is suggested to be the secretion of autocrine factors by the limb bud mesenchyme. This was demonstrated by Elder who observed an increase in GAG production and proliferation of chick limb bud cells during chondrogenesis carried out in media conditioned by mechanically-compressed limb bud cells [516].

The sensitivity of growth plate chondrocytes to mechanical cues for their lineage commitment was first suggested by Wolpert et al. They observed the generation of tension upon proliferation of growth plate chondrocytes of the developing limb, which was imposed by the surrounding perichondrium. This tension prevented cell growth, hypertrophy and endochondral ossification along the transverse axis and instead induces a longitudinal growth of the developing bone [517]. Foolen et al utilised a model in which developing chick tibia were stripped of their perichondrium, cultured on substrates of varying stiffness and compared with culturs in which the

perichondrium was left intact [518]. Explant cultures with their perchondrium intact exhibited no change in cartilage growth length in response to changes in ECM stiffness whereas the 3KPa surface induced cartilage growth relative to the 80KPa substrate in explants in which the perichondrium was removed. This growth advantage on the soft substrate was abolished by treatment of explants with an inhibitor of myosin contraction. This again was compared to cultures in which the perichondrium was left intact and in which the inhibition of myosin contraction had no effect on either substrate. Overall this study suggests a role of the perichondrium in regulating the mechanosensing ability of growth plate chondrocytes and that the proliferation of the growth plate and cartilage growth is in part, dependent on a cytoskeletal tension-mediated response to changes in ECM stiffness.

The mechanical properties of adult articular cartilage are products of the collagen-proteoglycan network and the osmotic pressure created by water-retention of the tissue. These together function to maintain the articular chondrocyte phenotype [519]. Darling et al identified the specific elastic modulus of both the pericellular matrix surrounding the articular chondrocytes as well as that of the ECM more distally–located from these cells [520]. These authors identified a softer ECM in the immediate area around the chondrocytes compared to that of the remaining ECM. Accordingly, adult articular cartilage is dependent on a specific, relatively low mechanical stiffness for maintenance of an articular chondrocyte phenotype. This was demonstrated by Kim et al who observed an increase in articular chondrocyte markers and decrease in hypertrophic markers on soft substrates compared to stiffer surfaces [352]. This was shown to be dependent on myosin-mediated cytoskeletal contraction due to observation that the articular chondrocyte phenotype on the soft

substrates were lost due to inhibitors of ROCK and myosin contraction. In addition these authors observed the requirement of ROCK-mediated cytoskeletal tension in protection from OA following surgical destabilisation of the medial meniscus.

Together the studies described above demonstrate a requirement of mechanosignalling throughout chondrogenic development. This is demonstrated by the mechanosensing ability of mesenchymal progenitors, immature chondrocytes and articular chondrocytes in order to generate stable articular cartilage. Another key set of observations which indicates the role of constitutive mechanosignalling throughout cartilage development is that of the ligand which stimulates these pathways. Unlike growth factor ligand bio-availability which is temporally-controlled during cartilage development, mechanical stimulation of the cell is not transient. This is due to the constitutive remodelling and perturbation of the ECM during sequential formation of the limb bud, growth plate and adult osteochondral tissue.

At the start of limb bud formation, the ECM is composed of Hyaluronic Acid. Maleski and Knudson demonstrated the function of HA in cell-cell adhesion at the limb bud stage by observation of a decrease in cell-cell binding upon treatment of chick limb bud cultures with the HA-digesting enzyme, hyaluronidase [178]. HA is then downregulated following onset of condensation and chondrogenesis, and this specific temporal regulation of HA was shown by Li et al to be a pre-requisite for cartilage development [177]. In the centre of the developing limb bud at the very start of mesenchyme condensation, both Collagen Type I and Fibronectin were shown to be expressed by Dessau et al [521].

Fibronectin has since been shown to also be required for mesenchymal condensation as demonstrated by Singh and Schwarzbauer who observed a decrease in MSC condensation *in vitro* in response to siRNA knockdown of fibronectin [522]. These authors also demonstrated the expression of Fibronectin-coding mRNA prior to condensation which increases following induction of cell compaction. Protein expression of collagen type I, fibronectin are then reduced following the initial induction of chondrogenesis and are eventually replaced by a matrix rich in Collagen Type II. [521].

Many studies are suggestive of the role of this changing ECM milieu of developing cartilage in stimulating mechanosensing pathways of the cells involved in chondrogenesis. Somaiah et al observed a change in actin organisation and RhoA activation of MSCs which was dependent on their culture on Collagen or Fibronectin-coated surfaces [523]. Varying the HA concentration within cell-laden hydrogels was also shown to induce changes in the mechanical properties of the construct and downstream changes in cell morphology and spreading [524]. Oberhauser et al demonstrated that the elasticity of fibronectin is significantly altered in response to mechanical loading of this protein due to conformation changes and unfolding of its tertiary structure. This therefore indicates the elasticity of Fibronectin-containing ECMs as being highly subject to change by mechanical forces which would have a knock-on effect on the stimulation of mechanosensing pathways in mesenchymal progenitors. Indeed, fibronectin-containing extracellular matrices have also been shown to upregulate specific integrin receptors and resulting in induction of RhoA/ROCK-mediated cytoskeletal tension [315]. Additionally, Kubow et al observed

in Collagen Type I-Fibronectin mixed ECM, that Collagen digestion reduces the mechanical strain of fibronectin [525].

The roles HA, fibronectin and Collagen Type I in regulating the mechanical properties of the ECM in which they reside, are suggestive of their stimulation of mechano-signalling pathways in limb bud cells and chondrocytes during cartilage development. The perturbations from the constantly remodelled ECM during articular cartilage development are sensed by integrin receptors [526]. The pathway which is downstream of integrin receptors is also key in maintaining the constitutive response of cells to the changing ECM as they transition from mesenchymal progenitor to resting articular chondrocyte. For example, the cytoskeleton is omnipresent within cells due the essential roles it plays during development and tissue homeostasis [527].The dependence of cells on this sub-cellular structure is also represented by the vast multitude of organelles to which it is connected [528]. The constitutive presence of the cytoskeleton is required for continued sensitivity to mechanical stimuli due to its role as a mediator of mechanical signal transduction from the cell surface to the nuclei where it induces transcriptional changes [529].

The nucleoskeleton which plays key roles in facilitating the transmission of force from the cytoplasm [340] is also constitutively present. This is due to the essential roles it plays during the maintenance of nuclear integrity [347] and regulation of chromatin epigenetics [530]. Other components of the mechanotransducive pathway have also been shown to be either primed constitutively for activation or are readily de-repressed following their initial stimulation. For example, the mature focal adhesions formed upon integrin activation are pre-meditated by the presence of nascent

complexes composed of α-actinin [531]. These structures couple myosin contraction with integrins even prior to the stimulation of these receptors, and have been shown to be integral in maturation of focal adhesion complexes through Talin and Kindlin2 [532]. In order to remain sensitive to mechanical signals, the mechanosensing pathway must 'reset' itself for repeated stimulation. Actin-myosin contraction which is stimulated by ROCK-mediated phosphorylation of myosin light chain 2, is subject to de-phosphorylation by myosin light chain phosphatase [533]. This results in a relaxation of the actin-myosin network, dissolution of stress fibres and a susceptibility of the cell to integrin-mediated tension once more.

In terms of the specific effect on chondrogenic lineage commitment of mesenchymal progenitors, the literature suggests an advantage of mechanical environments which promotes a round, less spread cytoskeletal arrangement and cortical actin fibres - e.g. substrates of a relative low stiffness. [354, 355]. Promotion of a cortical actin organisation and around cell shape is also conducive for maintenance of the articular chondrocyte phenotype as opposed to conditions which promote stress fibre formation and cell spreading [350, 352]. This has been investigated extensively as a strategy to improve protocols for MSC chondrogenesis. Bian et al observed an increase in *ACAN* expression and a decrease in *MMP13* and *COL10A1* mRNA upon encapsulation and differentiation in HA hydrogels of lower elastic modulus compared to relatively stiffer hydrogels [534]. Sun et al also observed a similar trend with increases in *SOX9, COL2A1* and *ACAN* expression observed in MSCs seeded on Poly Lactic Acid-PEG scaffolds of a lower compressive modulus compared to those of a greater compressive modulus [535].

Despite these improvements of CTE strategies, evidence in the literature is suggestive of unique mechano-regulatory mechanisms during chondrogenesis which could be exploited for *de novo* cartilage formation. Unlike other cell fates which are also promoted due to a lower relative substrate stiffness and reduced, round cell area, ROCK-mediated cytoskeletal tension appears to remain and play a role in chondrocyte specification. Adipogenesis is one of the classic examples used to describe the polar effects of cell stiffness and cytoskeletal tension on cell fate. McBeath et al observed that a round MSC morphology is conducive for an adipocyte cell fate, with treatment of a constitutively active RhoA inhibiting this effect and hyper-active ROCK treatment inducing osteogenesis instead [307]. Increased myosin contraction and cytoskeletal tension has also been shown to be inhibitory to other cell fates which constitute 'soft' tissues. This includes neuronal cells, the differentiation of which is the preferred cell fate on softer substrates where stress fibre formation and cell area is reduced [304] and in conditions in which myosin contraction is abolished [536].

In contrast to neurogenesis or adipogenesis, chondrogenesis appears to be an anomaly amongst those cell fates preferred on softer substrates. Studies such as that Allen et al by have demonstrated the preservation during chondrocyte differentiation, of RhoA/ROCK-mediated cytoskeletal tension, despite induction of a cortical actin arrangement and a rounder cell shape. This ROCK activity was subsequently shown to be required for full chondrogenic induction of ATDC5 cells on soft substrates. This was demonstrated by ROCK inhibition reducing chondrogenic mRNA and protein expression [355]. This was in contrast to that observed in cells on a relatively stiff substrate on which ROCK inhibition resulted in an increase in *SOX9*,

COL2A1 and *ACAN* expression. These observations are supported by Park et al who observed an increase in *COL2A1* expression in hMSCs in response to transfection of constitutively active RhoA on soft substrates compared to hMSCs expressing wild type RhoA [537].

Overall, the literature is suggestive of a role for ROCK activity and cytoskeletal tension during chondrogenesis on soft substrates. This is unlike other cell fate changes which are also favoured on softer substrates in which ROCK-mediated cytoskeletal tension is an inhibitory factor. This indicates that during cartilage development, factors which maintain ROCK-mediated actin-myosin tension in the round mesenchymal progenitors of the limb bud [353] may be essential for chondrogenesis. Hypoxia is a factor which mediates a plethora of pro-chondrogenic effects and akin to signalling in response to mechanical stimuli, is constitutively active during cartilage development. The evidence which describes hypoxia-mediated regulation of mechanotransducive pathways, indicates its potential in mediating the transduction of mechanical signals during chondrogenesis of the limb bud.

Hypoxia and HIF have been shown to influence activity of both RhoA and ROCK [372, 379] which induces corresponding changes on cytoskeletal arrangement via action-myosin contraction [375]. Reduced oxygen concentration has also been shown to induce F-Actin polymerisation [375]. No such studies exist which examine the crosstalk between hypoxic/HIF and mechanosensory pathways during MSC chondrogenesis. Answering such a question may provide further insight into the regulation of chondrocyte formation in the limb bud progenitor cell niche in addition

to aiding CTE efforts which may benefit from combinatorial modulation of the HIF and mechanotransducive pathways.

- **Aim**: To determine the existence of an effect of hypoxia on the mechanosensing ability of chondrogenically-induced progenitor cells.

- **Hypothesis**: Hypoxia upregulates ROCK-mediated cytoskeletal tension in MSCs with round morphologies on mechanically-soft substrates and in doing so, enhances downstream chondrogenesis.

- **Objectives**:
    - To identify an effect of hypoxia on the cytoskeletal arrangement of hBM-MSCs on 2D mechanically soft and stiff substrates
    - To identify an effect of hypoxia on pathways involved in, and downstream of, cytoskeletal tension in hBM-MSCs on 2D mechanically stiff and soft substrates.
    - To identify if hypoxia has a differential effect on hBM-MSC chondrogenesis on 2D mechanically stiff and soft substrates

5.2. Results

5.2.1. Validation of 40/0.5KPa polyacrylamide substrates for manipulation of cytoskeleton arrangement

Hypoxia has been shown to indue chondrogenesis of BM-MSCs both in the previous chapters here and previous studies. This is often described as occurring via direct mechanisms- HIF binding to chondrogenic target genes under low-oxygen conditions. However, hypoxia has also been shown to regulate a set of pathways which themselves have great impact on chondrocyte differentiation, maturation and cartilage ECM formation. These are the mechanosensory pathways which enable chondrogenically-induced cells to respond to substrates of varying stiffness, and which have been shown to dictate the chondrogenic differentiation program. The potential 'crosstalk' during chondrogenesis, between the hypoxia pathways and those which respond to mechanical stiffness, have largely been unexplored. Such a study may provide insights which are useful for the development of CTE strategies in which hypoxic culture of BM-MSCs is combined with biomaterial scaffolds of a defined stiffness.

PA gels have been established as a tool for assessing the effect of mechanical stimuli on cell behaviour. In the present study, these substrates were used to expose the cells to opposite extremes of stiffness with the purpose of inducing differential arrangement of the actin cytoskeleton via contraction of the associated myosin. 0.5KPa and 40KPa were selected as the low and high stiffness values due to the use of these ranges of stiffness in the study by Engler et al who initially indentified the

control of BM-MSC lineage commitment by substrate stiffness [304]. These stiffness values were utlised by Engler et al, and subsequently in the present study to induce completely polarising effects on the mechanotransducive pathways. Cell parameters such as substrate adhesion [538], actin-myosin contraction and cell morphology [304] are affected differentially by stiffness values in the 0.5-1 and 25-40KPa range. Critically, differential regulation of these cell characteristics by the magnitude induced by the 0.5-40KPa stiffness range has been shown to be key in differentially regulating BM-MSC fate decisions [304].

To confirm the function of fibronectin-coated PA gels, initial experiments were conducted to compare the cell response to stiff (40KPa) and soft (0.5KPa) gels. An established method for detecting cell response to mechanical stiffness is through visualisation of cytoskeleton rearrangement. This occurs due to the differential contraction of MLC2 on each substrates. Immunodetection of the actin cytoskeletal network was therefore performed, by binding to Phalloidin conjugated with a fluorophore . BM-MSCs on the 40Kpa surface exhibited a spread cytoskeleton with visible actin stress fibres (**Fig. 5.1A**) and cells on the 0.5KPa substrate forming a much round cell shape (**Fig. 5.1B**).

To provide a quantifier of actin rearrangement in response to 0.5 and 40KPa substrate, binary equivalents were created of each image in which the actin cytoskeleton was immunofluorescently labelled with Phalloidin. The cell area and circularity of each BM-MSC in each binary images was then quantified in ImageJ . The degree of spreading and circularity of the cells has been shown to be a key indicator of differential activation of mechanosensing pathways on stiff and soft substrates.

The qualitative observation of actin rearrangement on the 40 and 0.5KPa substrates were confirmed by this quantification analysis. The area of single BM-MSCs 40KPa were significantly larger (p=<0.05) than those on 0.5KPa surface (**Fig. 5.1C**). Quantification of the circularity of single BM-MSCs enabled the observation that cells on the 0.5KPa substrate were significantly more circular in morphology than those on the 40KPa substrate (**Fig. 5.1D**).

Regulation of cytoskeletal arrangement are normally thought to occur largely due to change in RhoA/ROCK activity rather than transcription or translation of their genes/mRNA. However studies such as that by Mih et al demonstrated the effect of ROCK1+2 siRNA in abolishing responses of lung fibroblasts to substrates of varying stiffness [305]. This indicates a role for ROCK1 and 2 at the mRNA level to play a role in mechanosensing. **Figure 5.2** illustrates the suitability of *RHOA, ROCK1, ROCK2, CTGF* and *ANKRD1*-specific primers for amplification of these genes. Each standard curve demonstrates a linear relationship between input [cDNA] and cycle number in addition to theoretical reaction efficiencies between 90-100%. When BM-MSCs were cultures for 24 hours on each substrates, no significant changes were induced due to 0.5KPa compared to 40KPa. However, *ROCK2* and *RHOA* expression demonstrated a trend towards increase (**Fig. 5.1E**).

YAP/TAZ localisation and their downstream function as binding partners for the TEAD family of transcription factors are markers of increased cytoskeletal tension on stiff substrates [330]. This therefore prompted investigation into their localisation on the substrates used here. **Figures 5.2F-5.2H** demonstrate the specificity of the anti-YAP antibody used in immunostaining here and that signal detected was due to this

primary antibody and not the fluorophore-conjugated secondary antibody. At 40KPa, YAP/TAZ were restricted to the nucleus of BM-MSCs (**Figs. 5.1F+5.1G**) and they showed a more dispersed pattern around the cell on the 0.5KPa substrate (**Figs. 1H+1I**). This difference between YAP/TAZ nuclear localisation on 40 and 0.5KPa substrates was confirmed by quantification of the percentage of each nuclei occupied by this protein pair. Cells on 40KPa induced a significantly greater nuclear YAP/TAZ localisation than on the 0.5KPa substrate (**Fig. 1J**). Finally, mRNA expression of TEAD targets were examined to validate our observation on YAP/TAZ nuclear localisation and neither *CTGF* nor *ANKRD1* expression were altered due to culture on the 0.5KPa substrate compared to that on 40KPa (**Fig. 5.1K**).

Overall, the PA gels of 40KPa and 0.5KPa stiffness are transduced by the seeded BM-MSCs to result in cell phenotypes which are typical of cells on stiff and soft substrates and which induce differential activation of the mechanosensory pathways. This therefore suggests the suitability of these substrates for investigation of the effect of hypoxia on the mechanosensory pathways which govern chondrogenesis of BM-MSCs.

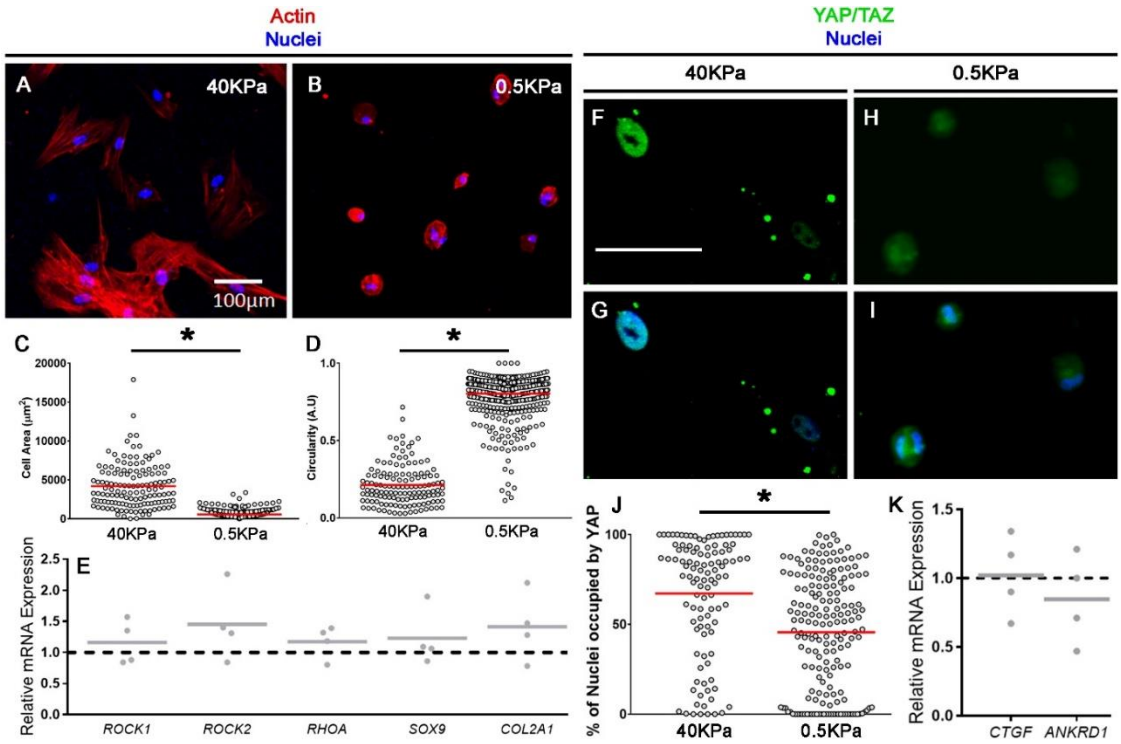

Figure 5.1. 40 and 0.5KPa induce differential cytoskeletal arrangement, cell shape and YAP/TAZ nuclear localisation in hBM-MSCs cultured in chondrogenic differentiating media. (A+B) Actin immunodetection by Phalloidin with DAPI counterstain at after 24 hours of culture on 40KPa (A) and 05KPa (B) substrates. Representative images of 4 independent repeats shown. Brightness and contrast were adjusted for all channels to an equal degree between all conditions. (C+D) Quantification of cell area (C) and circularity based on phalloidin staining. Values plotted represent the area/circularity of a single cell, with values from 4 independent repeats plotted and the mean values represented by the red line. (E+K) mRNA expression of *ROCK1*, *ROCK2*, *RHOA*¸ *SOX9*, *COL2A1* (E), *CTGF* and *ANKRD1* (K) following 24 hours of culture. Values plotted represent expression on the 0.5KPa substrate from 4 independent experiments, and are fold change compared to expression on the 40KPa substrate represented by the horizontal dotted line. The solid grey lines represent the mean expression value for each gene. (F-I) YAP/TAZ immunodetection with DAPI counterstain after 24 hours of culture on 40KPa (F+G) and 05KPa (H+I) substrates. Representative images of 3 independent repeats shown. Brightness and contrast were adjusted for all channels to an equal degree between all conditions. (J) Quantification of nuclear YAP/TAZ on each stiffness. Each value plotted represents the percentage of a single DAPI-marked nucleus that is occupied by YAP/TAZ. Values are from 3 independent repeats with the red horizontal lines representing the mean. Statistical analysis: **p*=<0.05.

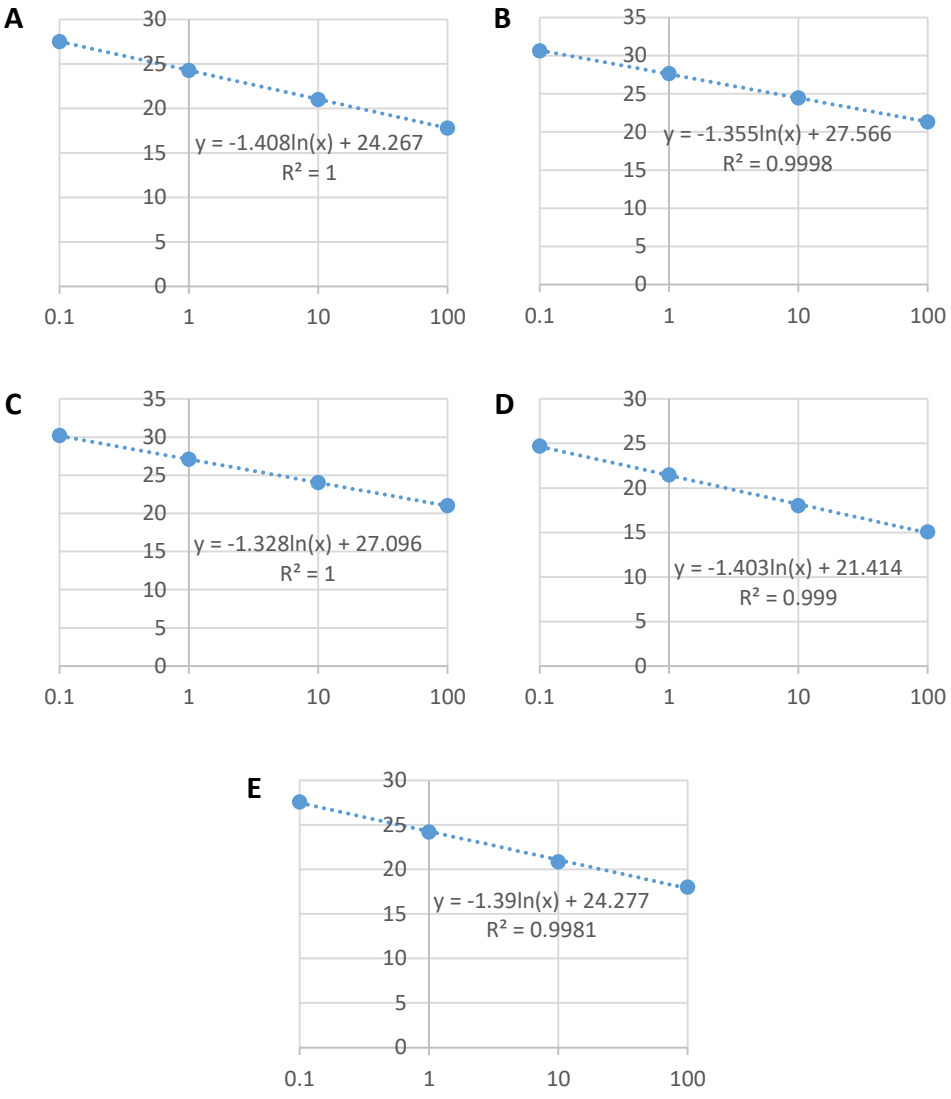
A
y = -1.408ln(x) + 24.267
R² = 1
B
y = -1.355ln(x) + 27.566
R² = 0.9998
C
y = -1.328ln(x) + 27.096
R² = 1
D
y = -1.403ln(x) + 21.414
R² = 0.999
E
y = -1.39ln(x) + 24.277
R² = 0.9981

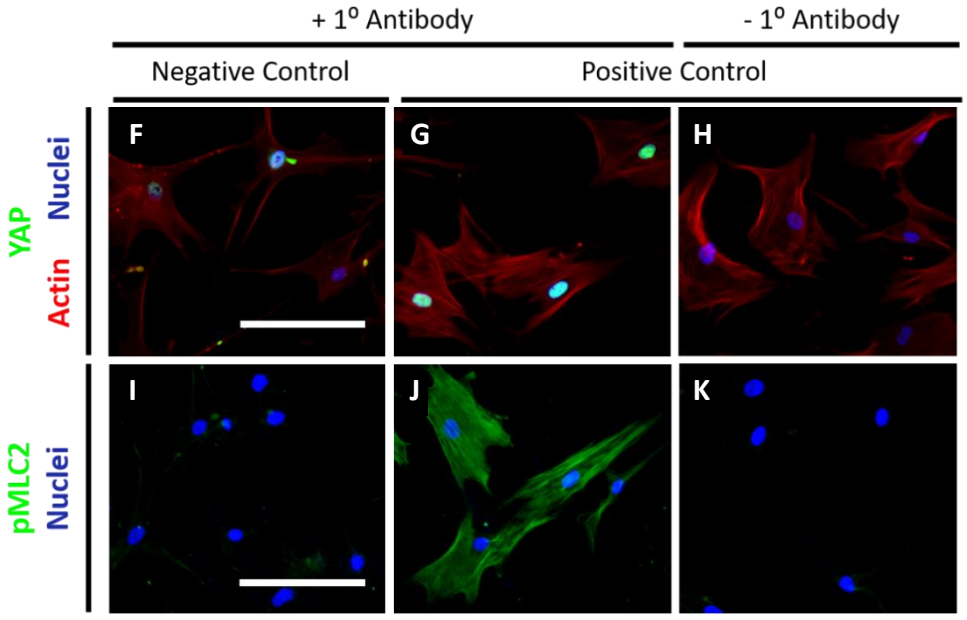
+ 1° Antibody
- 1° Antibody
Negative Control
Positive Control
YAP
Nuclei
Actin
pMLC2
Nuclei
F
G
H
I
J
K

Figure 5.2. Standard curves which demonstrate a linear relationship between input cDNA concentration and cycle (Ct) number when amplified using *RHOA*- (A), *ROCK1*- (B), *ROCK2*- (C) *CTGF- (D) and ANKRD1*-specific (E) primers (y axis = Ct, x axis = [cDNA] (%). (F-K) Immunostaining of YAP (F-H) and pMLC2 [230] in BM-MSC cultures incubated at 20%O_2, with (F+I) and without (G, H, J, K) ROCK inhibitor- Y-27632 for 24 hours. Images F, G, I and J demonstrate immunofluorescent signal following an immunostaining protocol in which the primary antibody was included. Images H and K were taken following an immunostaining protocol in which the primary antibody was omitted. Scale bar = 200µm.

5.2.2. ROCK governs cytoskeletal arrangement of hBM-MSCs on soft and stiff substrates

RhoA/ROCK activity has been established as the key mediator of cytoskeletal organisation in response to varying substrate stiffness, ligand availability and integrin engagement [307]. Therefore in order to confirm the role of ROCK in governing cell morphology of BM-MSCs cultured on 40 and 0.5KPa substrates, cultures here were incubated with and without the ROCK inhibitor- Y-27632. This compound acts to bind the ATP-binding pocket at the catalytic site of both ROCK1 and ROCK2, inhibiting myosin light chain phosphorylation and reducing stress fibre formation [539].

Following optimization of pMLC2 immunostaining as detailed in **Figure 5.2F-5.2H,** Immuno-detection of phosphorylated MLC2 was performed on BM-MSC cultures on substrates of both stiffness following a 24-hour treatment with Y-27632. BM-MSCs treated with the ROCK inhibitor (**Figs 5.3C+5.3D**) displayed abolished pMLC detection compared to the untreated control (**Figs 5.3A+5.3B**). In terms of actin organisation, Y-27632 appeared to reduce the formation of stress fibres in hBM-MSCs compared to that observed in the untreated control on the 40KPa substrate (**Figs 5.3E+5.3G**). Y-27632 also increased formation of protrusions from the cell body. On the 0.5KPa substrate compared to the control, Y-27632 treatment increases the cell area of hBM-MSCs and reduces the round morphology of these cells (**Figs 5.3F+5.3H**). These observed changed in cell area were confirmed by quantification of the phalloidin-stained images with a significant increase on the soft surface due to Y-27632 and no change on 40KPa substrates (**Figs 5.3I+5.3J**). The ROCK inhibitor also significantly reduced the circularity of BM-MSCs cultured on either substrate (**Figs 5.3K+5.3L**).

Overall, the characterisitic cell morphologies observed on the 0.5 and 40KPa substrates are govered by ROCK activity.

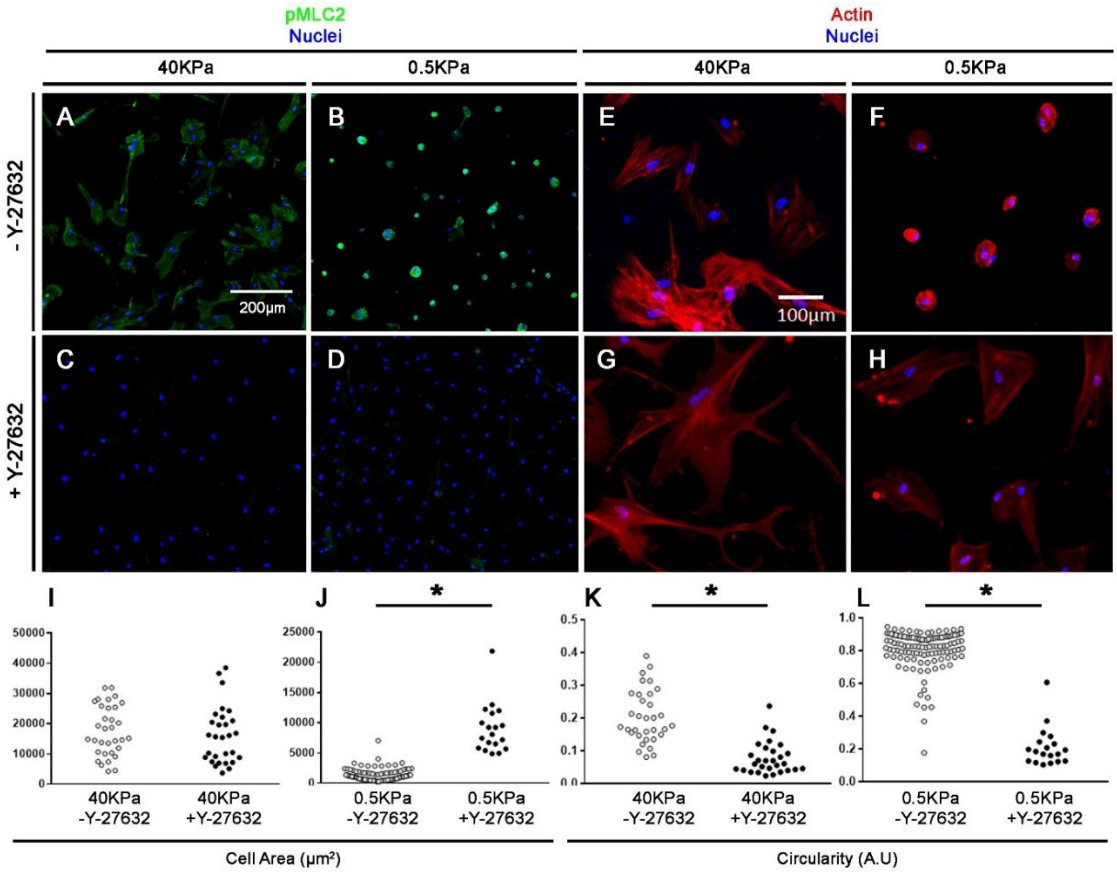

Figure 5.3. The ROCK inhibitor, Y-27632 reduces myosin light chain 2 phosphorylation and induces differential effects on the cytoskeletal arrangement and cell shape of hBM-MSCs cultured on 40 and 0.5KPa substrates. (A-D) pMLC2 immunodetection with DAPI counterstain after 24 hours of culture without Y-27632 on 40KPa (A) and 05KPa (B) substrates and with Y-27632 (C+D). Representative images of 3 independent repeats shown. Brightness and contrast were adjusted for all channels to an equal degree between all conditions. [375] Actin immunodetection by Phalloidin with DAPI counterstain after 24 hours of culture without Y-27632 on 40KPa (E) and 05KPa (F) substrates and with Y-27632 (G+H). Brightness and contrast were adjusted for all channels to an equal degree between all conditions. (I+J) Quantification of single cell area based on phalloidin staining in E-H on 40KPa (I) and 0.5KPa (J) **with** and **without** Y-27632. (K+L) Quantification of single cell circularity based on phalloidin staining in E-H on 40KPa (K) and 0.5KPa (L) **with** and **without** Y-27632. Statistical analysis: *p=<0.05.

5.2.3. Hypoxia partially inhibits small, round hBM-MSC morphology on 0.5KPa substrates and increases cell condensation on both surfaces.

As pertained to, hypoxia may regulate the mechanotransducive ability of BM-MSCs in response to culture on substrates of varying stiffness. As such pathways have themselves been shown to regulate chondrocyte differentiation, it is rational to hypothesize that hypoxia may regulate chondrogenesis through RhoA/ROCK-mediated mechantransducive signaling in BM-MSCs. This is demonstrated by studies in which the abrogation of stiffness-mediated cell proliferation and differentiation were observed in response to inhibition of actin polymerisation [540]. This may have significant implications for CTE strategies which aim to direct BM-MSCs down a chondrogenic cell fate by a combination of hypoxic culture and 3D biomaterial scaffolds of a defined stiffness.

Due to the relatively poor understanding of the crosstalk betweek the hypoxia and mechanotransducive pathways, the ability of hypoxia to induce changes in cytoskeletal organisation of hBM-MSCs on soft and stiff substrates was investigated here. Of the two hypoxic oxgen concentrations used thus far in chapters 3 and 4, 2%O_2 was selected for two reasons. The first of these is that oxygen levels below 5% are utilised by the majority of studies which investigate hypoxia's effect on mechanotransducive pathways [372, 541]. In addition, as seen in chapter 3, 2%O_2 raised expression of HIF targets- *VEGFA, PGK1* and *EGLN* by significant levels at both days 1 and 14 of chondrogenesis, whereas expression of these were raised significantly by 5%O_2 at day 1 only. This sustained expression of *VEGFA, PGK1* and *EGLN* by 2%O_2 indicates that this oxygen concentration may stably raise expression

of other HRE-containing genes whose products are involved in mechanotransduction, if indeed there exists crosstalk between these pathways during chondrogenesis. 2%O_2 was disregarded in chapter 4 due to the requirement of hypoxia in that chapter to inhibit hypertrophy in long-term differentiation experiments, which in chapter 3 was shown to occur due to 5%O only. This culture system also included TGF-β_3-containing chondrogenic media to mimic standard differentiating conditions.

On the 40KPa substrate, hypoxia did not induce changes on cytoskeletal organisation of hBM-MSCs compared to that at 20%O_2 (**Figs. 5.4D+5.4E**). Accordingly, no changes in cell area or circularity were observed, as confirmed by quantification of these cell parameters (**Figs 5.4A-5.4C**). On the 0.5KPa substrate, hypoxia increased the area of single cells (**Fig 5.4J**) and colonies (**Fig 5.4K**) in addition to reducing their circularity (**Fig 5.4L**). Hypoxia also appeared to increase the number of thin projection or protrusions extending from the centre of hBM-MSCs on the soft substrate. The changes in cell area and circularity on the 0.5KPa substrate were confirmed as significant by quantification of these parameters (**Figs 5.4G-5.4I**).

As a precursor to chondrogenic induction, the limb bud mesenchyme forms a condensation which initiates the transcriptional program required for chondrogenesis [178]. The mesenchyme at this stage of limb development is hypoxic as a result and this low-oxygen states plays keys role during chondrogenic induction at this stage of limb development [262]. This therefore prompted investigation of the effect of hypoxia on cell condensation and colony formation. On both the 40 and 0.5KPa substrates, hypoxia compared to normoxia induced an increasing trend of

cells present in colonies as a percentage of the total cell count. This was coupled with a trend towards a decrease observed in the proportion of single, isolated cells as a percentage of the total cell count (**Fig. 5.4M**). Hypoxia increased the ratio of colonies to single cells on substrates of both stiffness (**Fig. 5.4N**), whilst inducing no changes in the total cell count (**Fig. 5.4O**) and number of cells present per colony (**Fig. 5.4P**).

Overall hypoxia appears to affect cytoskeletal re-organisation on the soft substrate only. Addiotnally, whilst hypoxia increases condensation on both the 0.5kPa and 40KPa substrates, the condensations on the soft surface are more compact and therefore closely mimics the mesenchymal condensations of the limb bud.

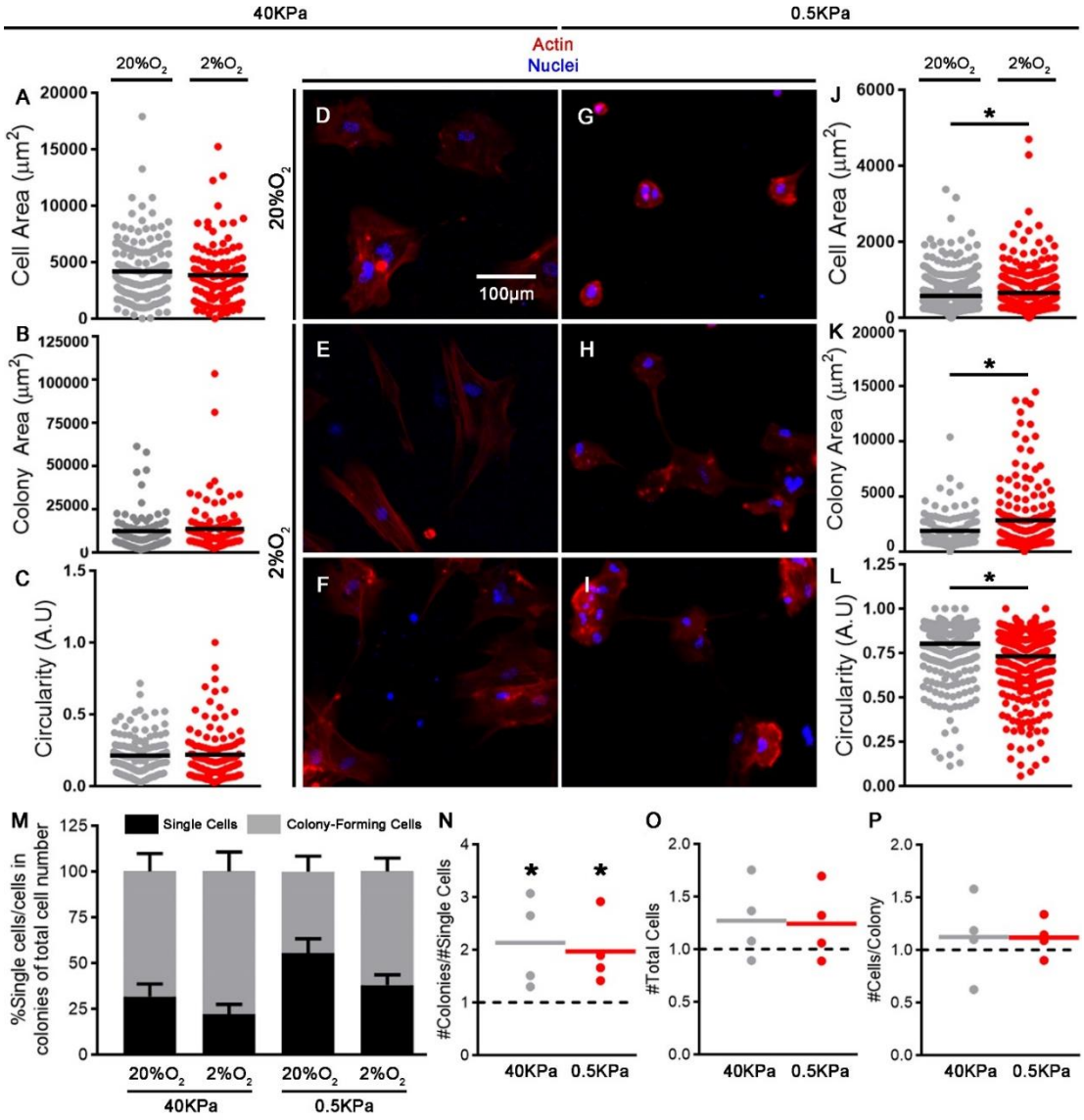

Figure 5.4. Hypoxic incubation induces changes in hBM-MSC morphology on 0.5KPa substrates and increases cell condensation on substrates of 40 and 0.5KPa. (A-C+J-L) Quantification of single cell (A+J) and colony (B+K) area and single cell circularity (C+L) based on phalloidin staining in images D-I on 40KPa (A-C) and 0.5KPa (J-L) at **20%** and **2%O_2**. Values plotted represent the area/circularity of single cells/colonies from 4 independent repeats with the mean values represented by the black lines. (D-I) Actin immunodetection by Phalloidin with DAPI counterstain after 24 hours of culture on 40KPa (D-F) and 0.5KPa (G-I) at 20%O_2 (D+G) and 2%O_2 (E, F, H, I). Representative images of 4 independent repeats shown. Brightness and contrast were adjusted for all channels to an equal degree between all conditions. (M) Number of **single** or **colony-forming** cells on 40KPa and 0.5KPa at 20% and 2%O_2 as a percentage of the total cell count within each condition. Values plotted are the means from 4 independent repeats, with error bars representing the standard error of the mean. [419] Quantification of colonies normalised to single cell count (N), total cell number (O) and number of cells per colony (P) in response to 2%O_2 on **40KPa** and **0.5KPa**. Values plotted are from 4 independent repeats and are fold change compared to that at 20%O_2 on the respective substrate, represented by the horizontal dotted line, with grey/red lines representing the mean values. Statistical analysis: *p=<0.05

5.2.4. Hypoxic incubation increases phosphorylation of myosin light chain 2 on 0.5KPa substrates

The ability of hypoxia to induce ROCK activity during its regulation of mechanotransductive pathways has been documented in a variety of cell types such breast cancer cells [372] and pulmonary artery smooth muscle cells [542]. In addition, regulation of ROCK activity represents the most plausible mechanism by which hypoxia induces the cytoskeletal re-arrangement observed on the 0.5KPa substrate. The effect of hypoxia on MLC2 phosphorylation was therefore investigated due to pMLC2 levels being indicative of ROCK activity [543]. Hypoxia did not induce any change in pMLC2 in hBM-MSCs on the 40KPa substrate compared to 20%O_2 (**Figs. 5.5A+5.5B**). However reduced oxygen levels did increase pMLC2 in cells cultured on 0.5KPa surfaces (**Figs. 5.5C+5.5D**). This significant increase due to hypoxia on only the soft substrate, was confirmed by quantification of pMLC2 immunostaining following normalisation to cell number and average area (**Figs. 5.5E**).

RHOA, *ROCK1* and *ROCK2* have been shown to contain HREs in their promoter regions in addition to their expression being induced by hypoxia [544]. Therefore, investigation of this phenomenon was carried out in the present study, but no significant changes were induced by hypoxia in the expression of *RHOA* (**Fig. 5.5F**), *ROCK1* (**Fig. 5.5G**) or *ROCK2* (**Fig. 5.5H**) mRNA on either substrate. However, a trend towards increase was observed in the mRNA of all three genes due to hypoxia on the 40KPa surface and that of *ROCK1* on the 0.5KPa substrate. Taken together, these results indicate that 2%O_2 induced changes in ROCK activity only in BM-MSCs on the 0.5KPa substrate and this effect appeared to be post-transcriptional.

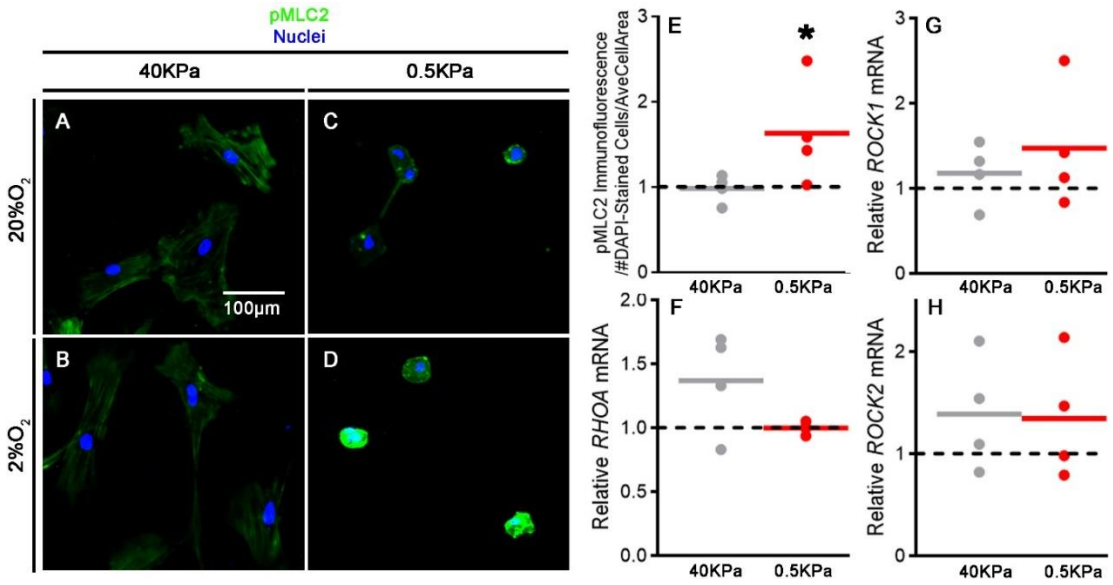

.

Figure 5.5. Hypoxic incubation increases phosphorylation of myosin light chain 2 on 0.5KPa substrates. (A-D) pMLC2 immunodetection with DAPI counterstain after 24 hours of culture at 20%O_2 (A+C) and 2%O_2 (B+D) on 40KPa (A+B) and 05KPa (C+D) substrates. Representative images of 4 independent repeats shown. Brightness and contrast were adjusted for all channels to an equal degree between all conditions. (E) Quantification of pMLC2 immunofluorescence in response to 2%O_2 on **40KPa** and **0.5KPa** substrates, normalised to DAPI-stained cell number and mean area of cells in each condition, calculated from Phalloidin images in figure 2D-I. (F-H) mRNA expression of *RHOA* (F), ROCK1 (G) and *ROCK2* (H) following 24 hours of culture at 2%O_2 on **40KPa** and **0.5KPa** substrates. Values plotted in E-H are from 4 independent experiments, and are fold change compared to pMLC2 immunofluorescence/mRNA expression at 20%O_2 which is represented by the horizontal dotted line. Mean values are represented by grey/red lines. Statistical analysis: *p=<0.05.

5.2.5. Hypoxia reduces the presence of YAP/TAZ in the nuclei of hBM-MSCs on the 40KPa substrate.

Reducing the oxygen concentration appears to reduce YAP protein expression, nuclear localisation and its downstream activity as a transcriptional co-factor [383]. The central role that YAP appears to play in the transduction of mechanical stimuli into transcriptional changes [545], prompted the investigation into YAP function in the present study.

Hypoxia appeared to reduce the overall presence of YAP/TAZ protein in hBM-MSCs cultured on the 40KPa substrate (**Fig. 5.6A-5.6D**) which resulted in a decrease in the nuclear localisation of this protein (**Fig. 5.6I**). This effect on the stiff substrate was not accompanied by a change in cytoplasmic localisation of YAP/TAZ. As observed previously, YAP/TAZ localisation on the 0.5KPa substrate at normoxia appeared to be more dispersed around the cell compared to that on the stiff substrate on which localisation was restricted to the nucleus of hBM-MSCs (**Fig. 5.6E-5.6H**). Quantification of YAP/TAZ localisation demonstrated a much more varied spread of YAP nuclear localisation on the soft substrate (**Fig. 5.6J**) compared to that due to 40KPa, which were polarised to the 50% level and above (**Fig. 5.6I**). However, no change in total or nuclear YAP/TAZ levels appeared to be induced by hypoxia on the 0.5KPa substrate.

Expression of TEAD targets were assessed to validate the observations of YAP/TAZ nuclear localisation. Hypoxia appeared to induce a trend towards increased expression of *CTGF* (**Fig. 5.6K**) and *ANKRD1* (**Fig. 5.6L**) on the 40KPa substrate, with a significant increase observed in *ANKRD1* mRNA on the 0.5KPa substrate (**Fig. 5.6L**).

Together, these results indicated that YAP localization and expression of its transcriptional targets are not subject to regulation by mechanotransducive pathways in response to hypoxia culture.

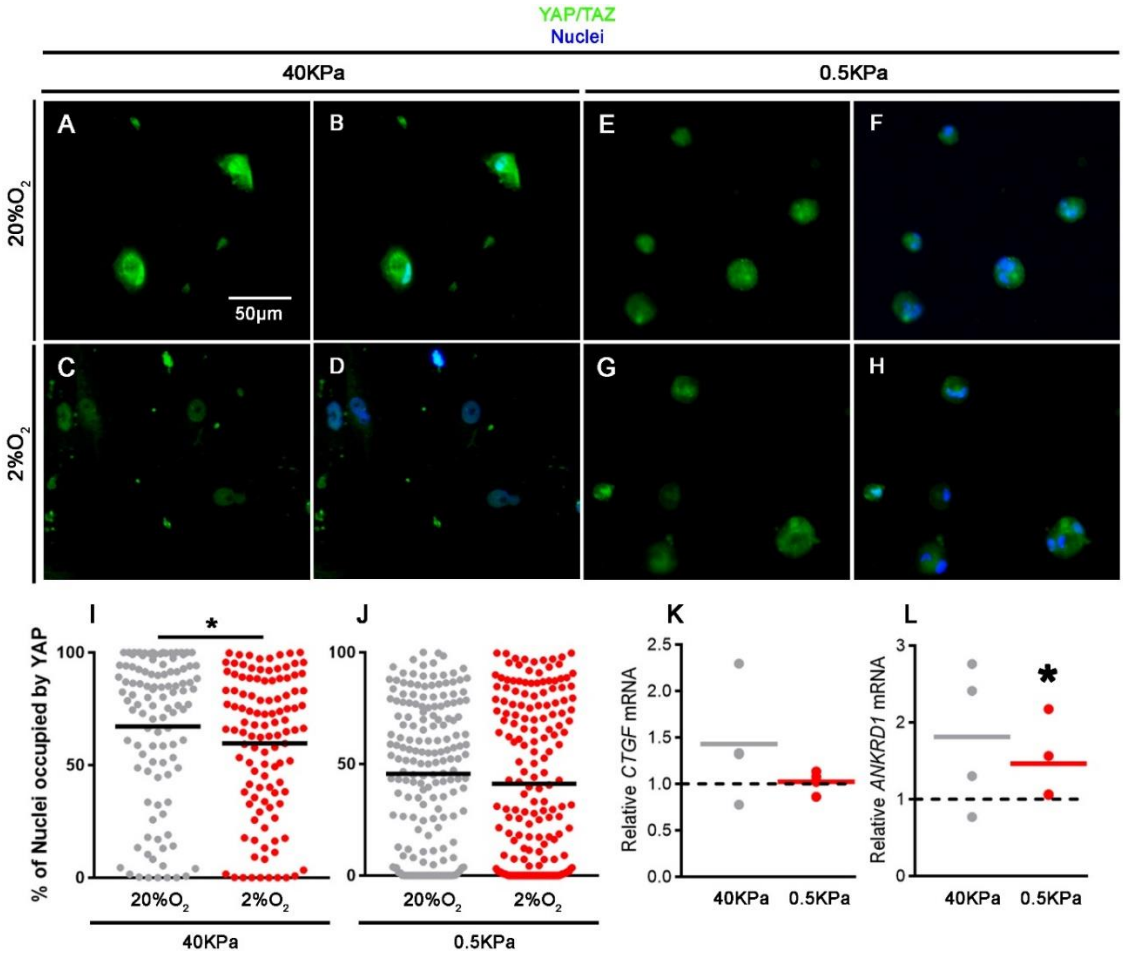

Figure 5.6. Hypoxia reduces the presence of YAP/TAZ in the nuclei of hBM-MSCs on the 40KPa substrate but does not induce corresponding changes in YAP-TEAD target genes. (A-H) YAP/TAZ immunodetection with DAPI counterstain after 24 hours of culture on 40KPa (A+D) and 0.5KPa (E+H) substrates at 20%O_2 (A, B, E, F) and 2%O_2 (C, D, G, H). Representative images of 3 independent repeats are shown. Brightness and contrast were adjusted for all channels to an equal degree between all conditions. (I+J) Quantification of nuclear YAP/TAZ on at 40KPa (I) and 0.5KPa (J) at **20%O_2** and **2%O_2**. Each value plotted represents the percentage of a single DAPI-marked nucleus that is occupied by YAP/TAZ. Values are from 3 independent repeats with the red horizontal lines representing the mean. (K+L) mRNA expression of *CTGF* (K) and *ANKRD1* (L) following 24 hours of culture at 2%O_2 on **40KPa** and **0.5KPa** substrates. Values plotted are from 4 independent experiments, and are fold change compared to expression at 20%O_2 represented by the horizontal dotted line. Mean values are represented by grey/red lines. Statistical analysis: *p=<0.05.

5.2.6. Hypoxia induces transcription of genes conducive for early chondro-induction on 0.5KPa substrates and increases cartilage ECM production on either substrate.

The cytoskeletal re-organisation, ROCK induction and increase in cell condensation observed due to hypoxia, motivated the decision to analyse expression of mRNA which denote mesenchymal limb bud progenitors specified down a chondrogenic cell fate. Hypoxia appeared to increase expression of the master chondrogenic factor, *SOX9* on the soft substrate only. The SOX9 target, *COL2A1* was induced on the 40KPa with a trend towards increase being induced on the 0.5KPa substrate (**Fig. 5.7A**).

In addition to those 'classic' markers of chondrogenesis, transcription of genes which are expressed in condensed limb bud mesenchymal cells prior to chondrocyte differentiation were investigated. *MSX1* is expressed within and surrounding the AER of the limb bud [546]. Msx1 plays an important function together with the Distal-less Homeobox 5/6 (Dlx5/6) set of transcription factors, in growth plate formation. This was shown by Vieux-Rochas et al who observed a further loss of Alcian Blue staining in the developing limb (E12.5) due to a combined *MSX1* and Dlx5/6 deletion compared to loss of Dlx5/6 only [546]. Msx1 has been shown to be a key mediator of BMP4 signalling required for maturation of the AER [547] and in the present study, hypoxia inhibited *MSX1* expression on the 40KPa substrate whilst not inducing any changes in expression on the softer surface (**Fig. 5.7A**).

PRX1 encodes another transcription factors whose expression also delineates pre-chondrogenic cells of the condensed limb bud mesenchyme. Genetic deletion targeted to *PRX1*-expressing cells is an established model for investigation into

cartilage development at the pre-chondrogenic stage, prior to cell fate commitment [94]. This transcription factor plays important roles during limb bud chondrogenesis such as the regulation of Tenascin-C which is an ECM protein required for limb bud progenitor condensation [49]. In this study, no significant changes in its expression were observed due to hypoxia on either the 40 or 0.5KPa substrates (**Fig. 5.7A**).

Other markers of the pre-chondrogenic limb bud mesenchyme include genes which encode cell-cell adhesion proteins, shown to be required for downstream chondrogenesis. Expression of *NCAM* was induced on only the 0.5KPa substrate due to hypoxia (**Fig. 5.7B**). To validate the induction of HIF in response to hypoxia in hBM-MSCs on either substrate, the upregulation of *VEGFA* and *EGLN* were assessed. Hypoxia upregulated both of these genes in hBM-MSCs cultured on either substrate (**Fig. 5.7C**).

Long-term chondrogenesis was investigated following a 21 day period. Collagen Type II in the ECM appeared to be upregulated due to hypoxia on both substrates. In addition, hBM-MSCs on the 40KPa appearing to induce higher levels of Collagen Type II at both 20% and 2%O_2 than observed on the soft substrate (**Fig. 5.7D-5.7G**). Gene expression at this time point was also analysed. At normoxia expression of *SOX9* and *COL2A1* mRNA were higher on the 0.5KPa substrate than on the 40KPa surface (**Fig. 5.7H**). Hypoxia did not have to effect on *SOX9* expression in hBM-MSCs on either substrate but on the 40KPa substrate, there was an increasing trend of *COL2A1, VEGFA* and *EGLN* expression due to hypoxia. This increase in *VEGFA* and *EGLN* expression due to hypoxia was not observed on the 0.5KPa substrate and a trend towards a decrease in *COL2A1* expression was observed due to 2%O_2 on the soft

substrate. No change occurred in *RUNX2* expression either in response to varying substrate stiffness or oxygen concentration. The involvement of ROCK in hypoxic induction of these gene was also analysed on TCP. The increases observed in *SOX9* at day 1 (**Fig. 5.7I**), *COL2A1* at day 21 (**Fig. 5.7J**) and HIF targets (**Fig. 5.7K+5.7L**) throughout the differentiation due to hypoxia, appeared to be reduced by ROCK inhibition.

Overall, hypoxia induced early transcriptional changes that are conducive for chondrocyte specification, in BM-MSCs on the soft substrate only. However at day 21, hypoxia appeared to increase chondrogenic at the mRNA level in BM-MSCs cultured on the stiff substrate.

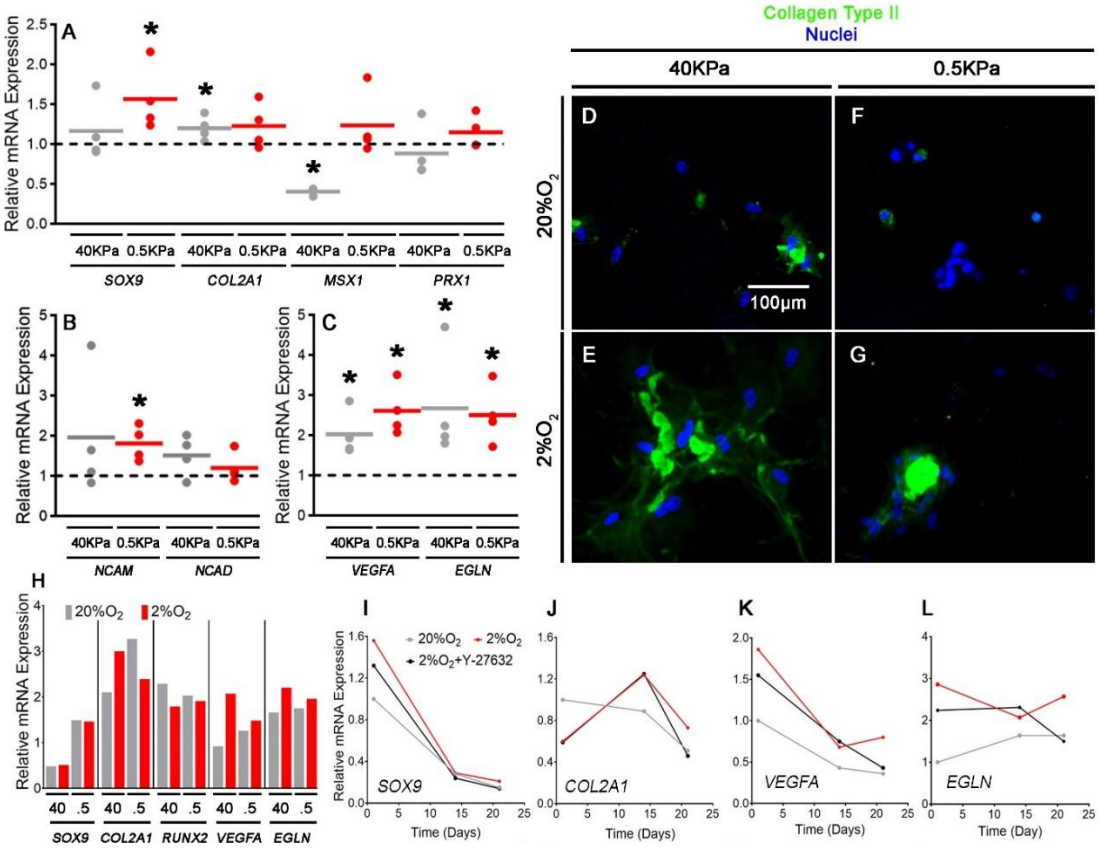

Figure 5.7. Hypoxia induces transcription of genes conducive for early chondro-induction on 0.5KPa substrates but it increases Collagen Type II in the ECM following 21-day chondrogenic induction on either stiffness. (A-C) mRNA expression of *SOX9*, *COL2A1*, *MSX1*, *PRX1* (A), *NCAM*, *NCAD* (B), *VEGFA* and *EGLN* (C) following 24 hours of culture at 2%O_2 on **40KPa** and **0.5KPa** substrates. Values plotted are from 4 independent experiments, and are fold change compared to expression at 20%O_2 represented by the horizontal dotted line. Mean values are represented by grey/red lines. (D-G) Collagen Type II immunodetection with DAPI counterstain after 21 days of chondrogenic induction 40KPa (D+E) and 0.5KPa (F+G) at 20%O_2 (D+F) and 2%O_2 (E+G). Brightness and contrast were adjusted for all channels to an equal degree between all conditions. (H) mRNA expression of *SOX9*, *COL2A1, VEGFA* and *EGLN* after 21 days of chondrogenic induction at 2%O_2 on **40KPa** and **0.5KPa** substrates. Values plotted are fold change compared to expression at 20%O_2 represented by the horizontal dotted line. [548] mRNA expression of *SOX9* (I), *COL2A1* (J), *VEGFA* (K) and *EGLN* (L) at days 1, 14 and 21 of chondrogenic induction at **20%O_2**, **2%O_2** and **2%O_2+Y-27632** on TCP. Values plotted are fold change compared to expression at day 1, **20%O_2**. Statistical analysis: *indicates significant difference compared to that at normoxia, where *p*=<0.05.

5.3. Discussion

The regulation of pathways induced in response to mechanical stimuli during cartilage development, may provide new potential strategies for CTE in the repair of acute chondral defects. The control of these pathways by the physical parameters of the ECM such as substrate elasticity however, may also be subject to regulation by other signalling pathways. Growth factor signalling for example, has also been shown to play keys role in regulating the activity of mechano-signalling pathways. TGF-β_1 has been observed to induce *RHOA* expression and actin re-organisation via a SMAD2/3-dependant mechanism [549]. This study is example of that which provides evidence that the mechanically-stimulated pathways (specifically RhoA/ROCK-mediated cytoskeletal tension) are themselves regulated by pathways not primarily associated with mechanotransducive signalling. Included in such pathways are those stimulated by physiological hypoxia. The plethora of pro-chondrogenic effects of hypoxia during MSC differentiation and evidence of its role in regulating RhoA and ROCK activity, suggests a role for hypoxia in regulating the mechano-transducive pathways involved during chondrogenesis. This therefore prompted the present study.

In summary the results in this chapter demonstrate that during BM-MSC chondrogenesis, hypoxic culture relative to that that observed at normoxia, induces cytoskeletal rearrangement, MLC phosphorylation and cell condensation. These hypoxia-induced changes occur on the 0.5KPa substrate however and not on the stiffer, 40KPa surface. These changes on the soft substrate, appear to correlate with a transcriptional profile that is conducive for early chondrogenic specification. This is

likened to that observed in limb bud progenitors prior to their differentiation into chondrocytes which constitute the growth plate prior during limb development. In contrast however, latent mRNA expression occurs of chondrogenic markers due to hypoxia on the 40KPa substrate. This indicates that the stiff substrate is more conducive for hypoxia mediated-chondrogenesis following intial chondro-specification of multipotent cells.

The established ROCK-mediated control of cytoskeleton dynamics on soft and stiff substrates was observed here. Actin stress fibre formation on the 40KPa substrates were reduced due to ROCK inhibition which also increased formation of filopodia-like projections from the cell body. Inhibition of ROCK has been shown to reduce cytoskeletal tension [305] concomitant with the result observed here and has also been shown to increase formation of projections from the cell body [330]. Such a fillopodia-rich morphology has been suggestive to be conducive for neural differentiation which corresponds to studies in which reduced cytoskeletal tension pre-disposes multipotent progenitors down a neural lineage [304].

In contrast to that on the stiff substrate, hBM-MSCs cultured on the 0.5KPa substrate adopted a small, round morphology as described previously [550]. The response of hBM-MSCs to ROCK inhibition on the soft substrate was also as previously described in which the cell area was increased in response to treatment. As described by Mih et al, the cytoskeletal tension of cells on a soft matrix significantly outweighs the strength of ECM-integrin interactions. This induces a net contraction of the cytoskeleton towards the centre of the cell which results in formation of an actin network that is condensed and concentrically-arranged around the nucleus [305].

Therefore when ROCK and cytoskeletal tension are inhibited in cells which adopt this actin arrangement on compliant ECM, the cytoskeletal tension directed towards the centre of the cell is ablated. This decrease in intracellular tension combined with a lack of interactions between the integrins and that of the surrounding ECM, induces a relax response in which the cell body flows freely outwards.

The majority evidence in the literature for the effect of hypoxia and HIF on actin-myosin dynamics, point to their role as inducers of cytoskeletal tension. For example in breast cancer cells, incubation at 1%O_2 induces actin stress fibre formation via RhoA and ROCK and was required for migration and metastasis of thesecells [372]. Inhibition of PHD2 in fibroblasts, which reduces HIF-1α hydroxylation, ubiquitination and degradation, enhanced Cofilin phosphorylation [406] which is required for F-Actin formation and cytoskeletal tension[375]. In addition, treatment of endothelial cells with the PHD2 inhibitor, DMOG also induced F-Actin stress fibre formation which again is suggestive of a role for hypoxia and HIF in inducing cytoskeletal reorganisation and tension [551]. Observations here suggest that hypoxia also increases cytoskeletal tension in hBM-MSCs. Increased phosphorylated myosin was observed due to hypoxia on the soft substrate, in addition to the rearrangement of actin on this substrate. A limitation of this system is the lack of quantification of the absolute levels of cytoskeletal tension of BM-MSCs in different conditions. Methods utilised here, including actin stress fibre immune-detection, cell morphology and semi-quantification of phosphorylated MLC2 are only suggestive of increased actin-myosin contraction. Techniques instead such as Traction Force Microscopy (TFM) would enable quantification of this parametre [305].

The effect of hypoxia on the soft substrate contrasts with the apparent lack of effect on the actin arrangement or pMLC2 in BM-MSCs on the stiff substrate. At normoxia, MSCs on a stiff substrate have been shown to exhibit higher cytoskeletal tension than that on a softer surface [305]. Therefore, it may be expected to observe a lack of change at 40KPa with regards to cytoskeletal tension due to this being at a maximal level on this substrate [304]. Again, it is important to note the limitations of this experiment in which the observations provide only correlative evidence of the regulation of cytoskeletal tension. As described above, direct quantification of cytoskeletal tension is most appropriate as opposed to indirect methods. In addition, semi-quantification of pMLC2 by Western Blotting may be required. This, and techniques such as TFM to quantify cytoskeletal tension, would enable determination of the magnitude by which hypoxia regulates actin-myosin contraction. TFM may also enable subtle changes to be detected in cytoskeletal tension on the stiff substrate due to hypoxia, which were not detected here.

Treatment of the carcinoma cell line- SCC-61 with Calyculin A on soft PA gels by Jerrell et al, resulted in an increase in cell protrusions required for ECM remodelling [552]. Calyculin A is a pan-phosphatase inhibitor and is used to increase MLC2 phosphorylation and contraction [553]. In the present study therefore, the increase in cell protrusions and decrease in circularity on the 0.5KPa substrates due to hypoxia, in view of the findings by Jerrel et al, are suggestive of hypoxia-mediated actin-myosin contraction. Once again, techniques such as TFM would be required to provide robust evidence of increased cytoskeletal tension induced by hypoxia. Based on observations here, it is possible to only suggest that hypoxia increases actin-myosin contraction of hBM-MSCs on a soft substrate.

The differences in the effect of hypoxia observed between the soft and stiff substrates may be due to an alterations in cell attachment sites. Hypoxia has been established as an inducer of ECM formation both in experiments conducted here and in the literature. Increased expression of ECM components such as fibronectin and collagens are induced by hypoxia for example during hESC proliferation and migration [541] and during hMSC chondrogenesis [272]. An increase in mRNA expression of genes encoding ECM-modifying enzymes has also been demonstrated by fibroblasts and chondrocytes cultured under hypoxic conditions [554]. Cell secreted ECM components have been demonstrated to increase cell attachment and spreading and proliferation of hMSCs [555]. In addition, fibronectin-coated surfaces which were observed to provide attachment sites for other ECM proteins in addition to a greater number of binding sites for seeded cells [556]. The use of fibronectin-coated surfaces here may suggest that hypoxic culture increases the number of cell attachment sites. This may rationalise the observation of increased cell and colony spreading on the 0.5KPa substrates which may not occur on the 40KPa substrate due to the maximal spreading already observed at normoxia on this surface.

Despite evidence of hypoxia inducing ECM formation and hBM-MSC spreading on the soft substrate, this theory of increased attachment sites remains speculative. ECM quantification on the soft substrate would need to be conducted in combination with quantification of cell attachment sites in response to hypoxic incubation. The latter suggestion may be conducted via semi-quantification of mature focal adhesions following their immunodetection. To robustly validate this theory, treatment of integrin-blocking antibodies/inhibitors would be required at the onset of chondrogenensis in normoxic and hypoxic conditions. If indeed, hypoxia-induced

increases in cell adhesions are mediating MSC spreading, then these cell shape changes would be abolished in the presence of an integrin blocker.

The increase in phosphorylated MLC2 observed in the present study on the 0.5KPa substrate, suggests an induction of RhoA/ROCK due to hypoxia. However unlike that previously demonstrated [372], an increase in *RHOA*/*ROCK1*/*ROCK2* mRNA was not observed, with a trend towards an increase in *ROCK1* transcription observed only. This suggests that hypoxia may induce its effect on MLC2 phosphorylation indirectly by regulating components upstream of RhoA/ROCK1/ROCK2. Indeed, reduced oxygen concentration has been shown to increase expression of specific integrins which would indirectly regulate RhoA/ROCK activity and MLC2 phosphorylation. Lee et al observed an increase in total expression of Integrin-β_1 in human ESCs due to hypoxic incubation. An Integrin-β_1-blocking antibody was subsequently shown to reduce hypoxia-mediated increases in cell attachment to cell-secreted fibronectin [541]. Indeed, with the use of integrin blocking molecules here, this theory can be investigated. Alternatively as suggested above, the upregulation of phosphorylated MLC2 may be due to increases in cell attachment sites which arise as a result of hypoxia-increased ECM. Increases in ECM ligand availability would induce integrin engagement and clustering followed by focal adhesion maturation and RhoA/ROCK activation [557].

In addition to the differences observed in hBM-MSC area between stiff and soft substrates at normoxia, the increased nuclear YAP localisation observed in cells on the 40KPa substrate contrasts with that observed on the 0.5KPa substrate in which a diffuse distribution of YAP/TAZ is exhibited. This suggests the suitability of this system

as inducing differential activation of integrin-mediated cytoskeletal tension due to demonstration that YAP/TAZ nuclear localisation is controlled by this pathway [330].

The increase in cell area and ROCK activity observed due to hypoxia on the 0.5Kpa substrate, prompted investigation of the oxygen-dependant regulation of YAP/TAZ. Interestingly, a decrease in nuclear YAP localisation occurred due to hypoxia on the 40KPa substrate, despite no changes observed in cell shape or ROCK activity due to this condition. Additionally, unlike that previously described of the mechano-regulation of YAP/TAZ, this decrease was not accompanied by an increase in cytosolic YAP/TAZ localisation. Rather, a decrease in global YAP/TAZ was observed due to hypoxia. This indicates that YAP/TAZ are not mechanosensitive in this context. This is also supported by lack of YAP/TAZ regulation on the soft substrate due to hypoxia, despite this oxygen state inducing changes in actin organization and ROCK activity on the soft surface. That observed may therefore be due to proteosomal degradation of YAP/TAZ under hypoxic conditions, which is induced by the Hippo pathway and YAP phosphorylation [558]. As conducted by Dupont et al, the involvement of the Hippo pathway may be assessed by siRNA of the Lats kinases which are responsible for phosphorylating YAP and targeting it for proteasomal degradation.

Hypoxia appeared to increase the number of colonies in relation to the number of single cells on both the 40 and 0.5KPa substrate. The total cell number on each substrate demonstrated a trend towards increase, but these changes were insignificant and to a lesser magnitude than the increases observed of colony number. Together with the lack of increase in cell number per colony, this suggest that the greater colony formation is not due to increased proliferation of single cells,

but rather a migration together or condensation of cultures. This is also supported by our observation of a hypoxia-induced increase in the proportion in cells that are present within colonies compared to single cells, as a percentage of the total cell number. However, a limitation of this study is a lack direct quantification of cell proliferation. This may be achieved via immune-detection of cell cycle markers which are indicative of cell division, for example the nuclear antigen Ki67. Alternatively incorporation and immuno-detection of 5-bromo-2'-deoxyuridine in newly synthesized DNA would delineate actively-dividing cells.

Provot et al observed that the limb bud condensations prior to chondrogenesis are hypoxic but that deletion of HIF-1α which was induced by this hypoxic state, did not inhibit formation of this condensation [262]. The observation that hypoxia induces HIF targets, *VEGFA* and *EGLN* in our study indicates that HIF-1α may be mediating the observed effects on the hBM-MSCs. This therefore, places discrepancy between that observed of the condensations due to hypoxia here and in the study by Provot et al. Therefore, we cannot rule out a HIF-1α-independent function of hypoxia during condensation, and the conditional knockdown of this transcription factor in the study by Provot et al does not take in account such mechanisms. Vogler et al observed that the increases in vinculin-containing focal adhesions, Integrin-β_1 immunodetection and cell spreading due to hypoxic culture of L292 fibroblasts which were not abolished upon HIF-1α knockdown [559]. The involvement or not of HIF-1α in hypoxia-induced condensation however, is purely speculative without genetic manipulation or chemical inhibition of HIF-1α during this process. Such an experiment could be conducted by the use of Acriflavine as in the chapter 4, or via siRNA knockdown of HIF-1α.

Despite hypoxia inducing cell-cell contact on both 40 and 0.5KPa substrates, there was a noticeable difference between the colonies formed on each substrate. As with single cells, hBM-MSC condensations on the 0.5KPa substrate exhibited a more compact shape than those on the stiff material with an almost ten-fold difference in colony area observed. As described by many studies, the compact colonies formed on the soft substrate may be more conducive for downstream chondrogenesis. One of the pioneering studies investigating this phenomenon was that by Tacchetti et al who observed a decrease in the chondrogenesis of chick limb bud mesenchymal progenitors upon their separation into single cell cultures [560].

The condensation of hBM-MSCs here on the 0.5KPa substrate due to hypoxia and the more compact nature of these compared to that of the stiff surface, corresponds to the increase in NCAM mRNA expression. This protein is essential for cell-cell adhesion and subsequent chondrogenesis. Widelitz et al observed a significant reduction in the aggregate size of chick limb bud micromass cultures upon incubation with an anti-NCAM antibody with a dose-dependent reduction in chondrogenesis also exhibited [561]. These authors also demonstrated an increase in aggregate formation due to NCAM overexpression, with an accompanying increase in Collagen Type II expression.

Studies investigating the expression pattern of cell-adhesion molecules during limb bud chondrogenesis such as that by Tavella et al, have observed a peak in expression of N-Cadherin which preceded that of NCAM [562]. These authors suggested the requirement of N-Cadherin in initiation of limb bud condensation with NCAM functioning to strengthen and maintain cell-cell adhesions. The lack of increase in N-Cadherin mRNA in the present study corresponding to NCAM induction by hypoxia,

suggests that reduced oxygen concentrations in this context does not initiate condensation, but acts to maintain it. A limitation of the study however, which would enable validation of this theory, is the lack of NCAM gene expression at time points following 24 hours. Latent expression of this gene would suggest the constitutive role of NCAM in hypoxia-induced condensations. In addition, the roles of N-Cadherin and NCAM, are not directly implicated in the hypoxia-induced condensations observed here of BM-MSCs. Blocking or genetic manipulation of these adhesion proteins would be required in order to confirm their role or lack thereof in these observations.

The rationale behind examining crosstalk between the hypoxic pathways and those stimulated in response to changes in the mechanical microenvironment, is for informing interaction of these pathways during chondrogenesis. Such a study would contribute to the knowledge of cartilage development from the mesenchymal limb bud. It would also aid cartilage tissue engineering strategies which aim to combine the effects of an appropriate mechanical environment with an oxygen gradient which mimics that of physiological levels in the limb bud and growth plate. Unlike other cell fates in which a round cell and low basal ROCK-mediated cytoskeletal tension is required for their differentiation [304, 307], chondrogenesis appears to be an anomaly. Strong evidence exists for the requirement of higher levels of ROCK activity and cytoskeletal tension during chondrogenesis of stem cells in which the actin cytoskeleton is in a cortical configuration. For example, ROCK inhibition or ablation of myosin light chain contraction appears to reduce chondrogenesis of ATDC5 cells on a relatively soft substrate in which actin fibres adopt a cortical arrangement [355]. This is also supported in the investigation carried out by Ray et al, who demonstrated the requirement for cytoskeletal tension in the round organisation of mesenchymal

progenitors of the limb bud and for subsequent mRNA expression of *SOX9* and *COL2A1* [353].

In the present study, hypoxic incubation of hBM-MSCs on the 0.5KPa substrate, appeared to express increased levels of mRNA conducive for induction. This includes that of *SOX9*, and a trend towards an increase of *COL2A1, PRX1* and *MSX1*. Despite inducing *COL2A1* expression, which may be also be stimulated by cell condensation as opposed to part of a specific differentiation program, hypoxia does not appear to induce expression of other early chondrogenic markers on the 40KPa substrate. Indeed, *MSX1* expression appears to be inhibited on this stiffness by hypoxia. A limitation of this study is represented by the relatively few genes chosen to represent early chondrogenic induction, and the even fewer genes whose expression were significantly altered due to hypoxia. As with any cellular process, expression of *SOX9* is not enough to robustly denote chondrogenesis and requires other early markers to confirm commitment down a chondrogenic lineage. For example expression of *SOX5* and *SOX6* may represent other suitable candidate genes, in addition to osteoblastic/hypertrophic markers such as *RUNX2* or *COL10A1.* Examination of these genes would enable confirmation or not of the single and specific lineage commitment of the BM-MSCs in hypoxic conditions.

The trend towards a chondrogenic expression due to hypoxia on the soft substrate only, appears to correlate with observations in which cell area increased and cell circularity decreased compared to no such effect on the stiff substrate. Together with the upregulation of MLC2 phosphorylation on the soft substrate only, this indicates that hypoxia may provide the signal for ROCK-mediated cytoskeletal tension that is

required for chondrogenesis in cells with a cortical actin arrangement. However it is important to note that this role of hypoxia is based only on correlative observations of cytoskeletal tension with changes in chondrogenic gene expression at the same time point. Therefore in order to robustly demonstrate the ability of hypoxia to induce chondrogenesis via increased ROCK-mediated cytoskeletal tension, it would be required to use chemical inhibitors of actin-myosin contraction during this process. Such experiments may be achieved through the use of inhibitors of both ROCK and myosin contraction (Y-27632 [305]) and Blebbistatin respectively during hBM-MSC chondrogenesis induced by hypoxia. Observation of differential chondrogenic mRNA when compared with that in which ROCK and myosin contraction are not inhibited, would enable a role to be determined of ROCK-mediated cytoskeletal tension.

The increase in number of compact condensations due to hypoxia on the 0.5KPa substrate and transcription of *NCAM*, suggests a mechanism behind the observed hypoxic-induction of *SOX9*. However as with suggested experiments which would directly implicate N-Cadherin and NCAM in hypoxia-induced condensations, it would be required to chemically or genetically manipulate these adhesion proteins to determine their role during downstream chondrogenesis. Furthermore, to enable demonstration of a direct relationship between cell condensation and cartilage differentiation, it may be required to analyse expression of early chondrogenic markers at time points following condensation at day 1. This may enable observation of a downstream, latent effect of cell condensation on chondrogenesis. This requirement for later time point analysis may also apply in order for a relationship to

be determined between chondrogenesis and actin re-arrangement/ROCK activity induction on the soft substrate due to hypoxia.

Results here which investigated the formation of more mature cartilage tissue demonstrate day 21 increases in *SOX9* and *COL2A1* mRNA on the 0.5KPa substrate compared to that on 40KPa as previously described [355, 358]. However, despite the greater effect of hBM-MSC chondrogenesis on the soft substrate at day 1, 21-day cultures exhibit greater chondrogenesis due to hypoxia on the stiff substrate. Hypoxia appeared to increase *COL2A1* transcription on the stiff substrate whilst inducing a reduction of this transcript on the soft surface. This also correlated with that of Collagen Type II protein levels which indicates that this effect of hypoxia is stable enough to induce changes in cartilage ECM composition. An important caveat to this observation is the lack of quantification of collagen type II which would clearly demonstrate this suggested advantage of the stiff substrate in response to hypoxic incubation. Additional observations which were not taken in this study would also more robustly demonstrate the synergistic role of hypoxia and mechanosignalling during chondrogenesis. One such example would be an increase in time points prior to day 21 at which articular chondrogenic gene expression is analysed. This would enable a more detailed examination of gene expression during chondrogenic lineage commitment in response to the combination of soft/stiff substrates with hypoxia. In addition, quantification of collagen type X protein would demonstrate the advantage of this combination for chondrogenesis over methods which do not utilise hypoxia or HIF induction for CTE.

Interestingly, hypoxia only raised levels of *VEFGA* and *EGLN* in cells on the 40KPa substrate only at day 21. This suggests that the signalling pathways stimulated in response to a stiff substrate are conducive for expression of genes which contain a HRE. This contrasts with that on the 0.5KPa surface at day 21 on which transcription of these genes by hypoxia appears to be suppressed. This is also at odds with day 1, at which hypoxia induced increases in *VEGFA* and *EGLN* expression on both substrates. This therefore suggests a change in the crosstalk between the HIF and mechanotransducive pathways from day 1 to day 21 of chondrogenesis which results in differential induction of HIF-mediated transcription and chondrogenesis. An improvement in the experiment design and one which would enable investigation of this phenomenon is the analysis of *VEGFA* and *EGLN* expression between days 1 and 21 of chondrogenesis. This would enable determination of the point at which the soft substrate becomes inhibitory to hypoxia-mediated expression of HRE-containing genes.

The involvement of the mechano-sensing pathways in HIF-mediated transcription was suggested by observations here of Y-27632 inhibiting hypoxia-mediated increases in *COL2A1*, *VEGFA* and *EGLN* mRNA in hBM-MSCs differentiated on TCP. This suggests that ROCK-mediated cytoskeletal tension on the stiff substrate is required for hypoxia-induced chondrogenic gene expression. The caveat to this observation is that TCP is magnitudes greater in stiffness than the 40KPa substrate and does not include the fibronectin-coated surface. It is therefore unable to fully represent the mechanically stiff substrate of 40KPa in terms of its effects on hBM-MSC chondrogenesis.

Taken together, the evidence in this chapter points to the ability of hypoxia to specifically regulate cell morphology, actin dynamics, cell condensation and downstream chondrogenic gene expression in hBM-MSCs. Interestingly, this effect of hypoxia appeared to be dependent on the mechano-sensing pathways stimulated by specific ECM stiffness values. The early induction of a milieu conducive for chondrogenesis on the soft substrate only, appeared to be via a unidirectional mechanism in which hypoxic pathways regulate those involved in sensing of mechanical signals, and not vice-versa. At day 21 however, there was a trend which indicated the dampening of hypoxic signalling in cells cultured on the soft substrate, with increases in hypoxia-mediated chondrogenesis observed on the stiff biomaterial only. This indicates that the pathways induced by hypoxia and those by mechanical stimuli are tightly intertwined with each regulating the activity of the other at different time points throughout chondrogenesis.

The differential effect of hypoxia on soft and stiff substrates throughout chondrogenesis suggests the requirement of a biomaterial system of dynamic stiffness is to be utilised in order to realise the potential of hypoxic signalling in CTE. Guvendiren and Burdick investigated the effect of hydrogels which are able to stiffen over a 14-day time period on the mechanosensing and lineage commitment of hMSCs [303]. In this study, hMSCs exhibited the characteristic features of cells on relative soft substrates with cortical actin arrangement, low cytoskeletal tension and adipogenic cell fate favoured prior to gel stiffening. This contrasted with stress fibre formation, increased cytoskeletal tension and osteogenesis of hMSCs following hydrogel stiffening via increased crosslinking of the free HA methacrylated arms. In addition, Caliari et al demonstrated the ability of UV-mediated stiffening of

methacrylated HA hydrogels to induce a cell response indicative of their culture on a stiff substrate compared to that exhibited on a soft material [563]. Biomaterial systems such as these which are able to stiffen *in situ* may be highly conducive for hypoxia-mediated chondrogenesis throughout the entire chondrogenic period. Such scaffolds would demonstrate the potential for hypoxia and mechano-signalling combinatorial strategies and may provide a proof of concept for their use in cartilage regeneration.

6. Discussion

Taken together, the results outlines in chapters 3, 4 and 5 demonstrate the complexity of regulatory mechanisms which govern hypoxia/HIF signalling and the activity of these pathways during hBM-MSC chondrogenesis. The requirement for lower oxygen concentrations than 5% is suggested due to the inability of this hypoxic level to induce expression of HIF target genes at day 14 of chondrogenesis compared to 2%O_2 which did so at day 1 and day 14 of culture. The literature is suggestive of the effect of differing oxygen concentrations on inducing differential HIF-1α upregulation only at a threshold hypoxic state [396]. This could be hypothesized to be due to a negative feedback loop in which HIF stimulation by milder hypoxic states is overcome by *EGLN* transcription and PHD2-mediated degradation of HIF-1α [411]. This may be investigated by utilising a hBM-MSC line in which HREs are deleted from the promoter of the *EGLN* locus [411]. The hypothesis for such a study would be that stimulation of HIF-mediated gene expression by 5%O_2 would not be subject to dampening by PHD2-mediated negative feedback in these transgenic HRE-deleted cell line compared to that conducted with wild type hBM-MSCs.

The mild induction of HIF by 5%O_2 could be due to factors present uniquely during chondrogenic differentiation. For example, Ascorbate as an essential co-factor for PHD2 which has been shown to reduce HIF-1α compared to basal conditions [430]. This may therefore result in an abolishment of any mild HIF induction by 5%O_2 whereas 2%O_2 is able to overcome this Ascorbate-mediated upregulation of PHD2 activity. TGF-β signalling has been shown to also raise HIF-1α levels in normoxic conditions. Inclusion of TGF-β may therefore raise basal levels of HIF-1α which may

be unable to be induced further by mild hypoxic states at later time points when subject to negative feedback loops.

The effects of both Ascorbate and TGF-β on hypoxic signalling may be investigated by the effects of their supplementation on HIF-1α upregulation and HIF activity in the presence of 5%O_2 and 2%O_2 at later time points in chondrogenesis. The hypothesis in such a study would be: Ascorbate treatment downregulates HIF-1α induction by 5%O_2 and downstream HIF activity, whereas 2%O_2 is able to overcome this. In terms of the effect of TGF-β signalling, treatment with this growth factor would be hypothesized to induce HIF-1α at normoxia and therefore this would be unable to be further induced by 5%O_2 but possible by 2%O_2. Together, the results here combined with that previously described, suggests that hypoxic signalling during BM-MSC chondrogenesis is not able to be easily induced by a mild lack of oxygen. Instead, lower oxygen levels beyond a specific threshold may be required for stimulation of HIF in chondrogenically-induced BM-MSCs.

The experiments conducted in the second chapter of this thesis investigated the effects of varying the bio-availability of a single PHD2/FIH substrate- oxygen, on downstream HIF activity. However, results in the second chapter instead demonstrate the effect of reducing the bio-availability of different PHD2/FIH co-factors on HIF-mediated gene expression, namely 2-OG and Fe^{2+}. DMOG, a 2-OG analogue has a greater effect on HIF target gene expression than that induced by either chelating or competing with Fe^{2+} using DFX or $CoCl_2$ respectively. These results therefore suggest that HIF regulation during BM-MSC chondrogenesis is subject to

mechanisms which are dependent more on 2-OG than those controlled by intracellular Fe^{2+} levels.

The relative roles of 2-OG and Fe^{2+} in HIF regulation could be investigated by examining the effect of 2-OG and Fe^{2+} supplementation on HIF-1α upregulation and HIF-mediated transcription during chondrogenesis. The hypothesis for such an investigation would be as follows: 2-OG supplementation more potently inhibits hypoxic induction of HIF compared to that induced by Fe^{2+} during BM-MSC chondrogenesis. Alternatively, inhibitors other than DMOG, DFX or $CoCl_2$ which either reduce 2-OG or Fe^{2+} bioavailability may be utilised. Such compounds include N-Oxaloylglycine (NOG), another 2-OG derivative and Ciclopirox Olamine (CPX), an iron chelator [564]. Observations of the effect of NOG and CPX on HIF-mediated transcription may enable confirmation or rejection of the hypothesis that the effects of DMOG, DFX and $CoCl_2$ in this study are not specific to these compounds but rather are representative of the effect of reducing 2-OG or Fe^{2+} availability. Results from such a study would uncover key regulatory elements of HIF during chondrogenesis.

The mechanisms of these 2-OG-dependant processes which regulate HIF are suggested by the literature. For example, DMOG has been shown to inhibit both FIH and PHD2-mediated hydroxylation of HIF-1α compared to inhibition of PHD2 alone due to DFX or $CoCl_2$ treatment [453]. This mechanism of action of DMOG may mediate its potent HIF-stimulation observed in the present study and is suggested due to observation that siRNA knockdown of FIH and PHD2 compared to PHD2 only, enhances HIF-mediated transcription [451]. Therefore it is a necessity to build on observations here to investigate if indeed, FIH and PHD2 inhibition mediates the

effect of DMOG in stimulating HIF-dependent transcription during cartilage development compared to that induced by DFX or $CoCl_2$. Such studies would be key in elucidating regulatory mechanisms of a pathway which are essential for chondrogenesis. It would also provide information of the specific chemical inhibition required for constitutive HIF stimulation throughout chondrogenic induction of hBM-MSCs. An initial requirement for such a study would be to identify if DMOG, compared to the effect of DFX or $CoCl_2$, inhibits both FIH and PHD2 and their respective hydroxylating functions of asparagine and proline residues of HIF-1α. It is possible to identify such post-translational modifications by the use of antibodies which are specific for hydroxylated asparagine and proline residues [453].

Following confirmation that DMOG inhibits both these hydroxylases compared to that due to DFX or $CoCl_2$, it would be required to investigate if this mechanism is responsible for the potent pro-chondrogenic effect of DMOG. This may be achieved by PHD and FIH overexpression [565, 566] in chondrogenically-induced BM-MSCs. The hypothesis for such a study would be as follows: Overexpression of both PHD2 and FIH reduces DMOG-induced HIF activity and BM-MSC chondrogenesis compared to that in which either hydroxylase alone, or neither, is overexpressed.

Chapters 3 and 4 suggest the differential effects of varying hypoxic states and bioavailability of different PHD2/FIH substrates on HIF signalling. In addition, hypoxic signalling that is conducive for chondrogenesis may also be subject to regulation by pathways which are stimulated in response to changes in ECM stiffness. In the present study, at an early stage of chondrogenesis, hypoxia induced expression of genes required for early chondrogenic induction including *SOX9* and *NCAM* in hBM-

MSCs cultured on mechanically soft substrates. This is in comparison to a lack of effect of hypoxia on stiffer substrates. These observations suggest that pathways stimulated in response to a relative low ECM mechanical stiffness, are conducive for hypoxia-induced chondrogenic gene expression. This is in contrast to that which occurs of hBM-MSCS on a stiff substrate in which hypoxia-mediated induction of chondrogenic gene expression is suppressed. As described previously, cells in which a cortical actin arrangement is exhibited, express higher levels of chondrogenic markers compared to cells in which a spread actin network and long stress fibres are observed [354]. Previous evidence in the literature suggests that ROCK-mediated responses to changes in ECM stiffness are required for this chondrogenic bias in cells of a rounded morphology [355]. This suggests the significance of findings in the present study, specifically the correlation on the soft substrate, between chondrogenic gene expression, ROCK activity and cytoskeletal rearrangement in hypoxic conditions.

The observations on the soft substrate in hypoxic conditions, prompt further experiments to investigate the role of ROCK-mediated actin re-arrangement during hypoxia-induced chondrogenesis. This aim may be addressed through the use of inhibitors of both ROCK and myosin contraction (Y-27632 and Blebbistatin respectively). Observation of changes in hypoxia-induced cartilage mRNA and protein due to Y-27632 and Blebbistatin, would enable a role to be determined of ROCK-mediated cytoskeletal tension during chondrogenesis in low-oxygen conditions. The findings of such experiments would be relevant for studies of cartilage development and tissue morphogenesis in which mechanotransduction and hypoxic pathways play key roles throughout. Functions of these pathways have been demonstrated from

the early mesenchymal limb bud stage, through to adult articular cartilage homeostasis [259, 262].

Observation that hypoxia induces formation of compact colonies and mRNA expression of *NCAM* is suggestive of another mechanism by which this oxygen state is conducive for chondrogenesis. NCAM plays a role in maintaining cell-cell adhesion in the mesenchyme of the limb bud following initiation of these adhesions by N-Cadherin [61]. Therefore, experiments which enable investigation of the role of hypoxia-induced *NCAM* expression during chondrogenesis of hBM-MSCs, would be informative of similar mechanisms which occur in the limb bud during cartilage development [567]. Such an experiment may involve siRNA knockdown of NCAM in hBM-MSCs which would enable observation of the role of NCAM in both condensation of these cultures and downstream chondrogenesis when compared to cells in which NCAM expression is not abolished [568].

Perhaps most importantly, this study informs strategies for cartilage tissue engineering and are suggestive of advantageous technologies for repair of acute chondral defects. The results from chapter 3 are suggestive of a role for either severe or mild hypoxia in inducing HIF-stabilisation and changes in Collagen Type II and X production during BM-MSC chondrogenesis. However, the potential disadvantages of physiological hypoxia include the induction of UPR and global inhibition of translation, both of which are inhibitory to stem cell differentiation. In addition, logistical issues may accompany incorporation of sub-atmospheric oxygen levels into biomaterial scaffolds for delivery into the patient injury site. Therefore, compounds which mimic hypoxia in terms of HIF stimulation may offer advantages compared to

CTE strategies in which only growth factors are used to promote chondrogenesis and which often result in hypertrophy and mineralisation of *de novo* tissue.

Results in chapter 4 indicate the ability of DMOG for stable HIF stimulation and hBM-MSC chondrogenesis. This demonstrates the potential for competitive 2-OG inhibitors in CTE. Incorporation of DMOG into a scaffold was demonstrated by Min et al for the purpose of increased angiogenesis in bone critical defects in a rat model [569]. These authors observed the sustained release of DMOG from 3D-printed polymer scaffolds over a 28-day period and demonstrated the ability of DMOG release in this manner to induce transcription of HIF target genes both at day 1 and 14 of hBM-MSC culture.

The potent HIF-mediated chondrogenic gene expression that was induced by DMOG however, was offset with the detrimental effect on Collagen Type II in the ECM of differentiated BM-MSCs. This was alleviated with treated of DMOG for the final third of the differentiating period, which also maintained expression of genes conducive for chondrogenesis. In order to address the requirement for late DMOG treatment in CTE, delayed-release scaffolds such as demonstrated by Jaklenec et al may be employed. These authors demonstrated the release of IGF-1 from PLGA scaffolds only between days 7 and 14, with no IGF-1 released prior to this time point [570]. As an alternative to DMOG, completion of suggested further experiments which examine the mechanism of action of this 2-OG analogue during chondrogenesis (e.g. FIH and PHD inhibition as opposed to PHD2 ablation alone), may highlight the usefulness of more specific inhibitors whose continuous treatment does not abolish collagen type II.

The results in chapter 5 suggest a crosstalk between the hypoxic pathways and those activated in response to changes in mechanical stiffness. Hypoxia-induced expression of chondrogenic markers, ROCK activation and cytoskeletal arrangement shown to be conducive for chondrogenesis were only stimulated in hBM-MSCs differentiated on a soft substrate. Therefore, it may be critical to ensure that DMOG/HIF stimulating compounds are incorporated into biomaterial scaffolds of a relatively low stiffness in which actin adopts a cortical arrangement. This combinatorial induction of hypoxic pathways and those activated in response to a soft microenvironment may offer greater levels of chondrogenesis compared to that in which either set of pathways are enhanced alone.

In order for robust conclusions to be made based on observations here and the described interpretations, the major experimental limitations of this study must be identified and addressed. The specifics of these have already been described in the discussion sections of each chapter, but one of the aims of this chapter is to summarise the caveats of the study presented here. One limitation of this study and one which may have omitted observations of key hypoxia-induced effects on chondrogenesis, are the time points chosen for analysis of gene expression. Evidence here suggests correlation between expression of specific gene products, such as *SOX9* with its target, *COL2A1* or *RUNX2* with that of *COL10A1.* However in order to validate these correlations, It would be a requirement to utilise more frequent time points throughout chondrogenesis. To confirm the role of a transcription factor in mediating the chondrogenic effect of hypoxia/a HIF-stimulating compound, genetic manipulation of these would need to be undertaken.

In addition to re-evaluation of time points at which samples are harvested during chondrogenesis, the number of genes chosen to denote a specific cellular process may need to be expanded. For example, HIF activity or early chondrogenic induction in this study have been delineated with expression of genes which represent only a subset of loci that are transcriptionally-active during these processes. By selecting a broader range of genes, the induction of these cellular processes will be more clearly demonstrated if they exist. This would also be enabled by quantification of specific proteins as oppose to a reliance placed solely on gene expression analysis. For example, quantification of HIF-1α or ECM proteins would enable the respective processes of HIF stabilisation and articular chondrocyte function to be more robustly assessed.

Another limitation to this study is represented by the nature of BM-MSCs. The adherence in this study to the ISCT criteria for BM-MSC characterisation, may negate sub-populations of cells which are adherent and capable of adipogenic, chondrogenic and osteogenic lineage commitment. This is due to observation by others of BM-MSC-like characteristics exhibited by cells sorted by markers such as Stro-1 and CD271 [170, 571] which were not used here. This lack of uniformity within the BM-MSC field in terms of the markers which define BM-MSCs, may suggest that the observations here are not representative of a true BM-MSC population. Such a population which would be viable for CTE or study of mesenchymal development, may consist of subgroups of cells defined by different subsets of markers. This represents a limitation of this study as each of these subgroups may exhibit different responses to hypoxic incubation and subsequent chondrogenesis.

Finally, the use of BM-MSCs from a single donor also represents a limitation of this study. This is due to the differential phenotype of BM-MSCs isolated from young/old patients, male/female or OA patients for example, and their potential differential response to hypoxia-mediated chondrogenic induction [572]. This is particularly important due to the requirement for harvesting autologous BM-MSCs for repair of chondral defects or for treatment of cartilage-related diseases. By discounting the effect of the experimental conditions used here on BM-MSCs derived from differing population groups such as age or sex, we may also omit key differences in their chondrogenic ability due to hypoxia.

7. Conclusions

The purpose of the research presented here was to investigate the potential role of hypoxia and its downstream signalling factor, HIF in CTE strategies for repair of acute chondral defects. The data here demonstrates, in the broadest sense, the complexity with which HIF/hypoxic signalling is regulated during chondrogenesis. By understanding this complexity, it may be possible to develop technologies which enable greater levels of HIF stimulation and downstream chondrogenesis. For example, it is important to understand the type of chemical inhibition required to achieve maximal HIF-mediated transcription, in addition to the mechanical environment that is conducive for HIF-mediated signalling.

Additionally, this study provides evidence for the multitude of effects of hypoxia which are beneficial for articular cartilage, be it chondrogenic induction of stem cells, collagen maturation, or inhibition of hypertrophy. Such insights may not only improve stem cell chondrogenesis in CTE, but may also inform the development of other cartilage-related treatments. For example, stimulation of ECM formation by articular chondrocytes may improve ACI/MACI-based strategies. Alternatively, work such as that presented here provide insights into HIF-related therapies for treatment of diseases such as OA in which cartilage is remodeled and degenerated. Finally, by taking the studies here forward and dissecting the mechanisms behind HIF-mediated chondrogenesis, it may be possible to further refine therapeutic strategies for damaged cartilage. This may be via stimulation of specific HIF-mediated effects, as opposed to induction of the entire complement of HIF's transcriptional targets.

8. Appendix

Plate (#wells)	Area/Well (cm^2)	[cell suspension] (cells/ml)	Volume pipetted into each well (ml)	Total number of cells/well	Final seeding density (cells/cm^2)
96	0.34	$5.1x10^4$	0.2	$1.02x10^4$	$3.0x10^4$
24	2	$6.0x10^4$	1.0	$6.0x10^4$	$3.0x10^4$
12	3.8	$5.7x10^4$	2.0	$1.146.0x10^5$	$3.0x10^4$
6	9	$9.0x10^4$	3.0	$2.706.0x10^5$	$3.0x10^4$

Appendix figure 1. Concentrations of cell suspensions made from master stock prior to seeding into well of each size to achieve final cell densities of $3.0x10^4$.

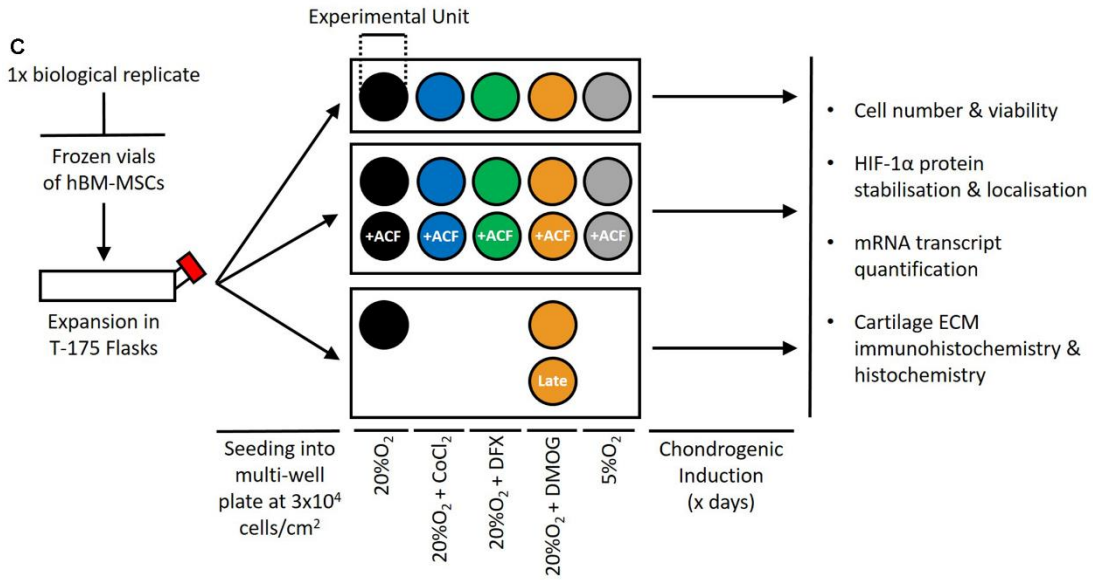

Appendix figure 2. Workflow detailing chondrogenic differentiation experiments.

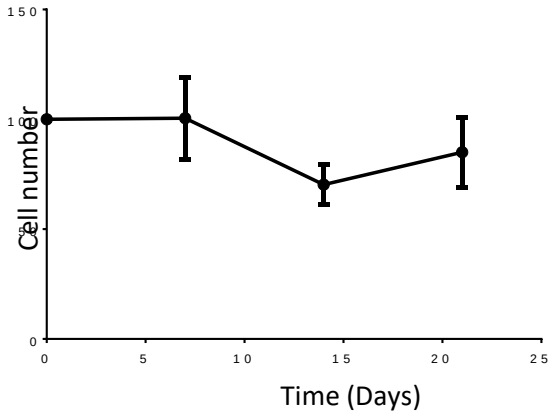

Appendix figure 3. Cell number throughout chondrogenesis in control conditions, utilising the PicoGreen Assay. Values plotted represent the mean from 3 independent experiments and are a percentage of the cell number at day 0. Error bars show the standard error of the mean.

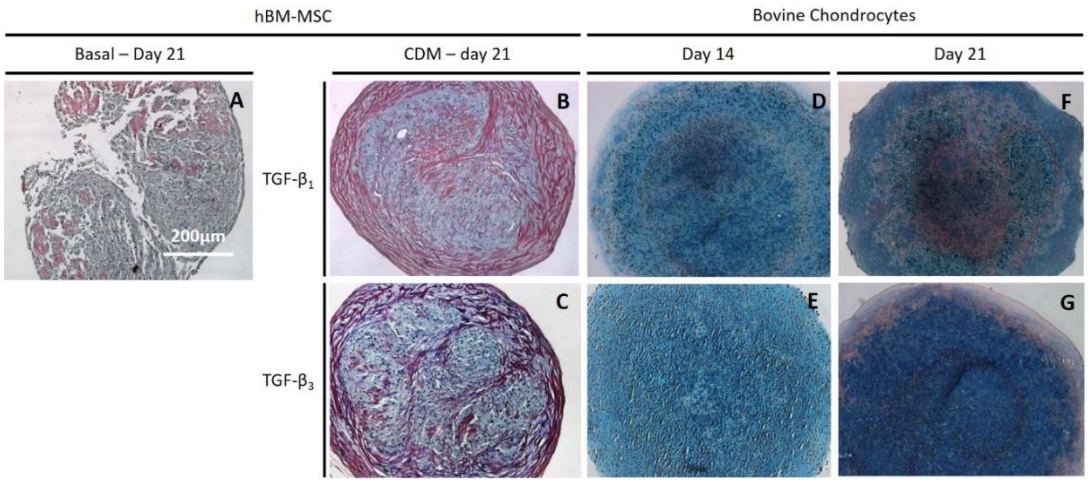

Appendix figure 4. Comparison of TGF-β_1 and TGF-β_3 for inducing presence of GAGs in ECM. Alcian Blue, Picosirius Red and Haemotoxylin staining of hBM-MSCs and Bovine Chondrocyte pellets in presence of TGF-β_1/TGF-β_3-containing chondrogenic media. A+B: hBM-MSCs at day 21 of culture in expansion conditions. C+D: hBM-MSCs at day 21 of chondrogenic induction in presence of TGF-β_1 (C) and TGF-β_3 (D). E+F: Bovine chondrocyte cultures at day 14 of culture in chondrogenic media consisting of TGF-β_1 (E) and TGF-β_3 (F). G+H: Bovine chondrocyte cultures at day 21 of culture in chondrogenic media consisting of TGF-β_1 (G) and TGF-β_3 (H).

Chemical processing of cell pellets for wax embedding	
Solution	**Treatment time**
70% (v/v) IMS	15 minutes
90% (v/v) IMS	15 minutes
100% (v/v) IMS	15 minutes
100% (v/v) IMS	15 minutes
100% (v/v) IMS	15 minutes
100% (v/v) IMS	15 minutes
Xylene	15 minutes
Xylene	15 minutes
Xylene	15 minutes
Ultraplast Wax	15 minutes
Ultraplast Wax	15 minutes
Ultraplast Wax	15 minutes

Appendix figure 5. Histological processing of hBM-MSC and bovine chondrocyte pellets.

Solution	Treatment time
Histoclear	2 x 10 minutes
100% (v/v) IMS	2 minutes
90% (v/v) IMS	2 minutes
70% (v/v) IMS	2 minutes
50% (v/v) IMS	2 minutes
Deionised water	2 minutes
Alcian Blue pH 1	10 minutes
Drain and blot dry	
Deionised water	Quick rinse
Ehrlich's Haematoxylin	2 minutes
Running water	10 minutes
Deionised water	Quick rinse
Phosphomolybdic acid (2.5% (v/v))	10 minutes
Deionised water	Quick rinse
Sirius Red F3B (0.5% (w/v) in saturated picric acid)	1 hour
Acetic acid 0.5% (v/v)	2x Quick rinse
Drain and blot dry	
100% IMS	3 x 5 minutes
Histoclear	2 x 5 minutes

Appendix figure 6. Alcian Blue, Picosirius Red and Haemotoxylin staining protocol of hBM-MSC and bovine chondrocyte pellets

A

No. Cycles	Cycle Duration	Temperature
1	3 mins	95°C
39	5 secs	95°C
	10 secs	60°C

B

Gene of Interest	Forward Primer Sequence	Reverse Primer Sequence	Concentration (nM)
VEGFA	AGGGCAGAATCATCACGAAGT	AGGGTCTCGATTGGATGGCA	250
PGK1	TGGACGTTAAAGGGAAGCGG	GCTCATAAGGACTACCGACTTGG	250
EGLN	AGGCGATAAGATCACCTGGAT	TTCGTCCGGCCATTGATTTTG	250
SOX9	AGCGAACGCACATCAAGAC	CTGTAGGCGATCTGTTGGGG	250
COL2A1	CCAGATGACCTTCCTACGCC	TTCAGGGCAGTGTACGTGAAC	500
ACAN	GTGCCTATCAGGACAAGGTCT	GATGCCTTTCACCACGACTTC	500
RUNX2	TGGTTACTGTCATGGCGGGTA	TCTCAGATCGTTGAACCTTGCTA	250
COL10A1	GGGGCTAAGGGTGAAAGGG	GGTCCTCCAACTCCAGGATCA	250
MMP13	ACTGAGAGGCTCCGAGAAATG	GAACCCCGCATCTTGGCTT	500
P4HA1	AGTACAGCGACAAAAGATCCAG	CTCCAACTCACTCCACTCAGTA	250
LOX	CGGCGGAGGAAAACTGTCT	TCGGCTGGGTAAGAAATCTGA	250
DKK1	ATAGCACCTTGGATGGGTATTCC	CTGATGACCGGAGACAAACAG	250
GREM1	CGGAGCGCAAATACCTGAAG	GGTTGATGATGGTGCGACTGT	250
IHH	AGACCGCGACCGCAATAAG	GCCTTTGACTCGTAATACACCCA	250
PTHRP	AAGGTGGAGACGTACAAAGAGC	CAGAGCGAGTTCGCCGTTT	250
LEF1	TGCCAAATATGAATAACGACCCA	GAGAAAAGTGCTCGTCACTGT	500
AXIN2	AGCCAAAGCGATCTACAAAAGG	AAGTCAAAAACATCTGGTAGGCA	500
RHOA	AGCCTGTGGAAAGACATGCTT	TCAAACACTGTGGGCACATAC	500
ROCK1	AACATGCTGCTGGATAAATCTGG	TGTATCACATCGTACCATGCCT	250
ROCK2	TCAGAGGTCTACAGATGAAGGC	CCAGGGGCTATTGGCAAAGG	500
CTGF	AAAAGTGCATCCGTACTCCCA	CCGTCGGTACATACTCCACAG	500
ANKRD1	GCCTACGTTTCTGAAGGCTG	GTGGATTCAAGCATATCACGGAA	250
PRX1	TGATGCTTTTGTGCGAGAAGA	AGGGAAGCGTTTTTATTGGCT	500
MSX1	CTCCGCAAACACAAGACGAAC	CACATGGGCCGTGTAGAGTC	250
NCAD	TCAGGCGTCTGTAGAGGCTT	ATGCACATCCTTCGATAAGACTG	250
NCAM	GGCATTTACAAGTGTGTGGTTAC	TTGGCGCATTCTTGAACATGA	500
RPL13A	GCCATCGTGGCTAAACAGGTA	GTTGGTGTTCATCCGCTTGC	250

Appendix figure 7. qPCR reaction conditions and primer sequences. A: qPCR reaction conditions. B: Primer sequences used to amplify the respective genes of interest.

A

Target Protein	Antibody	Species	Dilution	Detection Ab/Method
HIF-1α	h206 (Santa Cruz)	Rabbit	1:100	ab150077
Collagen Type II	ab34712 (Abcam)	Rabbit	1:200	ab150077
Collagen Type X	ab49945 (Abcam)	Mouse	1:250	Strep/Biotin
YAP	sc101199 (Santa Cruz)	Mouse	1:100	Strep/Biotin
pMLC2	3671S [573]	Rabbit	1:100	ab150077

B

1° Antibody Target	Culture substrate	Dilution
HIF-1α	TCP	1:200
Collagen Type II	TCP	1:1000
Collagen Type II	PA Gels	1:500
pMLC2	PA Gels	1:500

Appendix figure 8. Primary and secondary antibody details. A: Primary antibodies. B: α-Rabbit secondary antibody (ab150077) dilutions for conjugation to each primary antibody for detection of hBM-MSC proteins cultured on either TCP or PA gels.

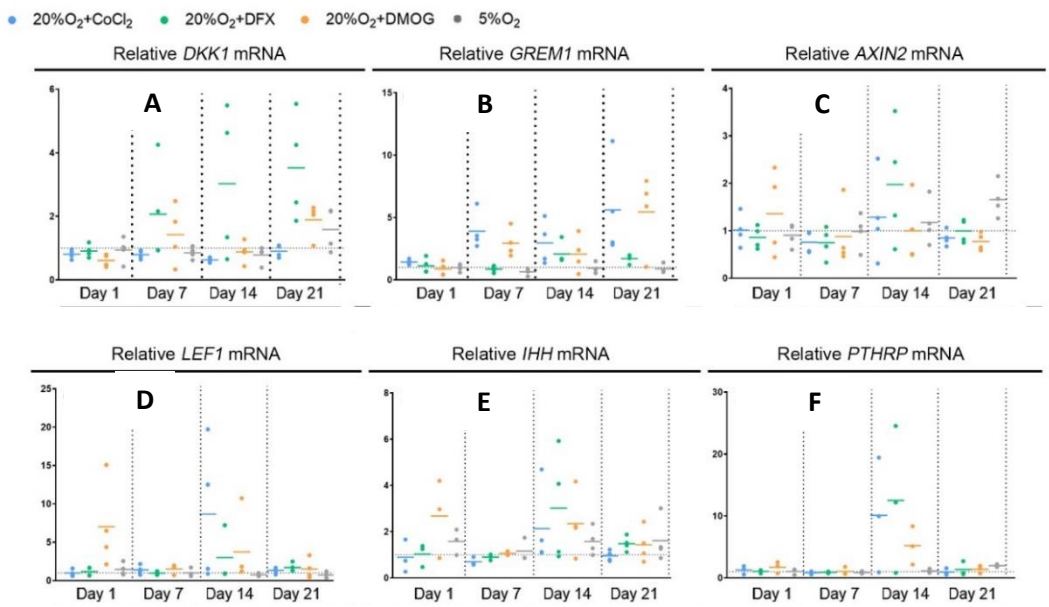

Appendix Figure 9. During BM-MSC chondrogenesis, CoCl2, DFX and DMOG induce changes in the mRNA of genes whose products are involved in the Bone Morphogenetic Protein, Wnt and Indian Hedgehog signalling pathways. mRNA expression of *DKK1* (A), *GREM1* (B), *AXIN2* (C), *LEF1* (D), *IHH* (E) and *PTHRP* (F) throughout chondrogenesis. Values plotted are from 4 independent experiments and are fold change compared to the untreated control which is represented by the horizontal dotted line. The solid coloured lines representing the mean for each condition.

A

Acrylamide (µl)	Bis acrylamide (µl)	PBS (µl)	APS (µl)	TEMED (µl)	E (kPa)
75	30	895	10	1	0.5
200	240	560	10	1	40

B

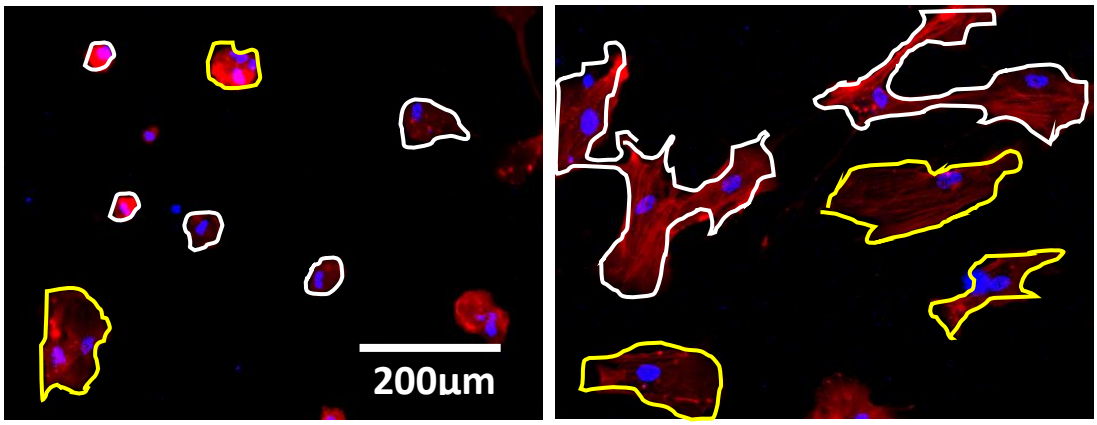

Appendix figure 10. A: Volume of reagents used for synthesis of PA gels. B: Classification of colonies and single cells on PA gels. Single cells are outlined in white and colonies outlined in yellow.

8. Bibliography

1. Krych, A.J., et al., *Activity levels are higher after osteochondral autograft transfer mosaicplasty than after microfracture for articular cartilage defects of the knee: a retrospective comparative study.* J Bone Joint Surg Am, 2012. **94**(11): p. 971-8.
2. Bhosale, A.M. and J.B. Richardson, *Articular cartilage: structure, injuries and review of management.* Br Med Bull, 2008. **87**: p. 77-95.
3. Sophia Fox, A.J., A. Bedi, and S.A. Rodeo, *The Basic Science of Articular Cartilage: Structure, Composition, and Function.* Sports Health, 2009. **1**(6): p. 461-8.
4. Akizuki, S., et al., *Tensile properties of human knee joint cartilage: I. Influence of ionic conditions, weight bearing, and fibrillation on the tensile modulus.* J Orthop Res, 1986. **4**(4): p. 379-92.
5. Wu, J.P., T.B. Kirk, and M.H. Zheng, *Study of the collagen structure in the superficial zone and physiological state of articular cartilage using a 3D confocal imaging technique.* J Orthop Surg, 2008. **3**: p. 29.
6. Aydelotte, M.B. and K.E. Kuettner, *Differences between sub-populations of cultured bovine articular chondrocytes. I. Morphology and cartilage matrix production.* Connect Tissue Res, 1988. **18**(3): p. 205-22.
7. Shepherd, D.E.T. and B.B. Seedhom, *Thickness of human articular cartilage in joints of the lower limb.* Annals of the Rheumatic Diseases, 1999. **58**(1): p. 27-34.
8. Kuettner, K.E. and A.A. Cole, *Cartilage degeneration in different human joints.* Osteoarthritis and Cartilage, 2005. **13**(2): p. 93-103.
9. Eger, W., et al., *Human knee and ankle cartilage explants: catabolic differences.* Journal of Orthopaedic Research, 2002. **20**(3): p. 526-534.
10. Goldring, M.B., *Update on the biology of the chondrocyte and new approaches to treating cartilage diseases.* Best Practice & Research Clinical Rheumatology, 2006. **20**(5): p. 1003-1025.
11. Hallmann, R., et al., *Regression of blood vessels precedes cartilage differentiation during chick limb development.* Differentiation, 1987. **34**(2): p. 98-105.
12. Calamia, V., et al., *Secretome analysis of chondroitin sulfate-treated chondrocytes reveals anti-angiogenic, anti-inflammatory and anti-catabolic properties.* Arthritis Res Ther, 2012. **14**(5): p. R202.
13. Hiraki, Y., et al., *Identification of chondromodulin I as a novel endothelial cell growth inhibitor. Purification and its localization in the avascular zone of epiphyseal cartilage.* J Biol Chem, 1997. **272**(51): p. 32419-26.
14. Zhang, X., R. Crawford, and Y. Xiao, *Anti-angiogenic factors are essential regulators in cartilage homeostasis and osteoarthritis.* Osteoarthritis and Cartilage. **22**: p. S132.
15. Zhang, X., et al., *Chondromodulin-1 ameliorates osteoarthritis progression by inhibiting HIF-2α activity.* Osteoarthritis and Cartilage, 2016. **24**(11): p. 1970-1980.
16. Verzijl, N., et al., *Effect of collagen turnover on the accumulation of advanced glycation end products.* J Biol Chem, 2000. **275**(50): p. 39027-31.
17. Maroudas, A., et al., *Aggrecan turnover in human articular cartilage: use of aspartic acid racemization as a marker of molecular age.* Arch Biochem Biophys, 1998. **350**(1): p. 61-71.
18. Vaughan-Thomas, A., et al., *Characterization of type XI collagen-glycosaminoglycan interactions.* J Biol Chem, 2001. **276**(7): p. 5303-9.
19. Kim, H.J. and T. Kirsch, *Collagen/Annexin V Interactions Regulate Chondrocyte.* J Biol Chem, 2008. **283**(16): p. 10310-7.
20. Makris, E.A., et al., *Repair and tissue engineering techniques for articular cartilage.* Nat Rev Rheumatol, 2015. **11**(1): p. 21-34.

21. Tiller, G.E., et al., *Dominant mutations in the type II collagen gene, COL2A1, produce spondyloepimetaphyseal dysplasia, Strudwick type.* Nat Genet, 1995. **11**(1): p. 87-9.
22. Ryan, M.C. and L.J. Sandell, *Differential expression of a cysteine-rich domain in the amino-terminal propeptide of type II (cartilage) procollagen by alternative splicing of mRNA.* J Biol Chem, 1990. **265**(18): p. 10334-9.
23. McAlinden, A., et al., *Alternative splicing of type II procollagen exon 2 is regulated by the combination of a weak 5' splice site and an adjacent intronic stem-loop cis element.* J Biol Chem, 2005. **280**(38): p. 32700-11.
24. Hyttinen, M.M., et al., *Inactivation of one allele of the type II collagen gene alters the collagen network in murine articular cartilage and makes cartilage softer.* Ann Rheum Dis, 2001. **60**(3): p. 262-8.
25. Gelse, K., E. Poschl, and T. Aigner, *Collagens--structure, function, and biosynthesis.* Adv Drug Deliv Rev, 2003. **55**(12): p. 1531-46.
26. Weis, M.A., et al., *Location of 3-Hydroxyproline Residues in Collagen Types I, II, III, and V/XI Implies a Role in Fibril Supramolecular Assembly.* J Biol Chem, 2010. **285**(4): p. 2580-90.
27. Notbohm, H., et al., *Recombinant human type II collagens with low and high levels of hydroxylysine and its glycosylated forms show marked differences in fibrillogenesis in vitro.* J Biol Chem, 1999. **274**(13): p. 8988-92.
28. Bergholt, M.S., et al., *Raman Spectroscopy Reveals New Insights into the Zonal Organization of Native and Tissue-Engineered Articular Cartilage.* ACS Central Science, 2016. **2**(12): p. 885-895.
29. Eyre, D.R. and J.J. Wu, *Collagen structure and cartilage matrix integrity.* J Rheumatol Suppl, 1995. **43**: p. 82-5.
30. Cao, L., et al., *beta-Integrin-collagen interaction reduces chondrocyte apoptosis.* Matrix Biol, 1999. **18**(4): p. 343-55.
31. Chang, D.P., et al., *Interaction of lubricin with type II collagen surfaces: Adsorption, friction, and normal forces.* Journal of Biomechanics, 2014. **47**(3): p. 659-666.
32. Waller, K.A., et al., *Role of lubricin and boundary lubrication in the prevention of chondrocyte apoptosis.* Proc Natl Acad Sci U S A, 2013. **110**(15): p. 5852-7.
33. Kiani, C., et al., *Structure and function of aggrecan.* Cell Res, 2002. **12**(1): p. 19-32.
34. Stattin, E.-L., et al., *A Missense Mutation in the Aggrecan C-type Lectin Domain Disrupts Extracellular Matrix Interactions and Causes Dominant Familial Osteochondritis Dissecans.* The American Journal of Human Genetics, 2010. **86**(2): p. 126-137.
35. Roughley, P.J. and J.S. Mort, *The role of aggrecan in normal and osteoarthritic cartilage.* J Exp Orthop, 2014. **1**.
36. Mow, V.C., et al., *The influence of link protein stabilization on the viscometric properties of proteoglycan aggregate solutions.* Biochim Biophys Acta, 1989. **992**(2): p. 201-8.
37. Mackie, E.J., L. Tatarczuch, and M. Mirams, *The skeleton: a multi-functional complex organ: the growth plate chondrocyte and endochondral ossification.* J Endocrinol, 2011. **211**(2): p. 109-21.
38. Long, F. and T.F. Linsenmayer, *Regulation of growth region cartilage proliferation and differentiation by perichondrium.* Development, 1998. **125**(6): p. 1067-73.
39. Minguillon, C., et al., *Hox genes regulate the onset of Tbx5 expression in the forelimb.* Development, 2012. **139**(17): p. 3180-8.
40. Naiche, L.A. and V.E. Papaioannou, *Loss of Tbx4 blocks hindlimb development and affects vascularization and fusion of the allantois.* Development, 2003. **130**(12): p. 2681-93.

41. Agarwal, P., et al., *Tbx5 is essential for forelimb bud initiation following patterning of the limb field in the mouse embryo.* Development, 2003. **130**(3): p. 623-33.
42. Ohuchi, H., et al., *The mesenchymal factor, FGF10, initiates and maintains the outgrowth of the chick limb bud through interaction with FGF8, an apical ectodermal factor.* Development, 1997. **124**(11): p. 2235-44.
43. Sun, X., F.V. Mariani, and G.R. Martin, *Functions of FGF signalling from the apical ectodermal ridge in limb development.* Nature, 2002. **418**(6897): p. 501-8.
44. Nguyen, L.K., et al., *A dynamic model of the hypoxia-inducible factor 1alpha (HIF-1alpha) network.* J Cell Sci, 2013. **126**(Pt 6): p. 1454-63.
45. Riddle, R.D., et al., *Sonic hedgehog mediates the polarizing activity of the ZPA.* Cell, 1993. **75**(7): p. 1401-16.
46. Fernandez-Teran, M., M.A. Ros, and F.V. Mariani, *Evidence that the limb bud ectoderm is required for survival of the underlying mesoderm.* Dev Biol, 2013. **381**(2): p. 341-52.
47. Moon, A.M. and M.R. Capecchi, *Fgf8 is required for outgrowth and patterning of the limbs.* Nat Genet, 2000. **26**(4): p. 455-9.
48. Koshiba, K., et al., *Expression of Msx genes in regenerating and developing limbs of axolotl.* J Exp Zool, 1998. **282**(6): p. 703-14.
49. Peterson, R.E., S. Hoffman, and M.J. Kern, *Opposing roles of two isoforms of the Prx1 homeobox gene in chondrogenesis.* Dev Dyn, 2005. **233**(3): p. 811-21.
50. Goldring, M.B., *Chondrogenesis, chondrocyte differentiation, and articular cartilage metabolism in health and osteoarthritis.* Ther Adv Musculoskelet Dis, 2012. **4**(4): p. 269-85.
51. Akiyama, H., et al., *Osteo-chondroprogenitor cells are derived from Sox9 expressing precursors.* Proc Natl Acad Sci U S A, 2005. **102**(41): p. 14665-70.
52. Zhou, G., et al., *Dominance of SOX9 function over RUNX2 during skeletogenesis.* Proc Natl Acad Sci U S A, 2006. **103**(50): p. 19004-9.
53. Leung, V.Y., et al., *SOX9 governs differentiation stage-specific gene expression in growth plate chondrocytes via direct concomitant transactivation and repression.* PLoS Genet, 2011. **7**(11): p. e1002356.
54. Lefebvre, V., R.R. Behringer, and B. de Crombrugghe, *L-Sox5, Sox6 and Sox9 control essential steps of the chondrocyte differentiation pathway.* Osteoarthritis Cartilage, 2001. **9 Suppl A**: p. S69-75.
55. Lefebvre, V., P. Li, and B. de Crombrugghe, *A new long form of Sox5 (L-Sox5), Sox6 and Sox9 are coexpressed in chondrogenesis and cooperatively activate the type II collagen gene.* Embo j, 1998. **17**(19): p. 5718-33.
56. Han, Y. and V. Lefebvre, *L-Sox5 and Sox6 drive expression of the aggrecan gene in cartilage by securing binding of Sox9 to a far-upstream enhancer.* Mol Cell Biol, 2008. **28**(16): p. 4999-5013.
57. LeClair, E.E., L. Bonfiglio, and R.S. Tuan, *Expression of the paired-box genes Pax-1 and Pax-9 in limb skeleton development.* Dev Dyn, 1999. **214**(2): p. 101-15.
58. Rodrigo, I., et al., *Pax1 and Pax9 activate Bapx1 to induce chondrogenic differentiation in the sclerotome.* Development, 2003. **130**(3): p. 473-82.
59. Kawato, Y., et al., *Nkx3.2 promotes primary chondrogenic differentiation by upregulating Col2a1 transcription.* PLoS One, 2012. **7**(4): p. e34703.
60. Jeong, D.U., J.Y. Choi, and D.W. Kim, *Cartilage-Specific and Cre-Dependent Nkx3.2 Overexpression In Vivo Causes Skeletal Dwarfism by Delaying Cartilage Hypertrophy.* J Cell Physiol, 2017. **232**(1): p. 78-90.
61. Tavella, S., et al., *N-CAM and N-cadherin expression during in vitro chondrogenesis.* Exp Cell Res, 1994. **215**(2): p. 354-62.

62. Oberlender, S.A. and R.S. Tuan, *Expression and functional involvement of N-cadherin in embryonic limb chondrogenesis.* Development, 1994. **120**(1): p. 177-187.
63. Vega, S.L., et al., *Single Cell Imaging to Probe Mesenchymal Stem Cell N-Cadherin Mediated Signaling within Hydrogels.* Annals of Biomedical Engineering, 2016. **44**(6): p. 1921-1930.
64. Behrens, J., et al., *Functional interaction of an axin homolog, conductin, with beta-catenin, APC, and GSK3beta.* Science, 1998. **280**(5363): p. 596-9.
65. Fischer, L., G. Boland, and R.S. Tuan, *Wnt signaling during BMP-2 stimulation of mesenchymal chondrogenesis.* J Cell Biochem, 2002. **84**(4): p. 816-31.
66. Day, T.F., et al., *Wnt/beta-catenin signaling in mesenchymal progenitors controls osteoblast and chondrocyte differentiation during vertebrate skeletogenesis.* Dev Cell, 2005. **8**(5): p. 739-50.
67. Akiyama, H., et al., *Interactions between Sox9 and β-catenin control chondrocyte differentiation.* Genes Dev, 2004. **18**(9): p. 1072-87.
68. Haas, A.R. and R.S. Tuan, *Chondrogenic differentiation of murine C3H10T1/2 multipotential mesenchymal cells: II. Stimulation by bone morphogenetic protein-2 requires modulation of N-cadherin expression and function.* Differentiation, 1999. **64**(2): p. 77-89.
69. Tuli, R., et al., *Transforming Growth Factor-β-mediated Chondrogenesis of Human Mesenchymal Progenitor Cells Involves N-cadherin and Mitogen-activated Protein Kinase and Wnt Signaling Cross-talk.* Journal of Biological Chemistry, 2003. **278**(42): p. 41227-41236.
70. Yoon, B.S., et al., *Bmpr1a and Bmpr1b have overlapping functions and are essential for chondrogenesis in vivo.* Proc Natl Acad Sci U S A, 2005. **102**(14): p. 5062-7.
71. Tsumaki, N., et al., *Bone morphogenetic protein signals are required for cartilage formation and differently regulate joint development during skeletogenesis.* J Bone Miner Res, 2002. **17**(5): p. 898-906.
72. Shu, B., et al., *BMP2, but not BMP4, is crucial for chondrocyte proliferation and maturation during endochondral bone development.* J Cell Sci, 2011. **124**(Pt 20): p. 3428-40.
73. Mi, M., et al., *Chondrocyte BMP2 signaling plays an essential role in bone fracture healing.* Gene, 2013. **512**(2): p. 211-8.
74. Tuli, R., et al., *Transforming growth factor-beta-mediated chondrogenesis of human mesenchymal progenitor cells involves N-cadherin and mitogen-activated protein kinase and Wnt signaling cross-talk.* J Biol Chem, 2003. **278**(42): p. 41227-36.
75. Zhang, X., et al., *Primary murine limb bud mesenchymal cells in long-term culture complete chondrocyte differentiation: TGF-β delays hypertrophy and PGE2 inhibits terminal differentiation.* Bone, 2004. **34**(5): p. 809-817.
76. Yang, X., et al., *TGF-beta/Smad3 signals repress chondrocyte hypertrophic differentiation and are required for maintaining articular cartilage.* J Cell Biol, 2001. **153**(1): p. 35-46.
77. Furumatsu, T., et al., *Smad3 induces chondrogenesis through the activation of SOX9 via CREB-binding protein/p300 recruitment.* J Biol Chem, 2005. **280**(9): p. 8343-50.
78. Hellingman, C.A., et al., *Smad signaling determines chondrogenic differentiation of bone-marrow-derived mesenchymal stem cells: inhibition of Smad1/5/8P prevents terminal differentiation and calcification.* Tissue Eng Part A, 2011. **17**(7-8): p. 1157-67.
79. Retting, K.N., *BMP canonical Smad signaling through Smad1 and Smad5 is.* 2009. **136**(7): p. 1093-104.
80. Dy, P., et al., *Synovial joint morphogenesis requires the chondrogenic action of Sox5 and Sox6 in growth plate and articular cartilage.* Dev Biol, 2010. **341**(2): p. 346-59.

81. Francis-West, P.H., et al., *Mechanisms of GDF-5 action during skeletal development.* Development, 1999. **126**(6): p. 1305-1315.
82. Chambers, M.G., et al., *Expression of collagen and aggrecan genes in normal and osteoarthritic murine knee joints.* Osteoarthritis Cartilage, 2002. **10**(1): p. 51-61.
83. Decker, R.S., et al., *Mouse limb skeletal growth and synovial joint development are coordinately enhanced by Kartogenin.* Developmental Biology, 2014. **395**(2): p. 255-267.
84. Deng, Y., et al., *Yap1 Regulates Multiple Steps of Chondrocyte Differentiation during Skeletal Development and Bone Repair.* Cell Rep, 2016. **14**(9): p. 2224-37.
85. Shibata, S., et al., *In situ hybridization and immunohistochemistry of bone sialoprotein and secreted phosphoprotein 1 (osteopontin) in the developing mouse mandibular condylar cartilage compared with limb bud cartilage.* J Anat, 2002. **200**(3): p. 309-20.
86. Inada, M., et al., *Critical roles for collagenase-3 (Mmp13) in development of growth plate cartilage and in endochondral ossification.* Proc Natl Acad Sci U S A, 2004. **101**(49): p. 17192-7.
87. McCulloch, D.R., et al., *Adamts5, the gene encoding a proteoglycan-degrading metalloprotease, is expressed by specific cell lineages during mouse embryonic development and in adult tissues.* Gene Expr Patterns, 2009. **9**(5): p. 314-23.
88. Sibole, S.C. and W. Herzog, *The mechanical effects of chondrocyte hypertrophy: a finite element study.* Osteoarthritis and Cartilage. **22**: p. S101-S102.
89. Ahmed, Y.A., et al., *Physiological death of hypertrophic chondrocytes.* Osteoarthritis and Cartilage, 2007. **15**(5): p. 575-586.
90. Hattori, T., et al., *SOX9 is a major negative regulator of cartilage vascularization, bone marrow formation and endochondral ossification.* Development, 2010. **137**(6): p. 901-911.
91. St-Jacques, B., M. Hammerschmidt, and A.P. McMahon, *Indian hedgehog signaling regulates proliferation and differentiation of chondrocytes and is essential for bone formation.* Genes Dev, 1999. **13**(16): p. 2072-86.
92. Rohatgi, R., L. Milenkovic, and M.P. Scott, *Patched1 regulates hedgehog signaling at the primary cilium.* Science, 2007. **317**(5836): p. 372-6.
93. Lanske, B., et al., *PTH/PTHrP receptor in early development and Indian hedgehog-regulated bone growth.* Science, 1996. **273**(5275): p. 663-6.
94. Akiyama, H., et al., *The transcription factor Sox9 has essential roles in successive steps of the chondrocyte differentiation pathway and is required for expression of Sox5 and Sox6.* Genes Dev, 2002. **16**(21): p. 2813-28.
95. Chung, U.I., et al., *Indian hedgehog couples chondrogenesis to osteogenesis in endochondral bone development.* J Clin Invest, 2001. **107**(3): p. 295-304.
96. Dann, C.E., et al., *Insights into Wnt binding and signalling from the structures of two Frizzled cysteine-rich domains.* Nature, 2001. **412**(6842): p. 86-90.
97. Stamos, J.L. and W.I. Weis, *The beta-catenin destruction complex.* Cold Spring Harb Perspect Biol, 2013. **5**(1): p. a007898.
98. Cadigan, K.M. and M.L. Waterman, *TCF/LEFs and Wnt Signaling in the Nucleus.* Cold Spring Harb Perspect Biol, 2012. **4**(11).
99. Lu, C., et al., *Wnt-mediated reciprocal regulation between cartilage and bone development during endochondral ossification.* Bone, 2013. **53**(2): p. 566-74.
100. Dong, Y.F., et al., *Wnt induction of chondrocyte hypertrophy through the Runx2 transcription factor.* J Cell Physiol, 2006. **208**(1): p. 77-86.
101. Leijten, J.C., et al., *Gremlin 1, frizzled-related protein, and Dkk-1 are key regulators of human articular cartilage homeostasis.* Arthritis Rheum, 2012. **64**(10): p. 3302-12.

102. Nukavarapu, S.P. and D.L. Dorcemus, *Osteochondral tissue engineering: current strategies and challenges.* Biotechnol Adv, 2013. **31**(5): p. 706-21.
103. Rai, V., et al., *Recent strategies in cartilage repair: A systemic review of the scaffold development and tissue engineering.* Journal of Biomedical Materials Research Part A, 2017. **105**(8): p. 2343-2354.
104. Wilson, D.J., *Development of avascularity during cartilage differentiation in the embryonic limb. An exclusion model.* Differentiation, 1986. **30**(3): p. 183-7.
105. Widuchowski, W., J. Widuchowski, and T. Trzaska, *Articular cartilage defects: study of 25,124 knee arthroscopies.* Knee, 2007. **14**(3): p. 177-82.
106. Wong, B.L. and R.L. Sah, *Effect of a Focal Articular Defect on Cartilage Deformation during Patello-Femoral Articulation.* J Orthop Res, 2010. **28**(12): p. 1554-61.
107. Cicuttini, F., et al., *Association of cartilage defects with loss of knee cartilage in healthy, middle-age adults: a prospective study.* Arthritis Rheum, 2005. **52**(7): p. 2033-9.
108. Lefkoe, T.P., et al., *An experimental model of femoral condylar defect leading to osteoarthrosis.* J Orthop Trauma, 1993. **7**(5): p. 458-67.
109. Davies-Tuck, M.L., et al., *The natural history of cartilage defects in people with knee osteoarthritis.* Osteoarthritis and Cartilage, 2008. **16**(3): p. 337-342.
110. Hunter, D.J., D. Schofield, and E. Callander, *The individual and socioeconomic impact of osteoarthritis.* Nat Rev Rheumatol, 2014. **10**(7): p. 437-41.
111. Nukavarapu, S.P. and D.L. Dorcemus, *Osteochondral tissue engineering: Current strategies and challenges.* Biotechnology Advances, 2013. **31**(5): p. 706-721.
112. Alford, J.W. and B.J. Cole, *Cartilage Restoration, Part 2.* The American Journal of Sports Medicine, 2005. **33**(3): p. 443-460.
113. Steadman, J.R., W.G. Rodkey, and J.J. Rodrigo, *Microfracture: surgical technique and rehabilitation to treat chondral defects.* Clin Orthop Relat Res, 2001(391 Suppl): p. S362-9.
114. Kreuz, P.C., et al., *Results after microfracture of full-thickness chondral defects in different compartments in the knee.* Osteoarthritis Cartilage, 2006. **14**(11): p. 1119-25.
115. Franke, O., et al., *Mechanical properties of hyaline and repair cartilage studied by nanoindentation.* Acta Biomater, 2007. **3**(6): p. 873-81.
116. Knutsen, G., et al., *A randomized trial comparing autologous chondrocyte implantation with microfracture. Findings at five years.* J Bone Joint Surg Am, 2007. **89**(10): p. 2105-12.
117. Saris, D.B., et al., *Characterized chondrocyte implantation results in better structural repair when treating symptomatic cartilage defects of the knee in a randomized controlled trial versus microfracture.* Am J Sports Med, 2008. **36**(2): p. 235-46.
118. Kitagaki, J., et al., *Activation of beta-catenin-LEF/TCF signal pathway in chondrocytes stimulates ectopic endochondral ossification.* Osteoarthritis Cartilage, 2003. **11**(1): p. 36-43.
119. Brittberg, M., et al., *Treatment of deep cartilage defects in the knee with autologous chondrocyte transplantation.* N Engl J Med, 1994. **331**(14): p. 889-95.
120. Peterson, L., et al., *Two- to 9-year outcome after autologous chondrocyte transplantation of the knee.* Clin Orthop Relat Res, 2000(374): p. 212-34.
121. Darling, E.M. and K.A. Athanasiou, *Rapid phenotypic changes in passaged articular chondrocyte subpopulations.* J Orthop Res, 2005. **23**(2): p. 425-32.
122. Yoo, J.U., et al., *The chondrogenic potential of human bone-marrow-derived mesenchymal progenitor cells.* J Bone Joint Surg Am, 1998. **80**(12): p. 1745-57.
123. Johnstone, B., et al., *In vitro chondrogenesis of bone marrow-derived mesenchymal progenitor cells.* Exp Cell Res, 1998. **238**(1): p. 265-72.

124. Pittenger, M.F., *Mesenchymal stem cells from adult bone marrow.* Methods Mol Biol, 2008. **449**: p. 27-44.
125. Wong, K.L., et al., *Injectable cultured bone marrow-derived mesenchymal stem cells in varus knees with cartilage defects undergoing high tibial osteotomy: a prospective, randomized controlled clinical trial with 2 years' follow-up.* Arthroscopy, 2013. **29**(12): p. 2020-8.
126. Pittenger, M.F., et al., *Multilineage potential of adult human mesenchymal stem cells.* Science, 1999. **284**(5411): p. 143-7.
127. Bruder, S.P., N. Jaiswal, and S.E. Haynesworth, *Growth kinetics, self-renewal, and the osteogenic potential of purified human mesenchymal stem cells during extensive subcultivation and following cryopreservation.* J Cell Biochem, 1997. **64**(2): p. 278-94.
128. Dell'Accio, F., C. Bari, and F.P. Luyten, *Molecular markers predictive of the capacity of expanded human articular chondrocytes to form stable cartilage in vivo.* Arthritis Rheum, 2001. **44**.
129. Ferretti, C. and M. Mattioli-Belmonte, *Periosteum derived stem cells for regenerative medicine proposals: Boosting current knowledge.* World J Stem Cells, 2014. **6**(3): p. 266-77.
130. O'Driscoll, S.W. and J.S. Fitzsimmons, *The role of periosteum in cartilage repair.* Clin Orthop Relat Res, 2001(391 Suppl): p. S190-207.
131. Stevens, M.M., et al., *A rapid-curing alginate gel system: utility in periosteum-derived cartilage tissue engineering.* Biomaterials, 2004. **25**(5): p. 887-94.
132. Gelse, K., et al., *Cell-based resurfacing of large cartilage defects: long-term evaluation of grafts from autologous transgene-activated periosteal cells in a porcine model of osteoarthritis.* Arthritis Rheum, 2008. **58**(2): p. 475-88.
133. Fellows, C.R., et al., *Adipose, Bone Marrow and Synovial Joint-Derived Mesenchymal Stem Cells for Cartilage Repair.* Front Genet, 2016. **7**.
134. Luo, L., et al., *The effects of dynamic compression on the development of cartilage grafts engineered using bone marrow and infrapatellar fat pad derived stem cells.* Biomed Mater, 2015. **10**(5): p. 055011.
135. Wu, L., et al., *Regeneration of articular cartilage by adipose tissue derived mesenchymal stem cells: perspectives from stem cell biology and molecular medicine.* J Cell Physiol, 2013. **228**(5): p. 938-44.
136. Rasini, V., et al., *Mesenchymal stromal/stem cells markers in the human bone marrow.* Cytotherapy, 2013. **15**(3): p. 292-306.
137. Méndez-Ferrer, S., et al., *Mesenchymal and haematopoietic stem cells form a unique bone marrow niche.* Nature, 2010. **466**(7308): p. 829-34.
138. Martin, G.R., *Isolation of a pluripotent cell line from early mouse embryos cultured in medium conditioned by teratocarcinoma stem cells.* Proc Natl Acad Sci U S A, 1981. **78**(12): p. 7634-8.
139. Friedenstein, A.J., R.K. Chailakhjan, and K.S. Lalykina, *The development of fibroblast colonies in monolayer cultures of guinea-pig bone marrow and spleen cells.* Cell Tissue Kinet, 1970. **3**(4): p. 393-403.
140. Grigoriadis, A.E., J.N. Heersche, and J.E. Aubin, *Differentiation of muscle, fat, cartilage, and bone from progenitor cells present in a bone-derived clonal cell population: effect of dexamethasone.* J Cell Biol, 1988. **106**(6): p. 2139-51.
141. Alev, C., et al., *Transcriptomic landscape of the primitive streak.* Development, 2010. **137**(17): p. 2863-74.
142. Alev, C., et al., *Decoupling of amniote gastrulation and streak formation reveals a morphogenetic unity in vertebrate mesoderm induction.* Development, 2013. **140**(13): p. 2691-6.

143. Tam, P.P. and R.S. Beddington, *The formation of mesodermal tissues in the mouse embryo during gastrulation and early organogenesis.* Development, 1987. **99**(1): p. 109-26.
144. Garcia-Martinez, V. and G.C. Schoenwolf, *Positional control of mesoderm movement and fate during avian gastrulation and neurulation.* Dev Dyn, 1992. **193**(3): p. 249-56.
145. Yonei-Tamura, S., H. Ide, and K. Tamura, *Splanchnic (visceral) mesoderm has limb-forming ability according to the position along the rostrocaudal axis in chick embryos.* Dev Dyn, 2005. **233**(2): p. 256-65.
146. Gros, J. and C.J. Tabin, *Vertebrate limb bud formation is initiated by localized epithelial-to-mesenchymal transition.* Science, 2014. **343**(6176): p. 1253-6.
147. Peled, A., et al., *Expression of alpha-smooth muscle actin in murine bone marrow stromal cells.* Blood, 1991. **78**(2): p. 304-9.
148. Logan, M., et al., *Expression of Cre Recombinase in the developing mouse limb bud driven by a Prxl enhancer.* Genesis, 2002. **33**(2): p. 77-80.
149. Banfi, A., et al., *Proliferation kinetics and differentiation potential of ex vivo expanded human bone marrow stromal cells: Implications for their use in cell therapy.* Exp Hematol, 2000. **28**(6): p. 707-15.
150. de Almeida D , C., et al., *Epigenetic Classification of Human Mesenchymal Stromal Cells.* Stem Cell Reports, 2016. **6**(2): p. 168-75.
151. Meyer, M.B., et al., *Epigenetic Plasticity Drives Adipogenic and Osteogenic Differentiation of Marrow-Derived Mesenchymal Stem Cells.* Journal of Biological Chemistry, 2016.
152. Herlofsen, S.R., et al., *Genome-wide map of quantified epigenetic changes during in vitrochondrogenic differentiation of primary human mesenchymal stem cells.* BMC Genomics, 2013. **14**(1): p. 105.
153. Brown, P.T., M.W. Squire, and W.J. Li, *Characterization and evaluation of mesenchymal stem cells derived from human embryonic stem cells and bone marrow.* Cell Tissue Res, 2014. **358**(1): p. 149-64.
154. Puissant, B., et al., *Immunomodulatory effect of human adipose tissue-derived adult stem cells: comparison with bone marrow mesenchymal stem cells.* Br J Haematol, 2005. **129**(1): p. 118-29.
155. Roemeling-van Rhijn, M., et al., *Human Bone Marrow- and Adipose Tissue-derived Mesenchymal Stromal Cells are Immunosuppressive In vitro and in a Humanized Allograft Rejection Model.* J Stem Cell Res Ther, 2013. **Suppl 6**(1): p. 20780.
156. Reinders, M.E., et al., *Autologous bone marrow-derived mesenchymal stromal cells for the treatment of allograft rejection after renal transplantation: results of a phase I study.* Stem Cells Transl Med, 2013. **2**(2): p. 107-11.
157. Pang, W.W., et al., *Human bone marrow hematopoietic stem cells are increased in frequency and myeloid-biased with age.* Proc Natl Acad Sci U S A, 2011. **108**(50): p. 20012-7.
158. Calvi, L.M., *Osteoblastic activation in the hematopoietic stem cell niche.* Ann N Y Acad Sci, 2006. **1068**: p. 477-88.
159. Clark, P., et al., *Lymphocyte subsets in normal bone marrow.* Blood, 1986. **67**(6): p. 1600-6.
160. Friedenstein, A.J., J.F. Gorskaja, and N.N. Kulagina, *Fibroblast precursors in normal and irradiated mouse hematopoietic organs.* Exp Hematol, 1976. **4**(5): p. 267-74.
161. Dominici, M., et al., *Minimal criteria for defining multipotent mesenchymal stromal cells. The International Society for Cellular Therapy position statement.* Cytotherapy, 2006. **8**(4): p. 315-317.

162. Barry, F.P., et al., *The monoclonal antibody SH-2, raised against human mesenchymal stem cells, recognizes an epitope on endoglin (CD105).* Biochemical and Biophysical Research Communications, 1999. **265**(1): p. 134-139.
163. Barry, F., et al., *The SH-3 and SH-4 antibodies recognize distinct epitopes on CD73 from human mesenchymal stem cells.* Biochemical and Biophysical Research Communications, 2001. **289**(2): p. 519-524.
164. Ode, A., et al., *CD73 and CD29 concurrently mediate the mechanically induced decrease of migratory capacity of mesenchymal stromal cells.* European Cells and Materials, 2011. **22**: p. 26-42.
165. Williams, A.F. and J. Gagnon, *Neuronal cell Thy-1 glycoprotein: Homology with immunoglobulin.* Science, 1982. **216**(4547): p. 696-703.
166. Narravula, S., et al., *Regulation of endothelial CD73 by adenosine: Paracrine pathway for enhanced endothelial barrier function.* Journal of Immunology, 2000. **165**(9): p. 5262-5268.
167. Ishii, M., et al., *Molecular markers distinguish bone marrow mesenchymal stem cells from fibroblasts.* Biochemical and Biophysical Research Communications, 2005. **332**(1): p. 297-303.
168. Battula, V.L., et al., *Isolation of functionally distinct mesenchymal stem cell subsets using antibodies against CD56, CD271, and mesenchymal stem cell antigen-1.* Haematologica, 2009. **94**(2): p. 173-84.
169. Calabrese, G., et al., *Potential Effect of CD271 on Human Mesenchymal Stromal Cell Proliferation and Differentiation.* Int J Mol Sci, 2015. **16**(7): p. 15609-24.
170. Simmons, P.J. and B. Torok-Storb, *Identification of stromal cell precursors in human bone marrow by a novel monoclonal antibody, STRO-1.* Blood, 1991. **78**(1): p. 55-62.
171. Nixon, A.J., et al., *A chondrocyte infiltrated collagen type I/III membrane (MACI(R) implant) improves cartilage healing in the equine patellofemoral joint model.* Osteoarthritis Cartilage, 2015. **23**(4): p. 648-60.
172. Bentley, G., et al., *Minimum ten-year results of a prospective randomised study of autologous chondrocyte implantation versus mosaicplasty for symptomatic articular cartilage lesions of the knee.* J Bone Joint Surg Br, 2012. **94**(4): p. 504-9.
173. Zeifang, F., et al., *Autologous chondrocyte implantation using the original periosteum-cover technique versus matrix-associated autologous chondrocyte implantation: a randomized clinical trial.* Am J Sports Med, 2010. **38**(5): p. 924-33.
174. Hinderer, S., S.L. Layland, and K. Schenke-Layland, *ECM and ECM-like materials - Biomaterials for applications in regenerative medicine and cancer therapy.* Adv Drug Deliv Rev, 2016. **97**: p. 260-9.
175. Chu, C.R., et al., *Articular cartilage repair using allogeneic perichondrocyte-seeded biodegradable porous polylactic acid (PLA): a tissue-engineering study.* J Biomed Mater Res, 1995. **29**(9): p. 1147-54.
176. Shafiee, A., et al., *Electrospun nanofiber-based regeneration of cartilage enhanced by mesenchymal stem cells.* J Biomed Mater Res A, 2011. **99**(3): p. 467-78.
177. Li, Y., et al., *Hyaluronan in limb morphogenesis.* Dev Biol, 2007. **305**(2): p. 411-20.
178. Maleski, M.P. and C.B. Knudson, *Hyaluronan-mediated aggregation of limb bud mesenchyme and mesenchymal condensation during chondrogenesis.* Exp Cell Res, 1996. **225**(1): p. 55-66.
179. Chung, C. and J.A. Burdick, *Influence of 3D Hyaluronic Acid Microenvironments on Mesenchymal Stem Cell Chondrogenesis.* Tissue Eng Part A, 2009. **15**(2): p. 243-54.
180. Amann, E., et al., *Hyaluronic acid facilitates chondrogenesis and matrix deposition of human adipose derived mesenchymal stem cells and human chondrocytes co-cultures.* Acta Biomater, 2017. **52**: p. 130-144.

181. Marcacci, M., et al., *Articular cartilage engineering with Hyalograft C: 3-year clinical results.* Clin Orthop Relat Res, 2005(435): p. 96-105.
182. Zhou, J., et al., *In vitro generation of osteochondral differentiation of human marrow mesenchymal stem cells in novel collagen-hydroxyapatite layered scaffolds.* Acta Biomater, 2011. **7**(11): p. 3999-4006.
183. Jeffrey, J.J. and G.R. Martin, *The role of ascorbic acid in the biosynthesis of collagen II. Site and nature of ascorbic acid participation.* Biochimica et Biophysica Acta (BBA) - General Subjects, 1966. **121**(2): p. 281-291.
184. Murad, S., et al., *Regulation of collagen synthesis by ascorbic acid.* Proc Natl Acad Sci U S A, 1981. **78**(5): p. 2879-82.
185. Myllylä, R., E.-R. Kuutti-Savolainen, and K.I. Kivirikko, *The role of ascorbate in the prolyl hydroxylase reaction.* Biochemical and Biophysical Research Communications, 1978. **83**(2): p. 441-448.
186. Temu, T.M., et al., *The mechanism of ascorbic acid-induced differentiation of ATDC5 chondrogenic cells.* Am J Physiol Endocrinol Metab, 2010. **299**(2): p. E325-34.
187. Grant, M.E. and D.J. Prockop, *The biosynthesis of collagen. 1.* N Engl J Med, 1972. **286**(4): p. 194-9.
188. Shintani, N. and E.B. Hunziker, *Differential effects of dexamethasone on the chondrogenesis of mesenchymal stromal cells: influence of microenvironment, tissue origin and growth factor.* Eur Cell Mater, 2011. **22**: p. 302-19; discussion 319-20.
189. Wang, W., D. Rigueur, and K.M. Lyons, *TGFβ Signaling in Cartilage Development and Maintenance.* Birth Defects Res C Embryo Today, 2014. **102**(1): p. 37-51.
190. Matsunaga, S., T. Yamamoto, and K. Fukumura, *Temporal and spatial expressions of transforming growth factor-betas and their receptors in epiphyseal growth plate.* Int J Oncol, 1999. **14**(6): p. 1063-7.
191. Sekiya, I., et al., *In vitro cartilage formation by human adult stem.* Proc Natl Acad Sci U S A, 2002. **99**(7): p. 4397-402.
192. Bian, L., et al., *Enhanced MSC chondrogenesis following delivery of TGF-beta3 from alginate microspheres within hyaluronic acid hydrogels in vitro and in vivo.* Biomaterials, 2011. **32**(27): p. 6425-34.
193. Diao, H., et al., *Improved cartilage regeneration utilizing mesenchymal stem cells in TGF-beta1 gene-activated scaffolds.* Tissue Eng Part A, 2009. **15**(9): p. 2687-98.
194. Pagnotto, M.R., et al., *Adeno-associated viral gene transfer of transforming growth factor-beta1 to human mesenchymal stem cells improves cartilage repair.* Gene Ther, 2007. **14**(10): p. 804-13.
195. Gonzalez-Fernandez, T., et al., *Gene Delivery of TGF-beta3 and BMP2 in an MSC-Laden Alginate Hydrogel for Articular Cartilage and Endochondral Bone Tissue Engineering.* Tissue Eng Part A, 2016. **22**(9-10): p. 776-87.
196. Abrahamsson, C.K., et al., *Chondrogenesis and mineralization during in vitro culture of human mesenchymal stem cells on three-dimensional woven scaffolds.* Tissue Eng Part A, 2010. **16**(12): p. 3709-18.
197. Orimo, H., *The mechanism of mineralization and the role of alkaline phosphatase in health and disease.* J Nippon Med Sch, 2010. **77**(1): p. 4-12.
198. Ichinose, S., et al., *Detailed examination of cartilage formation and endochondral ossification using human mesenchymal stem cells.* Clin Exp Pharmacol Physiol, 2005. **32**(7): p. 561-70.
199. Bakker, A.C., et al., *Overexpression of active TGF-beta-1 in the murine knee joint: evidence for synovial-layer-dependent chondro-osteophyte formation.* Osteoarthritis Cartilage, 2001. **9**(2): p. 128-36.
200. Steinert, A.F., et al., *Hypertrophy is induced during the in vitro chondrogenic differentiation of human mesenchymal stem cells by bone morphogenetic protein-2*

and bone morphogenetic protein-4 gene transfer. Arthritis Res Ther, 2009. **11**(5): p. R148.
201. Caron, M.M.J., et al., *Hypertrophic differentiation during chondrogenic differentiation of progenitor cells is stimulated by BMP-2 but suppressed by BMP-7.* Osteoarthritis and Cartilage, 2013. **21**(4): p. 604-613.
202. Franke, O., et al., *Mechanical properties of hyaline and repair cartilage studied by nanoindentation.* Acta Biomaterialia, 2007. **3**(6): p. 873-881.
203. Dewulf, N., et al., *Distinct spatial and temporal expression patterns of two type I receptors for bone morphogenetic proteins during mouse embryogenesis.* Endocrinology, 1995. **136**(6): p. 2652-63.
204. Spagnoli, A., et al., *TGF-beta signaling is essential for joint morphogenesis.* J Cell Biol, 2007. **177**(6): p. 1105-17.
205. Baffi, M.O., et al., *Conditional deletion of the TGF-beta type II receptor in Col2a expressing cells results in defects in the axial skeleton without alterations in chondrocyte differentiation or embryonic development of long bones.* Dev Biol, 2004. **276**(1): p. 124-42.
206. Horner, A., et al., *Expression and distribution of transforming growth factor-beta isoforms and their signaling receptors in growing human bone.* Bone, 1998. **23**(2): p. 95-102.
207. Thorp, B.H., I. Anderson, and S.B. Jakowlew, *Transforming growth factor-beta 1, -beta 2 and -beta 3 in cartilage and bone cells during endochondral ossification in the chick.* Development, 1992. **114**(4): p. 907-11.
208. Fisher, S.A. and W.W. Burggren, *Role of hypoxia in the evolution and development of the cardiovascular system.* Antioxid Redox Signal, 2007. **9**(9): p. 1339-52.
209. Gorr, T.A., M. Gassmann, and P. Wappner, *Sensing and responding to hypoxia via HIF in model invertebrates.* J Insect Physiol, 2006. **52**(4): p. 349-64.
210. Monahan-Earley, R., A.M. Dvorak, and W.C. Aird, *Evolutionary origins of the blood vascular system and endothelium.* J Thromb Haemost, 2013. **11 Suppl 1**: p. 46-66.
211. Stroka, D.M., et al., *HIF-1 is expressed in normoxic tissue and displays an organ-specific regulation under systemic hypoxia.* Faseb j, 2001. **15**(13): p. 2445-53.
212. Iwagaki, T., T. Suzuki, and T. Nakashima, *Development and regression of cochlear blood vessels in fetal and newborn mice.* Hear Res, 2000. **145**(1-2): p. 75-81.
213. Semenza, G.L. and G.L. Wang, *A nuclear factor induced by hypoxia via de novo protein synthesis binds to the human erythropoietin gene enhancer at a site required for transcriptional activation.* Mol Cell Biol, 1992. **12**(12): p. 5447-54.
214. Forsythe, J.A., et al., *Activation of vascular endothelial growth factor gene transcription by hypoxia-inducible factor 1.* Mol Cell Biol, 1996. **16**(9): p. 4604-13.
215. Kim, J.W., et al., *HIF-1-mediated expression of pyruvate dehydrogenase kinase: a metabolic switch required for cellular adaptation to hypoxia.* Cell Metab, 2006. **3**(3): p. 177-85.
216. Fukuda, R., et al., *HIF-1 regulates cytochrome oxidase subunits to optimize efficiency of respiration in hypoxic cells.* Cell, 2007. **129**(1): p. 111-22.
217. Rodesch, F., et al., *Oxygen measurements in endometrial and trophoblastic tissues during early pregnancy.* Obstet Gynecol, 1992. **80**(2): p. 283-5.
218. James, J.L., P.R. Stone, and L.W. Chamley, *The regulation of trophoblast differentiation by oxygen in the first trimester of pregnancy.* Human Reproduction Update, 2006. **12**(2): p. 137-144.
219. Sugishita, Y., et al., *Hypoxia-responsive signaling regulates the apoptosis-dependent remodeling of the embryonic avian cardiac outflow tract.* Developmental Biology, 2004. **273**(2): p. 285-296.

220. Fleming, I.N., et al., *Imaging tumour hypoxia with positron emission tomography.* Br J Cancer, 2015. **112**(2): p. 238-50.
221. Lu, H., R.A. Forbes, and A. Verma, *Hypoxia-inducible factor 1 activation by aerobic glycolysis implicates the Warburg effect in carcinogenesis.* J Biol Chem, 2002. **277**(26): p. 23111-5.
222. Caporarello, N., et al., *Classical VEGF, Notch and Ang signalling in cancer angiogenesis, alternative approaches and future directions (Review).* Mol Med Rep, 2017.
223. Mourcin, F., et al., *Galectin-1-expressing stromal cells constitute a specific niche for pre-BII cell development in mouse bone marrow.* Blood, 2011. **117**.
224. Kallio, P.J., et al., *Activation of hypoxia-inducible factor 1alpha: posttranscriptional regulation and conformational change by recruitment of the Arnt transcription factor.* Proc Natl Acad Sci U S A, 1997. **94**(11): p. 5667-72.
225. Arany, Z., et al., *An essential role for p300/CBP in the cellular response to hypoxia.* Proceedings of the National Academy of Sciences, 1996. **93**(23): p. 12969-12973.
226. Luo, W., et al., *Pyruvate kinase M2 is a PHD3-stimulated coactivator for hypoxia-inducible factor 1.* Cell, 2011. **145**(5): p. 732-44.
227. Wang, G.L. and G.L. Semenza, *Characterization of hypoxia-inducible factor 1 and regulation of DNA binding activity by hypoxia.* J Biol Chem, 1993. **268**(29): p. 21513-8.
228. Kimura, H., et al., *Identification of hypoxia-inducible factor 1 ancillary sequence and its function in vascular endothelial growth factor gene induction by hypoxia and nitric oxide.* J Biol Chem, 2001. **276**(3): p. 2292-8.
229. Ruas, J.L., L. Poellinger, and T. Pereira, *Functional analysis of hypoxia-inducible factor-1 alpha-mediated transactivation. Identification of amino acid residues critical for transcriptional activation and/or interaction with CREB-binding protein.* J Biol Chem, 2002. **277**(41): p. 38723-30.
230. Ema, M., et al., *A novel bHLH-PAS factor with close sequence similarity to hypoxia-inducible factor 1α regulates the VEGF expression and is potentially involved in lung and vascular development.* Proc Natl Acad Sci U S A, 1997. **94**(9): p. 4273-8.
231. Kilic, M., et al., *Role of hypoxia inducible factor-1 alpha in modulation of apoptosis resistance.* Oncogene, 2007. **26**(14): p. 2027-38.
232. Ghoshal, P., et al., *HIF1A induces expression of the WASF3 Metastasis Associated Gene under hypoxic conditions.* Int J Cancer, 2012. **131**(6): p. E905-15.
233. Krick, S., et al., *Hypoxia-driven proliferation of human pulmonary artery fibroblasts: cross-talk between HIF-1alpha and an autocrine angiotensin system.* Faseb j, 2005. **19**(7): p. 857-9.
234. Hu, C.J., et al., *Differential Roles of Hypoxia-Inducible Factor 1α (HIF-1α) and HIF-2α in Hypoxic Gene Regulation.* Mol Cell Biol, 2003. **23**(24): p. 9361-74.
235. Makino, Y., et al., *Inhibitory PAS domain protein is a negative regulator of hypoxia-inducible gene expression.* Nature, 2001. **414**(6863): p. 550-4.
236. Makino, Y., et al., *Inhibitory PAS domain protein (IPAS) is a hypoxia-inducible splicing variant of the hypoxia-inducible factor-3alpha locus.* J Biol Chem, 2002. **277**(36): p. 32405-8.
237. Wang, G.L., et al., *Hypoxia-inducible factor 1 is a basic-helix-loop-helix-PAS heterodimer regulated by cellular O2 tension.* Proc Natl Acad Sci U S A, 1995. **92**(12): p. 5510-4.
238. McDonough, M.A., et al., *Cellular oxygen sensing: Crystal structure of hypoxia-inducible factor prolyl hydroxylase (PHD2).* Proc Natl Acad Sci U S A, 2006. **103**(26): p. 9814-9.

239. Berra, E., et al., *HIF prolyl-hydroxylase 2 is the key oxygen sensor setting low steady-state levels of HIF-1alpha in normoxia.* Embo j, 2003. **22**(16): p. 4082-90.
240. Yu, F., et al., *HIF-1alpha binding to VHL is regulated by stimulus-sensitive proline hydroxylation.* Proc Natl Acad Sci U S A, 2001. **98**(17): p. 9630-5.
241. Cockman, M.E., et al., *Hypoxia inducible factor-alpha binding and ubiquitylation by the von Hippel-Lindau tumor suppressor protein.* J Biol Chem, 2000. **275**(33): p. 25733-41.
242. Maxwell, P.H., et al., *The tumour suppressor protein VHL targets hypoxia-inducible factors for oxygen-dependent proteolysis.* Nature, 1999. **399**(6733): p. 271-275.
243. Marxsen J , H., et al., *Hypoxia-inducible factor-1 (HIF-1) promotes its degradation by induction of HIF-α-prolyl-4-hydroxylases.* Biochem J, 2004. **381**(Pt 3): p. 761-7.
244. Liu, Y.V., et al., *RACK1 competes with HSP90 for binding to HIF-1alpha and is required for O(2)-independent and HSP90 inhibitor-induced degradation of HIF-1alpha.* Mol Cell, 2007. **25**(2): p. 207-17.
245. Isaacs, J.S., Y.J. Jung, and L. Neckers, *Aryl hydrocarbon nuclear translocator (ARNT) promotes oxygen-independent stabilization of hypoxia-inducible factor-1alpha by modulating an Hsp90-dependent regulatory pathway.* J Biol Chem, 2004. **279**(16): p. 16128-35.
246. Liu, Y.V., et al., *Calcineurin Promotes Hypoxia-inducible Factor 1α Expression by Dephosphorylating RACK1 and Blocking RACK1 Dimerization().* J Biol Chem, 2007. **282**(51): p. 37064-73.
247. Freedman, S.J., et al., *Structural basis for recruitment of CBP/p300 by hypoxia-inducible factor-1 alpha.* Proc Natl Acad Sci U S A, 2002. **99**(8): p. 5367-72.
248. Mahon, P.C., K. Hirota, and G.L. Semenza, *FIH-1: a novel protein that interacts with HIF-1α and VHL to mediate repression of HIF-1 transcriptional activity.* Genes Dev, 2001. **15**(20): p. 2675-86.
249. Lee, C., et al., *Structure of human FIH-1 reveals a unique active site pocket and interaction sites for HIF-1 and von Hippel-Lindau.* J Biol Chem, 2003. **278**(9): p. 7558-63.
250. Hudson, C.C., et al., *Regulation of hypoxia-inducible factor 1alpha expression and function by the mammalian target of rapamycin.* Mol Cell Biol, 2002. **22**(20): p. 7004-14.
251. Hui, A.S., et al., *Calcium signaling stimulates translation of HIF-alpha during hypoxia.* Faseb j, 2006. **20**(3): p. 466-75.
252. Wenger, R.H., et al., *Hypoxia-inducible factor-1α is regulated at the post-mRNA level.* Kidney International, 1997. **51**(2): p. 560-563.
253. Uchida, T., et al., *Prolonged hypoxia differentially regulates hypoxia-inducible factor (HIF)-1alpha and HIF-2alpha expression in lung epithelial cells: implication of natural antisense HIF-1alpha.* J Biol Chem, 2004. **279**(15): p. 14871-8.
254. Page, E.L., et al., *Induction of hypoxia-inducible factor-1alpha by transcriptional and translational mechanisms.* J Biol Chem, 2002. **277**(50): p. 48403-9.
255. Turcotte, S., R.R. Desrosiers, and R. Béliveau, *HIF-1α mRNA and protein upregulation involves Rho GTPase expression during hypoxia in renal cell carcinoma.* Journal of Cell Science, 2003. **116**(11): p. 2247-2260.
256. Yao, Y., et al., *MIF Plays a Key Role in Regulating Tissue-Specific Chondro-Osteogenic Differentiation Fate of Human Cartilage Endplate Stem Cells under Hypoxia.* Stem Cell Reports, 2016. **7**(2): p. 249-62.
257. Yudoh, K., et al., *Catabolic stress induces expression of hypoxia-inducible factor (HIF)-1 alpha in articular chondrocytes: involvement of HIF-1 alpha in the pathogenesis of osteoarthritis.* Arthritis Res Ther, 2005. **7**(4): p. R904-14.

258. Nilsson, O., et al., *Gradients in bone morphogenetic protein-related gene expression across the growth plate.* J Endocrinol, 2007. **193**(1): p. 75-84.
259. Schipani, E., et al., *Hypoxia in cartilage: HIF-1alpha is essential for chondrocyte growth arrest and survival.* Genes Dev, 2001. **15**(21): p. 2865-76.
260. Zhou, S., Z. Cui, and J.P. Urban, *Factors influencing the oxygen concentration gradient from the synovial surface of articular cartilage to the cartilage-bone interface: a modeling study.* Arthritis Rheum, 2004. **50**(12): p. 3915-24.
261. Maes, C., G. Carmeliet, and E. Schipani, *Hypoxia-driven pathways in bone development, regeneration and disease.* Nat Rev Rheumatol, 2012. **8**(6): p. 358-66.
262. Provot, S., et al., *Hif-1alpha regulates differentiation of limb bud mesenchyme and joint development.* J Cell Biol, 2007. **177**(3): p. 451-64.
263. Amarilio, R., et al., *HIF1alpha regulation of Sox9 is necessary to maintain differentiation of hypoxic prechondrogenic cells during early skeletogenesis.* Development, 2007. **134**(21): p. 3917-28.
264. Lam, J., et al., *Generation of Osteochondral Tissue Constructs with Chondrogenically and Osteogenically Pre-differentiated Mesenchymal Stem Cells Encapsulated in Bilayered Hydrogels.* Acta Biomater, 2014. **10**(3): p. 1112-23.
265. Lima, E.G., et al., *The effect of devitalized trabecular bone on the formation of osteochondral tissue-engineered constructs.* Biomaterials, 2008. **29**(32): p. 4292-9.
266. Maes, C., G. Carmeliet, and E. Schipani, *Hypoxia-driven pathways in bone development, regeneration and disease.* Nat Rev Rheumatol, 2012. **8**(6): p. 358-366.
267. Mohan, N., et al., *Continuous gradients of material composition and growth factors for effective regeneration of the osteochondral interface.* Tissue Eng Part A, 2011. **17**(21-22): p. 2845-55.
268. Nagel, S., et al., *Therapeutic manipulation of the HIF hydroxylases.* Antioxid Redox Signal, 2010. **12**(4): p. 481-501.
269. Robins, J.C., et al., *Hypoxia induces chondrocyte-specific gene expression in mesenchymal cells in association with transcriptional activation of Sox9.* Bone, 2005. **37**(3): p. 313-22.
270. Kanichai, M., et al., *Hypoxia promotes chondrogenesis in rat mesenchymal stem cells: a role for AKT and hypoxia-inducible factor (HIF)-1alpha.* J Cell Physiol, 2008. **216**(3): p. 708-15.
271. Zhou, N., et al., *HIF-1alpha as a Regulator of BMP2-Induced Chondrogenic Differentiation, Osteogenic Differentiation, and Endochondral Ossification in Stem Cells.* Cell Physiol Biochem, 2015. **36**(1): p. 44-60.
272. Duval, E., et al., *Molecular mechanism of hypoxia-induced chondrogenesis and its application in in vivo cartilage tissue engineering.* Biomaterials, 2012. **33**(26): p. 6042-51.
273. McMahon, S., et al., *Transforming growth factor beta1 induces hypoxia-inducible factor-1 stabilization through selective inhibition of PHD2 expression.* J Biol Chem, 2006. **281**(34): p. 24171-81.
274. Thoms, B.L., et al., *Hypoxia promotes the production and inhibits the destruction of human articular cartilage.* Arthritis Rheum, 2013. **65**(5): p. 1302-12.
275. Coyle, C.H., N.J. Izzo, and C.R. Chu, *Sustained hypoxia enhances chondrocyte matrix synthesis.* J Orthop Res, 2009. **27**(6): p. 793-9.
276. Tan, G.K., et al., *Effects of biomimetic surfaces and oxygen tension on redifferentiation of passaged human fibrochondrocytes in 2D and 3D cultures.* Biomaterials, 2011. **32**(24): p. 5600-14.
277. Pfander, D., et al., *HIF-1alpha controls extracellular matrix synthesis by epiphyseal chondrocytes.* J Cell Sci, 2003. **116**(Pt 9): p. 1819-26.

278. Thoms, B.L. and C.L. Murphy, *Inhibition of Hypoxia-inducible Factor-targeting Prolyl Hydroxylase Domain-containing Protein 2 (PHD2) Enhances Matrix Synthesis by Human Chondrocytes.* J Biol Chem, 2010. **285**(27): p. 20472-80.
279. Duval, E., et al., *Hypoxia-inducible factor 1alpha inhibits the fibroblast-like markers type I and type III collagen during hypoxia-induced chondrocyte redifferentiation: hypoxia not only induces type II collagen and aggrecan, but it also inhibits type I and type III collagen in the hypoxia-inducible factor 1alpha-dependent redifferentiation of chondrocytes.* Arthritis Rheum, 2009. **60**(10): p. 3038-48.
280. Aro, E., et al., *Hypoxia-inducible factor-1 (HIF-1) but not HIF-2 is essential for hypoxic induction of collagen prolyl 4-hydroxylases in primary newborn mouse epiphyseal growth plate chondrocytes.* J Biol Chem, 2012. **287**(44): p. 37134-44.
281. Makris, E.A., D.J. Responte, and N.K. Paschos, *Developing functional musculoskeletal tissues through hypoxia and lysyl oxidase-induced collagen cross-linking.* 2014.
282. Coimbra, I.B., et al., *Hypoxia inducible factor-1 alpha expression in human normal and osteoarthritic chondrocytes.* Osteoarthritis Cartilage, 2004. **12**(4): p. 336-45.
283. Lafont, J.E., S. Talma, and C.L. Murphy, *Hypoxia-inducible factor 2alpha is essential for hypoxic induction of the human articular chondrocyte phenotype.* Arthritis Rheum, 2007. **56**(10): p. 3297-306.
284. Lafont, J.E., et al., *Hypoxia promotes the differentiated human articular chondrocyte phenotype through SOX9-dependent and -independent pathways.* J Biol Chem, 2008. **283**(8): p. 4778-86.
285. Pelosi, M., et al., *Parathyroid hormone-related protein is induced by hypoxia and promotes expression of the differentiated phenotype of human articular chondrocytes.* Clin Sci (Lond), 2013. **125**(10): p. 461-70.
286. Tsuchida, S., et al., *HIF-1α-induced HSP70 regulates anabolic responses in articular chondrocytes under hypoxic conditions.* Journal of Orthopaedic Research, 2014. **32**(8): p. 975-980.
287. Leijten, J., et al., *Metabolic programming of mesenchymal stromal cells by oxygen tension directs chondrogenic cell fate.* Proc Natl Acad Sci U S A, 2014. **111**(38): p. 13954-9.
288. Bouaziz, W., et al., *Interaction of HIF1alpha and beta-catenin inhibits matrix metalloproteinase 13 expression and prevents cartilage damage in mice.* Proc Natl Acad Sci U S A, 2016. **113**(19): p. 5453-8.
289. Park, I.H., et al., *Constitutive stabilization of hypoxia-inducible factor alpha selectively promotes the self-renewal of mesenchymal progenitors and maintains mesenchymal stromal cells in an undifferentiated state.* Exp Mol Med, 2013. **45**: p. e44.
290. Edwards, M.M., et al., *Mutations in Lama1 disrupt retinal vascular development and inner limiting membrane formation.* J Biol Chem, 2010. **285**.
291. Chen, D., et al., *Synergistic inhibition of Wnt pathway by HIF-1alpha and osteoblast-specific transcription factor osterix (Osx) in osteoblasts.* PLoS One, 2012. **7**(12): p. e52948.
292. Mitchison, T.J., *Compare and contrast actin filaments and microtubules.* Mol Biol Cell, 1992. **3**(12): p. 1309-15.
293. Lutz, G.J. and R.L. Lieber, *Skeletal muscle myosin II structure and function.* Exerc Sport Sci Rev, 1999. **27**: p. 63-77.
294. Ingber, D.E., *Tensegrity I. Cell structure and hierarchical systems biology.* J Cell Sci, 2003. **116**(Pt 7): p. 1157-73.
295. Kroto, H.W., et al., *C60: Buckminsterfullerene.* Nature, 1985. **318**(6042): p. 162-163.
296. Fuller, R.B. *Tensegrity*. 1961; Available from: http://www.rwgrayprojects.com/rbfnotes/fpapers/tensegrity/tenseg01.html.

297. Chu, R.Z. *Mapping the Hidden Patterns in Sphere Packing*. 2003; Available from: http://verbchu.blogspot.co.uk/2010/07/mapping-hidden-patterns-in-sphere.html.
298. Tomasek, J.J. and E.D. Hay, *Analysis of the role of microfilaments and microtubules in acquisition of bipolarity and elongation of fibroblasts in hydrated collagen gels.* J Cell Biol, 1984. **99**(2): p. 536-49.
299. Tint, I.S., et al., *Evidence that intermediate filament reorganization is induced by ATP-dependent contraction of the actomyosin cortex in permeabilized fibroblasts.* Journal of Cell Science, 1991. **98**(3): p. 375-384.
300. Harris, A., P. Wild, and D. Stopak, *Silicone rubber substrata: a new wrinkle in the study of cell locomotion.* Science, 1980. **208**(4440): p. 177-179.
301. Banerjee, S.D., R.H. Cohn, and M.R. Bernfield, *Basal lamina of embryonic salivary epithelia. Production by the epithelium and role in maintaining lobular morphology.* J Cell Biol, 1977. **73**(2): p. 445-63.
302. Li, M. and D.S. Sakaguchi, *Inhibition of integrin-mediated adhesion and signaling disrupts retinal development.* Developmental Biology, 2004. **275**(1): p. 202-214.
303. Guvendiren, M. and J.A. Burdick, *Stiffening hydrogels to probe short- and long-term cellular responses to dynamic mechanics.* Nat Commun, 2012. **3**: p. 792.
304. Engler, A.J., et al., *Matrix Elasticity Directs Stem Cell Lineage Specification.* Cell, 2006. **126**(4): p. 677-689.
305. Mih, J.D., et al., *Matrix stiffness reverses the effect of actomyosin tension on cell proliferation.* J Cell Sci, 2012. **125**(Pt 24): p. 5974-83.
306. Vishavkarma, R., et al., *Role of Actin Filaments in Correlating Nuclear Shape and Cell Spreading.* PLOS ONE, 2014. **9**(9): p. e107895.
307. McBeath, R., et al., *Cell shape, cytoskeletal tension, and RhoA regulate stem cell lineage commitment.* Dev Cell, 2004. **6**(4): p. 483-95.
308. Al-Rekabi, Z. and A.E. Pelling, *Cross talk between matrix elasticity and mechanical force regulates myoblast traction dynamics.* Phys Biol, 2013. **10**(6): p. 066003.
309. Huveneers, S., et al., *Binding of soluble fibronectin to integrin alpha5 beta1 - link to focal adhesion redistribution and contractile shape.* J Cell Sci, 2008. **121**(Pt 15): p. 2452-62.
310. Jokinen, J., et al., *Integrin-mediated cell adhesion to type I collagen fibrils.* J Biol Chem, 2004. **279**(30): p. 31956-63.
311. Tadokoro, S., et al., *Talin binding to integrin beta tails: a final common step in integrin activation.* Science, 2003. **302**(5642): p. 103-6.
312. Ma, Y.Q., et al., *Kindlin-2 (Mig-2): a co-activator of beta3 integrins.* J Cell Biol, 2008. **181**(3): p. 439-46.
313. Kornberg, L.J., et al., *Signal transduction by integrins: increased protein tyrosine phosphorylation caused by clustering of beta 1 integrins.* Proc Natl Acad Sci U S A, 1991. **88**(19): p. 8392-6.
314. Humphries, J.D., et al., *Vinculin controls focal adhesion formation by direct interactions with talin and actin.* J Cell Biol, 2007. **179**(5): p. 1043-57.
315. Schiller, H.B., et al., *beta1- and alphav-class integrins cooperate to regulate myosin II during rigidity sensing of fibronectin-based microenvironments.* Nat Cell Biol, 2013. **15**(6): p. 625-36.
316. Pasapera, A.M., et al., *Myosin II activity regulates vinculin recruitment to focal adhesions through FAK-mediated paxillin phosphorylation.* J Cell Biol, 2010. **188**(6): p. 877-90.
317. Schaller, M.D., et al., *Autophosphorylation of the focal adhesion kinase, pp125FAK, directs SH2-dependent binding of pp60src.* Mol Cell Biol, 1994. **14**(3): p. 1680-8.
318. Zaidel-Bar, R., et al., *Early molecular events in the assembly of matrix adhesions at the leading edge of migrating cells.* J Cell Sci, 2003. **116**(Pt 22): p. 4605-13.

319. Zhai, J., et al., *Direct interaction of focal adhesion kinase with p190RhoGEF.* J Biol Chem, 2003. **278**(27): p. 24865-73.
320. Kopen, G.C., D.J. Prockop, and D.G. Phinney, *Marrow stromal cells migrate throughout forebrain and cerebellum, and they differentiate into astrocytes after injection into neonatal mouse brains.* Proc Natl Acad Sci U S A, 1999. **96**(19): p. 10711-6.
321. Amano, M., et al., *Formation of actin stress fibers and focal adhesions enhanced by Rho-kinase.* Science, 1997. **275**(5304): p. 1308-11.
322. Amano, M., et al., *Phosphorylation and activation of myosin by Rho-associated kinase (Rho-kinase).* J Biol Chem, 1996. **271**(34): p. 20246-9.
323. Kimura, K., et al., *Regulation of myosin phosphatase by Rho and Rho-associated kinase (Rho-kinase).* Science, 1996. **273**(5272): p. 245-8.
324. Yonezawa, N., E. Nishida, and H. Sakai, *pH control of actin polymerization by cofilin.* J Biol Chem, 1985. **260**(27): p. 14410-2.
325. Maekawa, M., et al., *Signaling from Rho to the actin cytoskeleton through protein kinases ROCK and LIM-kinase.* Science, 1999. **285**(5429): p. 895-8.
326. Sumi, T., K. Matsumoto, and T. Nakamura, *Specific activation of LIM kinase 2 via phosphorylation of threonine 505 by ROCK, a Rho-dependent protein kinase.* J Biol Chem, 2001. **276**(1): p. 670-6.
327. Crisan, M., et al., *A perivascular origin for mesenchymal stem cells in multiple human organs.* Cell Stem Cell, 2008. **3**(3): p. 301-13.
328. Huang, J., et al., *The Hippo signaling pathway coordinately regulates cell proliferation and apoptosis by inactivating Yorkie, the Drosophila Homolog of YAP.* Cell, 2005. **122**(3): p. 421-34.
329. Sansores-Garcia, L., et al., *Modulating F-actin organization induces organ growth by affecting the Hippo pathway.* Embo j, 2011. **30**(12): p. 2325-35.
330. Dupont, S., et al., *Role of YAP/TAZ in mechanotransduction.* Nature, 2011. **474**(7350): p. 179-83.
331. Aragona, M., et al., *A mechanical checkpoint controls multicellular growth through YAP/TAZ regulation by actin-processing factors.* Cell, 2013. **154**(5): p. 1047-59.
332. Hong, J.H., et al., *TAZ, a transcriptional modulator of mesenchymal stem cell differentiation.* Science, 2005. **309**(5737): p. 1074-8.
333. Cen, B., et al., *Megakaryoblastic leukemia 1, a potent transcriptional coactivator for serum response factor (SRF), is required for serum induction of SRF target genes.* Mol Cell Biol, 2003. **23**(18): p. 6597-608.
334. Vartiainen, M.K., et al., *Nuclear actin regulates dynamic subcellular localization and activity of the SRF cofactor MAL.* Science, 2007. **316**(5832): p. 1749-52.
335. Miralles, F., et al., *Actin dynamics control SRF activity by regulation of its coactivator MAL.* Cell, 2003. **113**(3): p. 329-42.
336. Esnault, C., et al., *Rho-actin signaling to the MRTF coactivators dominates the immediate transcriptional response to serum in fibroblasts.* Genes Dev, 2014. **28**(9): p. 943-58.
337. Kim, T., et al., *MRTF potentiates TEAD-YAP transcriptional activity causing metastasis.* The EMBO Journal, 2016.
338. Maniotis, A.J., C.S. Chen, and D.E. Ingber, *Demonstration of mechanical connections between integrins, cytoskeletal filaments, and nucleoplasm that stabilize nuclear structure.* Proc Natl Acad Sci U S A, 1997. **94**(3): p. 849-54.
339. Smith, J.R. and D.W. Lincoln, *Aging of cells in culture.* Int Rev Cytol, 1984. **89**.
340. Crisp, M., et al., *Coupling of the nucleus and cytoplasm: role of the LINC complex.* J Cell Biol, 2006. **172**(1): p. 41-53.

341. Kim, D.H. and D. Wirtz, *Cytoskeletal tension induces the polarized architecture of the nucleus.* Biomaterials, 2015. **48**: p. 161-72.
342. Driscoll, T.P., et al., *Cytoskeletal to Nuclear Strain Transfer Regulates YAP Signaling in Mesenchymal Stem Cells.* Biophys J, 2015. **108**(12): p. 2783-93.
343. Zwerger, M., et al., *Myopathic lamin mutations impair nuclear stability in cells and tissue and disrupt nucleo-cytoskeletal coupling.* Hum Mol Genet, 2013. **22**(12): p. 2335-49.
344. Taimen, P., et al., *A progeria mutation reveals functions for lamin A in nuclear assembly, architecture, and chromosome organization.* Proc Natl Acad Sci U S A, 2009. **106**(49): p. 20788-93.
345. Shumaker, D.K., et al., *Mutant nuclear lamin A leads to progressive alterations of epigenetic control in premature aging.* Proc Natl Acad Sci U S A, 2006. **103**(23): p. 8703-8.
346. Schermelleh, L., et al., *Subdiffraction multicolor imaging of the nuclear periphery with 3D structured illumination microscopy.* Science, 2008. **320**(5881): p. 1332-6.
347. Swift, J., et al., *Nuclear lamin-A scales with tissue stiffness and enhances matrix-directed differentiation.* Science, 2013. **341**(6149): p. 1240104.
348. Ho, C.Y., et al., *Lamin A/C and emerin regulate MKL1-SRF activity by modulating actin dynamics.* Nature, 2013. **497**(7450): p. 507-11.
349. Bertrand, A.T., et al., *Cellular microenvironments reveal defective mechanosensing responses and elevated YAP signaling in LMNA-mutated muscle precursors.* J Cell Sci, 2014. **127**(Pt 13): p. 2873-84.
350. von der Mark, K., et al., *Relationship between cell shape and type of collagen synthesised as chondrocytes lose their cartilage phenotype in culture.* Nature, 1977. **267**(5611): p. 531-2.
351. Zhang, T., et al., *Softening Substrates Promote Chondrocytes Phenotype via RhoA/ROCK Pathway.* ACS Applied Materials & Interfaces, 2016. **8**(35): p. 22884-22891.
352. Kim, J.H., et al., *Matrix cross-linking–mediated mechanotransduction promotes posttraumatic osteoarthritis.* Proc Natl Acad Sci U S A, 2015. **112**(30): p. 9424-9.
353. Ray, P. and S.C. Chapman, *Cytoskeletal Reorganization Drives Mesenchymal Condensation and Regulates Downstream Molecular Signaling.* PLoS One, 2015. **10**(8): p. e0134702.
354. Gao, L., R. McBeath, and C.S. Chen, *Stem cell shape regulates a chondrogenic versus myogenic fate through Rac1 and N-cadherin.* Stem Cells, 2010. **28**(3): p. 564-72.
355. Allen, J.L., M.E. Cooke, and T. Alliston, *ECM stiffness primes the TGFbeta pathway to promote chondrocyte differentiation.* Mol Biol Cell, 2012. **23**(18): p. 3731-42.
356. Stolz, M., et al., *Dynamic Elastic Modulus of Porcine Articular Cartilage Determined at Two Different Levels of Tissue Organization by Indentation-Type Atomic Force Microscopy.* Biophys J, 2004. **86**(5): p. 3269-83.
357. Mente, P.L. and J.L. Lewis, *Elastic modulus of calcified cartilage is an order of magnitude less than that of subchondral bone.* J Orthop Res, 1994. **12**(5): p. 637-47.
358. Kwon, H.J. and K. Yasuda, *Chondrogenesis on sulfonate-coated hydrogels is regulated by their mechanical properties.* J Mech Behav Biomed Mater, 2013. **17**: p. 337-46.
359. Coricor, G. and R. Serra, *TGF-β regulates phosphorylation and stabilization of Sox9 protein in chondrocytes through p38 and Smad dependent mechanisms.* Sci Rep, 2016. **6**.
360. Haudenschild, D.R., et al., *Rho Kinase-Dependent Sox9 Activation in Chondrocytes.* Arthritis Rheum, 2010. **62**(1): p. 191-200.
361. Bar Oz, M., et al., *Acetylation reduces SOX9 nuclear entry and ACAN gene transactivation in human chondrocytes.* Aging Cell, 2016. **15**(3): p. 499-508.

362. Xu, T., et al., *RhoA/Rho kinase signaling regulates transforming growth factor-beta1-induced chondrogenesis and actin organization of synovium-derived mesenchymal stem cells through interaction with the Smad pathway.* Int J Mol Med, 2012. **30**(5): p. 1119-25.
363. Deng, Y., et al., *Yap1 Regulates Multiple Steps of Chondrocyte Differentiation during Skeletal Development and Bone Repair.* Cell Reports, 2016. **14**(9): p. 2224-2237.
364. Karystinou, A., et al., *Yes-associated protein (YAP) is a negative regulator of chondrogenesis in mesenchymal stem cells.* Arthritis Research & Therapy, 2015. **17**(1): p. 147.
365. Zhong, W., et al., *Regulation of fibrochondrogenesis of mesenchymal stem cells in an integrated microfluidic platform embedded with biomimetic nanofibrous scaffolds.* PLoS One, 2013. **8**(4): p. e61283.
366. Zhong, W., et al., *YAP-mediated regulation of the chondrogenic phenotype in response to matrix elasticity.* Journal of Molecular Histology, 2013. **44**(5): p. 587-595.
367. Hao, Y., et al., *Tumor suppressor LATS1 is a negative regulator of oncogene YAP.* J Biol Chem, 2008. **283**(9): p. 5496-509.
368. Vogler, M., et al., *Hypoxia modulates fibroblastic architecture, adhesion and migration: a role for HIF-1alpha in cofilin regulation and cytoplasmic actin distribution.* PLoS One, 2013. **8**(7): p. e69128.
369. Yim, E.K.F., et al., *Nanotopography-induced changes in focal adhesions, cytoskeletal organization, and mechanical properties of human mesenchymal stem cells.* Biomaterials, 2010. **31**(6): p. 1299.
370. Glass, J.J., et al., *Hypoxia alters the recruitment of tropomyosins into the actin stress fibres of neuroblastoma cells.* BMC Cancer, 2015. **15**: p. 712.
371. Singleton, D.C., et al., *Hypoxic regulation of RIOK3 is a major mechanism for cancer cell invasion and metastasis.* Oncogene, 2015. **34**(36): p. 4713-22.
372. Gilkes, D.M., et al., *Hypoxia-inducible factors mediate coordinated RhoA-ROCK1 expression and signaling in breast cancer cells.* Proc Natl Acad Sci U S A, 2014. **111**(3): p. E384-93.
373. Wang, H.B., et al., *Focal adhesion kinase is involved in mechanosensing during fibroblast migration.* Proc Natl Acad Sci U S A, 2001. **98**(20): p. 11295-300.
374. Weidemann, A., et al., *HIF-1α activation results in actin cytoskeleton reorganization and modulation of Rac-1 signaling in endothelial cells.* Cell Commun Signal, 2013. **11**: p. 80.
375. Vogel, S., et al., *Prolyl hydroxylase domain (PHD) 2 affects cell migration and F-actin formation via RhoA/rho-associated kinase-dependent cofilin phosphorylation.* J Biol Chem, 2010. **285**(44): p. 33756-63.
376. Skuli, N., et al., *Alphavbeta3/alphavbeta5 integrins-FAK-RhoB: a novel pathway for hypoxia regulation in glioblastoma.* Cancer Res, 2009. **69**(8): p. 3308-16.
377. Brooks, D.L., et al., *ITGA6 is directly regulated by hypoxia-inducible factors and enriches for cancer stem cell activity and invasion in metastatic breast cancer models.* Mol Cancer, 2016. **15**: p. 26.
378. Gonzalez-Rodriguez, P., et al., *Hypoxic induction of T-type Ca(2+) channels in rat cardiac myocytes: role of HIF-1alpha and RhoA/ROCK signalling.* J Physiol, 2015. **593**(21): p. 4729-45.
379. Mizukami, Y., et al., *Hypoxic regulation of vascular endothelial growth factor through the induction of phosphatidylinositol 3-kinase/Rho/ROCK and c-Myc.* J Biol Chem, 2006. **281**(20): p. 13957-63.
380. Nakanishi, N., et al., *MURC deficiency in smooth muscle attenuates pulmonary hypertension.* Nat Commun, 2016. **7**.

381. Chen, H., Q. Chen, and Q. Luo, *Expression of netrin-1 by hypoxia contributes to the invasion and migration of prostate carcinoma cells by regulating YAP activity.* Exp Cell Res, 2016. **349**(2): p. 302-309.
382. Zhou, T.Y., et al., *Inactivation of hypoxia-induced YAP by statins overcomes hypoxic resistance tosorafenib in hepatocellular carcinoma cells.* Sci Rep, 2016. **6**: p. 30483.
383. Ma, B., et al., *Zyxin-Siah2-Lats2 axis mediates cooperation between Hippo and TGF-beta signalling pathways.* Nat Commun, 2016. **7**: p. 11123.
384. Yoshigi, M., et al., *Mechanical force mobilizes zyxin from focal adhesions to actin filaments and regulates cytoskeletal reinforcement.* J Cell Biol, 2005. **171**(2): p. 209-15.
385. Caniggia, I., et al., *Hypoxia-inducible factor-1 mediates the biological effects of oxygen on human trophoblast differentiation through TGFbeta(3).* J Clin Invest, 2000. **105**(5): p. 577-87.
386. Barry, F., et al., *Chondrogenic Differentiation of Mesenchymal Stem Cells from Bone Marrow: Differentiation-Dependent Gene Expression of Matrix Components.* Experimental Cell Research, 2001. **268**(2): p. 189-200.
387. Johnstone, B., et al., *In VitroChondrogenesis of Bone Marrow-Derived Mesenchymal Progenitor Cells.* Experimental Cell Research, 1998. **238**(1): p. 265-272.
388. Sekiya, I., et al., *In vitro cartilage formation by human adult stem cells from bone marrow stroma defines the sequence of cellular and molecular events during chondrogenesis.* Proc Natl Acad Sci U S A, 2002. **99**(7): p. 4397-402.
389. Wehling, N., et al., *Interleukin-1beta and tumor necrosis factor alpha inhibit chondrogenesis by human mesenchymal stem cells through NF-kappaB-dependent pathways.* Arthritis Rheum, 2009. **60**(3): p. 801-12.
390. Lauder, S.N., et al., *Interleukin-1beta induced activation of nuclear factor-kappab can be inhibited by novel pharmacological agents in osteoarthritis.* Rheumatology (Oxford), 2007. **46**(5): p. 752-8.
391. Meretoja, V.V., et al., *The effect of hypoxia on the chondrogenic differentiation of co-cultured articular chondrocytes and mesenchymal stem cells in scaffolds.* Biomaterials, 2013. **34**(17): p. 4266-73.
392. Tan, G.-K., et al., *Effects of biomimetic surfaces and oxygen tension on redifferentiation of passaged human fibrochondrocytes in 2D and 3D cultures.* Biomaterials, 2011. **32**(24): p. 5600-5614.
393. Bornes, T.D., et al., *Hypoxic culture of bone marrow-derived mesenchymal stromal stem cells differentially enhances in vitro chondrogenesis within cell-seeded collagen and hyaluronic acid porous scaffolds.* Stem Cell Res Ther, 2015. **6**: p. 84.
394. Foldager, C.B., et al., *Combined 3D and hypoxic culture improves cartilage-specific gene expression in human chondrocytes.* Acta Orthop, 2011. **82**(2): p. 234-40.
395. Collins, J., et al., *Oxygen and pH-sensitivity of human osteoarthritic chondrocytes in 3-D alginate bead culture system.* Osteoarthritis Cartilage, 2013. **21**(11): p. 1790-8.
396. Bracken, C.P., et al., *Cell-specific regulation of hypoxia-inducible factor (HIF)-1alpha and HIF-2alpha stabilization and transactivation in a graded oxygen environment.* J Biol Chem, 2006. **281**(32): p. 22575-85.
397. Siegel, G., et al., *Phenotype, donor age and gender affect function of human bone marrow-derived mesenchymal stromal cells.* BMC Medicine, 2013. **11**(1): p. 146.
398. Zayed, M., et al., *Donor-Matched Comparison of Chondrogenic Potential of Equine Bone Marrow- and Synovial Fluid-Derived Mesenchymal Stem Cells: Implications for Cartilage Tissue Regeneration.* Frontiers in Veterinary Science, 2017. **3**(121).
399. Goldstein, D.J. and R.W. Horobin, *Surface staining of cartilage by Alcian blue, with reference to the role of microscopic dye aggregates in histological staining.* Histochem J, 1974. **6**(2): p. 175-84.

400. Frenz, D.A., N.S. Jaikaria, and S.A. Newman, *The mechanism of precartilage mesenchymal condensation: a major role for interaction of the cell surface with the amino-terminal heparin-binding domain of fibronectin.* Dev Biol, 1989. **136**(1): p. 97-103.
401. Barbul, A., *Proline precursors to sustain Mammalian collagen synthesis.* J Nutr, 2008. **138**(10): p. 2021s-2024s.
402. Kulyk, W.M., J.L. Franklin, and L.M. Hoffman, *Sox9 expression during chondrogenesis in micromass cultures of embryonic limb mesenchyme.* Exp Cell Res, 2000. **255**(2): p. 327-32.
403. Wilkins, R.J. and A.C. Hall, *Control of matrix synthesis in isolated bovine chondrocytes by extracellular and intracellular pH.* Journal of Cellular Physiology, 1995. **164**(3): p. 474-481.
404. Sakai, K., et al., *Stage-and tissue-specific expression of a Col2a1-Cre fusion gene in transgenic mice.* Matrix Biol, 2001. **19**(8): p. 761-7.
405. Marxsen, J.H., et al., *Hypoxia-inducible factor-1 (HIF-1) promotes its degradation by induction of HIF-alpha-prolyl-4-hydroxylases.* Biochem J, 2004. **381**(Pt 3): p. 761-7.
406. Appelhoff, R.J., et al., *Differential function of the prolyl hydroxylases PHD1, PHD2, and PHD3 in the regulation of hypoxia-inducible factor.* J Biol Chem, 2004. **279**(37): p. 38458-65.
407. Robins, J.C., et al., *Hypoxia induces chondrocyte-specific gene expression in mesenchymal cells in association with transcriptional activation of Sox9.* Bone, 2005. **37**(3): p. 313-322.
408. Kallio, P.J., et al., *Signal transduction in hypoxic cells: inducible nuclear translocation and recruitment of the CBP/p300 coactivator by the hypoxia-inducible factor-1alpha.* Embo j, 1998. **17**(22): p. 6573-86.
409. Lin, C., et al., *Hypoxia induces HIF-1alpha and VEGF expression in chondrosarcoma cells and chondrocytes.* J Orthop Res, 2004. **22**(6): p. 1175-81.
410. Semenza, G.L., et al., *Transcriptional regulation of genes encoding glycolytic enzymes by hypoxia-inducible factor 1.* J Biol Chem, 1994. **269**(38): p. 23757-63.
411. Metzen, E., et al., *Regulation of the prolyl hydroxylase domain protein 2 (phd2/egln-1) gene: identification of a functional hypoxia-responsive element.* Biochem J, 2005. **387**(Pt 3): p. 711-7.
412. Foldager, C.B., et al., *Validation of suitable house keeping genes for hypoxia-cultured human chondrocytes.* BMC Mol Biol, 2009. **10**: p. 94.
413. Gibson, B.G. and M.D. Briggs, *The aggrecanopathies; an evolving phenotypic spectrum of human genetic skeletal diseases.* Orphanet J Rare Dis, 2016. **11**.
414. Pelttari, K., et al., *Premature induction of hypertrophy during in vitro chondrogenesis of human mesenchymal stem cells correlates with calcification and vascular invasion after ectopic transplantation in SCID mice.* Arthritis Rheum, 2006. **54**(10): p. 3254-66.
415. Yoshida, C.A., et al., *Runx2 and Runx3 are essential for chondrocyte maturation, and Runx2 regulates limb growth through induction of Indian hedgehog.* Genes Dev, 2004. **18**(8): p. 952-63.
416. Cheng, A. and P.G. Genever, *SOX9 determines RUNX2 transactivity by directing intracellular degradation.* J Bone Miner Res, 2010. **25**(12): p. 2680-9.
417. Zheng, Q., et al., *Type X collagen gene regulation by Runx2 contributes directly to its hypertrophic chondrocyte-specific expression in vivo.* J Cell Biol, 2003. **162**(5): p. 833-42.
418. Kobayashi, T., et al., *BMP signaling stimulates cellular differentiation at multiple steps during cartilage development.* Proceedings of the National Academy of Sciences of the United States of America, 2005. **102**(50): p. 18023-18027.

419. Worthley, Daniel L., et al., *Gremlin 1 Identifies a Skeletal Stem Cell with Bone, Cartilage, and Reticular Stromal Potential.* Cell. **160**(1): p. 269-284.
420. Lieven, O., J. Knobloch, and U. Rüther, *The regulation of Dkk1 expression during embryonic development.* Developmental Biology, 2010. **340**(2): p. 256-268.
421. Pacifici, M., et al., *Hypertrophic chondrocytes. The terminal stage of differentiation in the chondrogenic cell lineage?* Ann N Y Acad Sci, 1990. **599**: p. 45-57.
422. Royer, C., et al., *Effects of gestational hypoxia on mRNA levels of Glut3 and Glut4 transporters, hypoxia inducible factor-1 and thyroid hormone receptors in developing rat brain.* Brain Res, 2000. **856**(1-2): p. 119-28.
423. Neary, M.T., et al., *Hypoxia signaling controls postnatal changes in cardiac mitochondrial morphology and function.* J Mol Cell Cardiol, 2014. **74**(100): p. 340-52.
424. Mole, D.R., et al., *Genome-wide association of hypoxia-inducible factor (HIF)-1alpha and HIF-2alpha DNA binding with expression profiling of hypoxia-inducible transcripts.* J Biol Chem, 2009. **284**(25): p. 16767-75.
425. Kajimura, S., K. Aida, and C. Duan, *Understanding hypoxia-induced gene expression in early development: in vitro and in vivo analysis of hypoxia-inducible factor 1-regulated zebra fish insulin-like growth factor binding protein 1 gene expression.* Mol Cell Biol, 2006. **26**(3): p. 1142-55.
426. Spencer, J.A., et al., *Direct measurement of local oxygen concentration in the bone marrow of live animals.* Nature, 2014. **508**(7495): p. 269-73.
427. Ejtehadifar, M. and K. Shamsasenjan, *The Effect of Hypoxia on Mesenchymal Stem Cell Biology.* 2015. **5**(2): p. 141-9.
428. Fink, T., et al., *Induction of adipocyte-like phenotype in human mesenchymal stem cells by hypoxia.* Stem Cells, 2004. **22**(7): p. 1346-55.
429. Gelse, K., et al., *Chondrogenic differentiation of growth factor-stimulated precursor cells in cartilage repair tissue is associated with increased HIF-1alpha activity.* Osteoarthritis Cartilage, 2008. **16**(12): p. 1457-65.
430. Kuiper, C., et al., *Intracellular ascorbate enhances hypoxia-inducible factor (HIF)-hydroxylase activity and preferentially suppresses the HIF-1 transcriptional response.* Free Radic Biol Med, 2014. **69**: p. 308-17.
431. Miles, S.L., et al., *Ascorbic acid and ascorbate-2-phosphate decrease HIF activity and malignant properties of human melanoma cells.* BMC Cancer, 2015. **15**: p. 867.
432. Palomaki, S., et al., *HIF-1alpha is upregulated in human mesenchymal stem cells.* Stem Cells, 2013. **31**(9): p. 1902-9.
433. Simiantonaki, N., et al., *Hypoxia-inducible factor 1 alpha expression increases during colorectal carcinogenesis and tumor progression.* BMC Cancer, 2008. **8**: p. 320.
434. Brucker, P.U., N.J. Izzo, and C.R. Chu, *Tonic activation of hypoxia-inducible factor 1alpha in avascular articular cartilage and implications for metabolic homeostasis.* Arthritis Rheum, 2005. **52**(10): p. 3181-91.
435. Friedmann, E., et al., *YOS9, the putative yeast homolog of a gene amplified in osteosarcomas, is involved in the endoplasmic reticulum (ER)-Golgi transport of GPI-anchored proteins.* J Biol Chem, 2002. **277**(38): p. 35274-81.
436. Basciano, L., et al., *Long term culture of mesenchymal stem cells in hypoxia promotes a genetic program maintaining their undifferentiated and multipotent status.* BMC Cell Biology, 2011. **12**(1): p. 12.
437. Pigolotti, S., S. Krishna, and M.H. Jensen, *Oscillation patterns in negative feedback loops.* Proc Natl Acad Sci U S A, 2007. **104**(16): p. 6533-7.
438. Chan, D., et al., *A COL2A1 mutation in achondrogenesis type II results in the replacement of type II collagen by type I and III collagens in cartilage.* J Biol Chem, 1995. **270**(4): p. 1747-53.

439. Palotie, A., et al., *PREDISPOSITION TO FAMILIAL OSTEOARTHROSIS LINKED TO TYPE II COLLAGEN GENE.* The Lancet. **333**(8644): p. 924-927.
440. Loughlin, J., et al., *Differential allelic expression of the type II collagen gene (COL2A1) in osteoarthritic cartilage.* Am J Hum Genet, 1995. **56**(5): p. 1186-93.
441. Zhou, G., et al., *Three high mobility group-like sequences within a 48-base pair enhancer of the Col2a1 gene are required for cartilage-specific expression in vivo.* J Biol Chem, 1998. **273**(24): p. 14989-97.
442. Bell, D.M., et al., *SOX9 directly regulates the type-II collagen gene.* Nat Genet, 1997. **16**(2): p. 174-8.
443. Stokes, D.G., et al., *Regulation of type-II collagen gene expression during human chondrocyte de-differentiation and recovery of chondrocyte-specific phenotype in culture involves Sry-type high-mobility-group box (SOX) transcription factors.* Biochem J, 2001. **360**(Pt 2): p. 461-70.
444. Li, H., et al., *Comparative analysis with collagen type II distinguishes cartilage oligomeric matrix protein as a primary TGFbeta-responsive gene.* Osteoarthritis Cartilage, 2011. **19**(10): p. 1246-53.
445. Cheah, K.S., et al., *Expression of the mouse alpha 1(II) collagen gene is not restricted to cartilage during development.* Development, 1991. **111**(4): p. 945-53.
446. Gadjanski, I., K. Spiller, and G. Vunjak-Novakovic, *Time-dependent processes in stem cell-based tissue engineering of articular cartilage.* Stem Cell Rev, 2012. **8**(3): p. 863-81.
447. Martinez-Sanchez, A., K.A. Dudek, and C.L. Murphy, *Regulation of Human Chondrocyte Function through Direct Inhibition of Cartilage Master Regulator SOX9 by MicroRNA-145 (miRNA-145).* J Biol Chem, 2012. **287**(2): p. 916-24.
448. Pest, M.A., et al., *Disturbed cartilage and joint homeostasis resulting from a loss of mitogen-inducible gene 6 in a mouse model of joint dysfunction.* Arthritis Rheumatol, 2014. **66**(10): p. 2816-27.
449. Chang, D.M., et al., *Activin A suppresses interleukin-1-induced matrix metalloproteinase 3 secretion in human chondrosarcoma cells.* Rheumatol Int, 2007. **27**(11): p. 1049-55.
450. Zhao, Q., et al., *Parallel expression of Sox9 and Col2a1 in cells undergoing chondrogenesis.* Dev Dyn, 1997. **209**(4): p. 377-86.
451. Dayan, F., et al., *The oxygen sensor factor-inhibiting hypoxia-inducible factor-1 controls expression of distinct genes through the bifunctional transcriptional character of hypoxia-inducible factor-1alpha.* Cancer Res, 2006. **66**(7): p. 3688-98.
452. Tarhonskaya, H., et al., *Kinetic Investigations of the Role of Factor Inhibiting Hypoxia-inducible Factor (FIH) as an Oxygen Sensor.* J Biol Chem, 2015. **290**(32): p. 19726-42.
453. Tian, Y.M., et al., *Differential sensitivity of hypoxia inducible factor hydroxylation sites to hypoxia and hydroxylase inhibitors.* J Biol Chem, 2011. **286**(15): p. 13041-51.
454. Ono, N., et al., *A subset of chondrogenic cells provides early mesenchymal progenitors in growing bones.* Nat Cell Biol, 2014. **16**(12): p. 1157-1167.
455. Zhang, Q., et al., *SOX9 is a regulator of ADAMTSs-induced cartilage degeneration at the early stage of human osteoarthritis.* Osteoarthritis and Cartilage, 2015. **23**(12): p. 2259-2268.
456. Liu, C.-F. and V. Lefebvre, *The transcription factors SOX9 and SOX5/SOX6 cooperate genome-wide through super-enhancers to drive chondrogenesis.* Nucleic Acids Research, 2015. **43**(17): p. 8183-8203.
457. Bi, W., et al., *Sox9 is required for cartilage formation.* Nat Genet, 1999. **22**(1): p. 85-9.

458. Legendre, F., et al., *Enhanced chondrogenesis of bone marrow-derived stem cells by using a combinatory cell therapy strategy with BMP-2/TGF-beta1, hypoxia, and COL1A1/HtrA1 siRNAs.* Sci Rep, 2017. **7**(1): p. 3406.
459. Shahdadfar, A., et al., *Persistence of collagen type II synthesis and secretion in rapidly proliferating human articular chondrocytes in vitro.* Tissue Eng Part A, 2008. **14**(12): p. 1999-2007.
460. Hirao, M., et al., *Oxygen tension regulates chondrocyte differentiation and function during endochondral ossification.* J Biol Chem, 2006. **281**(41): p. 31079-92.
461. Eames, B.F., P.T. Sharpe, and J.A. Helms, *Hierarchy revealed in the specification of three skeletal fates by Sox9 and Runx2.* Dev Biol, 2004. **274**(1): p. 188-200.
462. Ding, M., et al., *Targeting Runx2 expression in hypertrophic chondrocytes impairs endochondral ossification during early skeletal development.* J Cell Physiol, 2012. **227**(10): p. 3446-56.
463. Mueller, M.B. and R.S. Tuan, *Functional characterization of hypertrophy in chondrogenesis of human mesenchymal stem cells.* Arthritis Rheum, 2008. **58**(5): p. 1377-88.
464. Herlofsen, S.R., et al., *Chondrogenic Differentiation of Human Bone Marrow-Derived Mesenchymal Stem Cells in Self-Gelling Alginate Discs Reveals Novel Chondrogenic Signature Gene Clusters.* Tissue Eng Part A, 2011. **17**(7-8): p. 1003-13.
465. Shen, G., *The role of type X collagen in facilitating and regulating endochondral ossification of articular cartilage.* Orthod Craniofac Res, 2005. **8**(1): p. 11-7.
466. Lee, H.H., et al., *Hypoxia enhances chondrogenesis and prevents terminal differentiation through PI3K/Akt/FoxO dependent anti-apoptotic effect.* Sci Rep, 2013. **3**: p. 2683.
467. Arsham, A.M., J.J. Howell, and M.C. Simon, *A novel hypoxia-inducible factor-independent hypoxic response regulating mammalian target of rapamycin and its targets.* J Biol Chem, 2003. **278**(32): p. 29655-60.
468. Browne, G.J. and C.G. Proud, *A novel mTOR-regulated phosphorylation site in elongation factor 2 kinase modulates the activity of the kinase and its binding to calmodulin.* Mol Cell Biol, 2004. **24**(7): p. 2986-97.
469. Wouters, B.G. and M. Koritzinsky, *Hypoxia signalling through mTOR and the unfolded protein response in cancer.* Nat Rev Cancer, 2008. **8**(11): p. 851-64.
470. Koumenis, C., et al., *Regulation of protein synthesis by hypoxia via activation of the endoplasmic reticulum kinase PERK and phosphorylation of the translation initiation factor eIF2alpha.* Mol Cell Biol, 2002. **22**(21): p. 7405-16.
471. Pan, Q., et al., *Sox9, a key transcription factor of bone morphogenetic protein-2-induced chondrogenesis, is activated through BMP pathway and a CCAAT box in the proximal promoter.* J Cell Physiol, 2008. **217**(1): p. 228-41.
472. Sanchez, Carlos G., et al., *Regulation of Ribosome Biogenesis and Protein Synthesis Controls Germline Stem Cell Differentiation.* Cell Stem Cell. **18**(2): p. 276-290.
473. Kristensen, A.R., J. Gsponer, and L.J. Foster, *Protein synthesis rate is the predominant regulator of protein expression during differentiation.* Mol Syst Biol, 2013. **9**: p. 689.
474. Romero-Ramirez, L., et al., *XBP1 is essential for survival under hypoxic conditions and is required for tumor growth.* Cancer Res, 2004. **64**(17): p. 5943-7.
475. Liu, M., et al., *Injectable hydrogels for cartilage and bone tissue engineering.* 2017. **5**: p. 17014.
476. Feng, Q., et al., *Sulfated hyaluronic acid hydrogels with retarded degradation and enhanced growth factor retention promote hMSC chondrogenesis and articular cartilage integrity with reduced hypertrophy.* Acta Biomaterialia, 2017. **53**: p. 329-342.

477. Wang, G.L. and G.L. Semenza, *Desferrioxamine induces erythropoietin gene expression and hypoxia-inducible factor 1 DNA-binding activity: implications for models of hypoxia signal transduction.* Blood, 1993. **82**(12): p. 3610-5.
478. Huang, Z., G. He, and Y. Huang, *Deferoxamine synergizes with transforming growth factor-beta signaling in chondrogenesis.* Genet Mol Biol, 2017: p. 0.
479. Gelse, K., et al., *Role of hypoxia-inducible factor 1 alpha in the integrity of articular cartilage in murine knee joints.* Arthritis Res Ther, 2008. **10**(5): p. R111.
480. Stolze, I.P., et al., *Genetic analysis of the role of the asparaginyl hydroxylase factor inhibiting hypoxia-inducible factor (FIH) in regulating hypoxia-inducible factor (HIF) transcriptional target genes [corrected].* J Biol Chem, 2004. **279**(41): p. 42719-25.
481. Huang, M., et al., *Double knockdown of prolyl hydroxylase and factor-inhibiting hypoxia-inducible factor with nonviral minicircle gene therapy enhances stem cell mobilization and angiogenesis after myocardial infarction.* Circulation, 2011. **124**(11 Suppl): p. S46-54.
482. Floyd, Z.E., et al., *Effects of prolyl hydroxylase inhibitors on adipogenesis and hypoxia inducible factor 1 alpha levels under normoxic conditions.* J Cell Biochem, 2007. **101**(6): p. 1545-57.
483. Makris, E.A., D.J. Responte, and N.K. Paschos, *Developing functional musculoskeletal tissues through hypoxia and lysyl oxidase-induced collagen cross-linking.* 2014. **111**(45): p. E4832-41.
484. Myllyharju, J., *Prolyl 4-hydroxylases, the key enzymes of collagen biosynthesis.* Matrix Biology, 2003. **22**(1): p. 15-24.
485. Makris, E.A., J.C. Hu, and K.A. Athanasiou, *Hypoxia-induced collagen crosslinking as a mechanism for enhancing mechanical properties of engineered articular cartilage.* Osteoarthritis Cartilage, 2013. **21**(4): p. 634-41.
486. D'Angelo, M., et al., *MMP-13 is induced during chondrocyte hypertrophy.* J Cell Biochem, 2000. **77**(4): p. 678-93.
487. Wang, M., et al., *MMP13 is a critical target gene during the progression of osteoarthritis.* Arthritis Res Ther, 2013. **15**(1): p. R5.
488. Kawakami, Y., et al., *WNT Signals Control FGF-Dependent Limb Initiation and AER Induction in the Chick Embryo.* Cell, 2001. **104**(6): p. 891-900.
489. Kobayashi, T., et al., *BMP signaling stimulates cellular differentiation at multiple steps during cartilage development.* Proc Natl Acad Sci U S A, 2005. **102**(50): p. 18023-7.
490. Caron, M.M., et al., *Hypertrophic differentiation during chondrogenic differentiation of progenitor cells is stimulated by BMP-2 but suppressed by BMP-7.* Osteoarthritis Cartilage, 2013. **21**(4): p. 604-13.
491. Lv, F.-J., et al., *Concise Review: The Surface Markers and Identity of Human Mesenchymal Stem Cells.* STEM CELLS, 2014. **32**(6): p. 1408-1419.
492. Partch, C.L. and K.H. Gardner, *Coactivators necessary for transcriptional output of the hypoxia inducible factor, HIF, are directly recruited by ARNT PAS-B.* Proc Natl Acad Sci U S A, 2011. **108**(19): p. 7739-44.
493. Lee, K., et al., *Acriflavine inhibits HIF-1 dimerization, tumor growth, and vascularization.* Proc Natl Acad Sci U S A, 2009. **106**(42): p. 17910-5.
494. Niebler, S., et al., *Hypoxia-Inducible Factor 1 Is an Inductor of Transcription Factor Activating Protein 2 Epsilon Expression during Chondrogenic Differentiation.* Biomed Res Int, 2015. **2015**: p. 380590.
495. Flamant, L., et al., *Anti-apoptotic role of HIF-1 and AP-1 in paclitaxel exposed breast cancer cells under hypoxia.* Molecular Cancer, 2010. **9**(1): p. 191.
496. Yoo, W., et al., *HIF-1alpha expression as a protective strategy of HepG2 cells against fatty acid-induced toxicity.* J Cell Biochem, 2014. **115**(6): p. 1147-58.

497. Lee, S.K., et al., *Iron chelator-induced growth arrest and cytochrome c-dependent apoptosis in immortalized and malignant oral keratinocytes.* J Oral Pathol Med, 2006. **35**(4): p. 218-26.
498. Berchner-Pfannschmidt, U., et al., *Nuclear oxygen sensing: induction of endogenous prolyl-hydroxylase 2 activity by hypoxia and nitric oxide.* J Biol Chem, 2008. **283**(46): p. 31745-53.
499. Tarhonskaya, H., et al., *Non-enzymatic chemistry enables 2-hydroxyglutarate-mediated activation of 2-oxoglutarate oxygenases.* Nat Commun, 2014. **5**: p. 3423.
500. Chan, M.C., et al., *Tuning the Transcriptional Response to Hypoxia by Inhibiting Hypoxia-inducible Factor (HIF) Prolyl and Asparaginyl Hydroxylases.* J Biol Chem, 2016. **291**(39): p. 20661-73.
501. Ma, Y., et al., *A controlled double-duration inducible gene expression system for cartilage tissue engineering.* Sci Rep, 2016. **6**.
502. Smits, P., et al., *The Transcription Factors L-Sox5 and Sox6 Are Essential for Cartilage Formation.* Developmental Cell, 2001. **1**(2): p. 277-290.
503. Sart, S., et al., *Three-Dimensional Aggregates of Mesenchymal Stem Cells: Cellular Mechanisms, Biological Properties, and Applications.* Tissue Eng Part B Rev, 2014. **20**(5): p. 365-80.
504. Sun, M.M. and F. Beier, *Chondrocyte hypertrophy in skeletal development, growth, and disease.* Birth Defects Res C Embryo Today, 2014. **102**(1): p. 74-82.
505. Da, H., et al., *The impact of compact layer in biphasic scaffold on osteochondral tissue engineering.* PLoS One, 2013. **8**(1): p. e54838.
506. Kon, E., et al., *A novel nano-composite multi-layered biomaterial for treatment of osteochondral lesions: technique note and an early stability pilot clinical trial.* Injury, 2010. **41**(7): p. 693-701.
507. Hirata, M., et al., *C/EBPbeta and RUNX2 cooperate to degrade cartilage with MMP-13 as the target and HIF-2alpha as the inducer in chondrocytes.* Hum Mol Genet, 2012. **21**(5): p. 1111-23.
508. Li, F., et al., *Runx2 contributes to murine Col10a1 gene regulation through direct interaction with its cis-enhancer.* J Bone Miner Res, 2011. **26**(12): p. 2899-910.
509. Saito, T., et al., *Transcriptional regulation of endochondral ossification by HIF-2alpha during skeletal growth and osteoarthritis development.* Nat Med, 2010. **16**(6): p. 678-86.
510. Jho, E.H., et al., *Wnt/beta-catenin/Tcf signaling induces the transcription of Axin2, a negative regulator of the signaling pathway.* Mol Cell Biol, 2002. **22**(4): p. 1172-83.
511. Hovanes, K., et al., *Beta-catenin-sensitive isoforms of lymphoid enhancer factor-1 are selectively expressed in colon cancer.* Nat Genet, 2001. **28**(1): p. 53-7.
512. Koivunen, P., et al., *Catalytic properties of the asparaginyl hydroxylase (FIH) in the oxygen sensing pathway are distinct from those of its prolyl 4-hydroxylases.* J Biol Chem, 2004. **279**(11): p. 9899-904.
513. Carrion, B., et al., *The Synergistic Effects of Matrix Stiffness and Composition on the Response of Chondroprogenitor Cells in a 3D Precondensation Microenvironment.* Adv Healthc Mater, 2016. **5**(10): p. 1192-202.
514. Damon, B.J., et al., *Limb bud and flank mesoderm have distinct "physical phenotypes" that may contribute to limb budding.* Developmental Biology, 2008. **321**(2): p. 319-330.
515. Takahashi, I., et al., *Compressive force promotes sox9, type II collagen and aggrecan and inhibits IL-1beta expression resulting in chondrogenesis in mouse embryonic limb bud mesenchymal cells.* J Cell Sci, 1998. **111 (Pt 14)**: p. 2067-76.
516. Elder, S.H., *Conditioned medium of mechanically compressed chick limb bud cells promotes chondrocyte differentiation.* J Orthop Sci, 2002. **7**(5): p. 538-43.

517. Wolpert, L., *Cellular basis of skeletal growth during development.* Br Med Bull, 1981. **37**(3): p. 215-9.
518. Foolen, J., C.C. van Donkelaar, and K. Ito, *Intracellular tension in periosteum/perichondrium cells regulates long bone growth.* J Orthop Res, 2011. **29**(1): p. 84-91.
519. Mow, V.C., C.C. Wang, and C.T. Hung, *The extracellular matrix, interstitial fluid and ions as a mechanical signal transducer in articular cartilage.* Osteoarthritis Cartilage, 1999. **7**(1): p. 41-58.
520. Darling, E.M., et al., *Spatial Mapping of the Biomechanical Properties of the Pericellular Matrix of Articular Cartilage Measured In Situ via Atomic Force Microscopy.* Biophysical Journal. **98**(12): p. 2848-2856.
521. Dessau, W., et al., *Changes in the patterns of collagens and fibronectin during limb-bud chondrogenesis.* J Embryol Exp Morphol, 1980. **57**: p. 51-60.
522. Singh, P. and J.E. Schwarzbauer, *Fibronectin matrix assembly is essential for cell condensation during chondrogenesis.* J Cell Sci, 2014. **127**(20): p. 4420-8.
523. Somaiah, C., et al., *Collagen Promotes Higher Adhesion, Survival and Proliferation of Mesenchymal Stem Cells.* PLoS One, 2015. **10**(12).
524. Ouasti, S., et al., *Network connectivity, mechanical properties and cell adhesion for hyaluronic acid/PEG hydrogels.* Biomaterials, 2011. **32**(27): p. 6456-70.
525. Kubow, K.E., et al., *Mechanical forces regulate the interactions of fibronectin and collagen I in extracellular matrix.* Nat Commun, 2015. **6**: p. 8026.
526. Ekholm, E., et al., *Diminished Callus Size and Cartilage Synthesis in α1β1 Integrin-Deficient Mice during Bone Fracture Healing.* Am J Pathol, 2002. **160**(5): p. 1779-85.
527. Bement, W.M., G.I. Gallicano, and D.G. Capco, *Role of the cytoskeleton during early development.* Microsc Res Tech, 1992. **22**(1): p. 23-48.
528. Jekely, G., *Origin and evolution of the self-organizing cytoskeleton in the network of eukaryotic organelles.* Cold Spring Harb Perspect Biol, 2014. **6**(9): p. a016030.
529. Wang, N., J.D. Tytell, and D.E. Ingber, *Mechanotransduction at a distance: mechanically coupling the extracellular matrix with the nucleus.* Nat Rev Mol Cell Biol, 2009. **10**(1): p. 75-82.
530. Lee, D.C., et al., *A-type nuclear lamins act as transcriptional repressors when targeted to promoters.* Exp Cell Res, 2009. **315**(6): p. 996-1007.
531. Choi, C.K., et al., *Actin and α-actinin orchestrate the assembly and maturation of nascent adhesions in a myosin II motor-independent manner.* Nat Cell Biol, 2008. **10**(9): p. 1039-50.
532. Bachir, Alexia I., et al., *Integrin-Associated Complexes Form Hierarchically with Variable Stoichiometry in Nascent Adhesions.* Current Biology, 2014. **24**(16): p. 1845-1853.
533. Valencia-Exposito, A., et al., *Myosin light-chain phosphatase regulates basal actomyosin oscillations during morphogenesis.* Nat Commun, 2016. **7**: p. 10746.
534. Bian, L., et al., *The influence of hyaluronic acid hydrogel crosslinking density and macromolecular diffusivity on human MSC chondrogenesis and hypertrophy.* Biomaterials, 2013. **34**(2): p. 413-21.
535. Sun, A.X., et al., *Chondrogenesis of human bone marrow mesenchymal stem cells in 3-dimensional, photocrosslinked hydrogel constructs: Effect of cell seeding density and material stiffness.* Acta Biomaterialia, 2017. **58**: p. 302-311.
536. Jiang, L., et al., *Cells Sensing Mechanical Cues: Stiffness Influences the Lifetime of Cell-Extracellular Matrix Interactions by Affecting the Loading Rate.* ACS Nano, 2016. **10**(1): p. 207-17.
537. Park, J.S., et al., *The Effect of Matrix Stiffness on the Differentiation of Mesenchymal Stem Cells in Response to TGF-β.* Biomaterials, 2011. **32**(16): p. 3921-30.

538. Engler, A.J., et al., *Surface probe measurements of the elasticity of sectioned tissue, thin gels and polyelectrolyte multilayer films: Correlations between substrate stiffness and cell adhesion.* Surface Science, 2004. **570**(1): p. 142-154.
539. Ishizaki, T., et al., *Pharmacological properties of Y-27632, a specific inhibitor of rho-associated kinases.* Mol Pharmacol, 2000. **57**(5): p. 976-83.
540. Young, D.A., et al., *Stimulation of adipogenesis of adult adipose-derived stem cells using substrates that mimic the stiffness of adipose tissue.* Biomaterials, 2013. **34**(34): p. 8581-8.
541. Lee, S.H., Y.J. Lee, and H.J. Han, *Role of hypoxia-induced fibronectin-integrin beta1 expression in embryonic stem cell proliferation and migration: Involvement of PI3K/Akt and FAK.* J Cell Physiol, 2011. **226**(2): p. 484-93.
542. Bailly, K., et al., *RhoA Activation by Hypoxia in Pulmonary Arterial Smooth Muscle Cells Is Age and Site Specific.* Circulation Research, 2004. **94**(10): p. 1383-1391.
543. Totsukawa, G., et al., *Distinct roles of ROCK (Rho-kinase) and MLCK in spatial regulation of MLC phosphorylation for assembly of stress fibers and focal adhesions in 3T3 fibroblasts.* J Cell Biol, 2000. **150**(4): p. 797-806.
544. Gilkes, D.M., et al., *Hypoxia-inducible factors mediate coordinated RhoA-ROCK1 expression and signaling in breast cancer cells.* Proceedings of the National Academy of Sciences, 2014. **111**(3): p. E384-E393.
545. Dupont, S., et al., *Role of YAP/TAZ in mechanotransduction.* Nature, 2011. **474**.
546. Vieux-Rochas, M., et al., *BMP-mediated functional cooperation between Dlx5;Dlx6 and Msx1;Msx2 during mammalian limb development.* PLoS One, 2013. **8**(1): p. e51700.
547. Pizette, S., C. Abate-Shen, and L. Niswander, *BMP controls proximodistal outgrowth, via induction of the apical ectodermal ridge, and dorsoventral patterning in the vertebrate limb.* Development, 2001. **128**(22): p. 4463-74.
548. Breu, A., et al., *Estrogen reduces cellular aging in human mesenchymal stem cells and chondrocytes.* J Orthop Res, 2011. **29**.
549. Vardouli, L., et al., *A novel mechanism of TGFbeta-induced actin reorganization mediated by Smad proteins and Rho GTPases.* Febs j, 2008. **275**(16): p. 4074-87.
550. Guo, W.H., et al., *Substrate rigidity regulates the formation and maintenance of tissues.* Biophys J, 2006. **90**(6): p. 2213-20.
551. Weidemann, A., et al., *HIF-1alpha activation results in actin cytoskeleton reorganization and modulation of Rac-1 signaling in endothelial cells.* Cell Commun Signal, 2013. **11**: p. 80.
552. Jerrell, R.J. and A. Parekh, *Cellular Traction Stresses Mediate Extracellular Matrix Degradation by Invadopodia.* Acta Biomater, 2014. **10**(5): p. 1886-96.
553. Suzuki, A. and T. Itoh, *Effects of calyculin A on tension and myosin phosphorylation in skinned smooth muscle of the rabbit mesenteric artery.* Br J Pharmacol, 1993. **109**(3): p. 703-12.
554. Gilkes, D.M., et al., *Hypoxia-inducible Factor 1 (HIF-1) Promotes Extracellular Matrix Remodeling under Hypoxic Conditions by Inducing P4HA1, P4HA2, and PLOD2 Expression in Fibroblasts.* J Biol Chem, 2013. **288**(15): p. 10819-29.
555. Subbiah, R., et al., *Tunable Crosslinked Cell-Derived Extracellular Matrix Guides Cell Fate.* Macromol Biosci, 2016. **16**(11): p. 1723-1734.
556. Prewitz, M.C., et al., *Tightly anchored tissue-mimetic matrices as instructive stem cell microenvironments.* Nat Methods, 2013. **10**(8): p. 788-94.
557. Cluzel, C., et al., *The mechanisms and dynamics of αvβ3 integrin clustering in living cells.* J Cell Biol, 2005. **171**(2): p. 383-92.

558. Zhao, B., et al., *Inactivation of YAP oncoprotein by the Hippo pathway is involved in cell contact inhibition and tissue growth control.* Genes Dev, 2007. **21**(21): p. 2747-61.
559. Vogler, M., et al., *Hypoxia Modulates Fibroblastic Architecture, Adhesion and Migration: A Role for HIF-1α in Cofilin Regulation and Cytoplasmic Actin Distribution.* PLOS ONE, 2013. **8**(7): p. e69128.
560. Tacchetti, C., et al., *Cell condensation in chondrogenic differentiation.* Exp Cell Res, 1992. **200**(1): p. 26-33.
561. Widelitz, R.B., et al., *Adhesion molecules in skeletogenesis: II. Neural cell adhesion molecules mediate precartilaginous mesenchymal condensations and enhance chondrogenesis.* J Cell Physiol, 1993. **156**(2): p. 399-411.
562. Tavella, S., et al., *N-CAM and N-Cadherin Expression during in Vitro Chondrogenesis.* Experimental Cell Research, 1994. **215**(2): p. 354-362.
563. Caliari, S.R., et al., *Stiffening hydrogels for investigating the dynamics of hepatic stellate cell mechanotransduction during myofibroblast activation.* Sci Rep, 2016. **6**.
564. Milosevic, J., et al., *Non-hypoxic stabilization of hypoxia-inducible factor alpha (HIF-alpha): relevance in neural progenitor/stem cells.* Neurotox Res, 2009. **15**(4): p. 367-80.
565. Takeda, K. and G.H. Fong, *Prolyl hydroxylase domain 2 protein suppresses hypoxia-induced endothelial cell proliferation.* Hypertension, 2007. **49**(1): p. 178-84.
566. Chen, T., et al., *Factor inhibiting HIF1alpha (FIH-1) functions as a tumor suppressor in human colorectal cancer by repressing HIF1alpha pathway.* Cancer Biol Ther, 2015. **16**(2): p. 244-52.
567. Bian, L., et al., *Hydrogels that mimic developmentally relevant matrix and N-cadherin interactions enhance MSC chondrogenesis.* Proc Natl Acad Sci U S A, 2013. **110**(25): p. 10117-22.
568. Yang, H.J., et al., *A novel role for neural cell adhesion molecule in modulating insulin signaling and adipocyte differentiation of mouse mesenchymal stem cells.* J Cell Sci, 2011. **124**(Pt 15): p. 2552-60.
569. Min, Z., et al., *3D-printed dimethyloxallyl glycine delivery scaffolds to improve angiogenesis and osteogenesis.* Biomaterials Science, 2015. **3**(8): p. 1236-1244.
570. Jaklenec, A., et al., *Sequential release of bioactive IGF-I and TGF-β1 from PLGA microsphere-based scaffolds.* Biomaterials, 2008. **29**(10): p. 1518-1525.
571. Battula, V.L., et al., *Isolation of functionally distinct mesenchymal stem cell subsets using antibodies against CD56, CD271, and mesenchymal stem cell antigen-1.* Haematologica, 2009. **94**.
572. Heathman, T.R.J., et al., *Characterization of human mesenchymal stem cells from multiple donors and the implications for large scale bioprocess development.* Biochemical Engineering Journal, 2016. **108**(Supplement C): p. 14-23.
573. Fahling, M., et al., *Translational control of collagen prolyl 4-hydroxylase-alpha(I) gene expression under hypoxia.* J Biol Chem, 2006. **281**(36): p. 26089-101.